The Role of Pocket Proteins pRb and p107 in Radial Migration and Axon Guidance through Cell Cycle Independent Mechanisms

Devon Sarah Svoboda

Thesis submitted to the Faculty of Graduate and Postdoctoral Studies in partial fulfillment of the requirements of the degree of Doctor of Philosophy in Neuroscience

Graduate program in Neuroscience
Department of Cellular and Molecular Medicine
Faculty of Medicine
University of Ottawa
Ottawa, Ontario
Canada

ABSTRACT

Pocket proteins (pRb, p107 and p130) are well studied in the role of regulating cell proliferation by controlling progression through the G1/S phase of the cell cycle. Increasing genetic and anatomical evidence suggests that these proteins also control early differentiation and even later stages of cell maturation including neural migration. However, the multifaceted functions of pocket proteins in the regulation of cell proliferation and cell death has complicated our interpretation of their role during development. As a result, the mechanisms through which pocket proteins regulate neuronal migration and neural maturation remain unknown. Using a pRb and p107 double knock out model, we show that a population of upper layer cortical neurons fails to pass through the intermediate zone into the cortical plate. Importantly, these neurons are born at the appropriate time and have exited the cell cycle. In addition, the role of pocket proteins in radial migration is independent cell death, since this migration defect cannot be rescued by eliminating ectopic cell death through Bax deletion. We also show a novel role of pRb and p107 in development of the dorsal midline and guidance of callosal axons. In the absence of pRb and p107, the structures of the commissural plate are highly disorganized and the callosal axons fail to cross the midline. We identify primary defects in axon extension and expression of multiple guidance cues, which can be observed prior to the disorganization of the midline axon guidance structures. Through the use of *in vitro* cortical explants and *in utero* electroporation, we identify defects in the rate of axon extension and directional guidance independent from the midline. In addition, protein levels of Netrin and Neuropilin-1 are decreased in the absence of pRb and p107, which could mediate the function of pocket proteins in guiding callosal axons. Indeed, we identify a previously undescribed population of Netrin expressing cells in the cingulate cortex of control embryos which is lost in the pRb/p107 deficient littermates. We propose that these cells play a significant role in callosal axon guidance

during normal development. The results presented in this dissertation define multiple novel roles of pRb and p107 in the regulation of radial migration and axon guidance, independent from the role of these pocket proteins in cell death and proliferation.

ACKNOWLEDGEMENTS

Writing this dissertation has been an exercise in looking back. And in looking back over my time at the University of Ottawa, I am very fortunate to remember the many people who have helped me along the way. It is with great pleasure that I take this opportunity to thank everyone who has contributed to my personal and professional achievements.

First, I would like to thank my PhD supervisor, Dr. Ruth Slack. From the very beginning, you have supplied me with a superb and supportive learning environment and have given me incredible opportunities to develop my skills, both technical and intellectual. I thank you for striking that perfect balance between giving me the independence to shape my research project and the encouragement I needed through the difficult periods. Under your mentorship, I feel that I have grown and developed as a scientist. Working in your lab has been a truly rewarding and enjoyable experience, and I look forward to continuing to work with you over the next year as a post-doc.

I would like to thank my colleagues in the Slack lab, both past and present. In particular I would like to thank Alysen Clarke, Ruthann Duivesteyn, Bensun Fong, Noel Ghanem, Ujval Anil Kumar, Kelly McClellan, David Patten and Delphie Dugal-Tessier. Special thanks go to Lisa Julian and Dr. Renaud Vandenbosch who helped train me when I first arrived, to Mireille Khacho who is always ready to talk when I have a question, and to Joelle Azzi for all her help cutting tissue and genotyping earclips. You have all contributed to the wonderful working environment and I have learned from each of you. I couldn't have done it without you!

Special thanks to Linda Jui for the hours and hours you spent cutting my tissue. Your meticulous work truly made my experiments easier to perform and made my images look better. I thank you for everything and wish you the best of luck.

And of course, a warm and special thanks to Jason MacLaurin, who has helped me in more ways than I could ever recount. Without you, we would be lost.

I would like to thank Dr. Freda Miller and Dr. Annie Paquin from the University of Toronto for teaching me how to perform in utero electroporation, and well as Dr. Pierre Mattar for coming to Ottawa to help me trouble shoot the technique when things were not going well. I thank my collaborators Dr. Tim Kennedy and James Correia from McGill University for teaching me how to perform cortical explant cultures. Also, thank you to Dr. Kelly McClellan for coming in on a Saturday to teach me how to prepare embryonic slice cultures. Your contributions to my technical skillset are invaluable.

I also wish to acknowledge the members of my Thesis Advisory Committee: Dr. Diane Lagace, Dr. Marc Ekker and Dr. Jean-Claude Beique. Thank you for your support, insight and advice throughout the progression of my PhD.

I would also like to thank the institutions which provided me with funding during my PhD: Heart and Stroke Foundation of Ontario, OGS/ OGSST, as well as the University of Ottawa International Admission and Excellence awards.

I would like to thank my horseback riding coach Ruth Allum and her husband Mark Nelson. You have provided me with immeasurable opportunities and pushed me to accomplishments I never thought possible.

And finally, I would like to thank my parents for supporting me in everything that I do. You have selflessly been there for me every day of my life and I know it wasn't easy. You have helped me grow into what I am, and I am grateful.

TABLE OF CONTENTS

LIST OF FIGURES

LIST OF TABLES

LIST OF ABBREVIATIONS

ABAM	anti-biotic anti-microbial
ABC	avidin biotin complex
AC3	active caspase 3
ANOVA	Analysis of Variance
ApoE	apolipoprotein E
Bcl2	B-cell lymphoma 2
bFGF	basic fibroblast growth factor
Bl6	Black 6 mouse strain
BLBP	brain lipid-binding protein
BMP	bone morphogenic protein
BMPR	BMP receptor
B-Myb	myeloblastosis related protein B
Boc	*Brother of CDO*
BrdU	bromodeoxyuridine
CB	calbindin
CC	corpus callosum
CDC42	cell division control protein 42
CDK	cyclin dependent kinase
CFN	corticofugal projection neuron
CIHR	Canadian Institute for Health Research
Cip/Kip	CDK interacting protein/ kinase inhibitory protein
ChIP	chromatin immunoprecipitation
CNS	central nervous system
CPN	cortical projection neuron
CR	calretinin
CR cells	Cajal Retzius cells
Cre	cyclization recombination enzyme
Ctip2	chicken ovalbumin upstream promoter transcription factor-interacting protein 2
Cux1	cut-like homeobox 1
Dab	3,3'-Diaminobenzidine
Dab1	disabled 1
DAPI	4',6-diamidino-2-phenylindole
DCC	deleted in colorectal cancer
DKO	double knockout
DMEM	Dulbecco's Modified Eagle Medium
DNA	deoxyribonucleic acid
DNMT1	DNA methyltransferase 1
DP	dimerization protein
DREAM	DP, Rb-like, E2F and MuvB protein complex
DSCAM	Down Syndrome call adhesion molecule
dUTP	2´-Deoxyuridine, 5´-Triphosphate
E__	embryonic day __
E2F	E2 promoter binding factor
Emx1	empty spiracles homeobox 1

Fez2	fasciculation and elongation protein zeta 2
flox	flanked loxP sites
FoxM1	forkhead box M1
FoxP1	forkhead box P1
FVBN	Friend virus B type susceptibility/NIH mouse
G0	interphase
G1	growth phase 1
G2	growth phase 2
GABA	gamma-aminobutyric acid
GE	ganglionic eminence
Gli3	GLI family zinc finger 3
GluN2B	NMDA receptor 2B
GFAP	glial fibrillary acidic protein
GFP	green fluorescent protein
GW	glial wedge
H2O2	hydrogen peroxide
HDAC1	histone deacetylase 1
HEK	human embryonic kidney
hPa	hectopascal
hr	hour
HSFO	Heart and Stroke Foundation of Ontario
IG	indusium griseum
IgG	immunoglobulin G
IP	intermediate precursor
ISH	*in situ* hybridization
IUE	*in utero* electroporation
IZ	intermediate zone
Jip1	JNK-interacting protein 1
JOVE	Journal of Visual Experiments
L1	L1-neural cell adhesion molecule
Lhx2	LIM homeobox 2
LoxP	locus of X-over P1
Lrp6	low density lipoprotein receptor-related protein 6
LxCxE	lysine – any amino acid – cysteine – any amino acid – glutamic acid
M	mitosis phase
Map2	microtubule associated protein 2
MEF2	myocyte enhancer factor-2
MGE	medial ganglionic eminence
min	minute
mRNA	messenger ribonucleic acid
MyoD	myogenic differentiation 1
NE	neuroephithelial cell
Nfia	nuclear factor 1/A
Nfib	nuclear factor 1/B
Nkx2.5	NK2 homeobox 5
NMDA	N-methyl-D-aspartate

NPC	neural precursor cell
Npn1	neuropilin1
NT3	neurotrophin 3
OGS	Ontario Graduate Scholarship
P__	postnatal day __
p107KO	p107 knock out
PBS	phosphate buffered saline
PCNA	Proliferating cell nuclear antigen
PCR	polymerase chain reaction
PFA	paraformaldehyde
PGC1α	Peroxisome proliferator-activated receptor gamma coactivator 1-alpha
PP1	Protein Phosphatase 1
pRb	Retinoblastoma protein
PSA-NCAM	polysialated neural cell adhesion molecule
RAC1	Ras-related C3 botulinum toxin substrate 1
RBKO	pRb knock out
RC2	radial glial cell marker 2
RGC	radial glial cell
RHOA	Ras homolog gene family, member A
RNA	ribonucleic acid
RNAi	RNA interference
Robo	roundabout, axon guidance receptor, homolog 1
RUNX2	Runt-related transcription factor 2
Ryk	receptor-like tyrosine kinase
S	synthesis phase
Satb2	special AT-rich sequence binding protein
SD	standard deviation
Sema	semaphorin
Shh	Sonic hedgehog
siRNA	silencing RNA
SNP	short neural precursor
Sox2	SRY (sex determining region Y)-box 2
SPARC-like 1	secreted *protein* acidic and rich in cysteine-like 1
Suv39h1	Su(var)3-9 homolog 1
SV40	Simian vacuolating virus 40
SVZ	subventricular zone
SWI/SNF	SWItch/Sucrose NonFermentable
Tbr1	T-box, brain, 1
Tle4	transducin-like enhancer of split 4
TUNEL	Terminal deoxynucleotidyl transferase dUTP nick end labeling
Unc5	Uncoordinated 5
Wnt	wingless (int-1)
VLDLR	very low density lipoprotein receptor
VZ	ventricular zone

CHAPTER 1

GENERAL INTRODUCTION

1. Preface: The overall aim of this dissertation is to determine whether the Retinoblastoma protein (pRB), and is close family member p107, are involved in the regulation of multiple aspects of cortical development. Studies aimed at understanding the basic mechanisms of cortical development are highly relevant to Canadian Health Research as many neurodevelopmental disorders, including autism spectrum disorder (ASD), Tourette's syndrome and schizophrenia exhibit defects in neural number (Carper, et al. 2002; Carper and Courchesne. 2005; Hazlett, et al. 2005), migration (Arnold, et al. 1991; Beckmann and Jakob. 1994; Akil and Lewis. 1997; Arnold, et al. 1997; Deutsch, et al. 2010) and errors in axon connectivity (Isler, et al. 2010; Yao, et al. 2010; Anderson, et al. 2011; Catarino, et al. 2013; Kern, et al. 2015; Hahamy, et al. 2015). In order to treat these disorders, it is crucial that scientists first understand the basic mechanisms which drive normal cortical development. In this dissertation I will examine the role of pocket proteins pRb and p107 in two aspects of neuronal maturation, radial migration and axon guidance. As the contents of this thesis will show, pocket proteins are required or the correct regulation of both cell cycle exit and neuronal maturation, such that they can be considered as prime candidates to be major regulators of cortical development, both in health and disease.

Pocket proteins are well known to regulate cell cycle exit and to control the transition from proliferating neural precursor cell (NPC) to differentiating neuroblast. Here, we specifically examine whether pRb and p107 are involved in regulating radial migration and axon guidance. We then ask whether pRb and p107 are required for neuronal maturation as a downstream consequence of their regulation of cell cycle exit and differentiation, or whether they regulate these processes through novel, cell cycle independent mechanisms. Because precise timing and coordination of different events is crucial during brain development, we

suspected that the defects in proliferation and cell cycle exit known to occur in the developing telencephalon following deletion of pRb or p107 could have severe downstream effects on the development of post-mitotic neurons. However, as the results presented in the following chapters will show, pRb and p107 seem to play a much larger, more direct role in both neuron migration and the growth and guidance of callosal axons than previously suspected. Furthermore, these pocket proteins seem to control migration and axon guidance through novel cell cycle independent mechanisms. In this introductory chapter, I will first describe the developmental processes of neurogenesis, radial migration and corpus callosum formation. I will then provide an overview of the molecular mechanisms of pRb/p107 function in cell cycle regulation and illustrate the role of pRb during development, through both cell cycle dependent and independent mechanisms. Although it is known that deletion of pRb can cause severe developmental defects in a variety of tissues, the mechanisms through which pocket proteins control development are essentially unknown. The possibility of cell cycle independent functions of pRb in controlling the development of post-mitotic cells is a relatively new and unexplored area of research. In this review, I will provide justification for the hypothesis that the pRb/p107 pathway has an extended role during neuronal development though cell cycle independent mechanisms.

2. Cortical Plate Development and Radial Migration

2.1 Overview of Neurogenesis: In order to appreciate the role of pRb and p107 in radial migration, it is first necessary to understand the processes by which the cortical plate is formed. This section will provide of an overview of these processes with special attention to neurogenesis and cell cycle regulation. As one of the main conclusions of this dissertation is that pRb and

p107 regulate cortical development through cell cycle independent mechanisms, it is crucial to discuss the importance of proper cell cycle regulation on normal cortical development.

The mammalian cortex consists of six layers of glutamatergic pyramidal neurons interspersed with a multitude of GABAergic interneurons. These two classes of neurons are derived from distinct populations of neural precursor cells (NPCs) (McConnell. 1995; Ferguson and Slack. 2001; Nadarajah and Parnavelas. 2002; Marin and Rubenstein. 2003; McClellan and Slack. 2006; Dehay and Kennedy. 2007; Stancik, et al. 2010a; Evsyukova, et al. 2013) (Figure 1-1A). Pyramidal neurons develop from proliferating NPCs in the ventricular and subventricular zones of the dorsal telencephalon, while the interneurons are derived from NPCs in the ganglionic eminences (GE) (Tarabykin, et al. 2001; Hevner, et al. 2001; Nadarajah and Parnavelas. 2002; Marin and Rubenstein. 2003; Gotz and Huttner. 2005; McClellan and Slack. 2006; Stancik, et al. 2010b). The GEs are ventrally located transient developmental structures that later give rise to the striatum (O'Rourke, et al. 1992; Tamamaki, et al. 1997; Nadarajah and Parnavelas. 2002). These interneurons reach the cortex though tangential migration around E15.5 in the mouse (O'Rourke, et al. 1992; Anderson, et al. 1997; Tamamaki, et al. 1997; Nadarajah and Parnavelas. 2002). The following overview of cortical development describes neurogenesis and focuses on radial migration of the glutamatergic pyramidal neurons in the dorsal telencephalon.

The cortex develops from a single layer of cells called the neuroepithelium of the neural tube (Figure 1-1B). Prior to the onset of neurogenesis, neuroepithelial (NE) cells undergo numerous rounds of self-renewing divisions to increase their numbers and build a thick pseudostratified neuroepithelium (Caviness, et al. 1995; Kriegstein and Gotz. 2003; Gotz and Huttner. 2005; Kriegstein, et al. 2006; Laguesse, et al. 2015). NEs are the first class of apical

neural progenitors and are characterized as having to two processes, a basal process attached to the basement membrane of the neuroepithelium and an apical process attached to the apical membrane (Miyata, et al. 2001; Noctor, et al. 2004; Gotz and Huttner. 2005; Laguesse, et al. 2015). As they progress through the cell cycle, the NE cell nucleus moves back and forth between the basal and apical membranes, which gives the neuroepithelium its pseudostratified appearance (Misson, et al. 1988; Gotz and Huttner. 2005; Spear and Erickson. 2012; Laguesse, et al. 2015).

Neurogenesis begins around E11-12 in the mouse telencephalon. At this point, NE cells transition into radial glial cells (RGs) and short neural precursors (SNPs), two other classes of apical progenitors, and adopt several astroglial characteristics (Caviness, et al. 1995; Noctor, et al. 2002; Kriegstein and Gotz. 2003; Laguesse, et al. 2015). Like NE cells, RGs have two long processes attached to the two membranes and undergo interkinetic nuclear migration within the ventricular zone (VZ) (Misson, et al. 1988; Miyata, et al. 2001; Kriegstein and Gotz. 2003; Laguesse, et al. 2015), which is the region of tightly packed cells adjacent to the ventricle (Figure 1B). RGs can undergo symmetric self-renewing divisions to generate two more RGs, or asymmetric neurogenic divisions to generate one RG and one intermediate precursor (IP) or a neuroblast (Malatesta, et al. 2000; Miyata, et al. 2001; Gotz, et al. 2002; Noctor, et al. 2004; Miyata, et al. 2004; Gotz and Huttner. 2005; Laguesse, et al. 2015). SNPs resemble RGs except that their shorter basal process doesn't reach the basement membrane and they often undergo asymmetric divisions to generate two neuroblasts (Haubensak, et al. 2004; Stancik, et al. 2010a). The type of division and origin of the neuroblasts is very important as neurons located in different cortical layers are derived from different categories of neural precursor cell, as will be discussed below.

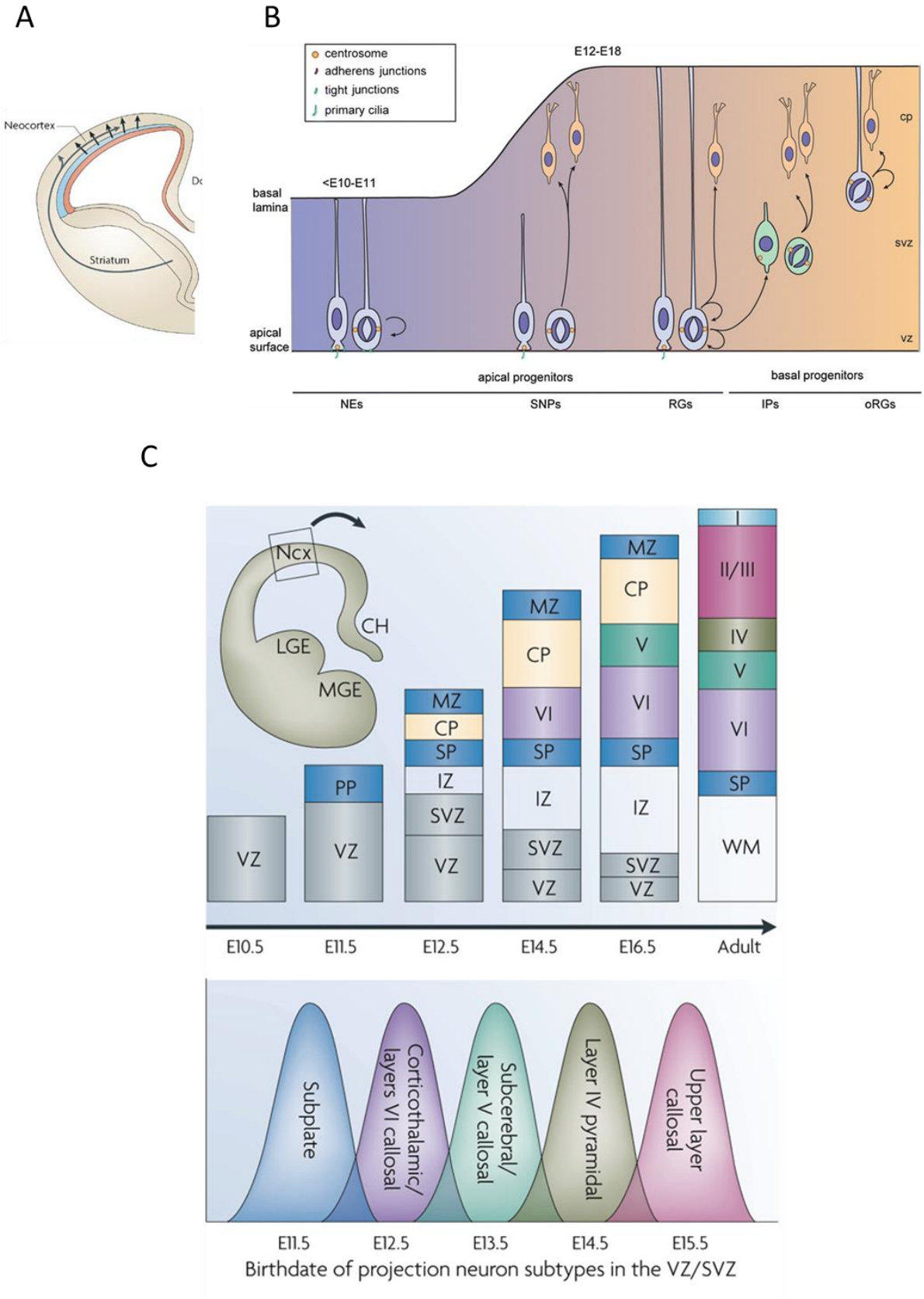
A
Neocortex
Striatum
B
centrosome
adherens junctions
tight junctions
primary cilia
E12-E18
<E10-E11
basal lamina
apical surface
cp
svz
vz
apical progenitors
basal progenitors
NEs
SNPs
RGs
IPs
oRGs
C
Ncx
CH
LGE
MGE
VZ
PP
MZ
CP
SP
IZ
SVZ
VI
V
II/III
IV
WM
E10.5
E11.5
E12.5
E14.5
E16.5
Adult
Subplate
Corticothalamic/ layers VI callosal
Subcerebral/ layer V callosal
Layer IV pyramidal
Upper layer callosal
E11.5
E12.5
E13.5
E14.5
E15.5
Birthdate of projection neuron subtypes in the VZ/SVZ

Figure 1-1

Figure 1-1: Neural Precursor Division and Corticogenesis. **A)** This coronal view of the mouse brain shows that the cortex is composed of two neural subtypes, pyramidal neurons which travel into the cortex from the ventricular zone (VZ) of the dorsal telencephalon via radial migration, and interneurons which reach the cortex of the ganglionic eminence of the ventral telencephalon via tangential migration. **B)** In the mouse brain, neural progenitor cells can be classified as apical progenitors (APs – light blue) and basal progenitors (BPs - green). Apical progenitors define neuroepithelial cells (NEs), short neural precursors (SNPs) and radial glial cells (RGs). NEs form the neural tube epithelium up to age E11 and undergo self-renewing divisions, generating two new daughter NEs. NEs transition into SNPs and RGs around E12, which undergo self-renewing symmetric divisions and neurogenic asymmetric divisions. SNPs primarily give rise directly to neurons, while RGs give rise to neurons and intermediate progenitors (IPs), which are the primary kind of BP in the developing mouse brain. IPs are located in the subventricular zone (SVZ) and undergo a few round of proliferative divisions, then give rise to neurons (orange). **C)** The earliest born neurons form the preplate (PP), which is later split into the more superficial marginal zone (MZ) and the deeply located subplate (SP). Later born neurons migrate past the subplate and previously deposited neurons to the top of the cortical plate (CP). This generates a multilayered neocortex in which the oldest neurons are in the deepest layers and the youngest neurons are in the uppermost layers. The birthdate of a neuron determines its cortical layer and functional classification, such that neurons born at a common age project axons to a common target. CH, cortical hem; E, embryonic day; Ncx, neocortex; IZ, intermediate zone; LGE, lateral ganglionic eminence; MGE, medial ganglionic eminence; WM, white matter.

Top: Modified from Laguesse et al., 2015. *Cell Tissue Res.*

Bottom: Modified from Molyneaux et al., 2007. *Nat Rev Neurosci*.

In asymmetric division of the RGs, the IP detaches from the apical membrane and migrates dorsally to the outer edge of the VZ (Tarabykin, et al. 2001; Noctor, et al. 2004; Laguesse, et al. 2015). This begins the formation of the subventricular zone (SVZ). The SVZ continues to expand during neurogenesis as the population of IPs grows until it peaks at E15.5, and then slowly shrinks towards the end of neurogenesis at E18.0, and is present only as a thin layer of cells in the adult brain (Caviness, et al. 1995; McConnell. 1995; Kriegstein, et al. 2006). IPsundergo one or two rapid symmetric proliferations to generate more IPs, and then complete one final division to yield two post-mitotic neuroblasts (Tarabykin, et al. 2001; Martinez-Cerdeno, et al. 2006; Kriegstein, et al. 2006). This point represents the "birthdate" of the neuroblast and the embryonic age at which the neuroblast is born is very important for defining the developmental trajectory and functional specificity of the mature neuron within the neocortex (Angevine and Sidman. 1961; Berry and Rogers. 1965; McConnell. 1988a; McConnell and Kaznowski. 1991; Frantz and McConnell. 1996).

2.2 Cortical Plate Development: Formation of the cortical plate begins with formation of the preplate, located along the top of the SVZ (Figure 1-1B) (Stewart and Pearlman. 1987; McConnell. 1988b). The first cohort of neurons are derived directly from neurogenic division of the SNPs or RGs (Noctor, et al. 2004) and reach the top of the SVZ through somal translocation (Nadarajah, et al. 2001; Nadarajah and Parnavelas. 2002), in which the basal process shortens to pull the soma vertically. These neurons form a structure known as the preplate (Stewart and Pearlman. 1987; Hevner, et al. 2001; Garcia-Moreno, et al. 2007). The next set of neuroblasts migrates to the middle of the preplate and thus splits the preplate into two parts (Stewart and Pearlman. 1987; Hevner, et al. 2001; Jimenez, et al. 2003; Garcia-Moreno, et al. 2007). The

bottom half becomes the subplate and can be identified throughout development as a loosely packed layer of neurons residing below the cortical plate (Hevner, et al. 2001; Jimenez, et al. 2003; Garcia-Moreno, et al. 2007). The upper half of the subplate becomes layer I of the cortex, also known as the marginal zone (Hevner, et al. 2001; Garcia-Moreno, et al. 2007). Of the multiple cell types found in layer I (Jimenez, et al. 2003), Cajal-Retzius (CR) cells are the most well described and serve a crucial function in radial migration through the secretion of Reelin (see section 2.4) (Tissir and Goffinet. 2003; Garcia-Moreno, et al. 2007; Frotscher, et al. 2009; Honda, et al. 2011; Hippenmeyer. 2014). Cell tracing studies have shown that CR cells are generated in the cortical hem at E10 and then migrate tangentially through the marginal zone to populate layer I throughout the cortical plate (Garcia-Moreno, et al. 2007). As neuroblasts are born, they migrate dorsally into the cortical plate by attaching to the basal processes of RGs and traveling along this scaffold, a process known as radial migration (Rakic. 1971; Rakic. 1972; Nadarajah and Parnavelas. 2002; Marin and Rubenstein. 2003; Ferguson, et al. 2005; Hippenmeyer. 2014; Wu, et al. 2014).

The six-layered cortical plate develops in an inside-out manner such that each successive population of migrating neurons travels past the previously deposited neurons to the outside of the cortex, just under the CR cells. Neuron birthdating experiments used BrdU incorporation to mark neurons born on different developmental days. These studies showed that neurons born early in neurogenesis, between E12.5 and E13.5, migrate to layer V/VI, while the neurons born later in neurogenesis, around E16.5 to E18.5, populate layers II/III (Figure 1-1C) (Angevine and Sidman. 1961; Berry and Rogers. 1965; Polleux, et al. 1997a; Shen, et al. 2006; Frotscher, et al. 2009; Honda, et al. 2011; Hippenmeyer. 2014). Neurons in the lower layers have been shown to have different cellular origins than upper layer neurons, with most lower layer neurons being

derived from direct neurogenic divisions of SNPs and RGs, while upper layer neurons are generated from divisions of IPs (Tarabykin, et al. 2001; Noctor, et al. 2004; Haubensak, et al. 2004; Martinez-Cerdeno, et al. 2006; Stancik, et al. 2010b). *In utero* electroporation of plasmids containing GFP controlled by cell-type specific promoters showed that SNP progeny were most likely to be deep layer neurons, while most RG progeny were shown to be a combination of IPs, and the upper layer neurons which are generated from IPs (Stancik, et al. 2010b).

2.3 Cell Cycle Regulation and Cortical Lamination: Regulation of the cell cycle is crucial for proper cortical development. The rate of proliferation regulates both the number of neurons produced and the intrinsic fate of daughter cells (Caviness, et al. 1995; Qian, et al. 2000; Shen, et al. 2006; Dehay and Kennedy. 2007). As pRb and p107 are canonical cell cycle regulators, and the purpose of this dissertation is to improve our understanding of the role of pRb and p107 in cortical development, this section will discuss the consequence of cell cycle deregulation on neural identity and cortical lamination.

The rate of cell cycle progression is determined by two factors, (1) the duration of one complete passage through the cell cycle, and (2) the decision to either remain in the cell cycle for another passage, or temporarily exit and adopt a state known as quiescence (Caviness. 1982; Misson, et al. 1988; Caviness, et al. 1995; Nowakowski, et al. 2002; Dehay and Kennedy. 2007). Because the rate of cell cycle progression controls the number of neurons produced at a given time, changes in the rate of cell division at different stages of neurogenesis can have direct impacts on the relative numbers of neurons within individual cortical layers. Studies have shown that differences in the rate of cell cycle progression correlate with differences in the relative thickness of the cortical layers between separate regions of the frontoparietal cortex (Polleux, et

al. 1997a; Polleux, et al. 1997b). For example, a decrease in cell cycle length at E14.5 correlates with an increase in neuron production and a wider layer IV. This can in turn alter cortical lamination and circuit formation (Polleux, et al. 1997a; Polleux, et al. 1997b). Similarly, deletion of core cell cycle regulator p57 (see section 4.1) was found to shorten the cell cycle by decreasing G1 length in both RGs and IPs early in neurogenesis at E14.5, while deletion of the very similar protein p27 was found to decrease G1 length specifically in IPs at E16.5 (Mairet-Coello, et al. 2012). The effect was that p57 deletion caused an increase in the production of layer V/VI neurons, while deletion of p27 caused an increase in the production of layer II-V neurons (Mairet-Coello, et al. 2012). This suggests regulation of cell cycle dynamics in all categories of NPCs can have profound effects on cortical development and lamination.

Cell cycle dynamics can also influence cell fate by regulating the type of division within a given developmental age. The length of the G1 phase of the cell cycle has been closely tied to daughter cell fate. Treatment of NPCs with bFGF, a mitogenic signal, was shown to promote proliferation through a decrease in G1 length, while treatment with NT3, which promotes differentiation, had the opposite effect in promoting neurogenic divisions through an increase in G1 length (Lukaszewicz, et al. 2002). Similarly, in proliferating NPCs in the VZ, G1 length was found to correlate with the type of division, with NPCs undergoing neurogenic divisions taking 20% longer to complete G1 than NPCs undergoing proliferative divisions (Calegari, et al. 2005). Forced expression of cyclinD/CDK4 led to a shortening of G1 in cycling NPCs, which resulted in increased proportion of proliferative division and caused an increase in the production of IPs at the expense of neurons and an expansion of the SVZ (Lange, et al. 2009). Together, these studies suggest that increasing G1 length leads to an increase in the proportion of differentiating

divisions at the expense of self-renewing divisions in NPCs, while decreasing G1 length promotes an increase in self-renewing divisions.

The length of the cell cycle is well known to progressively increase as neurogenesis proceeds (Caviness, et al. 1995; Takahashi, et al. 1996; Lukaszewicz, et al. 2002; Calegari, et al. 2005). Average NPC cell cycle length has been shown to increase from 8 hours at Ell to 20 hours at E17; this was shown to be due to a steady increase in the G1 length with no change in G2/M phase duration (Caviness, et al. 1995; Takahashi, et al. 1996). Furthermore, the G1 length has been shown to increase *in vivo* by 47% from E10.5 to E14.5 specifically in the NPCs undergoing neurogenic divisions (Calegari, et al. 2005). This suggests that the general increase in G1 length throughout neurogenesis is due to both an increase in the proportion of neurogenic divisions over self-renewing divisions, and an increase in G1 length during the neurogenic divisions (Caviness, et al. 1995; Takahashi, et al. 1996; Calegari, et al. 2005). This could indicate that G1 length controls not only the decision between neurogenic and self-renewing divisions, but also the identity of the subtype of neurons generated, with longer G1 promoting neuroblasts to adopt upper layer neuron identity (Calegari, et al. 2005). Modification of G1 length could therefore have profound effects on cortical structure and lamination, both through controlling the number of neurons generated and the laminar identity of the individual neurons. These observations greatly contributed to the early hypothesis of this thesis; that core cell cycle regulating proteins could affect neuronal maturation and brain development through regulation of cell cycle dynamics and the timing of generation of different neuron subtypes. Although we know that cell cycle regulation has far reaching downstream consequences on neuronal development, it is unknown whether this is the only, or even the primary, mechanism through which classical cell cycle regulators control cortical development and neuronal maturation.

2.4 Radial Migration: Radial migration and proper formation of the cortical layers, or cortical lamination, are highly important to normal neuronal development and brain function, as many neurodevelopmental and psychological disorders are characterized by abnormalities in cortical layer formation (Jakob and Beckmann. 1986; Arnold, et al. 1991; Beckmann and Jakob. 1994; Uribe and Wix. 2012; Catts, et al. 2013; Olson. 2014). In order for neuroblasts to travel from the SVZ to the top of the cortical plate, several barriers must be overcome. A list of the factors influencing radial migration are summarized in Table 1-1. First, the neuroblast must undergo complex cytoskeletal rearrangements to change from the multipolar morphology of an SVZ IP to the bipolar morphology a migrating neuroblast (Nadarajah and Parnavelas. 2002; Sato and Nagano. 2005; Pacary, et al. 2011; Boitard, et al. 2015). This process has been shown to be dependent on multiple factors, including Wnt signaling (Boitard, et al. 2015). Electroporation of a constitutively active form of Wnt3A caused neuroblasts to remain in a multipolar shape with an average of six highly branched processes randomly oriented around the soma, while control electroporated neuroblasts had two unbranched processes oriented parallel to the radial glial scaffold (Boitard, et al. 2015). The bipolar neuroblast then extends a leading process up the radial glial scaffold, forms an adhesive contact, and translocates the nucleus dorsally, a process calls nucleokinesis (Zheng, et al. 1996; Nadarajah, et al. 2001; Gongidi, et al. 2004; Nguyen, et al. 2006). Migration must occur at the correct speed, as delays in the rate of migration can affect the organization of the cortical layers (Kawauchi, et al. 2003; Konno, et al. 2005; Pacary, et al. 2011). Finally, the neuroblast must travel past the existing layers and detach from the scaffold at the correct location (Nadarajah, et al. 2001; Nadarajah and Parnavelas. 2002; Gongidi, et al. 2004; Frotscher, et al. 2009; Honda, et al. 2011). There seems to exist an additional barrier to

Table 1-1: Cell Autonomous and Non-Cell Autonomous Factors Regulating Radial Migration.

Feature	Intrinsic/Extrinsic	Function	Citation
Developmental age of cell cycle exit	Intrinsic	• Neuroblasts born early (E12.5-E13.5) adopt identity of layer V/VI neurons; neuroblasts born late in neurogenesis (E15.5-E18.5) adopt identity of layer II/III neurons. • Failure to exit the cell cycle completely could impair differentiation and migration	(McConnell. 1988b; McConnell and Kaznowski. 1991; Gotz and Huttner. 2005; Laguesse, et al. 2015)
Differentiation	Both	• Failure to differentiate properly impairs neuroblasts' ability to initiate migration and respond to migration signals. • Could be due to an intrinsic deregulation of neurogenic factors or an extrinsic signal which prevents differentiation.	(Tarabykin, et al. 2001; Ghanem, et al. 2012a; Boitard, et al. 2015)
Cytoskeletal Dynamics	Intrinsic	• Remodeling of the cytoskeleton required for transition to bipolar morphology. • Required for extension of leading process and nucleokinesis along radial glial scaffold. • Imbalance in polymerization and depolymerization could prevent movement of neuroblasts or change rate of translocation.	(Nguyen, et al. 2006; Boitard, et al. 2015; Azzarelli, et al. 2015)
Radial Glial Scaffold	Extrinsic	• Neuroblasts follow RG basal processes to the top of the cortical plate. • Disorganization or decreased numbers of the RG basal processes impairs radial migration.	(Hunter-Schaedle. 1997; Kriegstein and Gotz. 2003)
Expression of Guidance Cues	Extrinsic	• Many signals are expressed in the surrounding environment with permissive and directional roles in guiding migrating neuroblasts (see Table 2)	
Expression of Receptors for Guidance Cues	Intrinsic	• Neuroblasts must express appropriate transmembrane receptors and components of the cytoplasmic signal transduction pathways in order to respond to external signals (see Table 2).	

neuroblasts moving past the upper cortical layers. Time lapse imaging has shown that wild type neurons pause in layer IV entering the cell dense layer II/III and some radial migration phenotypes exhibit upper layer neurons able to enter the cortex, but being unable to enter these upper layers (Sekine, et al. 2011; Zhang, et al. 2015). Dab1, which mediates Reelin signaling (see below), has been shown to regulate migration through layer II/III, as deletion of Dab1 through *in utero* electroporation allows neurons to migrate to layer IV, but renders them unable to pass through these upper layers, which is sufficient to generate the inverted layer phenotype (Sekine, et al. 2011). Once neuroblasts have reached their appropriate location within the cortex, they continue to mature into functional neurons through axon extension and synaptogenesis.

Two well-known signals controlling migration are Reelin and Sema3a. Reelin is secreted by the CR cells located in layer I of the cortex and acts to allow immature neurons to pass through the intermediate zone and enter the correct cortical layer (Frotscher, et al. 2009; Honda, et al. 2011). Reelin binds the Apolipoprotein E (ApoE) or very low density lipoprotein receptor (VLDLR) on the neuroblast membrane (Hiesberger, et al. 1999; Jossin, et al. 2003; Bock, et al. 2004; Hippenmeyer. 2014). The importance of Reelin was discovered by examination of the reeler mouse, which is deficient in Reelin expression (Caviness. 1982). In this mouse, proliferation and preplate formation occur normally, but neuroblasts fail to migrate radially after cell cycle exit and accumulate under the subplate, where they displace previously born neurons dorsally (Caviness. 1982; Nadarajah and Parnavelas. 2002; Tissir and Goffinet. 2003; Hashimoto-Torii, et al. 2008a; Frotscher, et al. 2009; Honda, et al. 2011). This results in inverted cortical layers, with the oldest neurons at the top and the youngest neurons at the bottom. Many of the aspects of the Reelin-null phenotype, including failure to split the preplate and cortical layer disorganization, can be observed in slice cultures assays; growing these slice

cultures in the presence of Reelin was able to rescue these defects and restore normal development (Jossin, et al. 2004; Bock, et al. 2004). This shows that Reelin is a permissive cue rather than a directional cue, as Reelin protein was applied uniformly to the culture media and could not form a concentration gradient (Jossin, et al. 2004; Bock, et al. 2004). In addition, ectopic expression of Reelin in the VZ of the Reeler mice was able to partially rescue preplate splitting and cortical layer formation, even though neuroblasts were now moving away from the source of Reelin (Magdaleno, et al. 2002). Reelin has been shown to regulate radial migration through at least two mechanisms. First, Reelin-dependent phosphorylation and subsequent degradation of Dab1 is required for radial migration through cell intrinsic mechanisms. Knock-down of Dab1 though *in utero* electroporation of Dab1-RNAi caused GFP+ cells to be scattered throughout the cortical layers, rather than concentrated in layer II/III, as was seen in neurons electroporated with a control scramble RNAi (Sanada, et al. 2004; Olson, et al. 2006). In addition, Reelin is required for development of the radial glial processes, as Reelin-null mice exhibit a disorganized radial glial scaffold (Hunter-Schaedle. 1997).

While Reelin acts as a permissive cue (Polleux, et al. 1998; Chen, et al. 2008; Zhao, et al. 2011), Sema3a has been shown to act as a chemoattractant to guide neuroblasts up a concentration gradient toward the top of the cortex (Polleux, et al. 1998; Chen, et al. 2008; Zhao, et al. 2011). Sema 3a is expressed at highest levels in the marginal zone above the cortical plate and binds the Neuropilin1 (Npn1) receptor on the surface of the migrating neuroblasts (Polleux, et al. 1998; Zhao, et al. 2011). Sema3A was shown to attract migrating neuroblasts within organotypic slices, even when the source of the Sema 3A was placed in the "wrong" location, such as adjacent to the VZ (Polleux, et al. 1998; Zhao, et al. 2011). Furthermore, antibodies against Sema3A or Npn1 prevented migration in slice cultures (Chen, et al. 2008), and cell

autonomous knock-down of Npn1 or various members of Plexin family, which act as co-receptors (see section 3.2.3), caused GFP+ cells to be scattered throughout the cortex rather than located in layer II/III (Chen, et al. 2008). Sema3A-Npn1 signaling has been shown to be involved in orienting migrating neurons within the cortex, as deletion of Sema3A prevents neuroblasts from orienting their leading and trailing processes perpendicular to the cortical layers (Polleux, et al. 1998). Additional secreted cues involved in radial migration are listed in Table 1-2.

The many factors which influence radial migration can be categorized into cell autonomous factors, which are intrinsic to the migrating neuroblast, and non-cell autonomous factors, which originate in the surrounding environment, extrinsic to the neuroblast. Examples of cell autonomous factors include cell cycle exit (Tury, et al. 2011; Mairet-Coello, et al. 2012), neural differentiation (Methot, et al. 2013; Toyo-oka, et al. 2014), altered expression of transcription factor profiles and associated changes in gene regulation (Hevner, et al. 2001; Chen, et al. 2005; Alcamo, et al. 2008; Britanova, et al. 2008), regulation of cytoskeletal dynamics (Kawauchi, et al. 2003; Konno, et al. 2005; Pacary, et al. 2011; Hippenmeyer. 2014), and expression of transmembrane receptors to guidance cues (Hiesberger, et al. 1999; Bock, et al. 2004; Chen, et al. 2008; Senturk, et al. 2011; Zheng, et al. 2012; Zhang, et al. 2015; Jiang, et al. 2015). Non-cell autonomous factors include integrity of the radial glial scaffold (Hunter-Schaedle. 1997) and expression of secreted chemical signals (Jossin, et al. 2004; Chen, et al. 2008; Honda, et al. 2011; Hippenmeyer. 2014; Boitard, et al. 2015). Specific examples are summarized in Table 1-1. Failure of any of this multitude of requirements could result in migration defects, ranging from a complete failure of neurons to split the preplate and enter the cortical plate, resulting in inverted cortical layers as seen in the reeler mouse

Table 1-2: Selected Extrinsic Signaling Pathways Regulating Radial Migration.

Ligand/Receptor	Expression Pattern	Function	Citation
Reelin/ApoE/VLDLR/ Dab1	Reelin secreted by CR cells ApoE and VLDLR on migrating neuroblasts.	• Reelin is an essential permissive cue which instructs neuroblasts to split the preplate and migrate to the top of the cortex. • Dab1 necessary for passing through layer II/III.	(Hiesberger, et al. 1999; Bock, et al. 2004; Jossin, et al. 2004; Sekine, et al. 2011)
Sema3a/Npn1	Sema3a in marginal zone Npn1 on migrating neuroblasts	• Sema3a attracts migrating neuroblasts up a concentration gradient to the top of the cortical plate. • Orienting neuroblasts parallel to the radial glial scaffold by repelling the trailing process.	(Polleux, et al. 1998; Chen, et al. 2008)
Wnt – canonical pathway Wnt5A – non-canonical pathway	Neuroblasts responsive to canonical Wnt in VZ/SVZ, responsive to Wnt5A in IZ	• Decrease in canonical Wnt signaling necessary for multipolar to bipolar transition at the initiation of radial migration. This decrease in canonical Wnt mediated by an increase in Wnt5A signaling.	(Boitard, et al. 2015)
DSCAM	Throughout cortex	• Adhesion molecule hypothesized to function through isoform specific homophillic interactions, necessary for migration of upper layer neurons.	(Zhang, et al. 2015)
SPARC-like 1	Top of RG fibers	• Anti-adhesion function causes neuroblasts to detach from RG processes at the top of the cortical plate, terminating migration	(Gongidi, et al. 2004)
Robo4	Migrating neuroblasts	• Enhances motility by forming heterodimers with Robo1/2 and attenuating the repulsive effect of Slits.	(Zheng, et al. 2012)
Interleukin 1β/IL-1 Receptor 1	IL-1R1 found throughout developing cortex	• IL-1β attracts migrating neuroblasts in vitro shown through cell motility assay and in vivo through transfection of IL-1R1 siRNA.	(Ma, et al. 2014)
GluN2B	Migrating neuroblasts	• GluN2B is a subunit of the NMDA receptor expressed only during embryonic development. Knockdown of GluN2B causes cortical migration defects through unknown mechanisms.	(Jiang, et al. 2015)

(Caviness. 1982; Tissir and Goffinet. 2003; Honda, et al. 2011), to overlap and disorganization between the normally distinct cortical layers (Ferguson, et al. 2005; McClellan, et al. 2007). One of the primary goals of this thesis is to examine whether pocket proteins pRb and p107 regulate radial migration through cell autonomous or non-cell autonomous mechanisms (Chapter 2).

3 Axon Guidance Molecules and Mechanisms

3.1 Overview: The tremendous networks of neural connections present in the adult brain are initially formed through the mechanisms of axon guidance and axon extension during embryonic development. The importance of these processes is emphasized by the fact that many neurodevelopmental disorders including autism spectrum disorders, schizophrenia and cerebral palsy are characterized by developmental defects in white matter tract formation and axon connectivity (Paul, et al. 2007; He, et al. 2008; Isler, et al. 2010; Lo, et al. 2010; Anderson, et al. 2011; Catarino, et al. 2013; Paul, et al. 2014; Hahamy, et al. 2015). However, before it is possible to treat these disorders, it is necessary to develop a complete understanding of these mechanisms during normal development. While the signaling pathways and molecular mechanisms employed by many of the major axon guidance proteins have been analyzed, our understanding of the major regulators organizing the complex interplay of these proteins within the context of the developing brain remains incomplete. Indeed, the factors which control expression of these axon guidance proteins is essentially unknown. This section will provide a description of the relevant information necessary to appreciate the basic mechanisms of axon guidance and the challenges associated with creating the extensive neural networks present in the adult brain.

The process of wiring the brain and guiding axons toward their appropriate targets generates several unique challenges. First, the axons must often cover extremely long distances, often with complex trajectories including many turns and decision points. This is solved by dividing these long journeys into a series of small steps between intermediate targets (Shu and Richards. 2001; Rash and Richards. 2001a; Richards. 2002; Shu, et al. 2003c; Keeble, et al. 2006; Hatanaka, et al. 2009; Zhao, et al. 2011; Fothergill, et al. 2013). However, this strategy creates another dilemma; once an axon follows an attractive cue to an intermediate target, what can induce that axon to continue past that attractive cue and move on the next intermediate? This situation is especially relevant for commissural axons, such as callosal projection neurons (CPNs) of the CC, which must cross the midline of the central nervous system (CNS). The midline is an important intermediate target which expresses multiple attractive cues, yet axons must extend past these cues in order to reach their final target in the contralateral side of the nervous system. To solve this, the nervous system employs a large number of integrated attractive and repellant molecular signals (Shu, et al. 2000; Shu, et al. 2003a; Shu, et al. 2003c; Keeble, et al. 2006; Niquille, et al. 2009; Islam, et al. 2009; Piper, et al. 2009b; Unni, et al. 2012; Fothergill, et al. 2013). When used in combination, as is seen at the CC midline, these signals can enhance or attenuate each other to generate a complex language to guide axon tips. Furthermore, the expression of these axon guidance molecules on the growth cones changes as the axons cross the midline so that a signal which was attractive to a pre-crossing growth cone can become repulsive to a post-crossing growth cone (Fothergill, et al. 2013). This draws the pre-crossing axons into the midline, then pushes the post-crossing axons out the other side. The general principles of using 1) a series of intermediate targets and 2) combinations of interacting

molecular signals with temporally regulated patterns of expression can be used to understand the guidance of specific axon populations within an anatomical structure.

3.2 Guidance Molecules: Neurite tips express transmembrane receptors which bind to chemoattractant and chemorepulsive cues, which induce growth cone extension or collapse, respectively (Lowery and Van Vactor. 2009; O'Donnell, et al. 2009), and guide them through their complex environment to the appropriate destination (Figure 1-2). These receptors can bind diffusible cues which are secreted from a distant location, or bound cues which are attached to the extra cellular matrix or adjacent cells. The classic chemoattractant family in the CNS is the Netrins, which binds to DCC and Unc5 (Serafini, et al. 1996; O'Donnell, et al. 2009; Lowery and Van Vactor. 2009; Edwards, et al. 2014), while the classic chemorepellant families are the semaphorins (which bind the plexins and neuropilin 1) (Shimizu, et al. 2000; Kawasaki, et al. 2002; Gu, et al. 2003; de Wit and Verhaagen. 2003; Huber, et al. 2005; Piper, et al. 2009b; Zhao, et al. 2011), the ephrins (which bind Eph receptors) (Drescher. 2000; Hu, et al. 2003; Noren and Pasquale. 2004; Kadison, et al. 2006; Egea and Klein. 2007; Himanen, et al. 2007; Himanen, et al. 2010) and the Slits (which bind the Robos) (Shu, et al. 2003a; Shu, et al. 2003c; Lowery and Van Vactor. 2009; O'Donnell, et al. 2009; Unni, et al. 2012; Zheng, et al. 2012; Zelina, et al. 2014). In addition, several molecules previously identified as being involved in tissue patterning have recently been shown to also have important axon guidance function. These include Sonic Hedgehog (Shh) (which binds Boc and Patched), Wnt (which binds Frizzled) and Bone Morphogenic Protein (BMP) (which binds BMPR) (Yam and Charron. 2013; Sloan, et al. 2015). Cues from these receptors are transmitted to the cytoplasm through phosphorylation or conformational changes of the receptor, where they influence cytoskeletal dynamics

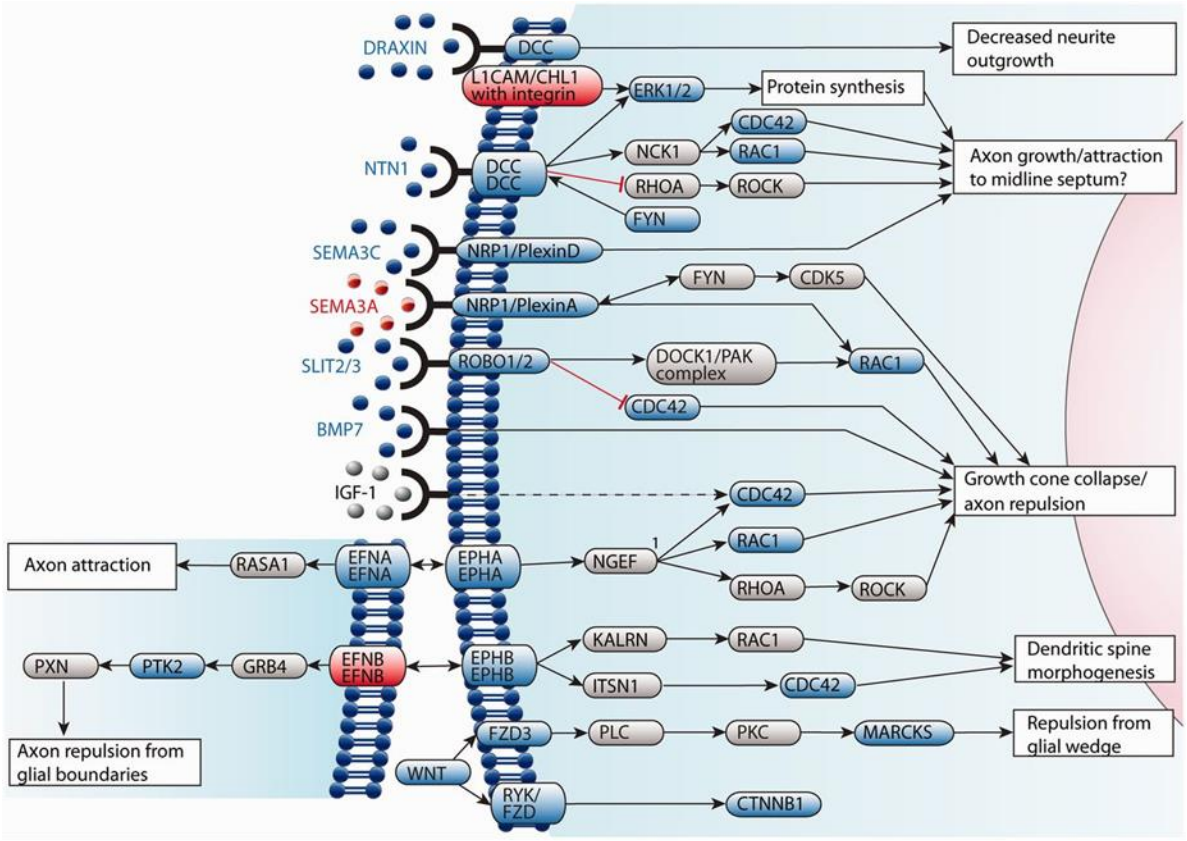

Figure 1-2

Figure 1-2: Major signaling pathways involved in guidance of callosal axons. Ligands are shown on the left, receptors are shown in the middle in the growth cone plasma membrane, and the cytoplasmic signaling pathways within the growth cone are shown on the right. When bound to their ligands, activated receptors influence cytoskeletal dynamics through GTPases such as RHOA, RAC1 and CDC42. In the case of the ephrins (EFNs), which bind the Eph receptors, both ligand and receptor are transmembrane proteins which can initiate downstream signaling and axon guidance. Growth cones express both ephrin and Eph family members so downstream signaling within the growth cone is shown on the left and right sides of the figure.

From Edwards et al., 2014, *Brain*

(Geraldo and Gordon-Weeks. 2009; Kaplan, et al. 2014). The major signaling pathways involved in axon guidance of callosal axons are summarized in Figure 1-2, and the secreted and adhesive axon guidance molecules involved in CC development are described in Tables 1-3 and 1-4, respectively. The current understanding of these molecules in commissural axon guidance is based predominantly on studies performed in vitro and in the spinal cord, so it remains largely unknown whether they function through the same mechanisms during CC development. The known roles of several key pathways in CC development in vivo are discussed in the following sections.

3.2.1 Netrin/DCC: Netrin is a diffusible molecule which binds dimers of the transmembrane receptors Deleted in Colorectal Cancer (DCC) and Uncoordinated 5 (Unc5) (Kennedy, et al. 1994; Serafini, et al. 1996; Kennedy, et al. 2006; O'Donnell, et al. 2009; Lowery and Van Vactor. 2009; Edwards, et al. 2014). When Netrin binds a DCC homodimer, it leads to stabilization and extension of the actin cytoskeleton and causes the growth cone to turn toward the source of Netrin secretion (Kennedy, et al. 1994; Shu, et al. 2000; Kennedy, et al. 2006). Conversely, when Netrin binds the DCC/Unc5 heterodimer, this activates different downstream signaling pathways and the growth cone collapses and retracts (Picard, et al. 2009; Antoine-Bertrand, et al. 2011; Purohit, et al. 2012; DeGeer, et al. 2013). The function of Netrin/DCC signaling is best understood in the developing spinal cord, where Netrin is secreted from the floorplate and attracts commissural axons (whose cell bodies are located in the dorsal half of the neural tube) to turn medially and cross the midline as part of the ventral commissure (Serafini, et al. 1996; Fazeli, et al. 1997; Sloan, et al. 2015). In the absence of Netrin, commissural axons have been shown to turn laterally as they descend and fail to cross the midline at the floorplate, which prevents formation of the ventral commissure (Serafini, et al. 1996; Fazeli, et al. 1997).

Table 1-3: Select Axon Guidance Molecule Families Important in CC development – Secreted Signals

Ligand	Receptor	Repulsion/ Attraction	Receptor Expression	Ligand Expression	Function	Sources
Netrin	DCC	Attraction	CPN axons and IG neurons	Septum, IG glia	• Attracts pioneering axons at midline. • Silences Slit2/Robo1 mediated repulsion in post-crossing CPN axons.	(Fothergill, et al. 2013)
Slit2	Robo1	Repulsion	CPN axons and IG neurons	GW, Ig glia	• Turns pre-crossing axons medially across corticoseptal boundary and pushes post-crossing axons out the midline.	(Shu, et al. 2003c)
Sema3a	Npn1	Repulsion	CPN axons, esp. pioneering axons, IZ	Marginal zone, lateral cortex	• Orients migrating neuroblasts within the cortex • Induces extension of the trailing process away from the cortex. • Instructs axons to turn medially at the IZ	(Polleux, et al. 1998; Hatanaka, et al. 2009; Zhao, et al. 2011)
Sema3c	Npn1	Attraction	CPN axons, esp. pioneering axons, IZ	Sling neurons, CR+ neurons within the CC	• Attracts axons towards the midline • Segregates axons from pioneering and cingulate cortexes.	(Niquille, et al. 2009)
Wnt5a	Ryk	Repulsion	CPN axons	GW, IG glia	• Turns post-crossing axons dorsally and pushes them away from the midline	(Keeble, et al. 2006)
Draxin	Lrp6	Repulsion	CPN axons	CPN axons, GW IG glia	• Repels neurite outgrowth. • Draxin knockout mouse is acallosal due to incomplete septal fusion	(Islam, et al. 2009)
Shh	Patched, Boc	Receptor Specific	Commissural spinal axons, RG axons	Floorplate, optic chiasm	• Shh attracts spinal commissural axons to the floor plate, then repels axons from floor plate post-crossing following Boc downregulation. • Not investigated in CC.	(Okada, et al. 2006; Yam and Charron. 2013; Sloan, et al. 2015)
BMP7	BMPR1B	Repulsion	Commissural spinal axons	Roofplate	• BMP7 repels spinal commissural axons from the roofplate in the spinal cord. Not investigated in CC.	(Sanchez-Camacho, et al. 2011)

Table 1-4: Select Axon Guidance Molecule Families Important in CC development – Adhesive Signals

Ligand	Repulsion/ Attraction	Expression	Function	Sources
Npn1	Attraction	CPN axons, IZ	• Promotes CPN axon fasciculation and prevents re-entry into ipsilateral cortex	(Hatanaka, et al. 2009)
PSA-NCAM	Attraction	Cortical axons	• Promotes fasciculation in vitro, specifically expressed on axon in vivo	(Wakade, et al. 2013)
L1	Attraction	Cortical axons	• Promotes fasciculation in vitro, specifically expressed on CPN axon in vivo	(Wolman, et al. 2007)
DSCAM	Attraction	Cortical axons	• Promotes growth of CPN axons, as DSCAM knockdown cell autonomously impaired axon extension through the IZ	(Zhang, et al. 2015)
EphB2/ephrinB1	Repulsion	EphB2: GW, Ig glia ephrinB2: CPN axons	• Turns pre-crossing axons medially across corticoseptal boundary and pushes post-crossing axons out the midline	(Palmer, et al. 2002; Zimmer, et al. 2003)
EphA5/ephrinA5	Attraction	EphA5: CPN axons	• EphA5 deletion leads to CPN axon crossing defect • ephrinA5 attracts neurites in vitro	(Hu, et al. 2003)
EphA4/ephrinB	Repulsion	EphA4: Regions surrounding commissures ephrinB: Commissural axons	• EphA4 deletion leads to guidance defects in forebrain commissures, primarily the anterior commissure	(Ho, et al. 2009)

3.2.1.1 Netrin in the CC: In the CC, Netrin plays a similar, although more complex and less well characterized role. Netrin is expressed by indusium griseum (IG) glial cells (see section 3.3.3.2) at the junction between the cingulate cortex and the septum (called the corticoseptal boundary) (Serafini, et al. 1996; Fothergill, et al. 2013) and is required for callosal axon crossing. Deletion of Netrin (Serafini, et al. 1996; Fothergill, et al. 2013) or DCC (Fazeli, et al. 1997; Shu, et al. 2000) in the brain prevents CC formation. However, pioneering axons from the cingulate cortex, which cross the midline first (see section 3.4.2), and neocortical axons from the lateral cortex, which cross the midline later, have been shown to process the Netrin signal differently. *In vitro*, Netrin has been shown to elicit an attractive response to neurites from cingulate cortex explants but not from lateral cortex explants (Fothergill, et al. 2013), which implies that Netrin/DCC signaling is attractive only to pioneering axons. However, Netrin-deficient neurites from the lateral cortex exhibit a much greater sensitivity to Slit2/Robo mediated repulsion due to an interaction between the DCC and Robo receptors which attenuates the Slit2/Robo signal (Fothergill, et al. 2013). This was interpreted as a mechanism to allow these lateral pre-crossing axons to overcome the repulsion of Slit2 (see following section) and approach the midline. DCC was shown to be downregulated once the axons reached the contralateral side, which seems to unmask the Slit2/Robo signal and encourage callosal axons to leave the midline and continue toward their final target (Fothergill, et al. 2013). Indeed, Netrin has been shown to have similar interactions with Slit and other signaling pathways in other systems (Kim, et al. 2014a; Sloan, et al. 2015). Thus far, differential regulation of DCC is the only mechanism described in the CC for changing cue sensitivity in pre-crossing and post-crossing axons at the midline (Fothergill, et al. 2013). The dual function of Netrin in pioneering axons and lateral axons illustrates that Netrin is crucial attractive and permissive signal in CC formation.

3.2.2 Slit/Robo: The Slit family of diffusible molecules contains three members, Slit1-3, while the Robo family has four members, Robo1-4 (Shu, et al. 2003a; Shu, et al. 2003c; Lowery and Van Vactor. 2009; O'Donnell, et al. 2009; Unni, et al. 2012; Zheng, et al. 2012; Zelina, et al. 2014). Robo1 and Robo2 are functionally similar in cortical neurons while Robo3 has very different function in axon guidance and has been shown to bind Netrin (Zelina, et al. 2014). Slit/Robo interactions are repulsive and lead to destabilization of the actin cytoskeleton. In the CC, Slit2 is expressed by the glial wedge (GW) and IG (Shu and Richards. 2001; Unni, et al. 2012), two support structures which form the outer boundaries of the corridor through which callosal axons traverse the midline (see section 3.3.3 for greater detail). Slit1 is expressed by the IG and the sling neurons located below the CC and the Robo1/2 receptors are expressed on growth cones (Shu and Richards. 2001; Unni, et al. 2012). Slit mediated repulsion is required to guide axons across the corticoseptal boundary as the Slit1/2 and Slit 1/3 double knock out mice fail to form a CC (Unni, et al. 2012). Furthermore, after dissecting out the GW from slice cultures and returning it in the opposite medial-lateral orientation, axons were induced to turn laterally, away from the midline, rather than medially, toward the midline (Shu and Richards. 2001), which further shows that Slit/Robo signaling is crucial to guiding callosal axons across the corticoseptal boundary.

3.2.3 Sema3/Npn1/PlexinA: Semaphorins (Semas) constitute a huge class of diffusible molecules which bind to the Plexin receptors (Shimizu, et al. 2000; Kawasaki, et al. 2002; Gu, et al. 2003; de Wit and Verhaagen. 2003; Huber, et al. 2005; Piper, et al. 2009b; Zhao, et al. 2011). Semas are subcategorized as Sema3 to Sema7, and each subcategory has multiple members. Likewise, the Plexins are divided into PlexinA and PlexinB subfamilies. Each Sema protein interacts with a specific subset of Plexin proteins, meaning that this huge group of proteins can

generate a vast number of specific interactions which are used by different cell types at different developmental stages (de Wit and Verhaagen. 2003). The Sema3 subfamily in particular is highly relevant to cortical development (Polleux, et al. 1998; Wolman, et al. 2007; Chen, et al. 2008; Piper, et al. 2009b; Zhao, et al. 2011) and the role of Sema3 as an attractive cue in radial migration was discussed in section 2.4 and Table 1-2. Sema3 proteins bind a receptor heterodimer composed of PlexinA1 and Neuropilin1 (Npn1) on axon growth cones (Polleux, et al. 1998; de Wit and Verhaagen. 2003; Hatanaka, et al. 2009; Piper, et al. 2009b; Zhao, et al. 2011). In CC formation, Sema3a functions as a repulsive signal through Npn1 to induce axons to leave the cortex and turn toward the midline (Piper, et al. 2009b; Zhao, et al. 2011). Sema3a is expressed at very high levels in the lateral portion of the cortex, and in the absence of Sema3a axons turn medially or laterally randomly upon reaching the IZ, such that descending axons are equally likely to turn away from the midline as toward it (Zhao, et al. 2011). Sema3a is also important at the midline as Sema3a knockout mice exhibit a thinning of the dorsal portion of the CC, which is composed of the axons from the cingulate cortex which express the highest levels of Npn1 (Piper, et al. 2009b).

Sema3c functions as an attractive signal, also through the Npn1 receptor, and is expressed by the subcallosal sling neurons at the midline (Niquille, et al. 2009; Piper, et al. 2009b). The importance of Sema3c in drawing axons toward the midline is illustrated by the observation that deletion of Sema3c prevents axons crossing (Niquille, et al. 2009). Furthermore, explants of Sema3c expressing HEK cells placed at ectopic locations within slice cultures has been shown to attract callosal axons into the septum, which they would not normally enter (Niquille, et al. 2009). Together with Netrin, Sema3C functions as an attractive signal to callosal axons and is necessary to CC development.

3.3 Corpus Callosum Development I - Establishing the Anatomy: The CC is the largest axon tract in both the murine and human brains. It connects the right and left hemispheres of the neocortex and allows more advanced information processing by enabling communication between the two sides of the brain (Demopoulos, et al. 2014; Kim, et al. 2014b). 1 in 4000 children are born with agenesis of the corpus callosum (ACC), and most neurodevelopmental disorders include callosal defects (Paul, et al. 2007; Collinson, et al. 2014; Demopoulos, et al. 2014; Kim, et al. 2014b). Children with ACC experience a wide range of symptoms, including mild to severe developmental delays, ASD and ADHD-like syndromes, defects in sensory processing, and cerebral palsy (Paul, et al. 2003; Paul, et al. 2004; Brown, et al. 2005; Paul, et al. 2007; Szabo, et al. 2011; Fairchild, et al. 2011; Paul, et al. 2014; Edwards, et al. 2014; Bridgman, et al. 2014; Demopoulos, et al. 2014). However, the causes of ACC are unknown. In order to understand the causes of ACC, it is crucial to understand the fundamental mechanisms that control the growth and guidance of callosal axons during normal development. This section will examine the early phases of CC development including formation of the support structures which express critical axon guidance cues, as well as mechanisms used by the pioneering axons.

3.3.1 Hemisphere Fusion: Formation of the CC begins with fusion of the two hemispheres and establishment of the callosal plate (Figure 1-3A). As the general patterning of the telencephalon proceeds (reviewed in (Borello and Pierani. 2010)), dorsal and ventral brain structures emerge. In particular, the establishment of the dorsally defined cingulate cortex and ventrally defined septum are crucial to commissural plate formation. Dorso-ventral patterning is controlled by a complex interplay of signaling pathways downstream of the morphogens Shh in the pre-optic

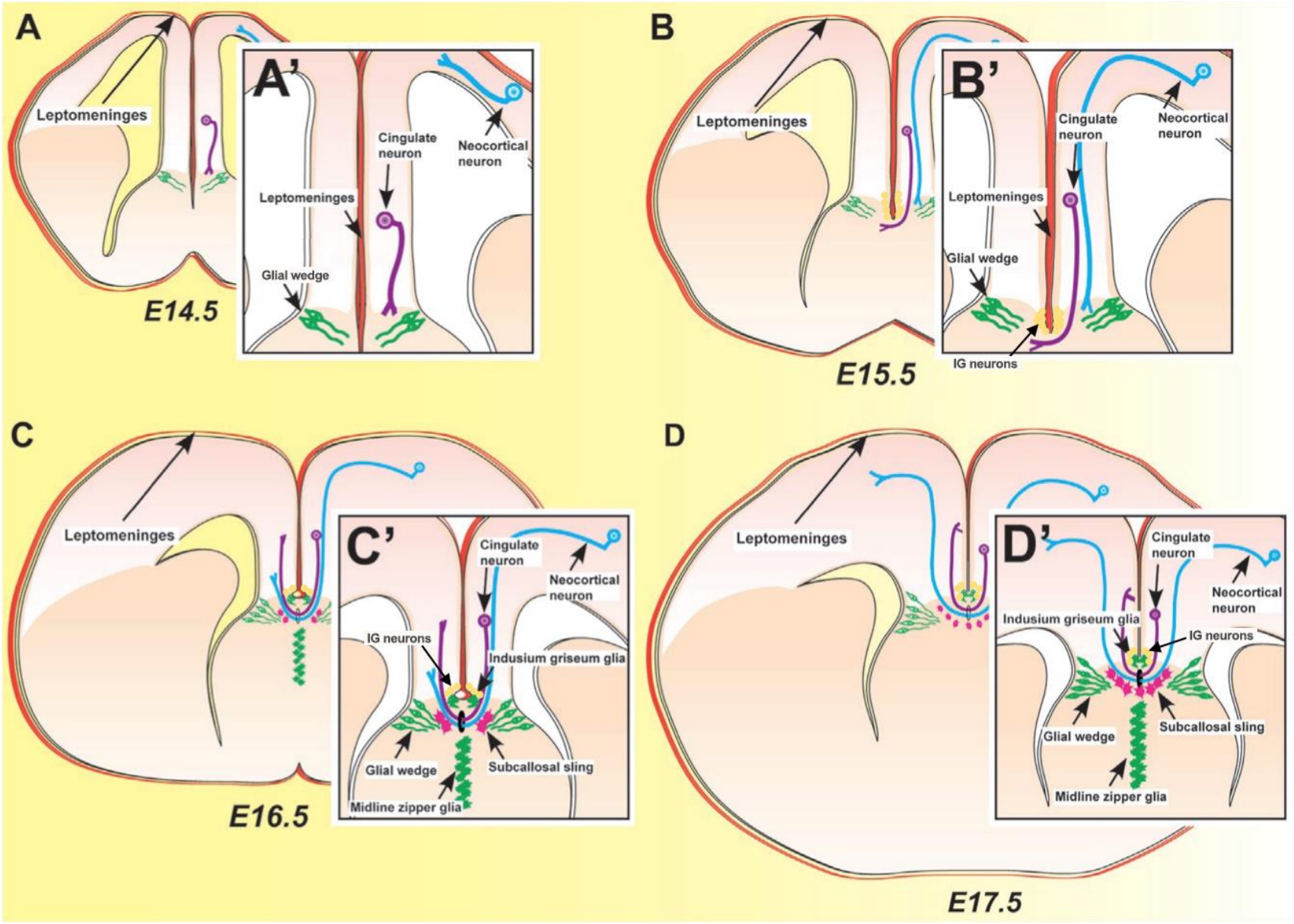
A
Leptomeninges
E14.5
A'
Leptomeninges
Glial wedge
Cingulate neuron
Neocortical neuron
B
Leptomeninges
E15.5
B'
Leptomeninges
Glial wedge
IG neurons
Cingulate neuron
Neocortical neuron
C
Leptomeninges
E16.5
C'
IG neurons
Glial wedge
Midline zipper glia
Cingulate neuron
Neocortical neuron
Indusium griseum glia
Subcallosal sling
D
Leptomeninges
E17.5
D'
Indusium griseum glia
Glial wedge
Midline zipper glia
Cingulate neuron
Neocortical neuron
IG neurons
Subcallosal sling

Figure 1-3

Figure 1-3: Development of the commissural plate and corpus callosum in the embryonic mouse brain. (A) Commissural plate formation begins with septal fusion from E13-E15. Complete septal fusion up to the corticoseptal boundary is necessary to provide a substrate for axons. Pioneering axons from the cingulate cortex and lateral axons from the neocortex initiate growth toward the midline around E14.5, while fusion is being completed. The glial wedge (GW) also starts to form at this stage. **(B)** The first pioneering axons from the cingulate cortex reach the midline at E15.5 and initiate crossing under the guidance of the GW, indusium griseum (IG) neurons (shown in yellow) and GABAergic interneurons (not shown). Axons from the lateral neocortex reach the corticoseptal boundary after the pioneer axons have already crossed. At this age, axons have already made the decision to extend out of the cortex, turn toward the midline and extend tangentially through the intermediate zone, under the guidance of Sema3a/Npn1 signaling. **(C)** Starting at E16.5, neocortical axons follow the scaffold established by the pioneering axons across the midline. They are guided by the GW, IG glia (shown in green), IG neurons, subcallosal sling neurons and GABAergic interneurons. Subcallosal sling neurons are in the process of migrating medially from the adjacent ventricle zones and will continue to form a complete sling under the axons, as well as within the CC between the cingulate and neocortical axonal compartments, until birth. Axons from the cingulate cortex have reached the contralateral hemisphere and are starting to find their targets. **(D)** Between E17.5 and P0, the majority of neocortical axons cross the midline and form the ventral compartment of the CC. During this stage, axons travel through the contralateral IZ to find their targets in the homotopic region of the cortex, where they undergo extensive axonal sprouting and pruning and eventually establish synaptic connections and functional circuits.

Modified from Gobius and Richards, *Colloquium Series in the Developing Brain*, 2011.

area (which confers ventral identity) (Chiang, et al. 1996; Yu, et al. 2009), Fgf8 in the anterior neural ridge (which becomes the commissural plate) (Crossley, et al. 2001; Fukuchi-Shimogori and Grove. 2001; Shimogori, et al. 2004; Okada, et al. 2008; Moldrich, et al. 2010) and Wnt/BMP in the cortical hem (which confers dorsal identity) (Shimogori, et al. 2004). Fgf8 is specifically expressed at the isthmus, which becomes the substrate on which the callosal axons eventually cross (Okada, et al. 2008; Moldrich, et al. 2010), and Fgf8 deletion leads to callosal agenesis in mice, as well as defects in dorsal/ventral patterning (Okada, et al. 2008; Moldrich, et al. 2010). Conversely, ectopic expression of Fgf8 has been shown to induce formation of an ectopic isthmus in the developing chick telencephalon (Crossley, et al. 2001), which illustrates that Fgf8 is crucial to establishing midline identity.

At E13.5 in the mouse, the two telencephalic vesicles are aligned along their medial edges and covered in a layer of meningeal fibroblasts known as the leptomeninges (McLone and Bondareff. 1975; Couly and Le Douarin. 1987; Siegenthaler and Pleasure. 2011). At E14.5, the two halves of the septum fuse into a single structure, starting at the ventro-caudal aspect and proceeding dorso-rostrally (Silver, et al. 1993). Although factors controlling this process are not well known, fusion is thought to be dependent on the midline zipper glia located between the septal halves, as well as on the glia of IG, located at the junction between the cingulate cortex and septum (Silver, et al. 1993). The requirement of complete midline fusion is exemplified by mice mutant for Nfia (Shu, et al. 2003a), Nfib (Piper, et al. 2009a), DCC (Fazeli, et al. 1997; Shu, et al. 2000), or Draxin (Islam, et al. 2009), which lack the midline glia and exhibit a small cleft between the dorsal portion of the two halves of the septum. When these glial population are absent, callosal axons fail to cross but instead swirl in complex Probst bundles adjacent to the midline. Fusion is also known to be dependent on expression of BMP7 by the meningeal

fibroblasts, as loss of BMP7 leads to loss of the midline glial cells and increased BMP7 induces premature differentiation of glial cells; both situations prevent proper midline fusion and lead to callosal agenesis (Sanchez-Camacho, et al. 2011).

3.3.2 Callosal Projection Neuron Specification: As described above, the cortex develops in an inside-out manner with early born neurons forming the deep cortical layers and later born neurons migrating through these layers to form the upper cortical layers. Neurons within a layer have a molecular identity shared with other neurons born at the same developmental age (Figure 1-1, bottom), and although there is still a large and often underestimated amount of diversity within pyramidal neuron populations, neurons within a given layer share the most molecular, anatomical and functional similarity, with greater differences being seen in comparisons between layers (Mitchell and Macklis. 2005; Molyneaux, et al. 2009; Fame, et al. 2011). These similarities are visible in terms of layer specific molecular markers as well as in examining the targets of the axonal projections, with neurons within a layer having a tendency to project to very similar targets (Mitchell and Macklis. 2005; Britanova, et al. 2008; Alcamo, et al. 2008; Molyneaux, et al. 2009; Fame, et al. 2011).

Cortical neurons are categorized by the target to which they project. Corticofugal neurons (CFNs) project to the striatum, basal ganglia, thalamus or spinal cord, callosal projection neurons (CPNs) project to the cortex of the opposite hemisphere, and ipsilateral circuit projection neurons project to distant regions of the cortex within their own hemisphere (Mitchell and Macklis. 2005; Chen, et al. 2005; Alcamo, et al. 2008; Britanova, et al. 2008; Fame, et al. 2011). A subpopulation of CPNs are born early and reside in layer V, while the majority of the CPNs are late born neurons located in layer II/III (Angevine and Sidman. 1961; Ozaki and Wahlsten. 1998; Rash and Richards. 2001b; Mitchell and Macklis. 2005; Alcamo, et al. 2008; Britanova, et

al. 2008). These two groups of CPNs have distinct functions and targets (Ozaki and Wahlsten. 1998; Rash and Richards. 2001b; Mitchell and Macklis. 2005; Petreanu, et al. 2007) and respond differently to axon guidance molecules in the IZ and at the midline (see example of Netrin responsiveness in section 3.2.1 (Fothergill, et al. 2013)). A primary difference is that the layer V CPNs of the cingulate cortex act as pioneering axons which are the first to cross the midline at the corticoseptal boundary and act as a scaffold for axons from the later born layer II/III CPN axons (Koester and O'Leary. 1994; Ozaki and Wahlsten. 1998; Rash and Richards. 2001b; Mitchell and Macklis. 2005).

Establishment of the CPN identity is thought to begin soon after exiting the cell cycle and to depend on the expression of a combination of crucial transcription factors including Cux1/2 (Nieto, et al. 2004) and Satb2 (Alcamo, et al. 2008; Britanova, et al. 2008). As was discussed during section 2.1 on neurogenesis, neurons in different layers express a unique combination of transcription factors, which instruct their identity and influence their mature function (Hevner, et al. 2001; Chen, et al. 2005; Alcamo, et al. 2008; Britanova, et al. 2008). Satb2 especially has been found to have a direct importance on CPN development and axon pathfinding. Satb2 is expressed specifically in CPN neurons and in Satb2 knockout embryos, upper layer neurons incorrectly adopt the identity of CFN neurons and express Ctip2 and Fez2 and extend axons toward the internal capsule (Alcamo, et al. 2008). In addition, Satb2 regulates expression of a broad range of transcription factors and axon guidance proteins involved in development and function of CPNs (Alcamo, et al. 2008; Britanova, et al. 2008). This establishment of the CPN molecular identity is a crucial first step which enables these neurons to send out axons which can navigate the complex system of guidance cues at the commissural plate and find their targets in the contralateral hemisphere.

3.3.3 Midline Guidance Structures: At the same time that early CPNs are being generated, several transient developmental structures are formed at the corticoseptal boundary (Figure 1-3). These structures include the glial wedge (GW), the indusium griseum (IG), the guidepost/sling neurons and GABAergic interneurons. Together, these structures will guide the CPN axons across the midline to the contralateral hemisphere. In order to appreciate the role of these structures in CC development, it is necessary to understand the development of each individual structure in turn.

3.3.3.1 The Glial Wedge: The radial glia of the GW are the first RGs in the developing brain to express detectable levels of GFAP as early as E13.5-E14.5 (Shu and Richards. 2001; Shu, et al. 2003c). The GW develops from the RGs located at the portion of the ventricle closest to the corticoseptal boundary. The medial endfoot of these cells detaches from the pial surface as the cortical plate thickens and the cells extend toward the midline along the lamina terminalis in a distinctive triangle shape (Figure 1-3 panels C and D) (Shu and Richards. 2001; Shu, et al. 2003c; Smith, et al. 2006). The first GW cells are born at E13.5 with the majority becoming post-mitotic at E14.5-E16.5, and these cells maintain their RG identity as they continue to express Nestin and RC2 as well as GFAP and BLBP (Shu, et al. 2003c). The GW functions by expressing repulsive cues which turn the descending callosal axons towards the midline and thus prevent them from extending straight downward and entering the septum (See Figure 1-3, panel B' at E15.5). The turn is completely dependent on the GW, since removal of the GW in slice cultures causes axons to continue straight past the corticoseptal boundary into the septum; if the GW is replaced in the opposite medial-lateral orientation, descending axons incorrectly turn laterally, away from the midline (Shu and Richards. 2001). The most well-known of these repulsive signals is the secreted molecule Slit2, which binds the Robo1/2 receptors on the axon

growth cones (Shu and Richards. 2001; Edwards, et al. 2014). GW cells also express Wnt5a which bind to the Ryk receptor on post-crossing axons leaving the corticoseptal boundary and causes them to turn dorsally and proceed through the IZ (Keeble and Cooper. 2006; Keeble, et al. 2006). In the absence of Wnt5a, axons are able to cross the midline normally, but rather than turning dorsally when they reach the contralateral GW, the axons stall and are unable to continue (Keeble, et al. 2006).

The size of the GW is important to CC formation as both an increase and decrease in the size of the GW can interfere with axon crossing. Deletion of Nf2 (Lavado, et al. 2014) and supplementation with BMP7 (Sanchez-Camacho, et al. 2011) have both been shown to increase the length and number of glial processes, so that GW processes maintain their connection with the pial surface and upregulate Slit2 expression. These effects combine to make an insurmountable barrier for the descending axons and prevent midline crossing. On the contrary, deletion of Slit2 (Shu and Richards. 2001; Unni, et al. 2012), Draxin (Islam, et al. 2009), Nfia (Shu, et al. 2003a; Piper, et al. 2009a), or Lhx2 (Chinn, et al. 2014) result in a decrease in GW cell number and process length, which removes the signal to turn and allows axons to continue into the septum. Mutation of Lhx2 is especially informative as this disrupts the GW but not the IG (see below), which confirms the specific requirement of the GW for axon turning (Chinn, et al. 2014). Proper location of the GW is also necessary as defects in Gli3 dependent midline patterning lead to disorganization of the glial populations and callosal agenesis (Magnani, et al. 2012a).

3.3.3.2 The Indusium Griseum: The indusium griseum (IG) is located at the corticoseptal boundary just underneath the pial membrane of the dorsomedial pallium, directly above the CC (Figure 1-3 panels B-D) (Shu and Richards. 2001; Shu, et al. 2003a; Shu, et al. 2003c). The IG

contains both neurons and glial cells (Di Ieva, et al. 2015), which can be marked with Calbindin (CB) or GFAP, respectively. Although much less is known about the development and function of the IG compared to the GW, the IG glia are known to be crucial to CC formation since loss of these cells in multiple knockout mouse models (Nfia/b, DCC, Draxin) causes an accollosal phenotype (Shu, et al. 2000; Shu, et al. 2003a; Islam, et al. 2009; Piper, et al. 2009a). Unfortunately, because most of the genetic deletions which lead to defects in the IG glia also lead to defects in the GW, the specific function of these cells is not known. Even more enigmatic, the IG neurons have a presumed axon guidance function due to their location and expression of multiple axon guidance cues including DCC and Robo1 (Shu, et al. 2000), yet the true importance and function of these cells in CC formation remains unknown.

The IG glia are derived from the RGs of the GW (Figure 1-3 panels C and D) (Shu, et al. 2003c). Between E14.5 and E15.5, these cells exit the cell cycle and translocate to the medial pallium by detaching their ventricular endfoot and shortening the processes between the cell body and pial surface (Shu, et al. 2003c; Smith, et al. 2006). IG glial cells differ from GW glial cells in that they adopt a more astroglial identity and upregulate GFAP much later, starting at E16.5-E17 (Shu, et al. 2003c). IG glial precursor translocation is dependent on Fgf8/FgfR1 signaling and is reminiscent of the RG translocation and astrogliosis that occurs throughout the cortex at the end of neurogenesis (Smith, et al. 2006). Once at the pial surface, the IG cells express multiple axon guidance cues including Netrin and Slit2 (Shu and Richards. 2001; Fothergill, et al. 2013), where they form the dorsal boundary of the CC. These cells are therefore necessary to the crucial balance between Netrin-mediated attraction and Slit2-mediated repulsion which allows CPN axons to cross the corticoseptal boundary (see section 3.2.1).

3.3.3.3 Guidepost/Sling Neurons: Sling neurons, also known as guidepost cells, are a thin band of glutamatergic neurons located just below the CC. These neurons were originally misidentified as glial cells and are referred to as the glial sling in older publications (Figure 1-3 panels C and D) (Shu, et al. 2003b). Sling neurons originate in the SVZ in the region of the GW, at the level of the corticoseptal boundary (Shu, et al. 2003b). Birthdating experiments show that the first of these neurons become post-mitotic at E15.5 and migrate tangentially towards the midline where they form a continuous band of cells underneath the immature CC (Shu, et al. 2003b). A second, smaller band of sling neurons is found in the middle of the CC and separates the dorsal axons of the cingulate cortex from the ventral axons of the lateral cortex (Shu, et al. 2003b; Niquille, et al. 2009). Similar to IG neurons, sling neurons express multiple axon guidance receptors, including DCC and Robo1/2 (Shu, et al. 2003b), as well as secreting Sema 3c (section 3.2.3 (Niquille, et al. 2009)). Sema3c has been shown to be an important attractive cue to callosal axons from the cingulate cortex (Fothergill, et al. 2013), which express the receptor Npn1, and ablation of Sema3c from sling neurons prevents axon crossing (Niquille, et al. 2009). Sema3c is one of only two attractive cues yet identified at the corticoseptal boundary (Niquille, et al. 2009; Fothergill, et al. 2013).

3.3.3.4 GABAergic Interneurons: A fourth population of CC support cells are the GABAergic interneurons dispersed throughout the CC (not shown in Figure 1-3) (Niquille, et al. 2009; Niquille, et al. 2013). These cells migrate tangentially from the medial (MGE) and caudal ganglionic eminences into the CC starting at E14.5 and reach maximal population density within the CC at E18.5 (Niquille, et al. 2013). After this, they decrease in number and are no longer present by P14 (Niquille, et al. 2013). These cells are attractive to callosal axons, as explants from the MGE are able to attract axons within slice cultures (Niquille, et al. 2013). This function

was suggested to be due to the expression of multiple axon guidance molecules, including Sema 3A, Npn2 and number ephrins and Eph receptors, as well as adhesion molecules such as L1 and N-cadherin (Niquille, et al. 2013).

3.4 Corpus Callosum Development II - From One Hemisphere to the Other: Once the morphology of the cortical plate and the support structures around the corticoseptal boundary are established, CPN growth cones must undertake a long and complex journey in order to reach the contralateral hemisphere. Due to the curvature of the mammalian cortex, axons must make several distinct turns before and after they cross the commissural plate (Figure 1-3). In this section, each stage of the journey will be examined in normal development. It should be noted that although the physical path of these axons has been described, the molecular mechanisms and interactions between competing signals remain incompletely understood. Furthermore, the mechanisms controlling the expression and establishment of these signals are completely unknown. As one of the primary goals of this dissertation is to examine how these processes are disrupted in the absence of pocket proteins (Chapter 4), this review is designed to provide a framework to appreciate these defects.

3.4.1 Importance of the Cingulate Cortex: The first axons to cross the corticoseptal boundary are the pioneering axons from layer V CPNs of the cingulate cortex (Figure 1-3) (Koester and O'Leary. 1994; Ozaki and Wahlsten. 1998; Rash and Richards. 2001b; Piper, et al. 2009b). The cingulate cortex is a specialized region of the cortex which contributes to the limbic system, similar to the entorhinal cortex and hippocampus (Koester and O'Leary. 1994; Ozaki and Wahlsten. 1998; Rash and Richards. 2001b; Piper, et al. 2009b). Also similar to the entorhinal cortex, the cingulate cortex has 3-5 layers, classifying it as an allocortex, rather than the full 6

layers seen in the more lateral neocortex (Koester and O'Leary. 1994). The junction between the cingulate and lateral cortexes occurs at the dorsal flexion, where the cingulate cortex invaginates inward (Yoshida, et al. 1997; Piper, et al. 2009b). Development of the cingulate cortex is dependent on expression of Emx2, which is expressed specifically in the medial portion of the developing neural tube (E9.5) and early telencephalon (E12.5) (Yoshida, et al. 1997). In the absence of Emx2, the roof plate is expanded and the cingulate cortex is greatly reduced (Yoshida, et al. 1997). In Emx2 deficient embryos, pioneering axons are absent and axons from the neocortex form Probst bundles rather than cross in the midline in the rostral portion of the corpus callosum (Piper, et al. 2009b). These results emphasize the crucial importance of pioneering axons from the cingulate cortex in the formation of the CC.

3.4.2 Pioneering Axons: Growth cones of pioneering axons from the cingulate cortex rely on several identified signaling pathways to traverse the corticoseptal boundary, the most important of which have already been discussed in detail in section 3.2 and will only be alluded to here. The path of a pioneering axon can be described as a series of steps:

1) The axon must leave the cingulate cortex and enter the IZ. The molecular signals behind this have only been studied in the lateral cortex and will be discussed in detail in section 3.4.3.1.

2) The axon must turn either dorsally or ventrally. The majority of pioneering axons turn ventrally toward the commissural plate (Figure 1-3 panel A), although a subset in fact turn laterally and travel through the IZ all the way to the lateral cortex (Ozaki and Wahlsten. 1998; Rash and Richards. 2001b). These axons are thought to function as an adhesive scaffold to guide axons from the lateral cortex (Rash and Richards. 2001b).

3) Pioneering axons then reach the corticoseptal boundary, where they encounter a complex interplay of repulsive and attractive signals, the receptors of which are expressed on the axon growth cones (Shu, et al. 2000; Shu and Richards. 2001; O'Donnell, et al. 2009; Piper, et al. 2009b; Unni, et al. 2012; Fothergill, et al. 2013). This review will focus on the molecules which will be tested in Chapter 4. Robo1 receptors bind to Slit2 secreted from the GW and IG glia (Shu and Richards. 2001) and DCC binds Netrin from IG glia (Fothergill, et al. 2013). As the axons extend down the IZ toward the midline, repulsion from the Slit2 causes them to turn medially and prevents them from entering the septum (Shu and Richards. 2001). After they have crossed, the Slit2 and Wnt5a from the contralateral GW similarly causes the growth cones to turn dorsally and continue to follow the IZ toward their destination (Shu and Richards. 2001; Keeble, et al. 2006). Although Netrin1 has been shown to be specifically attractive to pioneering axons from the cingulate cortex, and loss of Netrin prevents axon crossing (Shu, et al. 2000; Fothergill, et al. 2013), the exact role of Netrin in guiding pioneer axons across the midline has not been investigated. Finally, Sema3c expressed by the Calretinin+ neurons found within the medial IZ and in sling neurons attracts pioneering growth cones through interaction with the receptor Npn1 (Niquille, et al. 2009). All three of these pathways are necessary for pioneer axon crossing as disruption of any one of them prevents CC formation (Shu and Richards. 2001; Niquille, et al. 2009; Fothergill, et al. 2013). These and other signaling molecules important in CC formation are summarized in Figure 1-2 and Tables 1-3 and 1-4.

4) Once pioneering axons have crossed the midline, they continue through the IZ and reach their final targets in the contralateral cingulate cortex (Koester and O'Leary. 1994; Ozaki and Wahlsten. 1998; Rash and Richards. 2001b; Piper, et al. 2009b). These axons now serve as a scaffold for later crossing axons (Koester and O'Leary. 1994; Ozaki and Wahlsten. 1998; Rash

and Richards. 2001b; Piper, et al. 2009b). Axons from the lateral cortex are thought to bind them through adhesion molecules (Table 1-4) and the first axons have been shown to cross within the tract of pioneering axons already established (Koester and O'Leary. 1994; Rash and Richards. 2001b).

3.4.3 The Path of CPN axons: CPN axons follow a path that is very similar to that travelled by pioneering axons, except that these axons must travel a much greater distance. This journey can be summarized in a series of steps starting with 1) radial axon extension out of the cortex, 2) a medial turn to follow the IZ toward the midline, 3) fasciculation with other axons within the IZ, 4) another medial turn to cross the midline, 5) a dorsal turn to leave the midline, 6) and entering the contralateral cortex at the final destination. These stages are depicted in Figure 1-3.

3.4.3.1 Radial Axon Extension: Axon extension begins during radial migration, before the neuron has reached its final cortical layer (Polleux, et al. 1998; Zhao, et al. 2011). The bipolar neuroblast sends out a leading process extending in the direction the soma is traveling, and leaves behind a trailing process showing where the soma has been. This trailing process is converted into the rudimentary axon and extends back down towards the IZ (Polleux, et al. 1998). The orientation of the trailing process and the radial extension downward have been shown to be dependent on repulsion from Sema3a expressed in the marginal zone (Polleux, et al. 1998). Sema3a activity is mediated by binding the Npn1 receptor on the trailing process, although contradictory evidence has shown that expression of dominant negative form of Npn1 does not interfere with orientation or radial extension of the trailing process (Hatanaka, et al. 2009), implying that members of the Plexin receptor family, which are also known to bind Sema3, may be involved as well.

3.4.3.2 Turning Toward the Midline: Once the axon has reached the IZ, the tip must turn medially (Figure 1-3 panel A). Again, this decision is dependent primarily on repulsion from Sema3a (Zhao, et al. 2011). In addition to being found in the marginal zone, Sema3a is expressed in an increasing concentration gradient from medial to lateral within the cortex (Zhao, et al. 2011). The axons thus turn down the concentration gradient as they enter the IZ (Zhao, et al. 2011). Deletion of Sema3a or Npn1 randomizes the decision to turn medially or laterally in the both knockout mouse models (Zhao, et al. 2011). It is important to note that, although both pioneering and lateral CPN axons must make the decision to turn medially, neocortical CPN axons are much farther away from the midline, which means that the factors influencing this decision are very different. Pioneering axons could be close enough to the midline to respond directly to attractive cues, while axons from the lateral cortex are probably too distant from the midline to detect attractive cues such as Sema3c and Netrin. This may necessitate the existence of the additional repulsive signal of Sema3a pushing the axons to turn medially. Thus, while the medial turn is known to be governed by Sema3a in axons from the neocortex, it is unknown whether this turn is controlled via attraction towards to the midline or repulsion away from the lateral cortex in pioneering axons.

3.4.3.3 Axon Fasciculation in the IZ: The axons within the IZ represent a cohesive, tightly fasciculated tract throughout its length (Figure 1-3 panel B). This axon packing is achieved through the interaction of different adhesion molecules expressed on the surface of axons (Wolman, et al. 2007; Barry, et al. 2010). In fact, many of the molecules used to label axons, such as L1 and PSA-NCAM, are adhesion molecules specific to different axon tracts (Wolman, et al. 2007; Barry, et al. 2010; Niquille, et al. 2013). Molecular interactions can be either homophilic, such as L1-L1 interactions (Barry, et al. 2010), or heterophilic, such as between

different cadherin and protocadherin (Obst-Pernberg, et al. 2001; Treubert-Zimmermann, et al. 2002; Halbleib and Nelson. 2006; Ounkomol, et al. 2010; Hayano, et al. 2014) molecules. Npn1 in particular has been shown to be important in the fasciculation of CPN axons in the IZ (Hatanaka, et al. 2009). Axon defasciculation has been observed in both the Npn1 and Sema3a knockout mice (Gu, et al. 2003; Hatanaka, et al. 2009; Zhao, et al. 2011), and introduction of a dominant negative form of Npn1 causes axon defasciculation and re-entry into the ipsilateral cortex before reaching the midline (Hatanaka, et al. 2009). In addition to the classic Sema3 mediated signaling, Npn1 has been shown to homophillic adhesive activity (Shimizu, et al. 2000), and a mouse expressing a mutant form of Npn1 which is unable to bind Sema shows a milder phenotype than a full Npn-1 knock out (Gu, et al. 2003). It is therefore likely that some of the importance of Npn1 in axon fasciculation and guidance through the IZ is due to homophillic adhesive interactions between adjacent axons.

3.4.3.4 Crossing the Midline: Once the axons reach the midline, they must turn medially to cross the corticoseptal boundary (Figure 1-3 panel C). Similar to pioneering axons, lateral CPN axons also express Robo1/2 and are repelled by Slit2 from the GW (Shu and Richards. 2001). However, this Slit2 mediated repulsion is attenuated by Netrin/DCC signaling (Fothergill, et al. 2013), as was discussed in section 3.2.1, to allow precrossing axons to approach the midline despite this repulsive signal. Furthermore, Sema3c has been shown to be attractive to neurites from the lateral cortex as well as the medial cortex, even though Npn1 levels in neocortical axons are much lower (Niquille, et al. 2009; Piper, et al. 2009b). Numerous members of the ephrin and Eph classes are also expressed in the axons and at the midline, although the specific mechanisms controlling axon crossing have not been defined. EphrinB1 is present in the axons themselves, as well as the GW and IG, and deletion of ephrinB1 leads to an acallosal phenotype

(Mendes, et al. 2006; Bush and Soriano. 2009). Axonal ephrinB1 is thought to interact with EphB2, which is present on the GW and IG, to repel the axons and prevent them from entering the septum. Likewise, CC guidance errors have been detected in EphB4 and EphA5 mutant mice (Hu, et al. 2003; Ho, et al. 2009). Draxin, a newly discovered axon guidance molecule, has recently been shown to be expressed in the GW and IG and to cause neurite repulsion, possible through the Lrp6 receptor (Islam, et al. 2009). Draxin deletion leads to callosal agenesis in about 50% of mice due to incomplete septal fusion (Islam, et al. 2009). Finally, several morphogenic proteins, including Shh, Wnt and BMP, have also been shown to be important in crossing of commissural axons in the spinal cord (Okada, et al. 2006; Yam and Charron. 2013; Sloan, et al. 2015), although it has not yet been determined if they function in a similar way in the CC or other brain commissures.

3.4.3.5 Reaching the Target: After crossing the midline, the CPN axons must turn dorsally to follow the contralateral IZ (Figure 1-3 panel D). This is mediated through several repulsive signals from the contralateral GW. In addition to the unmasking of the Slit2 meditated repulsion following DCC downregulation (Fothergill, et al. 2013), Wnt5a from the GW repels axons through interaction with the Ryk receptor on the growth cone (Keeble, et al. 2006). The axons then continue along the IZ until reaching the homotopic region of the cortex. CPNs project to cortical targets in homotopic region of the contralateral hemisphere, meaning that their own location within the cortex defines the location of their axonal target (Fame, et al. 2011; Zhou, et al. 2013). This targeting is partially controlled by the location of an axon within the CC, such that axons arising from and projecting to the medial cortex are more dorsal within the CC than axons from the lateral cortex, and experimental disorganization of the axons within the CC lead to long lasting targeting defects in the contralateral hemisphere (Zhou, et al. 2013). Other

mechanisms, such as matching common patterns of electrical activity in homotopic regions in both hemispheres has also been suggested to be involved in CPN axon targeting as suppression of neuronal excitability has been shown to impair axon targeting in the primary somatosensory and visual cortexes (Wang, et al. 2007a; Mizuno, et al. 2010). However, the mechanisms through which growth cones detect this synaptic activity are completely unknown and an area of active research.

4. Mechanisms of Pocket Protein Dependent Gene Regulation

4.1 Overview of pocket protein function: Retinoblastoma protein (pRb) is well known for its role in regulating cell proliferation by controlling progression through the cell cycle. pRb plays a fundamental role both in regulating stem cell division during development and tissue repair (Jacks, et al. 1992; Lee, et al. 1994; Yoshikawa. 2000; Ferguson and Slack. 2001; Giacinti and Giordano. 2006; Khidr and Chen. 2006; Maddika, et al. 2007; McClellan and Slack. 2007; Sun, et al. 2007a; Gordon and Du. 2011), and in tumor suppression and the prevention of ectopic cell proliferation (Weinberg. 1991; Dannenberg and te Riele. 2006; Manning and Dyson. 2012). However, the role of pRb within cortical development remain largely uninvestigated, especially regarding mechanisms beyond neurogenesis and cell cycle regulation. This section will review the mechanisms of pRb function and the current evidence suggesting that this pathway has crucial cell cycle independent roles in neuron development and differentiation.

pRb is a member of the pocket protein family, together with the closely related proteins p107 and p130, which are named after the distinctive “pocket” domain required for the protein interactions through which all three pocket proteins function (Ewen, et al. 1991; Hannon, et al. 1993; Classon and Dyson. 2001; Burke, et al. 2010; Burke, et al. 2012; Dick and Rubin. 2013).

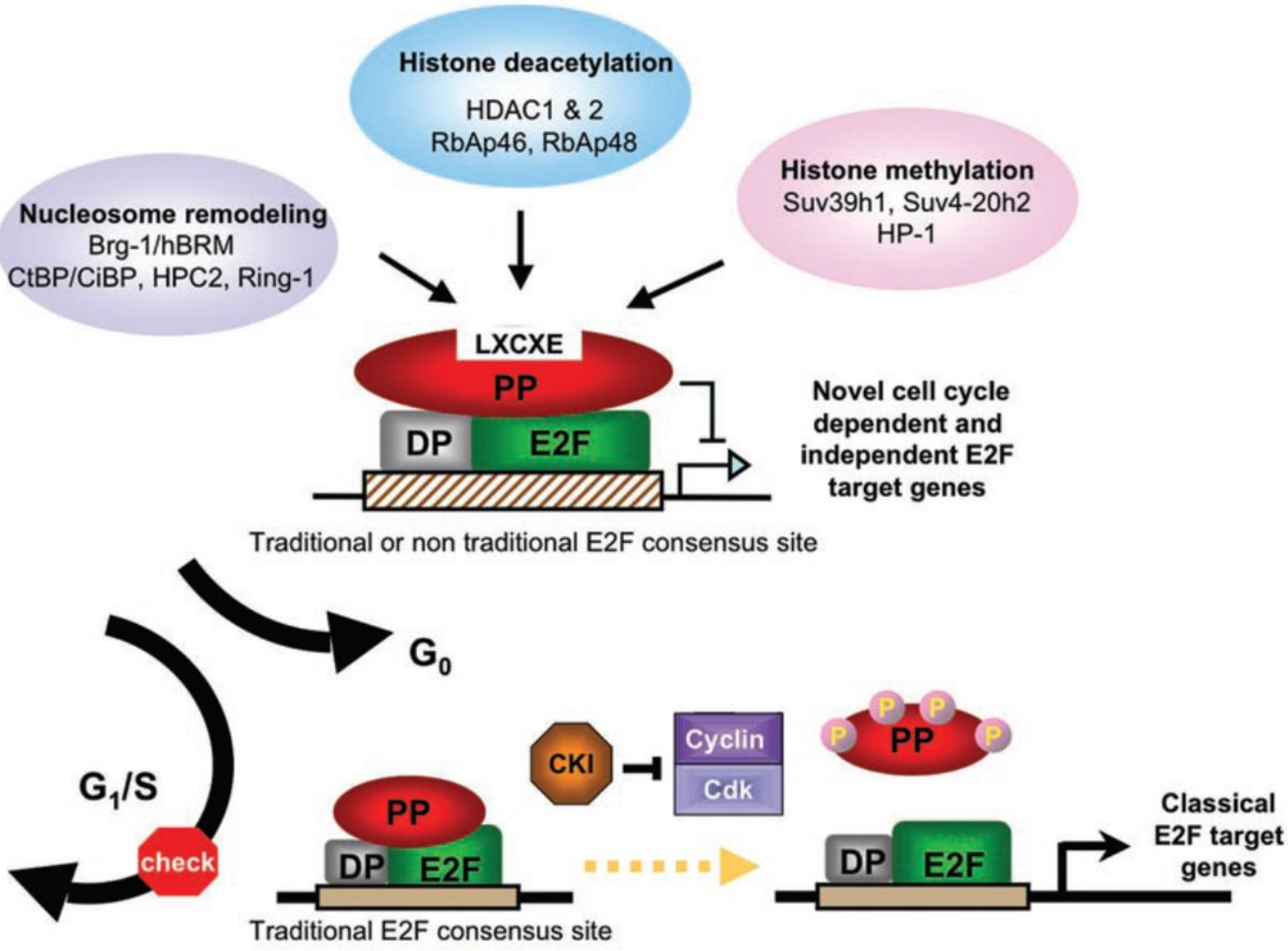
Histone deacetylation
HDAC1 & 2
RbAp46, RbAp48
Nucleosome remodeling
Brg-1/hBRM
CtBP/CiBP, HPC2, Ring-1
Histone methylation
Suv39h1, Suv4-20h2
HP-1
LXCXE
PP
DP
E2F
Novel cell cycle dependent and independent E2F target genes
Traditional or non traditional E2F consensus site
G0
G1/S
check
CKI
Cyclin
Cdk
P
PP
Classical E2F target genes
Traditional E2F consensus site

Figure 1-4

Figure 1-4: Mechanisms of pocket protein dependent regulation of transcription. pRb, p107 and p130 regulate transcription through two main mechanisms (top). The classical mechanism is through direct control over the activity of the E2F family of transcription factors. Additional levels of control are achieved by the recruitment of coregulators through interaction with the LXCXE binding domain. These co-regulators are often chromatin remodeling proteins which regulate transcriptional activity through modification of histones or DNA. These mechanisms are thought to be important in G0 for the long term silencing of pro-proliferation genes and the regulation of novel pRb targets involved in cell cycle independent functions such as differentiation, migration and other forms of cell maturation and specialization.

Traditional regulation of the G1/S checkpoint: During G1 phase, pocket proteins (PP) are hypophosphorylated and bind E2F factors on the DNA. As G1 progresses, CyclinD/CDK4/6 and CyclinE/CDK2 complexes progressively phosphorylate the pocket protein until it reaches a hyperphosphorylated state. At this point, the pocket protein releases E2F and allows it to activate transcription of pro-proliferation genes, which drives the cell through the checkpoint, into S phase. CDK activity is negatively regulated by CDK inhibitors Ink4 and Cip/Kip.

From McClellan and Slack, 2007, *Cell Cycle*

The classical function of pRb is to regulate the checkpoint between the growth phase 1 (G1) and synthesis (S) phases of the cell cycle (Figure 1-4). In this role, pRb acts to hold the cell in G1 until it reaches the appropriate developmental stage or receives a mitotic signal instructing it to divide (Giacinti and Giordano. 2006; Sun, et al. 2007a). In the canonical pathway, pRb achieves this by binding to E2F transcription factors and preventing their activation or repression of gene transcription (Bandara, et al. 1991; Chellappan, et al. 1991a; Frolov and Dyson. 2004; Korenjak and Brehm. 2005). The E2F family has nine members which can be categorized as transcriptional activators or transcriptional repressors (Kusek, et al. 2001; Frolov and Dyson. 2004; DeGregori and Johnson. 2006; Lammens, et al. 2009). pRb functions during G1 by inhibiting activating E2Fs and preventing them from promoting transcription of pro-proliferation genes, as well as by binding repressor E2Fs and enabling them to repress transcription at E2F target promoters (Figure 1-4).

Throughout G1, pRb becomes increasingly phosphorylated by the activity of cyclin dependent kinases (CDKs) (Santamaria and Ortega. 2006). CDKs are activated by binding to cyclins to make active cyclin/CDK complexes (reviewed in (Santamaria and Ortega. 2006)). As G1 progresses, mitogenic signals stimulate expression of D type cyclins, which bind CDK4/6 early in G1, and followed by increased levels of CyclinE and CyclinA which bind CDK2 late in G1 (Hinds, et al. 1992; Knudsen and Wang. 1997; Lundberg and Weinberg. 1998). This progressive phosphorylation of pRb culminates in late G1, when pRb achieves a hyperphosphorylated state and undergoes conformational changes resulting in detachment from E2F transcription factors (Dick. 2007; Burke, et al. 2010; Burke, et al. 2012). This frees activating E2F proteins to promote transcription of E2F target genes, while it simultaneously causes repressing E2Fs to detach from the chromatin and thus relieves their transcriptional

repression (Knudsen and Wang. 1997; Frolov and Dyson. 2004; Korenjak and Brehm. 2005; Chong, et al. 2009). The result is initiation of transcription at pro-proliferation genes and progression through the cell cycle. Through the subsequent growth 2 (G2) and mitosis (M) phases of the cell cycle, pRb is de-phosphorylated by multiple protein phosphatases including protein phosphatase 1 (PP1) and returned to its original hypophosphorylated state by the beginning of the subsequent G1 phase (Tamrakar, et al. 2000; Vietri, et al. 2006), thus completing an entire round of the cell cycle.

During early G1 and interphase (G0), pRb is maintained in a hypophosphorylated state by the activity of cyclin dependent kinase inhibitors (CDKIs) p16-INK4A, p21-CIP1, p27-KIP1 and p57-KIP2 (Serrano, et al. 1993; Kamb, et al. 1994; Cheng, et al. 1999; Blomen and Boonstra. 2007; Knudsen and Knudsen. 2008). Activity of these proteins serves to negatively regulate proliferation by either increasing the length of the G1 phase or promoting cell cycle exit and transitioning into a post-mitotic state.

The model presented in this overview represents the classically identified pathway of pRb function (Figure 1-4). Not surprisingly, the mechanisms of action are much more complex and show distinct specializations within different cell types and at different stages of development. Although most of these complications are beyond the scope of this thesis, the following sections will describe various aspects of the pRb pathway relevant to appreciating its role in neuronal development.

4.2 Comparisons between the three pocket proteins, pRb, p107 and p130: The three pocket proteins share a large degree of structural similarity and functional redundancy. All three proteins share the pocket domain crucial for interaction with E2Fs (Ewen, et al. 1991; Cao, et al.

1992; Hannon, et al. 1993; Mayol, et al. 1993; Litovchick, et al. 2007; Sun, et al. 2007b; Wirt, et al. 2010; Wirt and Sage. 2010; Dick and Rubin. 2013). Structurally, p107 and p130 share the most similarity, with 54% sequence identity, while pRb shows a greater degree of divergence and shares only 25% sequence identity with p107/p130, with the majority of this similarity being in the pocket domain (Ewen, et al. 1991; Hannon, et al. 1993; Mayol, et al. 1993; Pertile, et al. 1995; Huppi, et al. 1996; Chen, et al. 1996; Mulligan and Jacks. 1998). Together, all three pocket proteins function to regulate proliferation through similar mechanisms, and p107 or p130 can be substituted for pRb in the simplified canonical pathway outlined above (Chellappan, et al. 1991b; Cao, et al. 1992; Fattaey, et al. 1993a; Fattaey, et al. 1993b; Dagnino, et al. 1995; Classon and Dyson. 2001; Dick and Rubin. 2013). However, distinct functional differences arise in terms of binding partner specificity and activity in different cell types, which suggest that these proteins have non-redundant functions. For example, expression patterns within different proliferative cell types differ between pocket proteins, with pRb expressed in both proliferating and quiescent cells, p107 highest in proliferating cells and p130 highest in quiescent cells (Mayol, et al. 1993; Beijersbergen, et al. 1995; Kiess, et al. 1995; Hurford, et al. 1997; Garriga, et al. 1998; Callaghan, et al. 1999; Litovchick, et al. 2007; Burkhart, et al. 2008; Burkhart, et al. 2010; Litovchick, et al. 2011). This supports the idea that p107 functions primarily in regulating cell cycle progression while p130 is involved in long term repression of E2F targets in post-mitotic cells, and pRb has broader functions in both proliferation and differentiation. Another important distinction between pocket proteins is their preference for different E2F binding partners; pRb tends to interact most often with activating E2F1-3, as well as with repressing E2F4 (Moberg, et al. 1996; Thomas, et al. 1998; Trimarchi and Lees. 2002; Chong, et al. 2009; Guiley, et al. 2015), while p107 and p130 prefer to interact with repressing E2F4/5.

Despite these non-redundant functions, pocket proteins are able to compensate for deficiency of other family members in transgenic knockout models. In particular, p107 is able to compensate for loss of pRb during development (Callaghan, et al. 1999; Ferguson and Slack. 2001; McLear, et al. 2006). In the nervous system, there is a distinct upregulation of p107 in pRb deficient tissue, suggesting that p107 may substitute for pRb function during neuronal development (Callaghan, et al. 1999). Furthermore, pRb/p107 double knockout mice have similar but more exaggerated phenotypes as seen in pRb single knockout mice, with a greater degree of ectopic proliferation and cell death, as well as aggravated tissue specific defects (Lipinski and Jacks. 1999; Sage, et al. 2000; Marino, et al. 2003; Chen, et al. 2004; Haigis, et al. 2006; Berman, et al. 2009). For this reason, a double knockout mouse model deficient for both pRb and p107 can be used to examine to the full role of pRb in proliferation and development *in vivo*.

4.3 Mechanisms of pRb mediated transcriptional control: In addition to the classical pathway presented above, pRb has been shown to regulate gene transcription through a variety of mechanisms. Many pRb functions are achieved through binding and regulating the activity of E2F transcription factors, as described above (Dannenberg and te Riele. 2006; Giacinti and Giordano. 2006; Khidr and Chen. 2006; McClellan and Slack. 2007; Chen, et al. 2007a; Sun, et al. 2007a; Chong, et al. 2009; Andrusiak, et al. 2011; Gordon and Du. 2011; Ghanem, et al. 2012b). However, E2Fs often work through more complex pathways through interactions with co- activators or co-repressors as shown in Figure 1-5. Activating E2Fs have been shown to function as repressors in some situations, while repressing E2Fs have been shown to act as

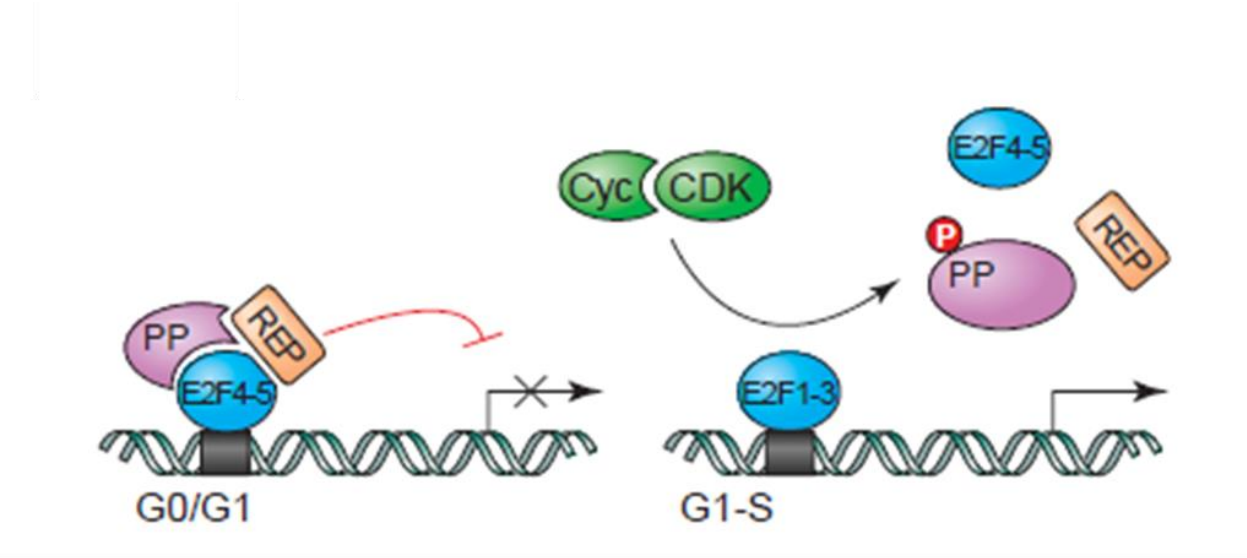

Figure 1-5

Figure 1-5: E2F activators and repressors. In the classical signaling pathway for the regulation of pro-proliferation genes, hypophosphorylated pocket proteins (PP) bind to repressing E2F family members, usually E2F4 and E2F5, during G0/G1 phase (left) which enables the PP/E2F complex to bind the E2F responsive element in the gene promotor (shown as a black box) and repress transcription, often through the recruitment of a co-repressor. When the pocket protein becomes hyperphosphorylated in late G1 (right), the PP/E2F complex disassembles and lifts off the chromatin, which opens the E2F responsive element for activating E2F family members, usually E2F 1-3. This allows the cell to pass through the G1/S checkpoint.. From McClellan and Slack, 2007, *Cell Cycle*

activators, implying that these proteins have context specific functions (Ziebold, et al. 2003; Chong, et al. 2009; Trikha, et al. 2011). For example, deletion of E2F3 in a pRb+/- mouse has been shown to have variable effects on proliferation and tumor formation in different tissues, such that the prevalence of pituitary tumors was decreased, while the incidence of metastatic thyroid carcinomas was dramatically increased (Ziebold, et al. 2003). This implies that E2F3 is acting as an oncogene in some tissues and a tumor suppressor in others, possibly through regulation of different genes in different cell types. In the small intestine, E2F1-3 have been shown to function as activators in proliferating cells where they are necessary for cell survival, but then function as transcriptional repressors in a complex with pRb in differentiating cells (Chong, et al. 2009). This furthers the classical model of pRb/E2F function because it shows that when activating E2Fs are bound to pRb on a gene promoter, they are capable of actively repressing transcription, rather than behaving as an inactive complex as was previously thought. In addition, this work shows that the E2F site is necessary both for the activation and the repression of a gene, since when E2F1-3 are absent, transcription of a pro-proliferation gene cannot be increased in proliferating cells, but neither can it be turned off in differentiating cells. In a similar reversed situation, E2F1-3 were found to function as transcriptional repressors to mediate cell survival in myeloid progenitors, but then switch to transcriptional activators to regulate proliferation in macrophages (Trikha, et al. 2011). Furthermore, expression profiling experiments in knockout models of a single E2F have shown that a similar number of genes are upregulated as are down regulated, regardless whether the E2F in question is an activator or repressor (Xu, et al. 2007; Asp, et al. 2009; Lee, et al. 2011; Julian, et al. 2015), further suggesting that E2Fs can function as either repressors or activators at different promotors in a context and tissue specific manner. These screens of E2F target genes have identified many

potential targets with functions beyond the cell cycle, such as differentiation or apoptosis (Xu, et al. 2007; Asp, et al. 2009; Lee, et al. 2011; Julian, et al. 2015), which first suggested the possibility that the pRb-E2F pathway has cell cycle independent functions. These observations show that the pocket protein and E2F proteins families regulate gene transcription through a variety of cell type specific mechanisms which lead to numerous tissue specific functions.

In addition to E2F mediated gene regulation, pRb has been shown to have additional protein interactions which mediate E2F-independent mechanisms of regulating expression. Many of these additional pRb interactors contain an LXCXE binding motif which interacts with the delta-L cleft on the pocket domain of all three pocket protein family members (Figure 1-4) (Dahiya, et al. 2000; Sutcliffe, et al. 2000; Wirt and Sage. 2010). This cleft is structurally separate from the E2F-pocket so that pRb can simultaneously bind E2F and additional co-regulators (Lee, et al. 1998; Kim, et al. 2001; Singh, et al. 2005; Dick and Rubin. 2013). Many of the LXCXE containing proteins are chromatin remodelers which are recruited to responsive promoters when pRb binds E2F to modify chromatin structure and change gene expression, such as to induce long term gene repression of pro-proliferative genes (Dahiya, et al. 2000; Sutcliffe, et al. 2000; Wirt and Sage. 2010). Examples of pRb binding chromatin remodeling proteins include histone deacetylases (such as HDAC1), histone methyl-transferases (such as Suv39h1/2), DNA methyl-transferases (such as DNMT1/2), and the ATP-dependent SWI/SNF modifiers (Ferreira, et al. 1998; Robertson, et al. 2000; Dahiya, et al. 2000; Pradhan and Kim. 2002; Dick and Rubin. 2013). Pocket proteins could therefore regulate gene expression in post-mitotic cells by recruiting chromatin remodeling factors to the promoters, which could represent a mechanism through which pRb can regulate neuronal maturation independent of the cell cycle.

4.4 pRb in development: Deletion of pRb in transgenic mouse models has provided invaluable evidence regarding the function of pRb during development. These studies have emphasized the complexity of the pRb pathway and made it evident that this pathway has much farther reaching tissue specific functions in development and cell survival. Knockout models of individual members of the pocket protein and E2F families have produced a wide variety of phenotypes which cannot be explained through regulation of cell cycle progression alone. These experiments have led to the discoveries of novel roles of the pRb pathway in maintaining chromosome stability (Ferreira, et al. 1998; Dahiya, et al. 2000; Sutcliffe, et al. 2000; Robertson, et al. 2000), regulating apoptosis (Jacks, et al. 1992; Feddersen, et al. 1995; Macleod, et al. 1996; Marino, et al. 2000; Chen, et al. 2004; Lazzerini Denchi and Helin. 2005; Ciavarra and Zacksenhaus. 2010a; Andrusiak, et al. 2012a) and promoting progenitor cell differentiation (Lee, et al. 1994; Korenjak and Brehm. 2005; Vanderluit, et al. 2007; McClellan and Slack. 2007; Chen, et al. 2007a; Ghanem, et al. 2012b) in multiple cell types.

The first indication that the pRb pathway has complex *in vivo* functions beyond cell cycle regulation came from the germline pRb knockout mice. pRb deletion results in embryonic lethality before E15.5 and is associated with high levels of ectopic apoptosis and mitosis throughout the body, with the greatest effect seen in the developing nervous system (Jacks, et al. 1992; Lee, et al. 1992; Clarke, et al. 1992; Morgenbesser, et al. 1994). Analysis of an embryo specific Cre line which deleted pRb from all tissues of the embryo but spared the placenta showed that the huge increase in cell death was due to oxygen deprivation caused by placental defects (de Bruin, et al. 2003a; de Bruin, et al. 2003b; MacPherson, et al. 2004; Wenzel, et al. 2007) while the ectopic proliferation and developmental defects in the CNS and muscular

systems were maintained. These finding led the way to a huge expansion of the pRb field into the role of cell cycle regulators in embryonic development.

The role of p107 and p130 during development are much more subtle than that of pRb, as single gene knockout animals are viable and fertile and exhibit no obvious tissue defects (Cobrinik, et al. 1996; Cobrinik, et al. 1996; LeCouter, et al. 1998; Classon and Dyson. 2001; Vanderluit, et al. 2004; Vanderluit, et al. 2007). However, a more detailed analysis of these animals has shown that p107 regulates NPC self-renewal and neurogenesis in the developing telencephalon. Deletion of p107 causes an increase in self-renewing divisions at the expense of neurogenic divisions, which led to increased neurogenesis in the adult (Vanderluit, et al. 2004; Vanderluit, et al. 2007). p107 was found to regulate neurogenesis through inhibition of transcription of Hes1, which is known to regulate the stem cell maintenance (Vanderluit, et al. 2004; Vanderluit, et al. 2007).

The use of tissue specific Cre lines led to the discovery that different pocket protein and E2F family members have tissue specific roles in differentiation. Results from *in vivo* anatomical and cell biological analysis as well as from studies examining the gene deregulation have revealed a huge degree of tissue specificity. In many tissues examined, including the CNS, retina and muscle, there in an increase in ectopic proliferation and apoptosis in pRb deficient cells (Lee, et al. 1992; Lee, et al. 1994; Feddersen, et al. 1995; Macleod, et al. 1996; LeCouter, et al. 1998; Padmanabhan, et al. 1999; Marino, et al. 2003; Chen, et al. 2004; MacPherson, et al. 2004; Sage, et al. 2006; Ciavarra and Zacksenhaus. 2010a; Gordon and Du. 2011; Chen, et al. 2013). In addition to these expected results, however, tissue specific differentiation defects were observed which have been shown to be mediated through a variety of mechanisms, giving rise to the idea that pRb is crucial for coupling cell cycle exit to differentiation. For example, deletion

of p107 or pRb has been shown to prevent the formation of white adipose tissue by preventing adipocyte precursors from completing differentiation (Scime, et al. 2005). This was found to be due to pRb repressing transcription of PGC1α, a pro-differentiation factor in adipogenesis (Scime, et al. 2005). Similarly, pRb was found to promote osteoblast differentiation by acting as a transcriptional co-factor with the osteogenic master regulator RUNX2, and thus increasing expression of pro-differentiation genes such as osteocalcin (Thomas, et al. 2001; Lee, et al. 2006). In the retina, deletion of pRb was shown to specifically prevent the differentiation and maturation of starburst amacrine cells, a category of interneuron, through a cell cycle and cell death independent mechanism (Chen, et al. 2007a). This was found to be mediated by increased E2F3 activity in the absence of pRb, as the phenotype was rescued by E2F3 deletion (Chen, et al. 2007a). pRb is also important in muscle fiber formation, as it was found to promote myoblast differentiation by interacting with MyoD, which in turn promotes MEF2 activity, which drives differentiation (Novitch, et al. 1999; Ciavarra and Zacksenhaus. 2010b). pRb has been shown to promote cardiomyocyte differentiation through increasing transcription of Nkx2.5 and MEF2c (Papadimou, et al. 2005), which is especially interesting since cardiomyocyte differentiation occurs prior to cell cycle exit. This implies that pRb involvement in differentiation must be truly uncoupled from cell cycle exit in these cells (Papadimou, et al. 2005). In addition, genomics studies have shown that many of the genes responsive to pRb and E2F family members have non-cell cycle functions, such as tissue specific differentiation, chromatin remodeling and apoptosis (Xu, et al. 2007; Asp, et al. 2009; Lee, et al. 2011; Julian, et al. 2015). Overall, studies suggest that the pRb family has cell-cycle independent roles in cell differentiation and potentially in later developmental stages of cell maturation. However, except for a few examples, the mechanisms through which pocket proteins regulate expression of proteins in post-mitotic cells

are unknown. Furthermore, the examples described above show that pRb employs highly tissue specific mechanisms to control differentiation, so that results from one tissue can often not be generally applied. In particular, the role of pRb in regulating neuronal maturation is essentially unknown, and could be mediated by a variety of mechanisms such as E2F-dependent gene activation following cell cycle withdrawal, chromatin remodeling, or interaction with yet uncharacterized binding partners. One of the primary goals of this thesis is to investigate the ability of pRb to control alternative aspects of neuronal maturation through cell cycle independent mechanisms.

4.5 pRb in Cell Death: The role of pRb family members in cell survival has been extensively studied both in the context of development and tumor suppression (Feddersen, et al. 1995; Marino, et al. 2003; Chen, et al. 2004; MacPherson, et al. 2004; Sage, et al. 2006; Berman, et al. 2009; Ciavarra and Zacksenhaus. 2010a). In the adult brain, overexpression of pRb has been shown to rescue the increase in cell death following infection with the oncogenic SV40 virus in Purkinje neurons (Feddersen, et al. 1995). Likewise, pRb deletion in post-mitotic cortical neurons *in vitro* has been shown lead to attempted cell cycle re-entry, DNA damage and apoptosis (Andrusiak, et al. 2012a), and a decrease in pRb expression was shown to precede apoptosis in cerebellar granular neurons undergoing KCl deprivation (Padmanabhan, et al. 1999), which together suggest that pRb activity is necessary for neuron survival. Increased apoptosis has been observed in many pRb deletion models during development, and this increase in cell death is often thought to accentuate the observed cell differentiation phenotypes in a variety of tissues (Lee, et al. 1994; Feddersen, et al. 1995; Chen, et al. 2004; MacPherson, et al. 2004; Berman, et al. 2009; Wu, et al. 2009; Ciavarra and Zacksenhaus. 2010a). In the retina, deletion

of pRb and p107 resulted in the absence of ganglion, bipolar a rod cells while cone, horizontal and Muller cells were maintained (Chen, et al. 2004). Further investigation showed that progenitors of all cell types were specified in pRb/p107 knockouts, but ganglion, bipolar and rod precursors underwent apoptosis upon cell cycle exit, whereas the other cell types were able to survive (Chen, et al. 2004). Similarly, pRb is known to cause severe defects in muscle development and myotube formation in the developing embryo. *In vitro*, pRb deficiency prevents myotube formation and causes an increase in myotube collapse and death (Novitch, et al. 1999; Ciavarra and Zacksenhaus. 2010b). However, this differentiation defect could be rescued by transfection with Bcl-2, an anti-apoptotic mitochondrial protein, which enabled the formation of mature twitching myotubes in pRb-deficient cultures (Ciavarra and Zacksenhaus. 2010b). Again, the presence of high levels of ectopic cell death in the absence of pRb significantly worsened the differentiation phenotype and complicated interpretation of the role of pRb during development. In the developing cerebellum, pRb loss has been shown to lead to defects in differentiation of granule neuron precursors (Marino, et al. 2003). However, because there was also an increase in cell death in granule cell precursors, it is difficult to determine whether pRb regulates differentiation of these cells directly, or is only important for their survival (Marino, et al. 2003). This increased apoptosis is primarily mediated through E2F1 dependent activation of the p53 pathway (Macleod, et al. 1996; Lazzerini Denchi and Helin. 2005; Wu, et al. 2009), although other p53 and even E2F1 independent pathways have been demonstrated in the retina (MacPherson, et al. 2004; Chen, et al. 2013) and cerebellum (Marino, et al. 2003). Therefore, the presence of ectopic cell death complicates interpretation of developmental phenotypes and makes it difficult to determine the true involvement of pRb in cell differentiation and maturation. This means that, in many tissues, the direct role of pRb in

differentiation independent of cell death is unknown. In this thesis, we attempt the answer this question by examining the role of pRb and p107 in neuronal maturation independent of their roles in survival.

4.6 pRb in CNS Development: The importance of pRb in nervous system development is emphasized by the severe phenotypes exhibited by pRb mutant embryos. Germline deletion of pRb has been shown to cause severe increases in cell death throughout the nervous system, although this defect was largely rescued by using embryo specific Cre lines which spared the placenta (Jacks, et al. 1992; Lee, et al. 1992; Clarke, et al. 1992; Morgenbesser, et al. 1994). Telencephalon specific Cre lines have suggested a number of additional cell cycle dependent and independent roles of pocket proteins in specific brain regions and cell types. Deletion of pRb has been shown to lead to ectopic proliferation of developing neuroblasts in the SVZ and cortex without significantly influencing cell division in the more immature NPCs in the VZ (Ferguson, et al. 2002; MacPherson, et al. 2004), indicating that pRb is important in establishing cell cycle exit prior to differentiation. In contrast, p107 is thought to regulate proliferation in NPCs within the VZ, as described above (Vanderluit, et al. 2004; Vanderluit, et al. 2007). Surprisingly, the increase in cell apoptosis observed in the telencephalon was much more modest than that seen in other tissues (Ferguson, et al. 2002; Ferguson, et al. 2005; McClellan, et al. 2007) or even other brain regions (Padmanabhan, et al. 1999; Marino, et al. 2000), suggesting that pRb does not regulate neural survival in the telencephalon to the same degree as seen in other tissues. An exception to this is the Cajal Retzius cells in layer I of the cortical plate, which were shown to be lost on pRb mutant embryos (Ferguson, et al. 2005). Cortical neuron differentiation was also found to be relatively normal in pRb-mutant embryos, as neurons are able to express cortical

markers such as Tbr1 (Ferguson, et al. 2005; McClellan, et al. 2007). To the contrary, expression of Dlx2 was found to be decreased in the ventral telencephalon of pRb mutant brain, which resulted in defects in interneuron differentiation (Ghanem, et al. 2012b). As pRb was found to directly modulate Dlx2 transcription (Ghanem, et al. 2012b), these results suggest that pRb could control differentiation in a cell type specific manner. In the cerebellum, pRb has been shown to be required for survival and differentiation of granule cells yet dispensable for Purkinje cells differentiation (Marino, et al. 2003). In the retina, the role of pRb is more complex, with ganglion and rod cells requiring pRb for survival and horizontal and cone cells showing the ability to differentiate and survive in the absence of pRb (Chen, et al. 2004; MacPherson, et al. 2004). Deletion of pRb has been shown to lead to defects in differentiation of amacrine cells (Chen, et al. 2007a) and rod cells (Zhang, et al. 2004) independent of cell cycle or cell death associated mechanisms, showing that pRb does seem to regulate differentiation and neuronal maturation directly in some cell types. The defect in amacrine cell differentiation was found to be due to increased E2F3 activity, while the increase in ectopic proliferation was found to be downstream of E2F1 (Chen, et al. 2007a), which supports the idea that the role of pRb in differentiation is mechanistically separate from its role in cell cycle progression.

4.6.1 pRb in neuroblast migration: In addition to its role in differentiation, pRb has been shown to have an important role in cortical lamination and radial migration. In pRb deficient embryos, the clear delineation between the subplate and the IZ is lost with ectopic Tbr1+ cells remaining scattered below the cortex in the IZ (Ferguson, et al. 2005; McClellan, et al. 2007). Injection of BrdU at E13.5 and examination of the brains at E18.5 showed that all BrdU labelled neurons reached the cortex in control brains, but some BrdU labelled cells were still present in the IZ in pRb-mutant brain, implying that pRb function is necessary for neuroblasts to migrate

radially into the cortical plate (Ferguson, et al. 2005). However, it was never determined whether this was a result of failure to exit the cell cycle properly or whether pRb regulated radial migration directly. These defects in radial migration were correlated with a loss of CR cells in the marginal zone of these brains, which led to the hypothesis that the defect in radial migration is due to death of the CR cells and subsequent loss of Reelin (Ferguson, et al. 2005), although this was never fully tested. This phenotype illustrates how the multifaceted functions of pocket proteins in neural survival and differentiation complicate the interpretation of developmental phenotypes. The full role and underlying mechanisms of pRb in radial migration, independent of its roles in cell death and cell proliferation, therefore remain unknown.

In addition, pRb has been shown to be involved in tangential migration of immature GABAergic interneurons from the ventral telencephalon into the cortex (Ferguson, et al. 2005; McClellan, et al. 2007; Andrusiak, et al. 2011) and into the olfactory bulb (Ghanem, et al. 2012b). pRb deletion led to a distinct decrease in the number of interneurons reaching the cortex (Ferguson, et al. 2005). pRb was shown to have a cell autonomous role in tangential migration using slice cultures, in which control or pRb-null explants from the ganglionic eminence were placed on top of wild type slice cultures and the migration of cells from the explant to the slice was measured. Immature neuroblasts from control explants were able to enter the marginal zone of the surrounding slice, while pRb deficient interneurons remained stuck in the explant and failed to migrate (McClellan, et al. 2007). pRb was found to regulate tangential migration through regulation of Neogenin transcription; deletion of pRb led to increases in Neogenin mRNA and protein levels, and ectopic expression of Neogenin was found to prevent interneuron migration, which mimicked the phenotype in pRb deficient brains (Andrusiak, et al. 2011). In the olfactory bulb, deletion of pRb impaired both tangential migration of neuroblasts along the

rostral migratory stream, and radial migration of neurons once they reached the bulb (Ghanem, et al. 2012b). Together these studies show that pRb has an important role in regulating multiple forms of neuronal migration. However, many unanswered questions remain, as the mechanisms through which pRb regulates various forms of migration are unknown. Further investigations are necessary to determine the whether pRb regulates migration through truly novel mechanisms that are independent of cell cycle dynamics, or whether these effects are downstream consequences of delays in cell cycle exit. Furthermore, the role of pRb in migration opens up the possibility that pRb is involved in many other aspects of brain development, such as axon extension and circuit formation, which remain completely uninvestigated.

5. Statement of Objectives

The pRb/E2F pathway has been convincingly shown through accumulating evidence to have multiple roles beyond its classically defined functions in controlling cell cycle progression and apoptosis. This has led to the hypothesis that pocket proteins are involved in coordinating cell cycle exit with later stages of differentiation and development. It has been suggested that this pathway has numerous tissue specific roles in cell differentiation, often independent from regulation of proliferation, and in the developing brain pRb has been shown to be involved in neuronal migration and differentiation. However, the multifaceted functions of the pRb pathway in cell proliferation and cell death have complicated interpretation of in vivo experiments and thus obscured the true function of this pathway functions during differentiation and cell maturation. As a result, the role of pocket proteins in later stages of neuraonal maturation and brain development remain unknown. In particular, it is unknown whether the defects in brain development observed following deletion of pRb are a direct consequence of the premature cell

cycle exit and increased apoptosis, or whether pRb regulates neuronal migration through a cell-cycle and cell-death independent mechanism. Understanding the functions of pocket proteins in later stages of neuronal maturation, such as migration and axon extension, is essential for our understanding of the functional mechanisms that regulate brain development. The research objectives of my PhD studies were as follows:

1. To examine whether pRb and p107 regulate radial migration through a cell cycle and cell death independent mechanism (Chapter 2);
2. To apply in utero electroporation to the pRb-flox model to study both migration and axon guidance (Chapter 3);
3. To determine the role of pRb and p107 in corpus callosum development, including development of the commissural plate and the growth and guidance of callosal axons (Chapter 4).

.

6. Hypotheses and Summary of Results

6.1 Chapter 2: pRb has been previously shown to regulate both radial and tangential migration. Although, pRb was thought to regulate migration through promoting survival of the Cajal-Retzius cells which secrete the migratory cue Reelin, this was never confirmed and the underlying mechanism through which pRb regulated radial migration remained unknown. In addition, it was unknown whether defects in radial migration were a direct results of failed cell cycle exit.

Hypothesis #1: pRb and p107 regulate radial migration though a cell cycle and cell death independent mechanism.

In this study, we describe a novel phenotype specific to the pRb/p107 double knock out (DKO) embryo in which a population of upper layer neurons are unable to migrate through the intermediate zone and fail to enter the cortical plate. Using a combination of birthdating and immunohistochemistry, we confirm that these delayed cells were born at the appropriate developmental stage and have exited the cell cycle, implying that pRb/p107 regulate migration though a cell cycle independent mechanism. By deleting Bax and generating a pRb/p107/Bax triple knock out embryo, we show that eliminating ectopic cell death fails to rescue the migration defect, implying that pRb/p107 regulate migration though a cell death independent mechanism, contrary to previous results. In addition, we use in utero electroporation to show that pRb regulates radial migration through a cell autonomous mechanism. **These findings represent a novel function of pRb in regulating radial migration through a cell autonomous mechanism independent of its roles in regulating cell death and cell cycle exit.**

6.2 Chapter 3: In order to study the cell autonomous role of pRb in neuraonal migration and axon guidance, it was necessary to perform in utero electroporation (IUE) on pRb-flox mice. Because none of the labs at the University of Ottawa used this technique, I visited the lab of Dr. Freda Miller at the University of Toronto to learn IUE, and then brought the technique back to Dr. Ruth Slack's lab. Here, I adapted the technique to a Cre mediated excision model and developed a system for confirming successful gene excision when an antibody or in situ hybridization probe is not available. Furthermore, I used this technique to target different regions of the developing telencephalon.

Technical Advance: Adapting in utero electroporation to Cre mediated gene excision in multiple regions of the developing telencephalon.

6.3 Chapter 4: The role of pocket proteins in radial migration suggested that pRb and p107 could have additional, unknown functions in neural maturation. In addition, a ChIP-on-chip screen designed to obtain a comprehensive list of E2F3 and E24F gene targets identified a surprising number of E2F3 targets involved in axon guidance, cytoskeletal dynamics and neurite extension. Beyond these preliminary results, the role of pocket proteins in axon growth are completely unknown.

Hypothesis #2: pRb and p107 regulate axon growth and guidance through a cell cycle and cell death independent mechanism.

In this study, we describe a novel function of pRb and p107 in regulating corpus callosum (CC) development. Pocket proteins were found to regulate both the development of the commissural plate and the growth and guidance of callosal axons. As with radial migration, further genetic deletion of Bax has no effect on the axon guidance defect, implying that pRb/p107 regulate CC development though a cell death independent mechanism. Analysis of the developmental progression of the CC defect in pRb/p107 brain shows that delays in axon growth rates and axon disorganization occur prior to and independently of the defect in commissural plate formation, suggesting that an initial defect in axon growth is the primary reason why the CC fails to form in the absence of pRb and p107. In addition, the defects in axon growth are not specific to the midline, but instead persist through the intermediate zone with callosal axons ectopically

entering the ipsilateral cortex. Through the use of in vitro explant cultures and IUE, we confirm that pRb and p107 regulate the rate of neurite extension. In order to identify the mechanism through which pocket proteins regulate CC formation, expression patterns of numerous axon guidance molecules were analyzed and we identified altered expression of Netrin and Neuropilin1 following deletion of pRb and p107. Indeed, we show that Netrin expression is specifically lost from a previously undescribed population of cells in the cingulate cortex of pRb/p107 deficient embryos. These cells could play a significant role in callosal axon guidance during normal development and deserve further investigation. **These findings represent a novel function of pRb in regulating commissural plate development and the growth and guidance of callosal axons.**

CHAPTER 2

Devon S Svoboda, Annie Paquin, David S Park, and Ruth S Slack. (2013). Pocket proteins pRb and p107 are required for cortical lamination independent of apoptosis. *Developmental Biology*. 384(1):101-13.

All experiments were performed by DSS. Experiments were conceptualized by DSS, with assistance from RSS. AP provided invaluable technical assistance with *in utero* electroporation. RSS provided technical training and conceptual insight. The manuscript was written by DSS, in collaboration with RSS.

Pocket proteins pRb and p107 are required for cortical lamination independent of apoptosis.

Devon S. Svoboda[1], Annie Paquin[2,3], David S Park[1], and Ruth S Slack[1]

[1]Department of Cellular and Molecular Medicine/Neuroscience, University of Ottawa, 451 Smyth Road, Ottawa ON, Canada, K1H 8M5
[2] Developmental & Stem Cell Biology, Hospital for Sick Children, Toronto ON, Canada, M5G 1L7
[3] Institute of Medical Science, University of Toronto, Toronto ON, Canada M5G 1L7

Corresponding Author: Ruth S. Slack
Department of Cellular and Molecular Medicine
University of Ottawa
451 Smyth Rd., Ottawa ON, K1H 8M5
Tel: 613-562-5800 x8458
Email: rslack@uottawa.ca

Character count: 35,788
Abstract word count: 191

Keywords: Retinoblastoma, cell cycle, radial migration, pocket proteins.

Abstract

Pocket proteins (pRb, p107 and p130) are well studied in the role of regulating cell cycle progression. Increasing evidence suggests that these proteins also control early differentiation and even later stages of cell maturation, such as migration. However, pocket proteins also regulate apoptosis, and many of the developmental defects in knock out models have been attributed to increased cell death. Here, we eliminate ectopic apoptosis in the developing brain through the deletion of Bax, and show that pocket proteins are required for radial migration independent of their role in cell death regulation. Following loss of pRb and p107, a population of cortical neurons fails to pass through the intermediate zone into the cortical plate. Importantly, these neurons are born at the appropriate time and this migration defect cannot be rescued by eliminating ectopic cell death. In addition, we show that pRb and p107 regulate radial migration through a cell autonomous mechanism since pRb/p107deficient neurons fail to migrate to the correct cortical layer within a wild type brain. These results define a novel role of pocket proteins in regulating cortical lamination through a cell autonomous mechanism independent of their role in apoptosis.

Introduction

Activating neurogenesis is a promising strategy for rehabilitating damage following traumatic injury or neurodegenerative disease. However, to use this therapeutic tool effectively it is crucial to understand the mechanisms which regulate neuronal birth and maturation. The retinoblastoma protein (pRb), together with its two family members p107 and p130, controls cell cycle progression and terminal mitosis (Ferguson and Slack. 2001; Giacinti and Giordano. 2006).

However, it remains unclear whether the pocket protein family plays additional roles in later stages of neuron maturation, such as terminal differentiation and migration.

During normal brain development, the progeny of proliferating neural precursor cells in the ventricular and subventricular zones exit the cell cycle and migrate dorsally through the intermediate zone, into the cortical plate (Nowakowski, et al. 2002). The first neurons born are the Cajal Retzuis cells of layer I (Garcia-Moreno, et al. 2007), which guide later born migrating neurons through secretion of Reelin (Honda, et al. 2011). These later born neurons migrate radially to the top of the cortical plate and reside in an "inside-out" pattern with the youngest neurons in the uppermost layers.

It is now well established that pocket proteins regulate both proliferation and cell death. In addition, increasing evidence suggests that cell cycle proteins also influence later stages of brain development (Nguyen, et al. 2006; Tury, et al. 2011), such as cortical plate formation (Ferguson, et al. 2005; McClellan, et al. 2007). Understanding developmental phenotypes in knockout models is complicated by increased apoptosis following pRb deletion through the E2F1/p53 pathway; thus it is often unknown whether a defect in cell maturation is due to a novel function of pRb or is an indirect result of this ectopic cell death. For example, Ciavarra and colleagues found a defect in pRb-null cardiomyocyte maturation, yet were able to completely rescue the phenotype by preventing apoptosis through expression of the anti-apoptotic protein Bcl2 (Ciavarra and Zacksenhaus. 2010a). In contrast, Chen et al. found that rescuing cell death and through E2F1 deletion does not rescue maturation defects in amacrine cells in the developing retina (Chen, et al. 2007b). Cell death has been shown to cause severe developmental defects in pRb null animals in the retina (Chen, et al. 2004), cerebellum, (Feddersen, et al. 1995; Padmanabhan, et al. 1999; Marino, et al. 2000), and the Organ of Corti (Sage, et al. 2006).

Similarly, in cases where morphological or functional defects were reported in pRb-null cells (Lee, et al. 1994; Sage, et al. 2006), it was often not possible to determine whether these differentiation defects were a secondary result of the increased cell death or represented a separate Rb function. Finally, we have previously shown that pRb deletion led to a defect in cortical lamination, where the delineation between the cortical plate and the intermediate zone was obscured; we were unable to determine whether this phenotype resulted from the established role of pocket proteins in cell death (Ferguson, et al. 2005; McClellan, et al. 2007). As examples of cell death dependent and independent developmental defects have been reported following loss of pocket proteins, the role of pRb and p107 in neuron maturation independent of cell death therefore remains an unanswered question in the field.

In the present study, we asked whether radial migration in the developing cortex is modulated by pocket proteins, independently from their role in cell death regulation. The pRb/p107 double mutants were used to avoid compensatory effects of p107 in pRb deficient tissues (Marino, et al. 2003; Chen, et al. 2004; Berman, et al. 2009). The contribution of apoptosis in the cortical migration phenotype observed in pRb/p107 double mutants, was evaluated by crossing these mice with animals carrying a null allele for Bax, a key apoptotic protein (Gavathiotis, et al. 2012). Here we show a defect in the migration of cortical neurons lacking pocket proteins pRb and p107, which could not be attributed to failed cell cycle exit or unchecked apoptosis. Notably, deletion of Bax did not rescue the defect in radial migration, despite the fact that apoptosis was returned to wild type levels. Furthermore, we show that pocket proteins regulate radial migration through cell autonomous mechanisms since *in utero* electroporation of Cre leads to migration defects in p107/pRb deficient neurons in the context of

an otherwise healthy brain. Overall, we show that pRb and p107 play an essential role in the regulation of radial migration, independent of their role in apoptosis.

Materials and Methods

Mice: pRb/p107 DKO mice were generated by crossing floxed Rb-F19 (Vooijs, et al. 1998; Marino, et al. 2000) with p107 germline knockout mice (LeCouter, et al. 1998). DKO mice were then crossed with Emx1-cre mice (Jackson Laboratories) to delete pRb specifically in the dorsal telencephalon. Mice were maintained on a mixed C57/Bl6/FVBN/Sv129 background and genotyped according to standard protocols with previously published primers for Rb (Jacks, et al. 1992) and p107 (LeCouter, et al. 1998). pRb f/f; p107 −/− females were crossed with pRb f/+; p107 +/−; Emx1-Cre+ males to generate wild type pRb f/+; p107 +/−; Emx1-Cre+ (WT), pRb f/f; p107 +/−; Emx1-Cre+ (RBKO), pRb f/+; p107 −/−; Emx1-Cre+ (p107KO) and double knock out pRb f/f; p107 −/−; Emx1-Cre+ (DKO) littermates. For embryonic time points, the time of plug identification was counted as embryonic day 0.5 (E0.5). Due to pRb autoregulation (Shan, et al. 1994), pRb expression in heterozygous mice is similar to that of wild-type controls. DKO-Bax−/− mice were bred by crossing pRb f/f; p107 −/− mice with Bax −/− mice (Jackson Laboratories) to generate pRb f/f; p107 −/−; Bax −/− females. These females were crossed with pRb f/+; p107 +/−; Bax +/−; Emx1-Cre+ males. These mice were also on a mixed C57/Bl6/FVBN/Sv129 background. All experiments were approved by the University of Ottawa's Animal Care ethics committee, adhering to the Guidelines of the Canadian Council on Animal Care.

Tissue fixation and Cryoprotection: Pregnant female mice were killed with a lethal injection of sodium pentobarbitol. P0 pups were killed by decapitation. Embryos were dissected and fixed overnight in 4% PFA in PBS, pH 7.4, and cryoprotected using a sucrose gradient of 10%, 15% and 20% in PBS. Brains were frozen, and 14-µm coronal cryosections were collected on Superfrost Plus slides (12–550-15; Fisher Scientific).

BrdU labelling and Immunohistochemistry: To mark neurons born at E13.5, a single intraperitoneal injection of BrdU (dissolved in 0.007 N/NaOH in 0.9% NaCl; 50 mg/kg body mass) was given to timed pregnant females at E13.5. Injected females were euthanized at E17.5 or pups were collected on the morning after birth (P0).

For all cell counts, images were taken from matching tissue sections, cut at equivalent locations along the rostro-caudal axis of the brain on the first section where a complete anterior commissure was visible crossing the midline. Images were taken from a portion of the cortex in between the dorsomedial and ventrolateral cortex, just as the cortex begins to slope downwards. For total cell counts, slides were treated with the Dako antigen retrieval protocol according to the manufacturer's protocol for 30 min and treated with combinations of the following antibodies: Cux1 (layers II–IV (Nieto, et al. 2004); 1/100; Santa Cruz), FoxP1 (layers III/IV (Ferland, et al. 2003); 1/750; Abcam), Ki67 (1/100; Cell Marque), Nestin (1/500; Abcam), SatB2 (layers II–IV (Britanova, et al. 2008); 1/500; Abcam), Tbr1 (layer V/VI (Hevner, et al. 2001); 1/1000; Abcam). Once equivalent sections of the cortex were identified and imaged, a 200 µm wide column of cortical tissue (450 µm for FoxP1 counts) was delineated within the image, extending vertically from the top of the cortical plate down through the ventricular zone. All cells expressing the marker of interest within this column were counted and binned according to their

anatomical layer. Cortical layers were identified as follows: layer II was defined as being marked by Cux1 and/or Satb2, but not by FoxP1. Layer III/IV was identified as expressing FoxP1 but not Tbr1. Layers V/VI were defined as expressing Tbr1. For total cell counts, cells were counted as being located either in the upper layers (II–IV) or lower layers (V/VI). For BrdU counts, BrdU detection was performed (Ferguson, et al. 2002), followed by Dako treatment for 15 min. Slides were then treated with combinations of the same antibodies, colabeling with anti-BrdU (1/250; Accurate Chemical and Scientific Corporation). All cells labeled with BrdU+, and with Foxp1 or SatB2 for co-labeling studies, were counted in 150 μm column of the cortex extending vertically from the top of the cortical plate through the ventricular zone, as described above. One-way ANOVA with Bonferroni was performed for all graphs in every figure. Significant differences were assessed at values of $p<0.05$. Four or five animals were used for each genotype at each age.

For Cajal Retzius cell counts, equivalent rostro-caudal sections were stained with Reelin (1/1000; Abcam) and Calretinin (1/500; Swant), two markers of Cajal Retzius cells. Six images of layer I of the cortex were taken from three different brain sections at 40×, covering a total distance of 1400 μm for each embryo. Only cells positive for both Reelin and Calretinin were counted. Cells from the six images were totaled for each animal, and totals for animals of the same genotype were averaged. Four to six animals were used for each genotype.

TUNEL Staining: Apoptotic cells were detected in equivalent rostro-caudal brain sections at E17.5 by Terminal deoxynucleotidyl transferase dUTP nick end labeling (TUNEL) using the Terminal Transferase Recombinant Kit (Roche Applied Science) together with dUTP-16-Biotin (Roche Applied Science) according to the manufacturer's protocol. In each brain, 6 fields of view were counted at 20× and the total number of TUNEL positive cells was totaled for each

animal. Fields of view were located in the same part of the cortex in each animal to ensure consistency. One-way ANOVA with Bonferroni post-hoc comparison test was performed to compare the mean numbers of TUNEL-positive cells and significant differences were assessed at values of $p<0.05$.

Western Blots: Protein was isolated from the dorsal cortex or ganglionic eminence at E15.5 and western blot analyses performed as previously described (Ferguson, et al. 2002) with antibodies directed toward pRb (1/1000; PharMingen), p107 (1/1000; Santa Cruz), Bax (1/1000; Santa Cruz) and β-actin (1/5000; Sigma).

In Utero **Electroporation:** Pups of pregnant DKO females were electroporated at E13.5 with a plasmid containing Cre fused to GFP under control of the pCAAG promoter. The fused Cre was used so that GFP would be localized to the nucleus to facilitate image analysis. Plasmids were prepped using the Qiagen Megaprep Kit, diluted to 2 µg/µl in sterile H_2O and mixed with trace amounts of Trypan Blue dye. The plasmid was injected into the lateral ventricle of the brain using an Eppendorf Femtojet Microinjector and electroporated into the dorsolateral cortex using a BTX ECM 830 Square Wave Electroporator. Animals were sacrificed 4 days later at E17.5. For analysis, electroporated sections at equivalent rostro-caudal levels of the brain, relative to the corpus callosum and anterior commissure, were selected. Tissue sections were treated with hot, non-boiling citric acid for 15 min and then stained with antibodies against GFP (1/4000; Abcam), FoxP1 (1/750) and Tbr1 (1/500). Amplification was performed on the GFP signal using the Avidin–Biotin Complex (ABC) kit according to the manufacturer's protocol (Vector Laboratories). Briefly, following binding of secondary IgG, slides were treated with 3% H_2O_2 for

30 min, followed by incubation with ABC complex for 1 hr. Finally slides were exposed to the Fluorescein Tyramide Reagent (Perkin Elmer) for 10 min. For counts, all GFP+ neurons which had reached the cortex were counted in two sections per brain. Neurons were binned according to whether they were found in layers II, (defined as being dorsal to FoxP1 staining), layer III/IV (within the Foxp1+ layer) or layer V/VI (within the Tbr1+ layer). GFP+ cells below the cortex were counted but not included in calculations since there was no difference between genotypes.

Results

pRb/p107 double knock out (DKO) embryos exhibit a defect in cortical lamination *in vivo*.

We have previously described minor defects in cortical lamination following loss of pRb in the developing brain (Ferguson, et al. 2005; McClellan, et al. 2007). However, members of the pocket protein family are known to compensate for each other in knock out models (Chen, et al. 2004; Haigis, et al. 2006; Berman, et al. 2009), so the full role of pocket proteins in radial migration has never been defined. To characterize the role of pRb and p107 in establishment of the cortical plate, we examined the cortical layers of pRb f/f; p107−/−; Emx1-Cre+ double knockout (DKO), pRb f/f; p107+/−; Emx1-Cre+ single knock out (RBKO), pRb f/+;p107−/−; Emx1-Cre+ (p107KO) and pRb+/f; p107+/−; Emx1-Cre+ wild type (WT) brains at E17.5, with the use of cortical layer-specific markers. Deletion of pRb and p107 was confirmed via Western blot at E15.5 (Figure 2-1A, B). Cortical layers were defined according to the following method: the delineation between the intermediate zone and the cortical plate was defined as the clear line between high cell density and low density according to Dapi staining (Figure 2-1C, D white and red lines), while the delineation between upper and lower layers was defined as the top of Tbr1 staining. Where relevant, layer II was defined as expressing Cux1 but not FoxP1, while layer

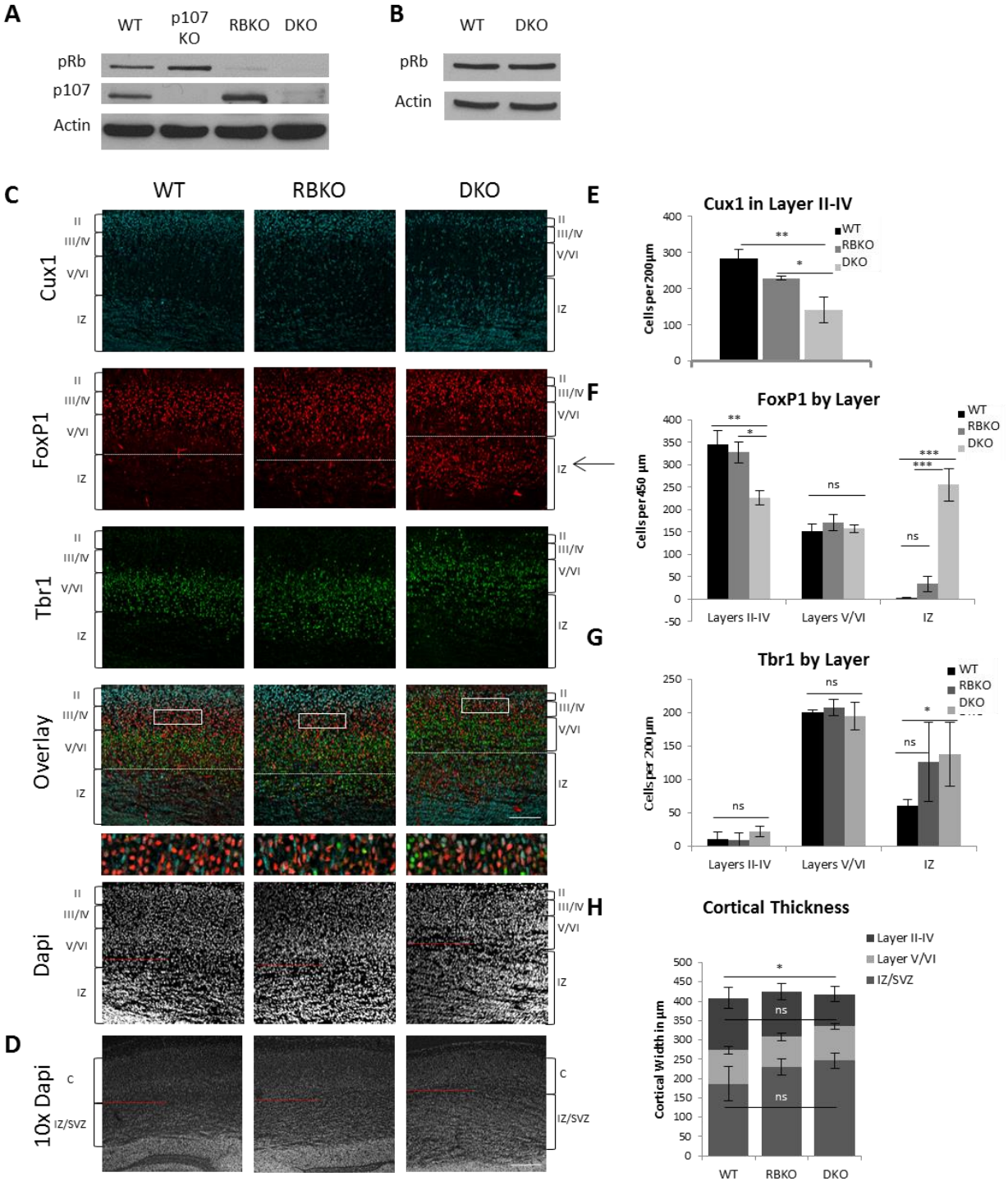
A
WT
p107 KO
RBKO
DKO
pRb
p107
Actin
B
WT
DKO
pRb
Actin
C
WT
RBKO
DKO
Cux1
FoxP1
Tbr1
Overlay
Dapi
II
III/IV
V/VI
IZ
D
10x Dapi
C
IZ/SVZ
E
Cux1 in Layer II-IV
Cells per 200µm
F
FoxP1 by Layer
Cells per 450 µm
Layers II-IV
Layers V/VI
IZ
G
Tbr1 by Layer
Cells per 200µm
H
Cortical Thickness
Layer II-IV
Layer V/VI
IZ/SVZ
Cortical Width in µm

Figure 2-1

Figure 2-1: Cortical neurons are mislocalized in Rb/p107 double knock out (DKO) mice. **A-E)** Expression of cortical layer markers was examined in Rb f/+; p107 +/- (WT), Rb f/f; p107 +/- (RBKO) and Rb f/f; p107 -/- (DKO) brains at E17.5. Brains were stained for Cux1 (blue; marker of layer II), FoxP1 (red; marker of layer III/IV), Tbr1 (green; marker of layer V/VI) and Dapi (gray; nuclear stain). We observed a population of cells expressing FoxP1 in the intermediate zone of DKO embryos (arrow), but not WT or RBKO embryos, with a concurrent decrease in the number of FoxP1+ neurons in layers II-IV of the cortex in DKO brains relative to both RBKO and WT brains **(D)** (layers II-IV were defined as being above the Tbr1+ layers; layers V/VI were defined as expressing Tbr1). Cells were counted in a 450 μm wide (FoxP1) or 450 μm wide (Cux1 and Tbr1) column of cortex extending from the top of the cortical plate to the ventricular zone. The delineation between the cortical plate and intermediate zone, defined using Dapi staining, is shown with a white line (red line in the Dapi panel). An inset is provided below the merged images to show nuclear staining in greater detail. There was a similar decrease in the number of cells expressing Cux1 in DKO brains compared to both WT and RBKO brains **(C)**. Tbr1 cells were found to be disorganized and increased in the intermediate zone but there was no change in the number of Tbr1 cells in the cortical plate **(E)**. Cortical plate width was also found to be decreased in DKO brains compared to WT brains **(F)** as shown at a lower magnification (10x) Dapi image **(B)**. Deletion pRb and p107 expression in the E15.5 cortex was confirmed in the Emx1-cre model by Western blot **(G)**. pRb deletion was specific to the dorsal telencephalon as expected, since it was not deleted in tissue collected for the ventral telencephalon **(H)**. Three to five embryos were used for each phenotype. Error bars show standard deviation. *** $p < .001$ ** $p < .01$ * $p < .05$ Scale bars = 100 μm.

III/IV was defined as expressing FoxP1 but not Tbr1. In DKO animals, where low levels of Tbr1 staining sometimes extended into the upper cortical layers, or there was a scattering of Tbr1+ cells in the upper layers, the delineation between layers was defined as the top of intense, high cell density Tbr1 staining. In WT, p107KO and RBKO brains, upper layer markers FoxP1 (layers III/IV) and SatB2 (layers II–IV) (data not shown) were confined to their expected locations. In DKO brains, however, a population of cells expressing these upper layer markers was found below the cortical plate in the intermediate zone, with a corresponding 34.4% decrease in the average number of FoxP1+ neurons in the upper layers of the cortical plate (Figure 2-1C, F). Note that FoxP1 is normally only expressed in mature neurons which have reached their final location (Ferland, et al. 2003). Cortical lamination in p107KO brains was indistinguishable from that in WT brains (data not shown). These observations suggest that pRb and p107 play a necessary role in radial migration and cortical lamination.

As FoxP1 cell numbers were decreased in the DKO cortical plate, we further investigated whether pocket proteins have a specific role in the development of the upper cortical layers. To test this, we asked whether layer II formed normally, using a more comprehensive upper layer marker CuxI (layers II–IV), which in our wild type mice is found above FoxP1 staining. Our results revealed a 50% decrease in the number of Cux1 cells in layers II–IV of DKO brains compared to WT animals (Figure 2-1C, E). Cux1 counts could not be done in layers V/VI since recently born neurons migrating through this area express Cux1 (Nieto, et al. 2004) and could not be differentiated from misplaced neurons, which failed to migrate correctly.

Interestingly, there was no difference in the number of Tbr1+ neurons in layers V/VI (defined by Dapi staining), although there was an increase in the number of Tbr1+ neurons in the IZ and the Tbr1 layer appeared disorganized in DKO brains (Figure 2-1C, G). Consistent with

the layer specific changes in neuron number, the thickness of the upper layers is reduced in DKO brains relative to WT brains, with no change in the thickness of the lower layers (Figure 2-1D, H). The total thickness of the cortical plate was not different between WT and DKO brains since there was a trend toward an increase in the thickness of the subventricular zone in the DKO to compensate for the decrease in thickness of layers II–IV (Figure 2-1D, H). As the upper layer neurons are visibly split into two populations, with an associated drop in the number of layer II neurons reaching the cortical plate, the migration phenotype in these later born neurons in DKO brains is much more striking and severe than in the early born neurons in the layer V/VI. For this reason, we chose to focus our studies on the formation of layers II–IV. These findings suggest that the pocket proteins pRb and p107 are required for the proper migration or specification of upper cortical layer neurons.

One potential explanation for this defect in lamination is that radial migration is delayed due to a delay in cell cycle exit. If neurons migrate normally following a delayed cell cycle exit, the defect should be corrected with further development. To determine if these migrating neurons reach their layer II/IV destination at a later age, we examined cortical lamination two days later at P0. At this later time point, misplaced FoxP1+ neurons were still found in the intermediate zone of DKO, but not RBKO or WT brains (Figure 2-2A, D). Importantly, the numbers of FoxP1+ cells in the intermediate zone at P0 and at E17.5 were similar, with 256±40 FoxP1+ cells in DKO brains at E17.5, and 293±43 FoxP1+ cells in this same region at P0, indicating that there is not even a small rescue of this phenotype. Furthermore, there was still a 33% decrease in the number of FoxP1 neurons (Figure 2-2D) and a 41% decrease in the number of Cux1 neurons (Figure 2-2C) in the upper layers of DKO brains relative to WT brains, as well as a 40% decrease in thickness of the upper layers (Figure 2-2F). As seen at E17.5, there was an increase

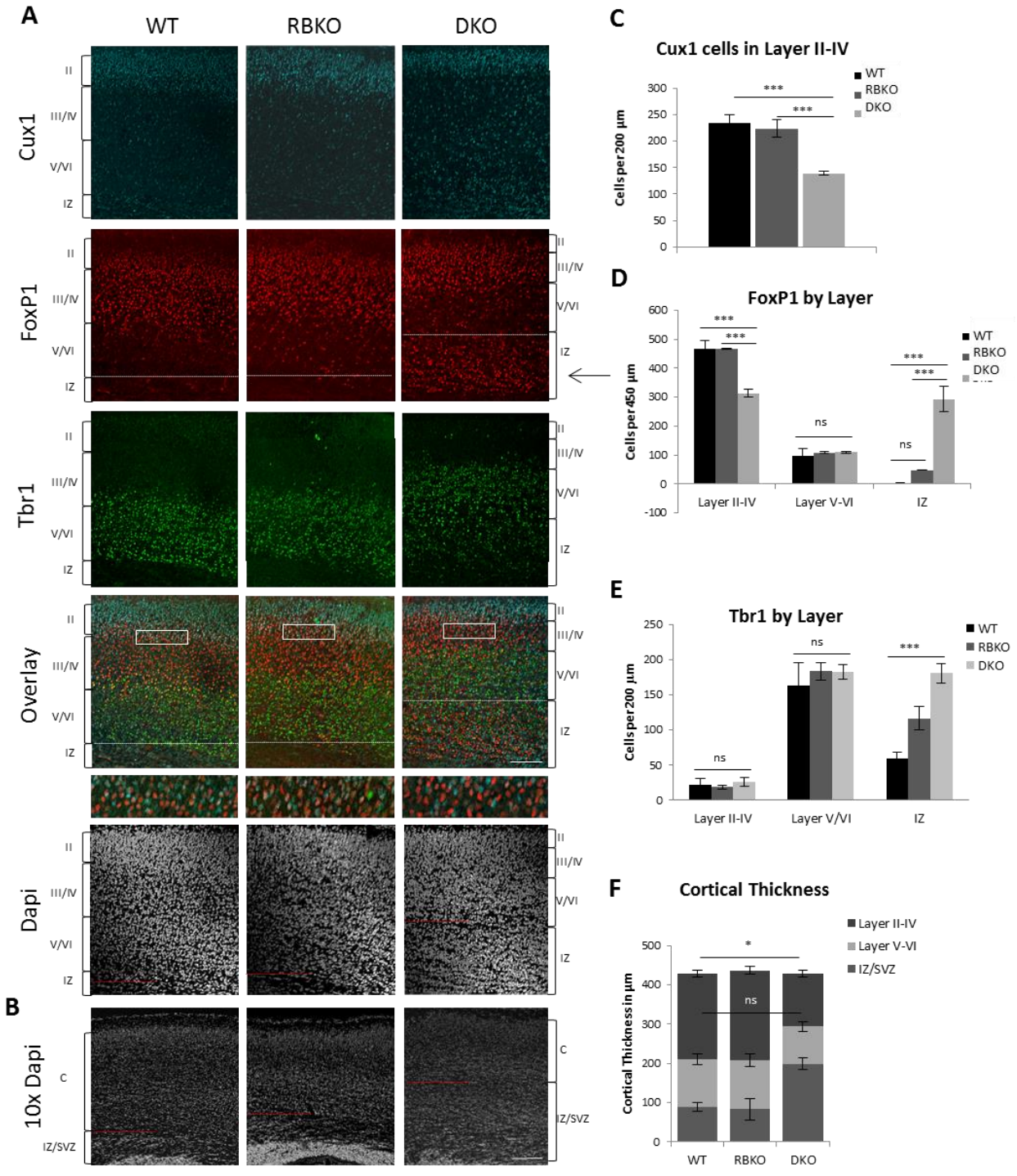
A
WT
RBKO
DKO
Cux1
FoxP1
Tbr1
Overlay
Dapi
II
III/IV
V/VI
IZ
B
10x Dapi
C
IZ/SVZ
C
Cux1 cells in Layer II-IV
Cells per 200 µm
WT
RBKO
DKO
***
D
FoxP1 by Layer
Cells per 450 µm
ns
Layer II-IV
Layer V-VI
IZ
E
Tbr1 by Layer
Cells per 200 µm
Layer V/VI
F
Cortical Thickness
Cortical Thickness in µm
Layer II-IV
Layer V-VI
IZ/SVZ
*

Figure 2-2

Figure 2-2: Cortical neuron mislocalization is not corrected. To determine whether the migration defect was due to a delay in migration, expression of cortical layer markers was examined at P0. Brains were stained for Cux1 (blue; marker of layer II), FoxP1 (red; marker of layer III/IV), Tbr1 (green; marker of layer V/VI) and Dapi (gray; nuclear stain) **(A)**. The population of FoxP1 cells in the intermediate zone of DKO embryos seen at E17.5 (Figure 1) was still present at P0 **(D)**, and there was still a decrease in FoxP1 cells **(D)** and Cux 1 cells **(C)** within the cortical plate. Cells were counted in a 450 μm wide (FoxP1) or 450 μm wide (Cux1 and Tbr1) column of cortex extending from the top of the cortical plate to the ventricular zone. The delineation between the cortical plate and intermediate zone, defined using Dapi staining, is shown with a white line (red line in the Dapi panel). An inset is provided below the merged images to show nuclear staining. Cortical plate width was also found to be decreased in DKO brains compared to WT brains **(F)** as shown at a lower magnification (10x) Dapi image **(B)**.

in the thickness of the subventricular zone in DKO brains to compensate for this decrease in the thickness of the upper layers. Again, there was no detectable decrease in the number of Tbr1 neurons within layer V/VI, although there was an increase in Tbr1+ neurons in the intermediate zone (Figure 2-2E). Although it would have been useful to determine if cortical lamination was corrected at P7, when migration is complete in the mouse, this was not possible due to neonatal lethality of the DKO pups. Together, these findings show that the misplacement of the cortical neurons in DKO brains is not due to a delay in migration. Again, since delayed migration due to delayed cell cycle exit would have been corrected, this data also indicates that the errors in migration in the DKO are unlikely to result simply from delayed cell cycle dynamics in affected cells.

Pocket proteins are required for radial migration of upper layer neurons. To resolve whether the Foxp1+ cells in the DKO intermediate zone were fated for the cortical plate, we performed a birthdating assay to determine if these neurons had exited the cell cycle at a time appropriate for neurons of the upper cortical layers. Pregnant mothers were injected with BrdU at E13.5 and embryos were collected at E17.5 or P0. BrdU injection was done at E13.5 because, on our mouse background strain, this time point revealed the highest level of colocalization with upper layer markers, while later injections at E15.5 targeted neurons still migrating through the intermediate zone. We then analyzed the location of neurons born at E13.5 to determine whether these neurons had migrated into the cortex or remained stalled in the intermediate zone. In WT and RBKO brains, 78.6±8% and 83.9±11% of the BrdU+ cells were found in the cortical plate, respectively, while only 43.7±5% of the BrdU+ cells reached the cortical plate in the DKO brains (Figure 2-3A, B). Due to variation in BrdU labeling between litters, total BrdU+ cell

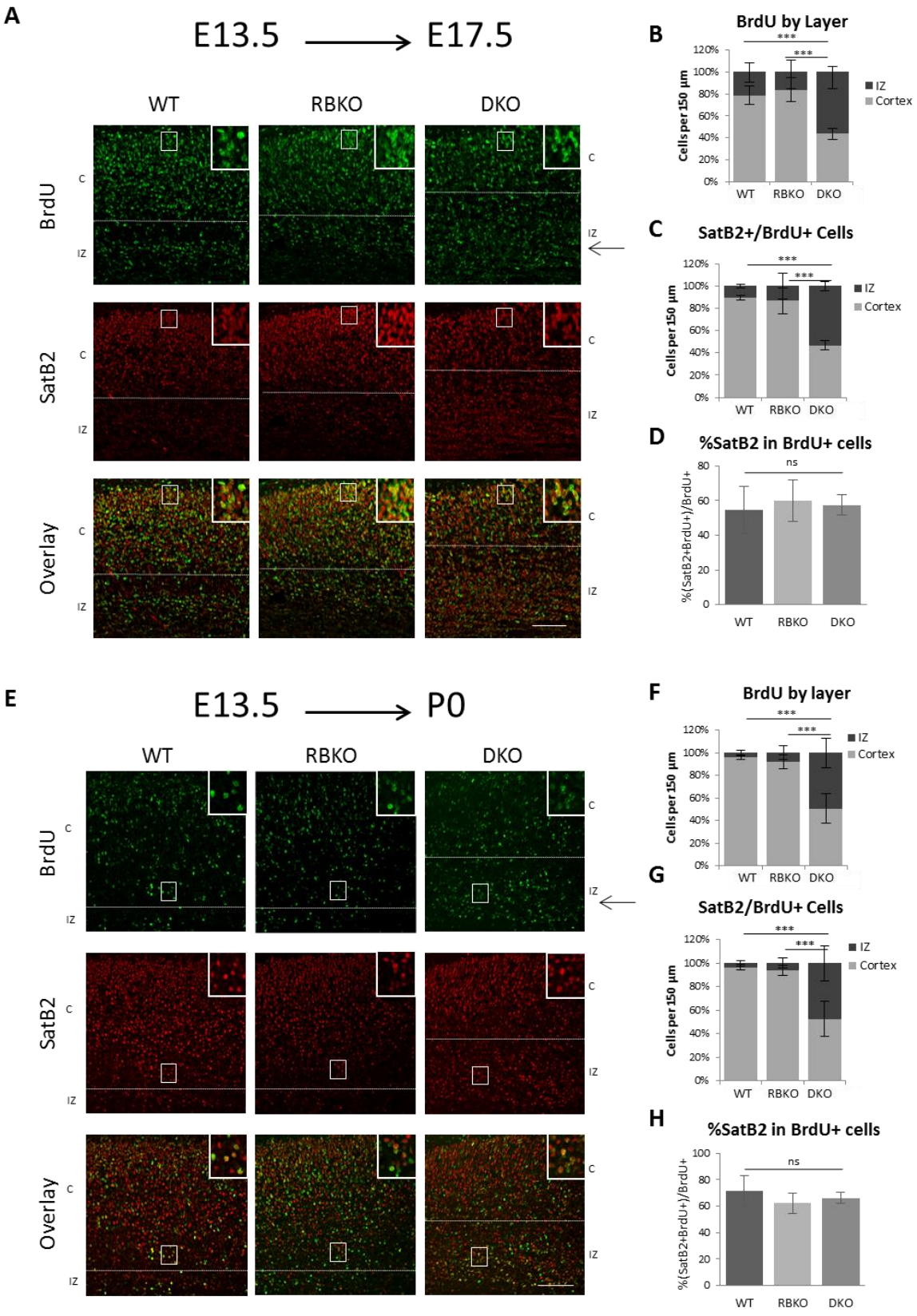
A
E13.5 ⟶ E17.5
WT
RBKO
DKO
BrdU
SatB2
Overlay
C
IZ
B
BrdU by Layer
Cells per 150 µm
IZ
Cortex
C
SatB2+/BrdU+ Cells
D
%SatB2 in BrdU+ cells
%(SatB2+BrdU+)/BrdU+
ns
E
E13.5 ⟶ P0
F
BrdU by layer
G
SatB2/BrdU+ Cells
H
%SatB2 in BrdU+ cells

Figure 2-3

Figure 2-3: Misplaced neurons exhibit a defect in radial migration. A,E) To determine if cells born 4 days ago were located in the correct layer and expressed the correct cortical layer markers, pregnant moms were injected with BrdU at E13.5 and pups collected at E17.5 **(A)** and P0 **(E)**. The delineation between the cortical plate and intermediate zone, defined using Dapi staining, is shown with a white line. Brains were stained for BrdU incorporation (green) and SatB2 (red), a marker for layers II-IV. An inset is provided to show double labelling. Cells were counted in a 150 μm wide strip of cortex extending from the top of the cortical plate to the ventricular zone. Approximately 50% of the BrdU+ neurons remain in the intermediate zone in DKO brains at both ages, while only 5-20% of these BrdU+ cells stay in the intermediate zone in RBKO and WT brains (see text for exact percentages) **(B,F)**. Arrows **(A,E)** indicate the increase in BrdU staining in the intermediate zone of DKO brains. Similar values were obtained at both E17.5 and P0 when the percentages of BrdU+/SatB2+ **(C,G)** or BrdU+/FoxP1+ cells **(D,H)** in the intermediate zone and cortical plate were quantified. Three to five embryos were used for each phenotype. Error bars show standard deviation. *** $p < .001$ ** $p < .01$ * $p < .05$ Scale bars = 100 μm.

counts for all layers ranged from 248±46 (average±SD) cells in DKO brains, 186±74 in RBKO, and 250±102 in WT. At P0, 97.6±2% of BrdU+ cells reached the cortical plate in WT brains, but only 51.8±1% of BrdU+ cells reached the same destination in DKO brains (Figure 2-3E, F). Total cell counts ranged between 208±24 in DKO, 177±27 in RBKO and 149±40 in WT. Similar results were found when the locations of double stained BrdU+/SatB2+ (Figure 2-3C, G) or BrdU+/FoxP1+ (data not shown) cells were quantified, with 91±33 FoxP1+/BrdU+ and 133±43 SatB2+/BrdU+ total cells counted per brain regardless of genotype or age. There was no difference in the percentage of BrdU+ cells which co-labeled with SatB2 at either E17.5 or P0, indicating that the identity of the cells born at E13.5 is similar in WT and DKO brains (Figure 2-3D, H). These results show that the misplaced Foxp1+ cells in the intermediate zone of DKO brains were born at the correct time for upper layer cortical neurons, but were unable to migrate to the correct location. This evidence supports the hypothesis that pocket proteins play a direct role in regulating radial migration.

Misplaced neurons in the DKO intermediate zone have exited the cell cycle. Many of the developmental phenotypes described in pRb mutants result from defects in cell cycle exit, even in cells expressing markers normally associated with terminal differentiation (Chen, et al. 2004; Haigis, et al. 2006; Berman, et al. 2009). To determine whether the migration defect in DKO embryos results from misplaced neurons having failed to exit the cell cycle, we injected pregnant mothers with BrdU at E13.5 and collected brains at E17.5, as described above, and examined whether BrdU+ neurons expressed the cell cycle progression marker Ki67. We found that 98±0.4% of BrdU+ cells in DKO brains no longer expressed Ki67 (Figure 2-4), compared to 99.8±0.1% of BrdU+ cells in WT brains (203±55 cells counted per brain). Although there are

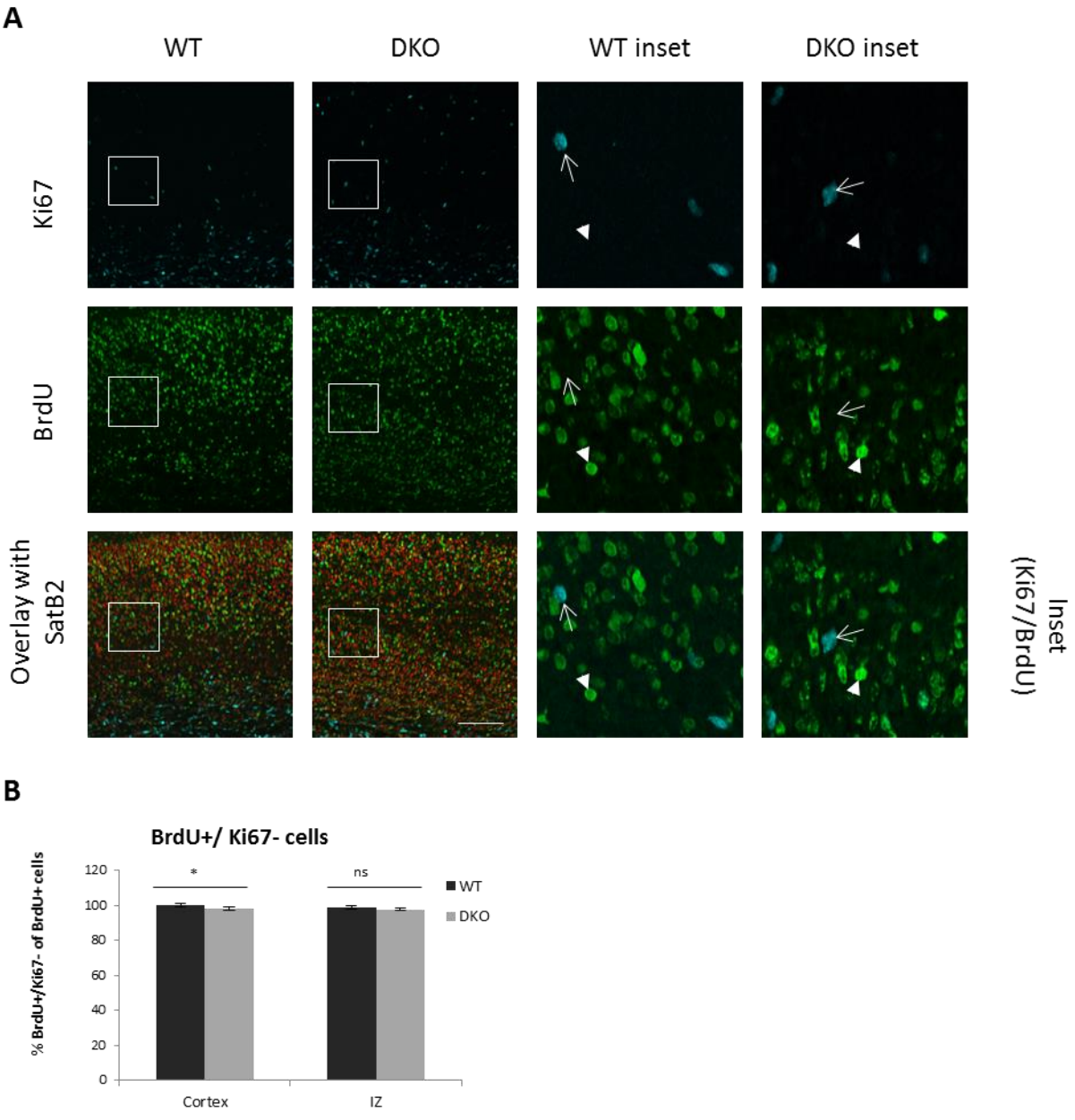
A
WT
DKO
WT inset
DKO inset
Ki67
BrdU
Overlay with SatB2
Inset (Ki67/BrdU)
B
BrdU+/ Ki67- cells
% BrdU+/Ki67- of BrdU+ cells
120
100
80
60
40
20
0
*
ns
WT
DKO
Cortex
IZ

Figure 2-4

Figure 2-4: Assessment of cell cycle exit in misplaced neurons of DKO brains. (A) To determine if misplaced neurons in the intermediate zone inappropriately express the marker of cell cycle progression Ki67, pregnant moms were injected at E13.5 and pups collected at E17.5. Sections were stained for BrdU incorporation (green), Ki67 (blue) and SatB2 (red). The percentage of BrdU+ cells, born 4 days prior to tissue collection, which do not stain for Ki67 was quantified **(B)**. Cells were counted in a 450 µm wide strip of cortex extending from the top of the cortical plate to just above the subventricular zone. In both WT and DKO brains, at least 97% of the BrdU+ neurons did not express Ki67, indicating that they have left the cell cycle. High magnification insets (right side of **A**) show examples of a BrdU+/Ki67- neurons (arrowheads) and BrdU-/Ki67+ neurons (arrows). Overlay is shown with SatB2 staining to show the location of the layers. Three to five embryos were used for each phenotype. Error bars show standard deviation.* $p < .05$ Scale bars = 100 µm.

significantly more Ki67+/BrdU+ cells in DKO brains, these cells represent such a small percentage of the total BrdU+ cells that they could not account for the observed migration phenotype. Furthermore, the 2% of BrdU+ cells which do express Ki67 were evenly distributed throughout the cortex and intermediate zone, rather than concentrated in the intermediate zone like the misplaced FoxP1+ neurons. Together, the observations that radial migration does not correct with time and that misplaced neurons have exited the cell cycle by E17.5, suggest that the defect in migration in DKO brains is not due to ectopic proliferation or a failure to exit the cell cycle.

Inhibition of cell death does not rescue the migration defect in DKO neurons. pRb loss has been shown to lead to increased apoptosis which may cause or accentuate many of the phenotypes described in RBKO mutants (Lee, et al. 1994; Feddersen, et al. 1995; Chen, et al. 2004; MacPherson, et al. 2004; Berman, et al. 2009; Wu, et al. 2009; Ciavarra and Zacksenhaus. 2010a), while in other cases maturation defects are cell death independent (Chen, et al. 2007b). It remains an outstanding question whether pocket proteins regulate post-mitotic cell maturation directly or if this role is attributable to the role of pRb in apoptosis. We have previously shown that the defect in radial migration in the RBKO mutant coincides with a decrease in Cajal Retzius cells (Ferguson, et al. 2005; McClellan, et al. 2007). However, it remains unknown whether the defect in radial migration shown in Figure 2-1 and Figure 2-2 is a result of deregulated apoptosis following loss of pRb and p107, or whether these pocket proteins regulate radial migration directly. To determine whether migration is impaired in DKO brains due to increased apoptosis and subsequent loss of a crucial migratory signal, we crossed the pRb/p107 DKO mice with Bax −/− mice to generate DKO;Bax −/− mice and examined cortical lamination at E17.5. First, we

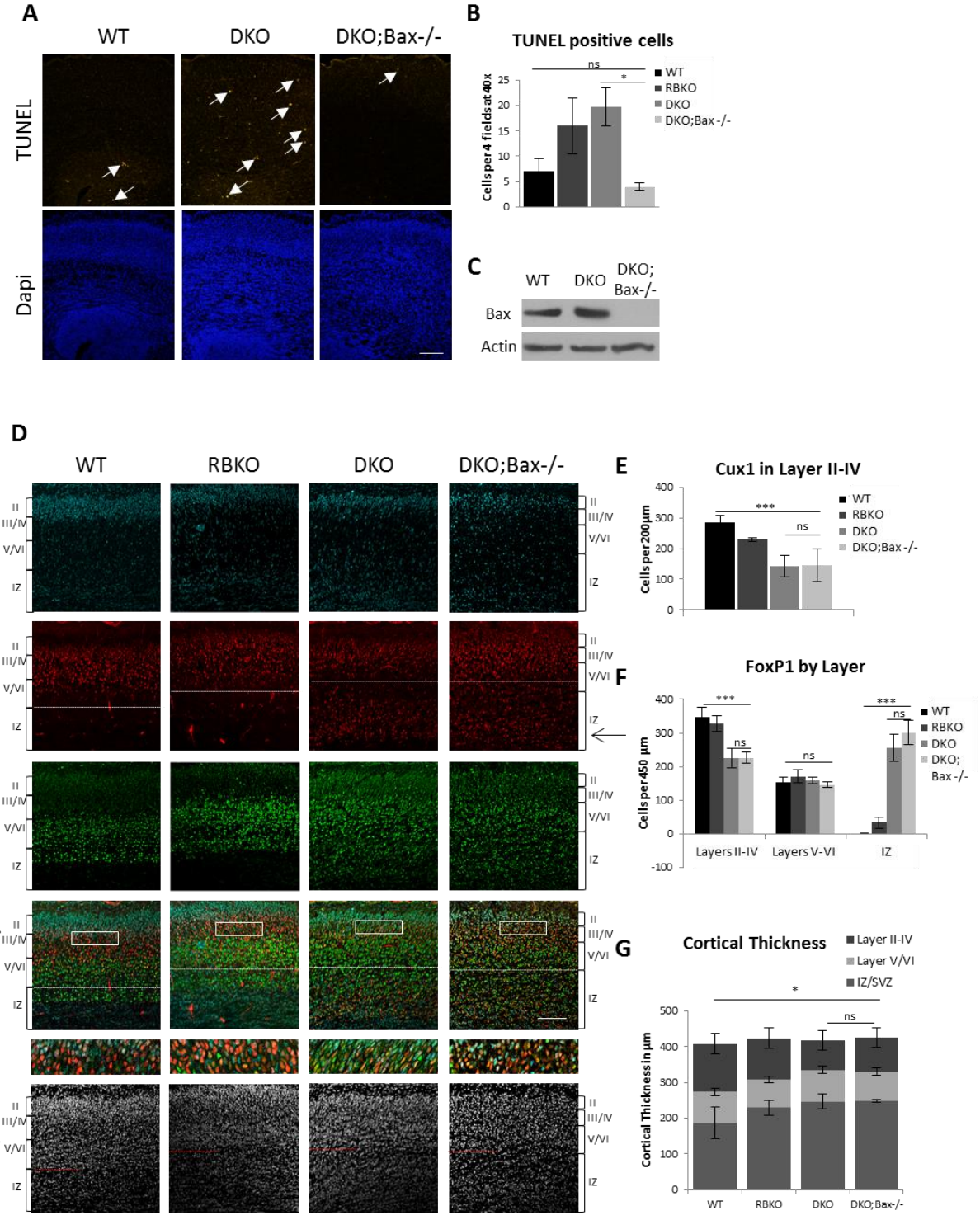
A
WT
DKO
DKO;Bax-/-
TUNEL
Dapi
B
TUNEL positive cells
ns
*
WT
RBKO
DKO
DKO;Bax -/-
Cells per 4 fields at 40x
C
WT
DKO
DKO; Bax-/-
Bax
Actin
D
WT
RBKO
DKO
DKO;Bax-/-
Cux1
FoxP1
Tbr1
Overlay
Dapi
II
III/M
V/VI
IZ
III/IV
E
Cux1 in Layer II-IV
***
ns
Cells per 200µm
F
FoxP1 by Layer
Cells per 450 µm
Layers II-IV
Layers V-VI
IZ
DKO; Bax -/-
G
Cortical Thickness
Layer II-IV
Layer V/VI
IZ/SVZ
Cortical Thickness in µm

Figure 2-5

Figure 2-5: The migration defect in DKO brains is not due to increased cell death. To determine if the migration defect is due to increased apoptosis, cortical lamination was examined DKO-Bax-/- brains at E17.5. **(A,B)** TUNEL staining was used to confirm that the increase in cell death seen in DKO brains was returned to wild type level in DKO-Bax-/- brains. **(C)** Deletion of Bax in cortical tissue was confirmed by Western blot at E17.5. **(D)** Cortical lamination was examined by staining for Cux1 (blue; marker of layer II), FoxP1 (red; marker of layer III/IV), Tbr1 (green; marker of layer V/VI) and Dapi (gray; nuclear stain). The delineation between the cortical plate and intermediate zone, defined using Dapi staining, is shown with a white line (red line in the Dapi panel). The population of FoxP1+ cells in the intermediate zone of DKO brains is maintained in DKO-Bax-/- brains (arrow). Quantification of FoxP1 cells **(F)**, Cux1 cells **(E)**, and cortical width **(G)** showed no difference between DKO and DKO-Bax brains, indicating that rescuing cell death failed to rescue these phenotypes. Quantifications were done the same way as those described in Figure 1. Error bars show standard deviation. *** $p < .001$ ** $p < .01$ * $p < .05$ Scale bars = 100 μm.

used TUNEL staining to confirm that the increased levels of cell death seen in DKO brains was rescued to wild type levels following deletion of Bax (Figure 2-5A–C). We then asked if cortical migration was rescued in DKO;Bax−/− brains by staining for layer specific markers. Deletion of Bax did not rescue the migration defect, as no differences in cortical lamination or layer specific cell counts could be found between DKO and DKO;Bax−/− embryos (Figure 2-5D–G) (counts were performed as described for Figure 2-1). Specifically, DKO;Bax−/− brains have an average of 302±36 FoxP1+ neurons stalled in the intermediate zone, with a corresponding 35% decrease in the number of FoxP1+ neurons in layers II–IV compared to WT. There is a 50% decrease in the number of Cux1+ cells in the upper layers and a 30% decrease in cortical thickness compared to WT, as seen in absence of pRb/p107 alone. Loss of Bax alone could therefore not account for these phenotypes, as there was no difference in FoxP1 or Cux1 cell number or localization, or cortical thickness between Bax+/+ and Bax−/− brains (these brains were wild type for pRb and p107) (Figure 2-S1). This evidence indicates that apoptosis cannot account for the migration defect in DKO embryos and that pocket proteins influence cortical lamination and neuron migration through a mechanism that is independent from its role in regulating neuron survival.

Pocket proteins regulate cortical migration through a combination of cell autonomous and environmental mechanisms. Given that the migration defect could not be rescued by inhibition of apoptosis, we next asked whether pocket proteins regulate radial migration through a cell autonomous mechanism, or whether the migration defect is the result of a failing environment. We have previously shown a decrease in Cajal Retzius cells in pRb mutants (Ferguson, et al. 2005; McClellan, et al. 2007). As we had hypothesized that loss of the migratory signal Reelin

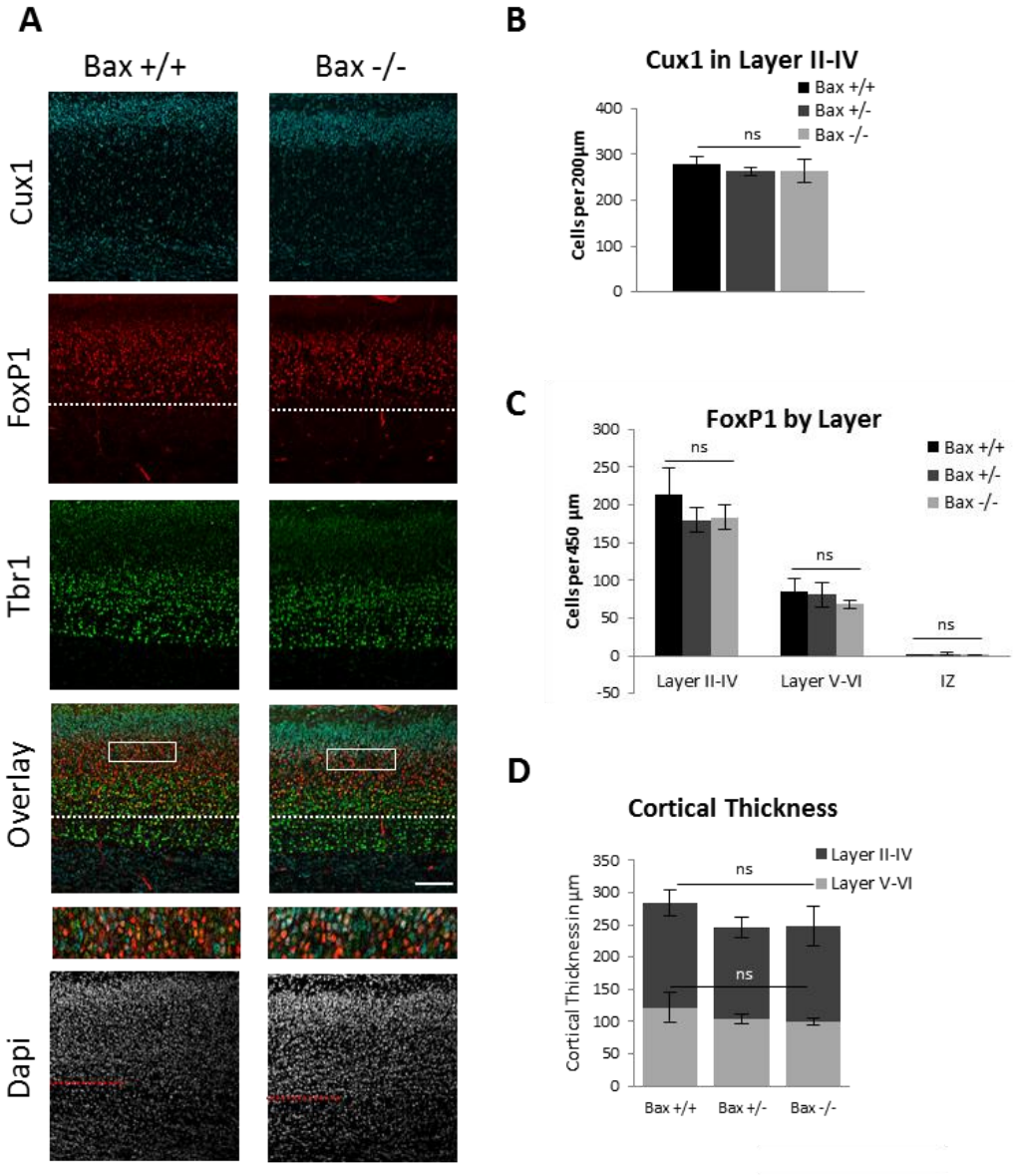
A
Bax +/+
Bax -/-
Cux1
FoxP1
Tbr1
Overlay
Dapi
B
Cux1 in Layer II-IV
Bax +/+
Bax +/-
Bax -/-
ns
Cells per 200µm
400
300
200
100
0
C
FoxP1 by Layer
Bax +/+
Bax +/-
Bax -/-
Cells per 450 µm
300
250
200
150
100
50
0
-50
ns
ns
ns
Layer II-IV
Layer V-VI
IZ
D
Cortical Thickness
Layer II-IV
Layer V-VI
Cortical Thickness in µm
350
300
250
200
150
100
50
0
ns
ns
Bax +/+
Bax +/-
Bax -/-

Figure 2-S1

Figure 2-S1: Cortical lamination is not effected by deletion of Bax. To determine whether deletion of Bax led to a radial migration phenotype in brains wild type for pRb and p107, cortical lamination was examined at E17.5 by staining for Cux1 (blue; marker of layer II-IV), FoxP1 (red; marker of layer III/IV), Tbr1 (green; marker of layer V/VI) and Dapi (gray; nuclear stain) (**A**). Quantification of FoxP1 cells (**C**), Cux1+ cells (**B**), and cortical thickness (**D**) showed no difference between Bax+/+ and Bax−/− brains. Quantifications were done the same way as those described in Figure 2-1. Error bars show standard deviation. ns = not significant, Scale bars=100 μm.

from these Cajal Retzius cells might account for the lamination defect in RBKO brains, we asked whether there was a further decrease in Cajal Retzius cells in DKO and DKO-Bax−/− brains. Surprisingly, Cajal Retzius cells were similarly decreased in both RBKO and DKO embryos, but the migration defect is specific to DKO brains. Staining with two markers of Cajal Retzius cells, Reelin and Calretinin, revealed a 65% and 58% decrease in DKO and RBKO, respectively, which was not rescued by Bax deficiency (also a 65% decrease in DKO;Bax−/− brains) (Figure 2-6A, B). These results show that Cajal Retzius cell loss cannot explain the migration phenotype and that pocket proteins regulate migration through an alternative mechanism.

The radial glial scaffold provides structural support for migrating neurons. To determine whether defects in this scaffold are responsible for the migration phenotype in DKO brains, we asked whether this scaffold is intact in DKO brains by staining for Nestin. We found that the glial scaffold appeared normal in both DKO and WT brains (Figure 2-S2), indicating that these cells are unlikely to be involved in the migration defect in DKO brains.

Cortical migration depends on a complex array of environmental factors, such as secreted migratory cues (e.g. Reelin), intact radial glial scaffolding, as well as cell autonomous factors, such as migratory cue receptors and regulation of cytoskeletal dynamics. To further pursue the mechanism by which pocket proteins modulate cortical migration, we asked whether their role in migration was cell autonomous. To address this question, we performed *in utero* electroporation to track the migration of Rb/p107 deficient neuroblasts in the context of a healthy environment, where migratory cues remain intact. Embryos (Rbf/f; p107−/− and Rbf/+; p107+/−) were electroporated with Cre-GFP at E13.5, and brains were collected 4 days later at E17.5. The efficiency of Cre mediated recombination was confirmed both *in vivo* and *in vitro* (Figure 3-3). The location of GFP+ neurons relative to cortical layer markers FoxP1 and Tbr1 was analyzed.

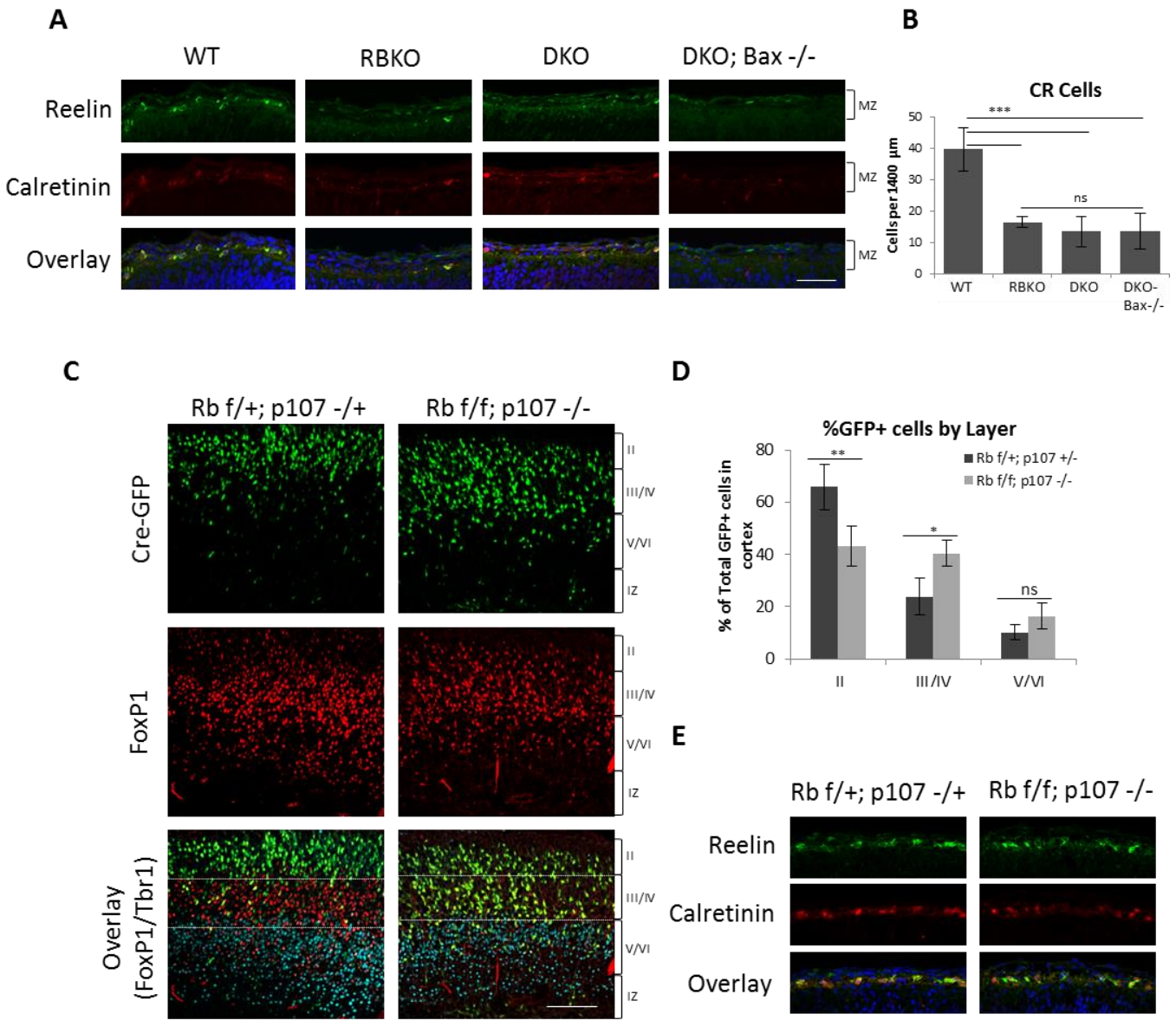
A
WT
RBKO
DKO
DKO; Bax -/-
Reelin
Calretinin
Overlay
MZ
B
CR Cells
***
ns
Cells per 1400 µm
WT
RBKO
DKO
DKO-Bax-/-
C
Rb f/+; p107 -/+
Rb f/f; p107 -/-
Cre-GFP
FoxP1
Overlay (FoxP1/Tbr1)
II
III/IV
V/VI
IZ
D
%GFP+ cells by Layer
Rb f/+; p107 +/-
Rb f/f; p107 -/-
% of Total GFP+ cells in cortex
**
*
ns
II
III/IV
V/VI
E
Rb f/+; p107 -/+
Rb f/f; p107 -/-
Reelin
Calretinin
Overlay

Figure 2-6

Figure 2-6: Pocket proteins regulate radial migration through a cell autonomous mechanism. A,B) To determine if the migration defect correlated with a decreased in Cajal Retzius cells, WT, RBKO and DKO brains were stained for Reelin (green) and Calretinin (red) at E17.5. All double labeled layer I cells were counted in a total of 1400µm per brain **(B)**. White lines outline layer I to distinguish from background staining in meninges. Scale bars = 50 µm. **C)** To determine if pocket proteins regulate radial migration cell autonomously, pRb f/f;p107-/- and pRb f/+;p107-/+ embryos were electroporated in utero at E13.5 and brains were collected at E17.5. The location of GFP+ neurons was quantified according to cortical layer. Layer II was defined as being above FoxP1 staining (red), layer III/IV was defined as within FoxP1 staining, above Tbr1 (blue) and layer V/VI was defined as within the Tbr1positive layer **(D)**. We show that a portion pRb and p107 deficient neurons fail to reach layer II but instead remain in layer III/IV. **E)** Cajal Retzius cells were normal in all electroporated brains, which emphasizes that Reelin signaling is not involved in this migration defect. *** $p < .001$ ** $p < .01$ * $p < .05$ Scale bars = 100 µm.

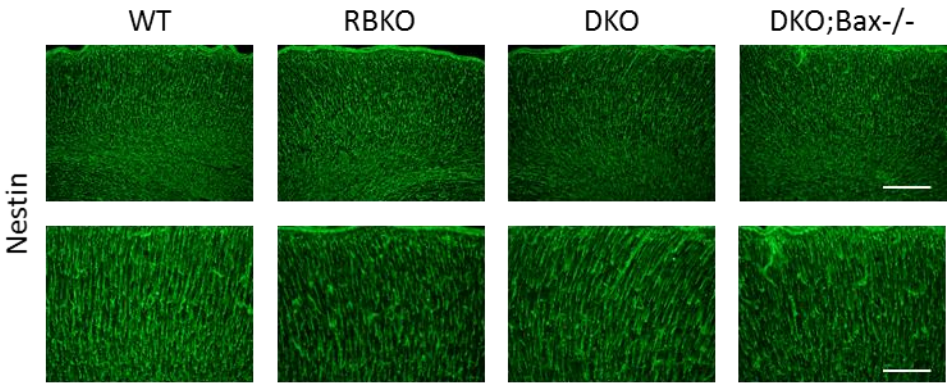

Figure 2-S2

Figure 2-S2: The radial glial scaffold is intact in DKO and DKO;Bax−/− brains. To determine if the migration defect in DKO brains is due to disorganization of the radial glia, WT, RBKO, DKO and DKO;Bax−/− brains were stained for Nestin at E17.5. No difference in the integrity of the scaffold could be seen between phenotypes. Top panels, scale bar=200 μm. Lower panels, scale bar=100 μm.

In WT brains, 65.8±8.7% GFP+ neurons migrated to layer II, and 23.9±7.1% were found in layer III/IV (Figure 2-6C, D). In DKO brains, however, only 43.2±7.6% of GFP+ neurons reached layer II, with 40.4±4.9% of GFP+ neurons scattered throughout layers III/IV. A minimum of 250 cells were counted for each brain. Layer II was defined as being above the FoxP1+ layer, while layer III/IV was defined as being within the FoxP1+ layer, above the Tbr1+ layer. There was no difference in the number of GFP+ neurons in the intermediate zone between the two phenotypes, and no defect was seen in electroporated RBKO brains (data not shown). Unlike in conditional knockouts (Figure 2-6A), here there was no difference in the number of Cajal Retzius cells between pRb f/f;p107−/− and wild type electroporated brains (Figure 2-6E). Given that pRb/p107 deficient neurons failed to migrate correctly in a healthy environment, we conclude that pocket proteins are essential to modulate radial migration through a cell autonomous mechanism.

Discussion

In this study, we evaluated the role of pocket proteins pRb and p107 in the regulation of radial migration in the developing cortex. Our results support a number of conclusions. First, we present a novel defect in radial migration which is specific to the pRb/p107 DKO brains. We then show that this defect is not due to unchecked cell death, despite the importance of pocket proteins in regulating apoptosis. Finally, we show that pRb and p107 regulate radial migration through a combination of cell autonomous and non-cell autonomous mechanisms. These results are summarized in Table 2-1. Together, our results describe a novel function of pocket proteins in regulating cortical plate formation in the developing brain.

Table 2-1: Phenotype Summary

	WT	RBKO	DKO	DKO;Bax-/-
FoxP1+ neurons in IZ	-	-	++	++
Thinning of Cux+ layer	-	+	++	++
BrdU+ cells in IZ	-	-	++	ND
Loss of CR cells	-	+	+	+
GFP+ neurons in layer III/IV following IUE	-	-	+	ND

Negative sign indicates not observed, + indicates mild phenotype, and ++ indicates severe phenotype.
IZ = Intermediate Zone CR = Cajal Retzius ND = Not Done

pRB and p107 are required for radial migration in the developing cortex. pRb is known to play a variety of roles during brain development, namely control of cell cycle progression, apoptosis and early fate specification (Jacks, et al. 1992; Ferguson and Slack. 2001; MacPherson, et al. 2004; Vanderluit, et al. 2004; McClellan and Slack. 2006; Wu, et al. 2009; Ghanem, et al. 2012a). Indeed, we have shown that pRb regulates early differentiation factors and tangential migration in ventrally derived neurons (Ferguson, et al. 2005; Andrusiak, et al. 2011; Ghanem, et al. 2012a), independently of its role in proliferation. pRb was also shown to be involved in cortical lamination as deletion of pRb caused the normally well-organized delineation between cortical plate and intermediate zone to become indistinct (McClellan, et al. 2007). However, p107 has been shown to compensate for loss of pRb in various models (Marino, et al. 2003; Chen, et al. 2004; Haigis, et al. 2006; Berman, et al. 2009). Pocket proteins may therefore have additional roles in neuron maturation which could not be detected in single knock-out models. To address this issue, we used the pRb/p107 double knock out (DKO) mouse to test the hypothesis that pocket proteins have more extensive roles in radial migration in the developing brain.

Here we show a defect in radial migration in DKO brains with a concurrent decrease in the number of upper layer neurons within the cortical plate. Our data implies that the phenotype in DKO brains is due to a primary defect in migration rather than the result of a delay in cell cycle exit for two reasons. First, if the misplaced neurons were migrating normally but were delayed because they exited the cell cycle late, they would continue migration and approach their destination at P0 (Figure 2-2), which does not occur. Second, the misplaced neurons do not express the cell cycle marker, Ki67 (Figure 2-4); at E17.5, only 2% of the migrating population exhibited ectopic proliferation. Together, these findings suggest that the defect in radial

migration does not result from failed cell cycle exit. Whether this migration defect results from other cell cycle related mechanisms, such as delayed exit, disruption of polarity or impaired precursor differentiation cannot be determined at this time and requires further investigation.

In this study we have focused on the migration defect in the upper layers neurons of DKO brains. However, there is also a defect in lamination in the lower layers as seen by the increased Tbr1+ neurons in the IZ of RBKO and DKO at E17.5 (Figure 2-1). Interestingly, this defect appears to be distinct from that seen in the upper layers, since there is no decrease in the number of Tbr1+ neurons which reach the cortical plate in DKO brains, as is seen with FoxP1+ and Cux1+ neurons. Likewise there is no difference in the thickness of the lower cortical layers between DKO and WT brains. For these reasons, the defect in formation of layers V/VI cannot result solely from Tbr1+ neurons failing to migrate through the intermediate zone. An alternate possibility is that pocket proteins control the relative rates of proliferation during development such that neurogenesis is increased early when layers V/VI are formed, but later slows when layers II–IV are formed. This increase in neurogenesis would then account for the increased Tbr1+ neurons in the intermediate zone, rather than, or in addition to, a defect in migration of these neurons. At this point it is only possible to conclude that pocket proteins regulate formation of upper cortical layers differently than the formation of lower cortical layers and further analysis is required to understand the responsible mechanisms.

Pocket protein regulation of radial migration does not depend on cell death. pRb was first identified as a tumor suppressor and has been extensively studied in its role in regulation of cell division and apoptosis (Chen, et al. 2004; Lazzerini Denchi and Helin. 2005; Giacinti and Giordano. 2006; Ciavarra and Zacksenhaus. 2010a; Gordon and Du. 2011; Manning and Dyson.

2012). Ectopic cell death has been shown to contribute to many developmental phenotypes in pRb knockout models (Feddersen, et al. 1995; Marino, et al. 2003; MacPherson, et al. 2004; Chen, et al. 2004; Sage, et al. 2006; Berman, et al. 2009; Ciavarra and Zacksenhaus. 2010a). Increased apoptosis found in pocket protein knock out models is primarily due to deregulated E2F1 activity and subsequent activation of the p53 pathway (Macleod, et al. 1996; Lazzerini Denchi and Helin. 2005; Wu, et al. 2009), although increased apoptosis has been found to sometimes be p53 and even E2F1 independent in the retina (MacPherson, et al. 2004; Chen, et al. 2013). pRb has also been shown to be crucial for survival in post-mitotic neurons (Andrusiak, et al. 2012a). This dual role of pRb in regulating both cell proliferation and death has obscured our understanding of other important developmental roles of pocket proteins. It was therefore unclear whether the migration phenotype in the DKO brains was due to death of cells providing regulatory signals necessary for radial migration, or whether it represented a primary migratory function of pocket proteins. To resolve this question, we eliminated this ectopic apoptosis through deletion of the apoptotic regulator Bax (Gavathiotis, et al. 2012) in the DKO and determine whether the defect radial migration persisted. Surprisingly, despite the fact that cell death was successfully restored to wild type levels in the DKO;Bax−/− brains (Figure 2-5A), none of the migratory phenotypes described in DKO brains were rescued by Bax deletion (Figure 2-5D–G; Table 2-1). The FoxP1+ cells are still present in the intermediate zone of these DKO;Bax−/− brains and the upper cortical layers were still thinner, indicating that this migration defect does not result from apoptosis. Furthermore, a migration defect was observed in GFP+ neurons following *in utero* electroporation of Cre (see below); because these neurons migrate in a healthy environment, and have clearly survived, cell death does not seem to be involved. This

shows that, in the developing brain, pocket proteins regulate migration and apoptosis through separate, independent mechanisms.

Pocket proteins have a cell autonomous role in radial migration. We have previously shown that Cajal Retzius cells are decreased in the RBKO mouse and hypothesized first, that these cells were lost to apoptosis, and second that their loss was responsible for the minor defect in radial migration. However, we show here that deletion of Bax fails to rescue these Cajal Retzius cells (Figure 2-6A) and that there was no difference in the number Cajal Retzius cells between RBKO and DKO mice (Figure 2-6B). There are two possible explanations for the absence of Cajal Retzius cells in DKO brains; these cells could either be lost through an alternative apoptotic pathway or there could be a defect in their differentiation following loss of pRb and p107. Further experimentation is necessary in order to distinguish between these scenarios. More importantly, the fact that both RBKO and DKO brains show the same decrease in Cajal Retzius cell number while only DKO brains have a migration defect implies that the loss of Cajal Retzius cells cannot explain why a subset of DKO neurons fails to pass through the intermediate zone.

Radial migration is dependent on numerous factors which can be categorized as being either cell autonomous or non-cell autonomous. Here we show that pocket proteins control radial migration through a cell autonomous mechanism independent of environmental factors through the use of *in utero* electroporation, as the pRb and p107 deficient neurons failed to migrate correctly through a healthy cortical plate. It should be noted that these animals are genome knockouts for p107. However, since there is no migration phenotype following p107 deletion (data not shown) and there is no apparent defect in cortical lamination in non-electroporated

regions of the pRb flox/flox;p107−/− electroporated brains, we conclude that the defect requires the loss of both pRb and p107 in GFP+ neurons.

Following pRb deletion in electroporated pRb flox/flox;p107−/− brains, GFP+ neurons reach the cortical plate but are highly disorganized, while in DKO Emx1-Cre brains the misplaced neurons fail to migrate past the intermediate zone. One possible explanation for this difference is that pRb and p107 regulate migration through a combination of cell autonomous and non-cell autonomous mechanisms. In electroporated brains, the pRb/p107 deficient neurons may have been able to reach the cortex since environmental support was still intact, while in the full cortex knockout both environmental and cell autonomous mechanisms were compromised. For example, it is possible that, in the DKO;Emx1-Cre+ cortex, the cell autonomous defect makes these neurons more sensitive to the drop in Reelin and this contributes to their failure to migrate through the intermediate zone, while in the RBKO cortex the low levels of Reelin are sufficient. Another possibility is that the time required for Cre to be expressed, excise pRb and for pRb target genes to become deregulated, allows neurons electroporated at E13.5 to have time to pass through the intermediate zone and into the cortical plate before migration is disrupted. Further experimentation is required to fully understand the mechanism through which pocket proteins regulate cortical migration.

These results represent the first description of a cell autonomous role of pRb in radial migration in the developing cortex. We have shown in previous work that pRb is involved in tangential migration of ventrally derived immature interneurons, also in a cell autonomous manner through regulation of the Netrin receptor Neogenin (Ferguson, et al. 2005; McClellan, et al. 2007; Andrusiak, et al. 2011). When considered together, these studies suggest that neither phenotype is a single phenomenon but that pRb may regulate migration in a wide variety of cell

types. It remains to be determined whether pocket proteins control migration in non-neural cells, or whether migration is regulated through similar mechanisms in different cell types. Further exploration into the mechanisms through which pocket proteins regulate cell migration in various tissues will greatly increase our understanding of how this protein family influences both normal development and tumor formation.

In conclusion, these results demonstrate that pocket proteins are required for radial migration. This is achieved through a combination of cell autonomous and environmental factors which are independent of cell death. These finding strongly support our hypothesis that pocket proteins are important in later stages of neuron maturation through mechanisms independent of their role in cell cycle progression or apoptosis.

Acknowledgements

We are indebted to Pierre Mattar and Freda Miller for their assistance with the *in utero* electroporation. We thank Linda Jui, Angela Nguyen, and Jason G. MacLaurin for excellent technical assistance. Equipment was supported by the Centre for Stroke Recovery.

This work was supported by a CIHR grant to R.S.S.

CHAPTER 3

Devon S Svoboda, Alysen Clark, David D Park, and Ruth S Slack. (2015). Induction of Protein Deletion Through *In Utero* Electroporation to Define Deficits in Neuronal Migration in Transgenic Models. *Journal of Visual Experiments.* (95), e51983, doi:10.3791/51983.

All experiments were performed by DSS. Experiments were conceptualized by DSS, with assistance from RSS. AC provided technical assistance. RSS provided technical training and conceptual insight. The manuscript was written by DSS, in collaboration with RSS. Special thanks to Benson Fong for image credit.

Induction of Protein Deletion Through *In Utero* Electroporation to Define Deficits in Neuronal Migration in Transgenic Models

Devon S. Svoboda[1], Alysen Clarke[1], David S Park[1], and Ruth S Slack[1]

[1]Department of Cellular and Molecular Medicine/Neuroscience, University of Ottawa, 451 Smyth Road, Ottawa ON, Canada, K1H 8M5

Corresponding Author: Ruth S. Slack
Department of Cellular and Molecular Medicine
University of Ottawa
451 Smyth Rd., Ottawa ON, K1H 8M5
Tel: 613-562-5800 x8458
Email: rslack@uottawa.ca

Character count: 25,957
Abstract word count: 238

Keywords: Developmental Biology, Issue 95, *In utero* electroporation, brain development, neural migration, transgenic, cell autonomous, mouse model.

Abstract

Genetic deletion using the Cre-Lox system in transgenic mouse lines is a powerful tool used to study protein function. However, except in very specific Cre models, deletion of a protein throughout a tissue or cell population often leads to complex phenotypes resulting from multiple interacting mechanisms. Determining whether a phenotype results from disruption of a cell autonomous mechanism, which is intrinsic to the cell in question, or from a non-cell autonomous mechanism, which would result from impairment of that cell's environment, can be difficult to discern. To gain insight into protein function in an *in vivo* context, *in utero* electroporation (IUE) enables gene deletion in a small subset of cells within the developing cortex or some other selected brain region. IUE can be used to target specific brain areas, including the dorsal telencephalon, medial telencephalon, hippocampus, or ganglionic eminence. This facilitates observation of the consequences of cell autonomous gene deletion in the context of a healthy environment. The goal of this protocol is to show how IUE can be used to analyze a defect in radial migration in a floxed transgenic mouse line, with an emphasis on distinguishing between the cell autonomous and non-cell autonomous effects of protein deletion.

By comparing the phenotype resulting from gene deletion within the entire cortex versus IUE-mediated gene deletion in a limited cell population, greater insight into protein function in brain development can be obtained than by using either technique in isolation.

Video Link

The video component of this article can be found at http://www.jove.com/video/51983/

Introduction

Radial migration is a central process to early cortical development. It depends on a variety of cell autonomous factors, such as correct mitotic exit and neuronal differentiation, cell polarity, regulation of cytoskeletal dynamics and expression of transmembrane receptors, as well as non-cell autonomous factors, such as formation of the radial glial scaffold and secretion of migratory guidance molecules (Evsyukova, et al. 2013; Hippenmeyer. 2014; Wu, et al. 2014). Since disruption of any of these mechanisms can impair neuronal migration in a transgenic mouse model (Nguyen, et al. 2006; McClellan, et al. 2007; Hashimoto-Torii, et al. 2008a; Ori-McKenney and Vallee. 2011; Svoboda, et al. 2013), determining the underlying cause of a defect in migration can be a complex and difficult process. *In utero* electroporation (IUE) can be used to complement and simplify interpretation of the phenotype of a genetic knock-out model and thereby elucidate important mechanisms required for radial migration (Wang, et al. 2007b; Heng, et al. 2008; Hashimoto-Torii, et al. 2008a; Alfano, et al. 2011). *In utero* electroporation (IUE) is the process by which a plasmid carrying both a gene of interest and a reporter is injected into the ventricle in the brain of a mouse or rat embryo and then drawn into the cells lining the ventricle through use of an electric current (Saito. 2006; De Vry, et al. 2010; Dixit, et al. 2011). This allows the investigator to analyze the effect of up or down regulation of a gene of interest in development or function of electroporated neurons. Following IUE, brains can be processed for immunohistochemistry (Wang, et al. 2007b; Heng, et al. 2008; Hashimoto-Torii, et al. 2008a; Alfano, et al. 2011), electrophysiology (Elias, et al. 2008) or cell culture (Rice, et al. 2010; Bhuiyan, et al. 2013). The major advantage of IUE is that is allows for highly specific manipulation of gene expression. Furthermore, IUE can be used to target a specific region of the developing brain through a directed current (Figure 3-2). IUE can also be used to target a

specific cell type through injection of plasmids carrying genes under control of various promoters or plasmid activation systems (tetracycline induced gene expression is an example) (Miyagi, et al. 2004; Wang, et al. 2007b; Heng, et al. 2008; LoTurco, et al. 2009; Yoshida, et al. 2010). IUE can be used in conjunction with the Cre-Lox mediated gene excision system (Hashimoto-Torii, et al. 2008a; Ori-McKenney and Vallee. 2011; Alfano, et al. 2011; Wang, et al. 2011; Bouabe and Okkenhaug. 2013). A plasmid containing a gene encoding the message for the Cre protein can be electroporated into an embryo homozygous for the floxed allele (in which the gene or specific DNA regions are flanked by two *loxP* sites for Cre mediated DNA recombination). Cre will then induce recombination of the gene of interest specifically in electroporated neural precursors, generating a knock-out of the floxed allele. The effect of protein knockdown on neural migration and development within individual neurons can then be studied. Electroporation of Cre induces recombination in only a small population of affected cells, leaving the supporting environment intact. In contrast, tissue specific expression of Cre under control of a cell type specific promoter, occurs throughout the entire tissue so that both migrating neuroblasts and the surrounding environment could be affected. Thus, juxtaposition of these two approaches can determine whether a given migration defect is due to cell autonomous or cell non-autonomous mechanisms. Defective migration in both experimental systems suggests that the observed phenotype results from a cell autonomous mechanism; normal migration following electroporation of Cre with defective migration in a tissue specific Cre model indicates that the gene of interest is acting through a non-cell autonomous mechanism.

IUE can also be used to perform rescue experiments by electroporating potential interacting genes into knock out animals (Heng, et al. 2008; Hashimoto-Torii, et al. 2008a; Wang, et al. 2011). For example, an investigator could attempt to rescue a migration phenotype

in a transgenic model by electroporating a downstream target and determining if the migration defect is corrected in the electroporated neurons. This has the additional benefit that a successful rescue indicates that normal migration can be restored by manipulating protein expression in a specific neuron, even though the surrounding environment is still deficient for the targeted gene. Again, this approach is more time and cost effective than crossing or generating transgenic lines, with the added benefit of determining whether the defective mechanism is cell autonomous.

IUE can be used to track migrating neurons through electroporation of a reporter plasmid into knock out embryos (Figure 3-4C). As only the neurons lining the ventricle at the time of surgery are electroporated (Rice, et al. 2010), IUE can be used to follow the neurons born at a specific time with the advantage of visualization of their morphology *in vivo*.

Finally, it is possible to use IUE to target brain regions such as the medial or dorsal telencephalon, hippocampus or ganglionic eminence (Figure 3-2). This gives researchers the power to investigate gene function in a specific area independent of complications resulting from protein knockdown in neighboring structures.

Retinoblastoma protein (pRb), p107 and p130 comprise the pocket protein family and are well established regulators of cell cycle exit. However, there is increasing evidence that these proteins also regulate cell cycle independent aspects of neural development. As we have previously shown, pRb and p107 play a crucial role in both tangential (Ferguson, et al. 2005; McClellan, et al. 2007) and radial migration (Svoboda, et al. 2013). Here, we demonstrate the role of pocket protein family members pRb and p107 on neural migration (Svoboda, et al. 2013) to exemplify the use of *in utero* electroporation of Cre in a transgenic model. In summary, IUE provides a powerful way of analyzing cell autonomous effects of gene deletion (or

overexpression). When combined with tissue specific knock out models, IUE can provide additional information regarding the mechanisms controlling neural migration.

Procedure

NOTE: All experiments were approved by the University of Ottawa's Animal Care ethics committee, adhering to the Guidelines of the Canadian Council on Animal Care.

1. Pre-surgical Preparation and Materials

    1.1. Plasmid Preparation:

        1.1.1. Prepare plasmids using the Qiagen MegaPrep according to the manufacturer's protocol. Innoculate at least 400 ml of LB broth with transformed bacteria to ensure a high DNA yield and incubate overnight.

        1.1.2. Resuspend plasmid in 100-200 µl TE to a final concentration of at least 5 µg/µl. Aliquot DNA and store at -20 °C. If the concentration is too low, do not precipitate and resuspend as this can add impurities. Start over with a new preparation.

        1.1.3. Before surgery, dilute a single plasmid (Cre-GFP for example) to 2 µg/µl in sterile water with 1 µl of 0.1% (w/v) Fast Green dye per 10 or 20 µl of diluted plasmid solution. If GFP and the gene of interest are to be co-electroporated on separate plasmids, inject the GFP plasmid and the plasmid carrying the gene of interest at a ratio of 1:4 to maximize the likelihood that all cells marked with GFP are co-electroporated with both plasmids.

    1.2. Pull glass microcapillary tubes (1 mm outer diameter - hereafter referred to as needles) on a standard needle puller, using a single step pull at 62 °C.

1.3. Autoclave a surgical pack containing the following: needle holders, wound retractor, forceps, scissors for surgery, scissors for needles, stapler, staples, gauze, wound covers, surgical drapes (Figure 3-1A, B; Materials Table 3-1).

1.4. Collect other required tools: Electroporator, Femtojet Microinjecter, Tweezertrodes (5 or 7 mm), saline, suture, 5 ml syringe (Materials Table 3-1).

2. Prepare Mouse for Surgery

2.1. For pain management, inject a timed-pregnant mouse with Buprenorphine (0.05 mg/kg body weight) one hour before surgery. Apply this protocol to mice timed anywhere from embryonic day 12.5 (E12.5) to E17.5.

2.2. Use microloader pipette tips to back-load pulled needles with the plasmid solution. Do not fill all the way into the tip of needle yet as this will cause the needle to become clogged.

2.3. Anaesthetize mouse using 2-5% isoflurane gas with 1 L/min O2. Once immobile, place in face mask and apply ointment to eyes to prevent drying. Inject with 1 ml saline (0.9% NaCl) subcutaneously in back.

NOTE: When working with isoflurane gas, use a gas scavenger to recapture excess gas and prevent it from escaping into the room.

2.4. Shave abdomen. Wash abdomen with Chlorohexadine scrub, rinse with water, and apply a final prep solution of chlorohexadine and 70% ethanol. Cover mouse with sterile drape or gauze to cover fur but leave abdomen exposed (Figure 3-1C, D).

3. *In utero* Electroporation

3.1. Make an incision in the skin over the abdomen between the lower teats. Pull the skin away from the underlying muscle layer by tearing the connective tissue, then cut

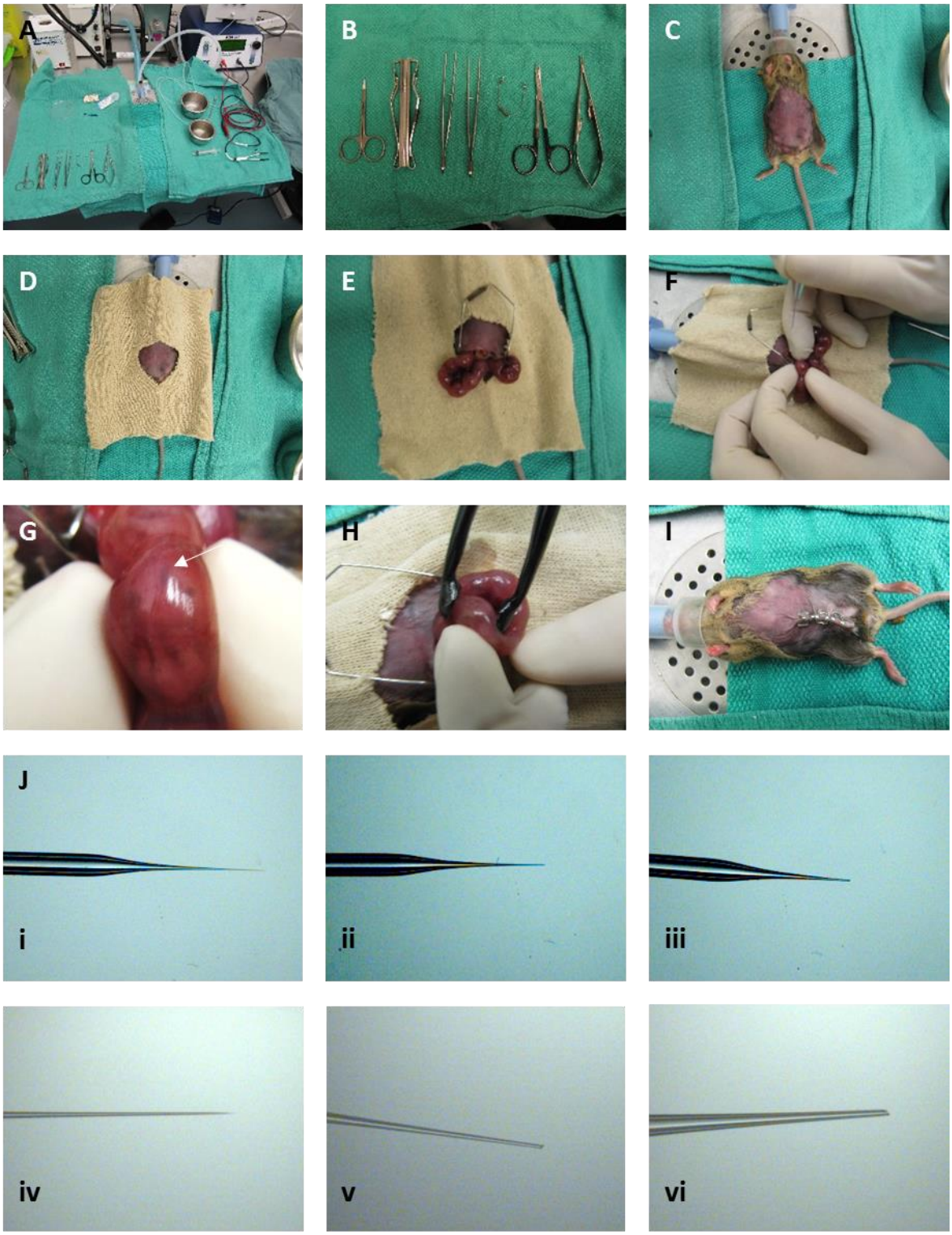

Figure 3-1

Figure 3-1: Performing *In Utero* Electroporation. A) Sterile surgical set up. **B)** Surgical tools from left: fine scissors for cutting needle tips; stapler; forceps; wound retractor; surgical scissors; needle holder. **C)** Prepped pregnant mouse with shaved and disinfected abdomen. **D)** Mouse covered with sterile drape prior to incision. **E)** Uterus with E13.5 embryos removed from abdominal cavity. **F)** Injecting pups in the ventricle. **G)** Close up of injected pup; note the blue crescent on the embryo's head indicating that the ventricle was successfully injected with the plasmid solution (arrow). H) Paddles are placed to electroporate the lateral cortex. **I)** Mouse post-surgery. **J)** Preparing sharp needles is a crucial part of *in utero* electroporation. Examples of uncut needles **(i, iv)**, good needles **(ii, v)** and poor needles **(iii, vi)** are shown at low **(i-iii)** and high **(iv-vi)** magnification.

Table 3-1: Equipment and Materials

Product Name	Company	Catalog Number	Description	Autoclave
ECM 830 Square Wave Electroporator	BTX Harvard Apparatus	**45-0052**	Electroporator only – buy cables separately (45-0204)	
1250FS Footswitch for ECM 830	BTX Harvard Apparatus	45-0211	Foot paddle is necessary for hands-free electroporation	
Tweezertrodes	BTX Harvard Apparatus	**45-0489 (5mm) 45-0488 (7mm)**	Platinum forcep style electrodes	
Femtojet	Eppendorf	920010504	Microinjector	
Griphead 0	Eppendorf	920007414	Holds the pulled needle	
Universal Capillary Holder	Eppendorf	920007392	Connects griphead to tube	
Injection Tube	Eppendorf	920007431	Connects capillary holder to Femtojet	
Foot Control	Eppendorf	920005098	Foot paddle for hands-free injection	
Microloader Tips	Eppendorf	930001007	Tips for loading the pulled capillary tubes	
Plasmid Mega Kit	Qiagen	12181	5 QIAGEN-tip 2500, Reagents, Buffers	
Fast Green FCF	Sigma-Aldrich	F7252-5G	Non-toxic dye	
Extra Fine Bonn Scissors	Fine Science Tools	14084-08	For trimming the needles	X
Bonn Strabismus Scissors	Fine Science Tools	14084-09		X
Graefe Forceps	Fine Science Tools	11050-10	Straight	X
Colibri Retractors	Fine Science Tools	17000-03		X
Stapler	Fine Science Tools	12031-07	For 7mm clips	X
Castroviejo Needle Holder	Medical Tools	SNH-6737	Straight, with lock	X
Needle Puller	Narishige	PC-10	For pulling microcappillaries	
Microcapillaries	Drummond	1-000-800	0.4 mm inner diameter glass capillary tubes	

through the peritoneum into the abdominal cavity along the linea alba. Insert the wound retractor to pull the edges of the wound apart.

3.2. Remove the uterus from the abdominal cavity and lay it out as shown (Figure 3-1E).

3.2.1. If different pups are to be injected with different plasmids (such as GFP *vs.* GFP with the gene of interest), count the pups on each side and decide which ones and how many to inject with each plasmid. Replace one side of the uterus back into the abdomen to keep the embryos warm and lubricated. Immediately moisten the exposed uterus with saline (preferably warmed to body temperature).

3.2.2. If injecting all pups with the same plasmid (such as when injecting Cre-GFP into transgenic embryos) only remove one horn of the uterus at a time.

3.3. Put a loaded needle in the grip head of the injection wand and carefully cut the tip with a pair of small surgical scissors or fine forceps. Cut the tip so the needle stays as long as possible while still allowing fluid to pass through (Figure 3-1Ji-iv).

3.3.1. Adjust length of injection (in seconds) and injection pressure on the microinjector so that a small yet easily visible droplet of 0.1-0.2 µl appears on the tip of the needle when the foot paddle is pressed. Keep the volume of this droplet as consistent as possible between different needles.

NOTE: this step is crucial for embryo survival (see discussion).

3.3.2. Use the following injection parameters for the Femtojet: injecting pressure (pi) = 250-300 hPa; injection time (ti) = 0.8-1.2 sec; compensation pressure = 10-50 hPa. If required, adjust these parameters to accommodate variation between needles.

3.4. Select an embryo and gently position it on its back, head tilted upward (Figure 3-1F).

NOTE: This may require turning or shifting the embryo; be careful not to apply too much pressure and avoid rupture of the amniotic sac while manipulating the embryo.

3.5. Once the embryo is in place, locate the ventricle, which presents as a crescent shaped shadow parallel to the sagittal sinus. Touch the tip of the needle to the uterus above the ventricle at a slight angle and guide the needle through the uterine wall. The amount of pressure required depends on the sharpness of the needle. Push the needle through the cortex into the ventricle.

NOTE: Although there is rarely any additional detectable resistance, the embryo's head is often pushed away slightly and then recoils as the needle passes through the cortex into the ventricle.

3.6. Pump the foot paddle to inject the plasmid solution. Continue to pump until a green area is visible and conforms to the arc shape of the ventricle (Figure 3-1G). In young embryos (E12.5 to E14.5) the dye will often diffuse into the contralateral ventricle.

NOTE: The number of pumps depends on the diameter of the needle tip, the age of the embryo (and resulting size of the ventricle) and the desired injection volume. Keep volume injected as consistent as possible between embryos.

3.7. Inject three or four embryos. Keep all exposed embryos moist with saline throughout procedure.

3.8. Go back to the first embryos injected and place the paddles such that the positive electrode will draw the plasmid into the desired region of the brain (Figure 3-1H). Angle the negative electrode so that the shortest path between the electrodes passes directly through the structure targeted for electroporation (Figure 3-2).

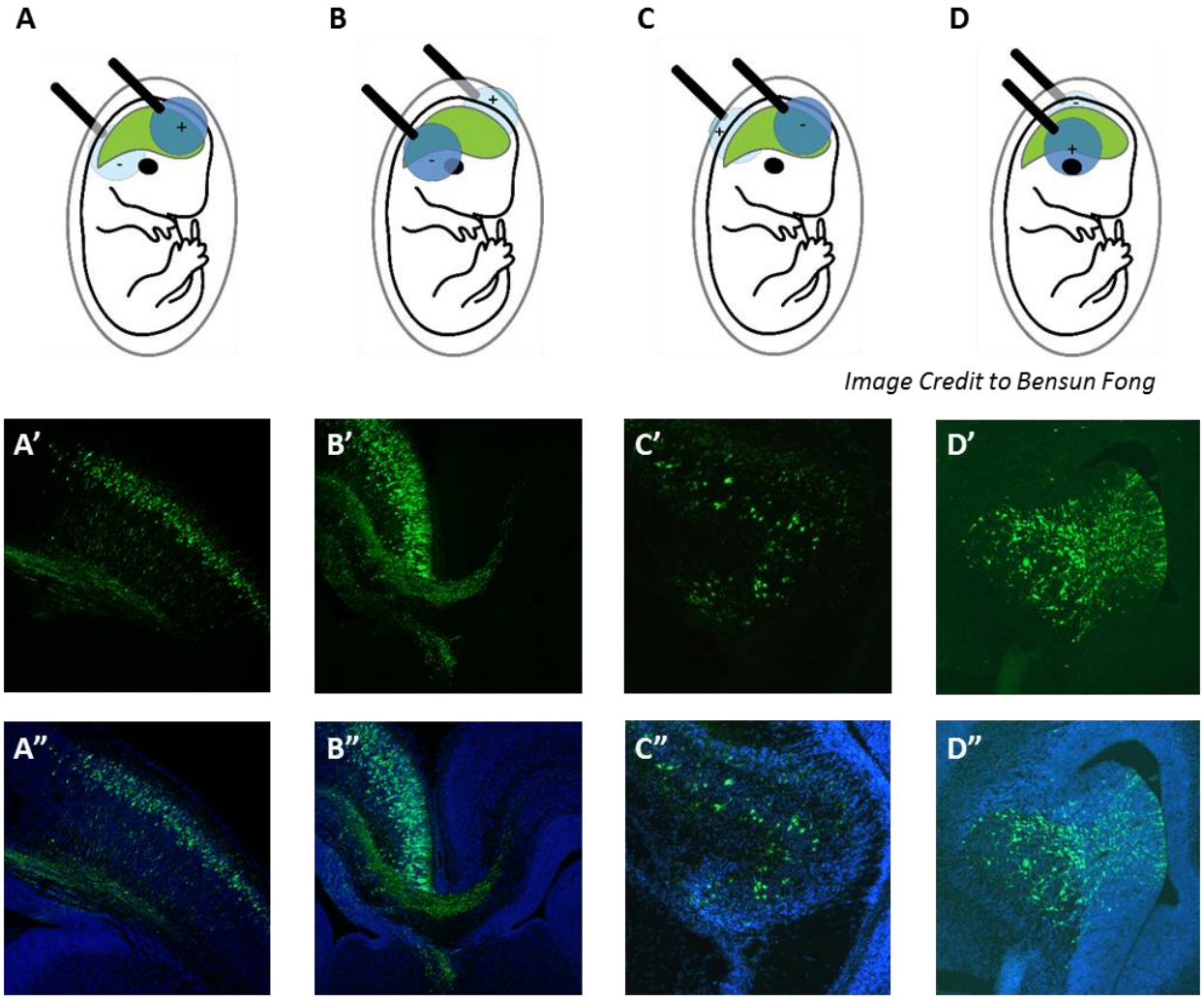

Figure 3-2

Figure 3-2: Targeting different brain regions. Diagrams **A-D** show paddle placement for targeting different regions of the forebrains. The dark blue circle represents the paddle in front of the embryo while the light blue circle represents the paddle behind the embryo. Positive and negative electrodes are indicated with the appropriate sign. **A)** Electrodes angled to target the lateral cortex. **A', A")** Example of electroporation of the lateral cortex, three days after surgery. **B)** Electrodes angled to target the medial cortex. **B', B")** Example of electroporation of the medial cortex. **C)** Electrodes angled to target the hippocampus. **C', C")** Example of electroporation of the hippocampus. **D)** Electrodes angled to target the ganglionic eminence (GE). **D', D")** Example of electroporation of the GE.

3.9. Once the paddles are in place, apply the shock. Depending on the age and size of the embryos, use 5 pulses of 35-50 V (see Table 3-2). Use the following electroporation parameters: pulse length of 5 msec with a pulse interval of 950 msec. Repeat with all injected embryos.

3.10. Cut the tip of new pre-loaded needle as in step 3.3 as the last needle likely dried and clogged during step 3.9. Inject the next set of three or four embryos with either the same plasmid or a different plasmid and then apply the shock as in step 3.9. When all the pups in one side of the uterus are injected, remove the second side of the uterus from the female's abdomen and then replace the completed side to keep it warm.

3.11. Return both sides of the uterus to the female being careful to keep the surface moist with saline and not to apply too much pressure to prevent trauma to the amniotic sacs. Suture the muscle layer closed using a simple continuous stitch. Staple the skin closed. If staples are not available, suture the skin with a simple interrupted stitch. (Figure 3-1I)

3.12. While suturing, progressively turn down the isoflurane to allow the pregnant female's anesthesia to lighten.

NOTE: This will expedite arousal of the dam after the surgery is complete; keeping the female anesthetized for as short a time as possible will improve embryo survival. Total surgery time, starting from when the female is first anaesthetized, should be approximately 30 min.

4. Aftercare

4.1. Place the sutured female in an incubator or on a heating pad to recover from anesthesia. Bed her on clean bedding and place a standard recovery gel in the cage

Table 3-2: Electroporation voltage by embryo age

Embryo Age	Voltage
E12.5 – E13.5	35V
E14.5 – E15.5	40V
E16.5	45V
E17.5	50V

to maintain hydration. For pain management following surgery, give the female three doses of Buprenorphine (0.05 mg/ kg body weight) at 8 hr intervals following surgery, then four additional doses at 12 hr intervals.

5. Harvesting Brains

NOTE: Brains can be harvested at any age up to adulthood. The following applies for collecting brains prior to birth. Note that once pups are born, the order within the uterus is lost, so either every pup in the litter must be injected with the same plasmid, or another method of differentiating between control and experimental animals must be devised.

5.1. Prepare cold (4 °C), filtered 4% paraformaldehyde (PFA) prior to euthanizing female.

5.2. Euthanize the female using an intraperitoneal injection of a lethal dose of sodium pentobarbital (100 mg/kg body weight) and cut open abdomen. Pull out both sides of the uterus and lay out as when pups were initially injected.

5.2.1. In the case where all pups received the same plasmid, such as when injecting Cre into a transgenic litter, embryo order is not important, therefore cut the uterus out of the female and place in PBS.

5.2.2. If pups were injected with different plasmids, be sure to locate each pup, noting any dead pups, and determine which ones were injected with control and experimental plasmids before removing the uterus from the female. Be careful to keep track of which pup belongs to which group after the uterus is in PBS.

5.3. Remove each pup individually, decapitate with sharp scissors or a razor blade and place the head in PBS. In the case of transgenic mice, collect tissue samples for genotyping and keep each head separate, such as in a 12-well plate.

5.4. Under a dissecting scope, remove the brain from the skull, being careful not to nick the cortex or tear the midline. Using a fluorescent microscope, check to see if brains have a GFP+ patch, indicating that they were electroporated successfully.

5.5. Fix brains by immersion in PFA at 4 °C overnight.

NOTE: Check brains for expression of GFP prior to fixation since PFA often quenches the signal.

5.6. Cryoprotect brains through immersion in 20% sucrose for at least three days prior to freezing. Use a sucrose gradient of 10%, 15% and 20% (24 hr in each solution) to prevent tissue damage due to osmotic pressure. Store frozen brains at -80 °C and cut on a cryostat at 10-14 μm thick sections.

6. Co-staining with anti-GFP

NOTE: If antigen retrieval is necessary in order to co-stain with anti-GFP, it is important to use a gentle antigen retrieval protocol that does not compromise the GFP signal. Some antigen retrieval protocols are too harsh to use in conjunction with GFP staining (even with an antibody against GFP). A basic citric acid pre-treatment prior to application of the primary antibody is successful for most epitopes (Lagace, et al. 2007).

6.1. Make a 0.01 M solution of citric acid in ddH2O. pH to 6 using a calibrated pH meter.

6.2. Heat citric acid in staining chamber in microwave or water bath until citric acids reaches 75-80 °C. Put slides in staining chamber for 10-15 min. Maintain temperature as stable as possible.

6.3. Wash slides in PBS 3x for 3 min at room temperature. Apply the primary antibody and proceed with immunostaining according to a standard protocol.

6.4. Validate Cre mediated excision by co-labelling for GFP and the gene of interest to confirm knock down (Figure 3-3A).

Representative Results

Different regions of the brain can be targeted for electroporation by varying the orientation of the paddle electrodes over the embryo's head (Figure 3-2). For all parts of the forebrain, the plasmid is injected into the lateral ventricle (the hind brain can be targeted by injecting into the fourth ventricle). In general, place the electrodes so that the straight line between them passes through the region of interest, with DNA being drawn toward the positive electrode. To target the lateral cortex (Figure 3-2A), place the positive electrode on top of the green crescent, with a slight rostral angle. For the medial cortex (Figure 3-2B), switch the orientation so that the positive electrode is over the contralateral non-injected ventricle, this time with an even larger forward angle. To target the hippocampus (Figure 3-2C), place the positive electrode over the contralateral side, but instead angle the positive electrode caudally (electroporations must be done at an age when the neural precursors are still part of the cortical hem, prior to migration to the final location of the hippocampus). To target the ganglionic eminence (Figure 3-2D) place the paddles on the embryo in line with the ears, with the positive electrode slightly lower than the negative electrode. Representative images of these electroporated regions are shown in Figure 3-2.

It is important to validate Cre-mediated excision in electroporated brains. The ideal approach is to perform *in situ* hybridization or immunohistochemistry against the transcript or protein in question. Unfortunately, as is the case for pRb, reliable probes or antibodies are not always available against the deleted gene. In these cases, alternative approaches, such as staining

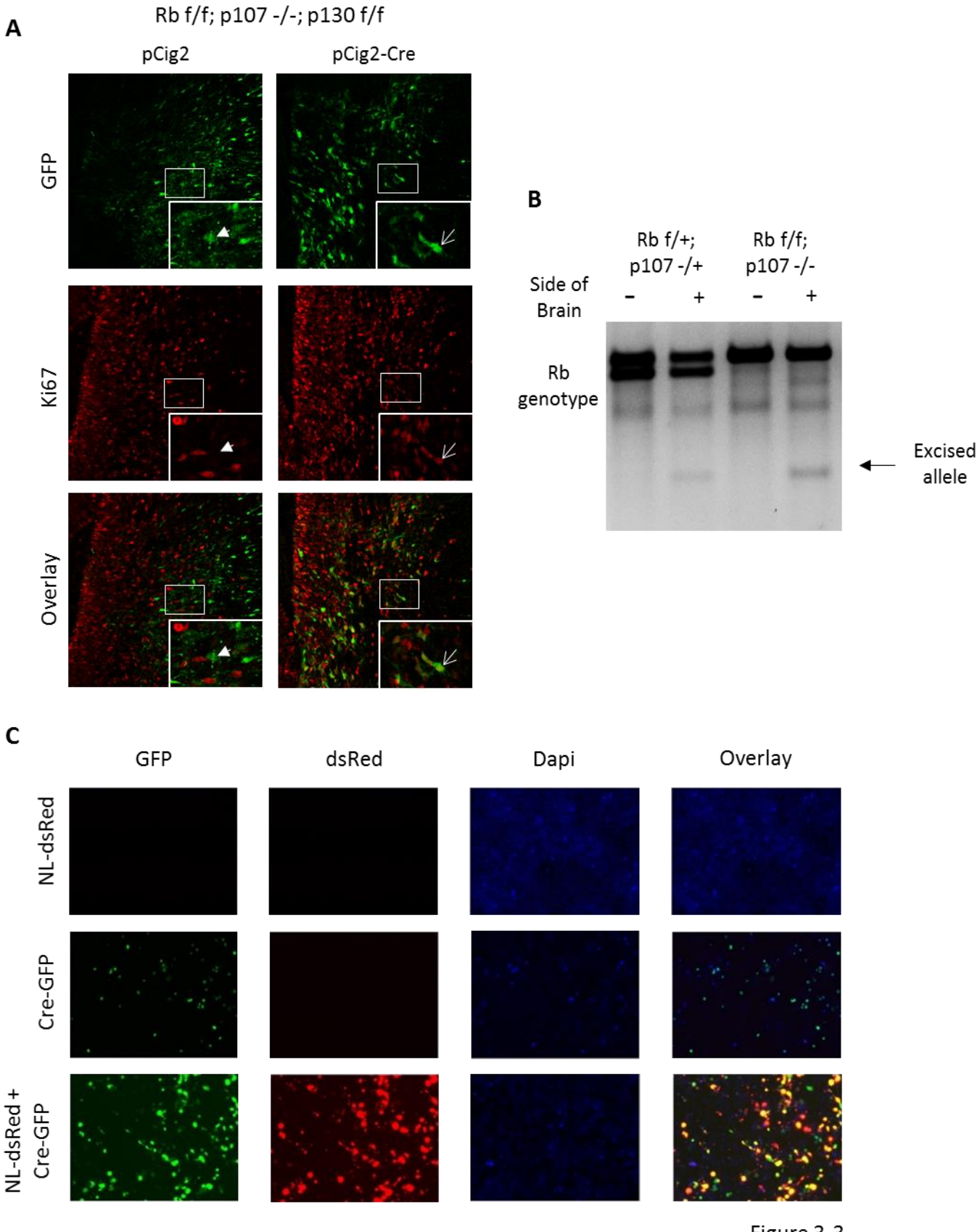
A
Rb f/f; p107 -/-; p130 f/f
pCig2
pCig2-Cre
GFP
Ki67
Overlay
B
Rb f/+; p107 -/+
Rb f/f; p107 -/-
Side of Brain
–
+
–
+
Rb genotype
Excised allele
C
GFP
dsRed
Dapi
Overlay
NL-dsRed
Cre-GFP
NL-dsRed + Cre-GFP

Figure 3-3

Figure 3-3: Confirming Cre-mediated gene excision in electroporated neurons. A) Cre mediated excision can be confirmed by co-staining for a downstream target of the deleted gene. pRb f/f; p107 -/-; p130 f/f embryos were electroporated with either the empty pCig2 plasmid or the pCig2-Cre plasmid and stained for GFP and Ki67, a marker of cell cycle entry. Double stained cells were seen in neurons electroporated with Cre (arrows in inset) but not in neurons electroporated with pCig2 alone (arrowheads). **B)** Excision of pRb was also confirmed by performing PCR with genotyping primers on DNA extracted from the tissue sections removed from the slides. Sections were divided down the midline and the electroporated side of the section was pooled. The upper band represents the floxed allele and the lower band represents the wild type allele. The arrow indicates the excised allele in the electroporated side of the brain only. Because pRb f/+; p107 +/- heterozygotes were used as controls, an excised allele can be seen in the electroporated side of the brain in both the control and knockout brains. **C)** Cre-mediated excision can also be confirmed *in vitro* using plasmids with floxed stop codons upstream of RFP, such as NL-dsRed. RFP is only expressed in HEK cells when co-transfected with Cre-GFP in Hek293 cells (bottom row), indicating that excision was successful.

for a downstream target regulated by the deleted gene (Figure 3-3A) or confirming excision of the targeted allele in electroporated sections by PCR (Figure 3-3B), can be used. For example, Figure 3-3A confirms Cre mediated excision by reproducing a well-documented effect of pRb/p107/p130 gene deletion in electroporated neurons.

Following electroporation of pRb f/f; p107 -/-; p130 f/f neuronal precursors with the pCig2-Cre plasmid, these triple knock out GFP+ cells continue to express the cell cycle progression marker Ki67, which is a known effect following excision of pocket proteins (Andrusiak, et al. 2012b). Control GFP+ neurons electroporated with the empty pCig2 plasmid do not express Ki67. The Cre plasmid should also be tested *in vitro* through co-transfection with a plasmid carrying a reporter gene behind a floxed stop codon, such as the NL-dsRed plasmid (Figure 3-3C), but this should only be used in combination with other *in vivo* techniques.

Due to the variation between electroporated brains, analysis of electroporated neurons requires calculating the percentage of total GFP+ transfected cells that portray a specific characteristic, such as expression of a protein marker or location within a given cortical layer. It is crucial to compare electroporated sections from similar anatomical locations within the brain relative to known landmarks. For example, images for Figure 3-4 were taken at the level of the anterior commissure. Furthermore, due to horizontal migration, images taken near the edge of the electroporated regions have a higher proportion of mature neurons that have reached the cortex, while images taken near the middle of the electroporated region have both mature and immature GFP+ cells. To insure consistency, it is important to quantify images selected from similar places within the electroporated patch.

Following Emx1-Cre mediated deletion of pRb and p107 in dorsal neural precursors in the telencephalon, a population of neurons expressing the upper cortical layer marker FoxP1

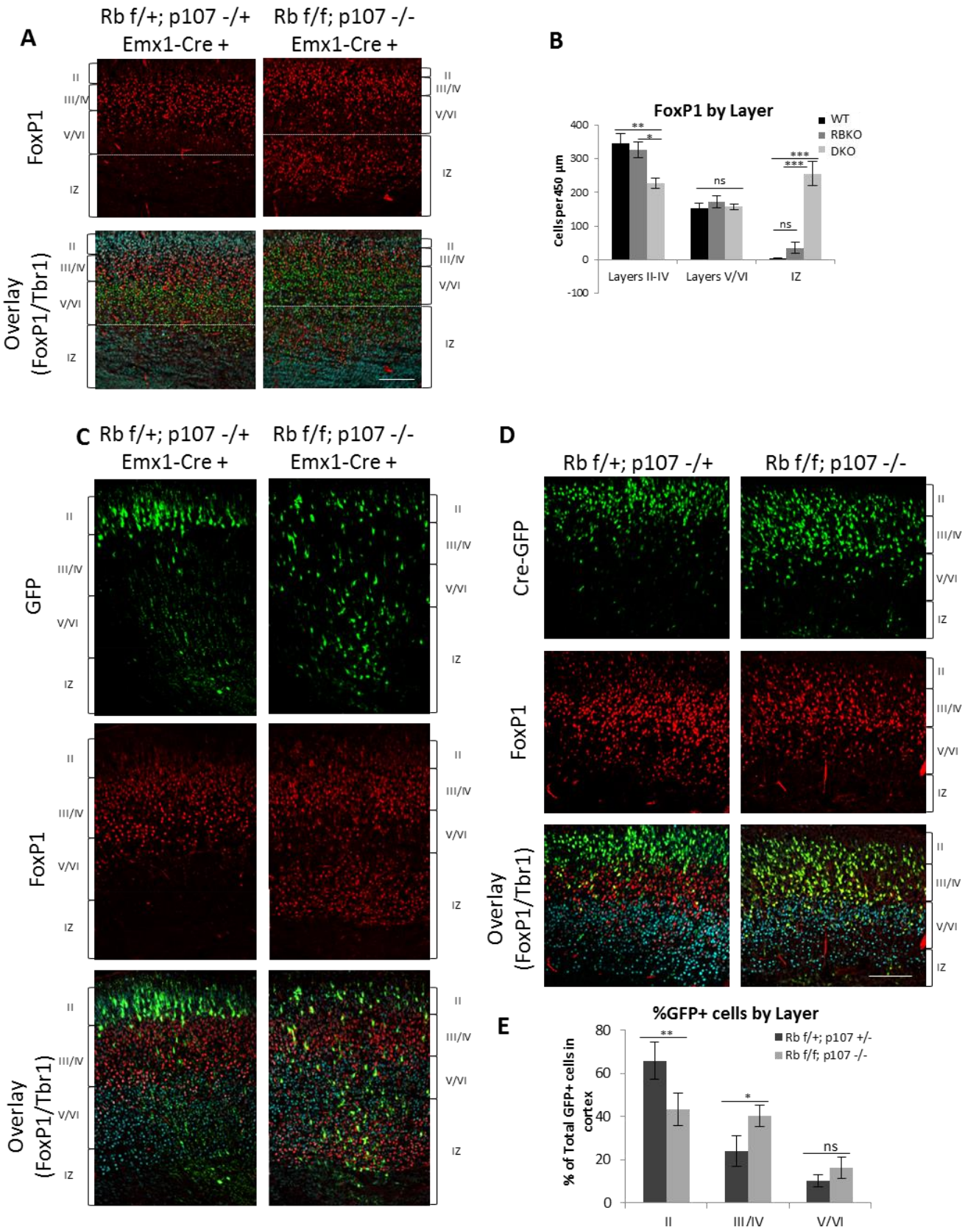
A
Rb f/+; p107 -/+
Emx1-Cre +
Rb f/f; p107 -/-
Emx1-Cre +
FoxP1
Overlay (FoxP1/Tbr1)
II
III/IV
V/VI
IZ
B
FoxP1 by Layer
WT
RBKO
DKO
Cells per 450 µm
400
300
200
100
0
-100
**
*
ns
***
***
ns
Layers II-IV
Layers V/VI
IZ
C
Rb f/+; p107 -/+
Emx1-Cre +
Rb f/f; p107 -/-
Emx1-Cre +
GFP
FoxP1
Overlay (FoxP1/Tbr1)
D
Rb f/+; p107 -/+
Rb f/f; p107 -/-
Cre-GFP
FoxP1
Overlay (FoxP1/Tbr1)
E
%GFP+ cells by Layer
Rb f/+; p107 +/-
Rb f/f; p107 -/-
% of Total GFP+ cells in cortex
80
60
40
20
0
**
*
ns
II
III/IV
V/VI

Figure 3-4

Figure 3-4: Using IUE to study migration in transgenic mouse models. A) Expression of FoxP1, a marker for layer III/IV cortical neurons, was examined in pRb f/+; p107 +/-; Emx1-Cre + (WT), and pRb f/f; p107 -/-; Emx1-Cre + (DKO) brains at E17.5. Overlay includes Cux1 (blue - marker for layers II-IV) and Tbr1 (green - marker for layers V/VI). A population of cells expressing FoxP1 was observed in the intermediate zone of DKO embryos (arrow), but not WT embryos, with a concurrent decrease in the number of FoxP1+ neurons in layers II-IV of the cortex in DKO brains relative to WT brains **(B)**. The white line indicates the delineation between the cortical plate and intermediate zone, which was determined using DAPI staining (not shown). **C)** To trace the migration of a discrete population of late born neurons, WT and DKO embryos were electroporated with GFP at E14.5 and collected the brains at E18.5. Brains were co-stained with FoxP1 (red) and Tbr1 (blue) to show that GFP+ neurons are found almost exclusively in layer II in the WT brain but are delayed in the intermediate zone (IZ) and lower cortical layers in the DKO. **D)** To determine if pRb and p107 regulate radial migration cell autonomously, pRb f/f; p107-/- and pRb f/+; p107-/+ embryos were electroporated with Cre-GFP at E13.5 and brains were collected at E17.5. The location of GFP+ neurons was quantified according to cortical layer. Layer II was defined as being above FoxP1 staining (red), layer III/IV was defined as within FoxP1 staining, above Tbr1 (blue) and layer V/VI was defined as within the Tbr1 positive layer **(E)**. We show that a portion pRb and p107 deficient neurons fail to reach layer II but instead remain in layer III/IV. The figure has been modified from Svoboda et al., 2012.

were mislocalized to the intermediate zone (IZ) (Figure 3-4A). There are significantly more FoxP1+ cells in the IZ of double knock out (DKO) brains compared to control brains with a corresponding decrease in the number of FoxP1+ cells in the upper cortical layers (above layer IV) of DKO brains than found in the upper layers of control brains (Figure 3-4B). There was no corresponding defect in the radial glial scaffold (Figure 2-S2 of Chapter 2, (Svoboda, et al. 2013)). Here we compare expression of cortical layer markers Tbr1, FoxP1 and Cux1 in pRb f/+; p017 +/-; Emx1-Cre + (wild type (WT)) brains to expression of these same markers in pRb f/f; p107 -/-; Emx1-Cre + (DKO) brains. Heterozygote embryos can be used as controls since pocket proteins exhibit autoregulation at the protein level and heterozygote animals are aphenotypic (Shan, et al. 1994).

It was unclear whether these FoxP1+ cells were found in the IZ because these cells were immature neurons inappropriately expressing FoxP1, or whether they were earlier born neurons that had failed to migrate. To distinguish between these possibilities, we electroporated GFP into the wild type (WT) and double knock out (DKO) embryos at E14.5 and tracked the progress of these neurons over 4 days. Although this technique does not conclusively identify the final cell division, as with BrdU birthdating, it does allow the tracking of newborn neurons since it marks the discrete set of neurons derived from cells lining the ventricle at the time of electroporation (Rice, et al. 2010). As shown in Figure 3-4C, all of the GFP+ neurons reach the uppermost cortical layer in the WT brains, but only a subset of these neurons reach the top of the cortex in DKO brains, indicating that there is in fact a defect in the migration of upper layer neurons, rather than improper expression of neuronal markers (similar results were obtained through traditional BrdU birthdating (Svoboda, et al. 2013)).

Neuronal migration is a highly complex process that is regulated by a multitude of interconnected mechanisms (Evsyukova, et al. 2013; Hippenmeyer. 2014; Wu, et al. 2014) As it is very difficult to identify the mechanism underlying a migration defect in an uncharacterized transgenic model, distinguishing cell autonomous versus non cell autonomous defects can facilitate phenotype characterization. If following electroporation of Cre-GFP, GFP+ neurons fail to migrate in an otherwise wild type brain, this indicates that the mechanism disrupted by gene deletion is specific to the electroporated cell. Alternatively, if the electroporated neurons migrate normally in the wild type brain, this suggests that the cause of aberrant migration in the transgenic embryo is due to an environmental defect. Following electroporation of Cre-GFP in control pRb f/+; p107 +/- and double knock out pRb f/f; p107 -/- embryos, GFP+ neurons were found to migrate into the cortex in pRb f/f; p107 -/- brains, but many of these neurons failed reach the upper cortical layers as they did in control brains (Figure 3-4D) (Svoboda, et al. 2013). There were significantly lower percentage of GFP+ neurons within the layer III/IV, marked by expression of FoxP1 (Ferland, et al. 2003), in pRbf/f; p107 -/- electroporated brains than in control brains (Figure 3-4E). A Cre-GFP fusion protein was used to limit GFP fluorescence to the cell body and facilitate localization of the neuron to a specific cortical layer. Since the phenotype following electroporation of Cre is less severe than the phenotype following gene deletion throughout the cortex, this suggests that the original phenotype shown in Figure 3-4A is a combination of multiple mechanisms, both cell autonomous and not cell autonomous. Alternatively, it is possible that the time delay following electroporation, during which Cre is expressed, DNA recombination is performed, pRb is downregulated and the effects are manifested, is long enough to allow the electroporated neurons to reach the cortex before a migration defect becomes apparent.

It should be noted that the distinction between cell autonomous and non-cell autonomous mechanisms should be interpreted with caution in brains with high electroporation efficiencies, where 100-200 or more neurons are electroporated in a single 14 μm thick section. If a high enough proportion of neurons are electroporated, GFP+ neurons may influence each other and create a small microenvironment. To be truly cell autonomous, migration defects must be detected even when electroporation efficiency is very low (10-30 GFP+ neurons per section). If necessary, the number of transfected cells can be lowered by decreasing voltage, pulse number or DNA concentration. All of these factors must be taken into consideration when analyzing the results following electroporation of Cre in a transgenic model.

Discussion

Two of the primary challenges in performing *in utero* electroporations are 1) preventing embryo lethality and 2) decreasing variability between electroporations. One of the most important factors in preventing lethality is needle quality, as blunt needles inflict more damage to the embryo.

When cutting the needle, keep the tip as long as possible while still allowing a visible droplet of 0.1-0.2 μl of fluid to appear following a pump of the foot paddle **(**Figure 3-1J**)**. If the needle is too dull or the shaft too short, the resulting tissue damage could kill the embryo. Conversely, if the tip of the needle is too fine, it will take too long to inject sufficient plasmid volume; leaving the needle in the brain for too long causes damage due to unavoidable vibrations of the investigator's hands and slight rotations of the embryo. Furthermore, use a microbeveler to make needles with a sharp, beveled tips to allow injections into younger, more fragile embryos, although this should not be necessary for embryos E13.5 and older.

The stress level of the pregnant female is another key factor affecting embryo survival. The higher the dam's stress level, the more likely she will abort the litter. For this reason it is important to minimize anesthesia time and change housing as little as possible before and after surgery. The background strain can also affect stress level and it may be necessary to outcross colonies prone to anxiety onto a strain such as CD1, assuming that the phenotype under investigation is maintained across different background strains.

The single biggest limitation to IUE is the inherent variability between electroporations. Each electroporated brain is different due to variations in injection volume, paddle placement, paddle contact and embryo age. Since needles are variable, it is not possible to inject a fixed volume – rather the investigator must approximate the size of the green patch to deliver similar amounts to all embryos. Similarly, because the embryo is floating in a fluid filled sac, it is not possible to systematically measure the location and orientation of the paddles over the embryo's head, as is done for stereotactic injections. Finally, slight differences in embryonic age can have significant effects on experimental results. For this reason, comparison between littermates is recommended.

Disclosures

The authors have nothing to disclose.

Acknowledgements

We are indebted to Pierre Mattar and Freda Miller for their assistance with the *in utero* electroporation and to Noel Ghanem and Bensun Fong for creating diagrams. We thank Linda

Jui and Jason G. MacLaurin for excellent technical assistance. Equipment was supported by the Centre for Stroke Recovery.

This work was supported by a scholarship from HSFO and OGS to D.S.S. and a CIHR grant to R.S.S.

CHAPTER 4

Devon S Svoboda, Joelle Azzi, Kelly A McClellan, David S Park, Timothy E Kennedy and Ruth S Slack. Pocket Proteins pRb and p107 Regulate Growth and Guidance of Callosal Axons. *In preparation*.

All experiments were performed by DSS. Experiments were conceptualized by DSS, with assistance from RSS. TEK provided technical assistance with cortical explant cultures. KAM and JA provided technical assistance. RSS and TEK provided technical training and conceptual insight. The manuscript was written by DSS, in collaboration with RSS.

Pocket Proteins pRb and p107 Regulate Growth and Guidance of Callosal Axons.

Devon S. Svoboda[1], Joelle Azzi[1], Kelly A McClellan[1], David S Park[1], Timothy E Kennedy[2], and Ruth S Slack[1]

[1]Department of Cellular and Molecular Medicine/Neuroscience, University of Ottawa, 451 Smyth Road,K1H 8M5, Ottawa ON, Canada.
[2] Department of Neurology and Neuroscience, Montreal Neuroscience Institute at McGill University, 3801 Rue University, Montréal, QC H3A 2B4

Corresponding Author: Ruth S. Slack
Department of Cellular and Molecular Medicine
University of Ottawa
451 Smyth Rd., Ottawa ON, K1H 8M5
Tel: 613-562-5800 x8458
Email: rslack@uottawa.ca

Character count: 51,355
Abstract word count: 280

Keywords: Corpus callosum, Netrin, Neuropilin, indusium griseum, axon growth, commissural plate, telencephalon development, cell cycle.

Highlights:

1. Deletion of pRb and p107 leads to an acallosal phenotype.
2. Defects in axon growth and guidance precede defects in glial wedge and indusium griseum, implying that pocket proteins regulate axon growth directly.
3. Axons show growth and guidance defects independent of the midline, including re-entry into the ipsilateral cortex.
4. Netrin and Neuropilin-1 are decreased in the absence of pRb and p107.
5. Netrin is expressed by two separate cell populations at the midline in control animals; the dorsal population of cell is currently undescribed in the literature and absent in DKO animals.

Abstract

Pocket proteins (pRb, p107 and p130) are well studied in the role of regulating cell cycle progression. Increasing genetic and anatomical evidence suggests that these proteins also control early differentiation and even later stages of cell maturation including neural migration. However, the role of pocket proteins in the regulation of later stages of neuronal maturation, such as axon growth and synaptogenesis, remain unknown. Here, we examine the role of pRb and p107 in regulating development of the commissural plate and the guidance of callosal axons. Following loss of pRb and p107, the structures of the commissural plate are highly disorganized and callosal axons are unable to cross the midline to form the corpus callosum. The failure of pRb/p107 deficient axons to cross seems to result from primary defects in axon extension and expression of guidance cues, rather than from defects in formation of the glial wedge or indusium griseum. Through the use of *in vitro* cortical explants and *in utero* electroporation, we identify defects in the rate of axon extension and directional guidance. This includes premature axon re-entry into the ipsilateral cortex independent from the midline throughout the length of the axon's trajectory. In addition, we identify altered regulation of Netrin and Neuropilin-1 following loss of pRb and p107, which could mediate the function of pocket proteins in regulating guidance of callosal axons. Indeed, we show that Netrin expression is specifically lost from a previously undescribed population of cells in the cingulate cortex of pRb/p107 deficient embryos. These cells could play a significant role in callosal axon guidance during normal development. These results define a novel role of pocket proteins in regulating axon growth and guidance during corpus callosum formation.

Introduction

The development of tools and therapies aimed at generating new neurons to heal injured brains following a stroke is an extremely active area of neuroscience research. Though there is a surge of cell division following the initial injury (Zhang, et al. 2001; Kuge, et al. 2009; Kernie and Parent. 2010; Merson and Bourne. 2014), the vast majority of these neuroblasts fail to enter the existing neural networks and do not survive to become functional neurons (Zhang, et al. 2001; Kuge, et al. 2009; Kernie and Parent. 2010; Merson and Bourne. 2014). It is well established that the proteins which regulate cell cycle progression are activated following brain injury and in diseased states (Park, et al. 2000; Iyirhiaro, et al. 2014; Kuhla, et al. 2015). It is also becoming increasingly clear that classic cell cycle regulators are involved in controlling neuronal differentiation and aspects of maturation such as migration and synapse formation (Chen, et al. 2004; Ferguson, et al. 2005; McClellan and Slack. 2006; Nguyen, et al. 2006; McClellan, et al. 2007; McClellan and Slack. 2007; Chen, et al. 2007a; Andrusiak, et al. 2011; Tury, et al. 2011; Odajima, et al. 2011; Ghanem, et al. 2012b). This suggests that cell cycle regulatory pathways coordinate cell cycle exit with later stages of neuron development. Manipulation of cell cycle regulators and their downstream targets therefore represents an important source for potential therapies designed to promote maturation and survival of new neurons as well as cell proliferation following injury. Furthermore, developmental models can be used to efficiently study and understand the mechanisms through which cell cycle proteins regulate the processes of neural maturation, such as axon extension and network formation, before these concepts are applied to therapy development.

pRb and p107, two members of the pocket protein family, are well known for controlling the G1/S phase checkpoint during cell cycle progression (Giacinti and Giordano. 2006;

Dannenberg and te Riele. 2006; Gordon and Du. 2011). Increasing evidence shows that these proteins are also important in regulating numerous aspects of neuron development, including terminal differentiation, tangential migration, and radial migration (Ferguson, et al. 2005; McClellan, et al. 2007; Vanderluit, et al. 2007; Chen, et al. 2007a; Andrusiak, et al. 2011; Gyda, et al. 2012; Ghanem, et al. 2012b; Svoboda, et al. 2013). However, all of the processes examined to date occur early in the complex process of neuron and brain maturation. It remains unknown whether these proteins also control events in later stages of maturation, such as axon extension and directional guidance.

Corpus callosum (CC) formation is initiated by pioneering axons from neurons in the cingulate cortex (Koester and O'Leary. 1994; Rash and Richards. 2001b; Piper, et al. 2009b). These are the first axons to cross the midline at the corticoseptal boundary, the junction between the ventral edge of the cingulate cortex and the dorsal edge of the GE, between E15.5 and E16.5 (Koester and O'Leary. 1994; Rash and Richards. 2001b). Cingulate axons serve as a guiding scaffold for later crossing axons derived from neurons located in more lateral portions of the cortex (Koester and O'Leary. 1994; Rash and Richards. 2001b). In order to reach their destinations, growth cones on both pioneering and lateral axons must pass through a series of decision points controlled by a combination of secreted and adhesive signals (Price, et al. 2006a; Canty and Murphy. 2008). Neurite extension begins during the final stages of radial migration when the trailing process of the migrating neuron extends downward toward the IZ to become the rudimentary axon (Polleux, et al. 1998; Hatanaka, et al. 2009; Zhao, et al. 2011). Once it reaches the intermediate zone (IZ), the growth cone turns medially and extends tangentially, which involves a ventral turn to follow the IZ through the dorsal flexure to reach the midline corticoseptal boundary (Hatanaka, et al. 2009; Zhao, et al. 2011; Leyva-Diaz and Lopez-Bendito.

2013). The axon tip must then turn medially, cross the midline, turn dorsally, and then continue to extend through the contralateral IZ until it enters the cortex to reach its final destination (Price, et al. 2006b; Hatanaka, et al. 2009; Piper, et al. 2009b; Zhao, et al. 2011). Pioneering axons are sensitive to a different set of guidance signals than axons from the lateral cortex and can be identified by their high levels of Neuropilin1 (Npn1) (Hatanaka, et al. 2009; Piper, et al. 2009b; Fothergill, et al. 2013), although low levels of Npn1 are important for proper guidance of axons from the lateral cortex as well (Hatanaka, et al. 2009). Axons derived from the cingulate cortex are located in the dorsal portion of the mature CC while axons from the lateral cortex are located in the ventral portion of the CC (Niquille, et al. 2009; Zhou, et al. 2013).

Neurite tips express transmembrane receptors which bind to chemoattractant and chemorepulsive cues to induce growth cone extension or collapse, respectively (Lowery and Van Vactor. 2009; O'Donnell, et al. 2009). The Netrins are the classic chemoattractant family in the CNS, which bind to DCC and Unc5, while the classic chemorepellant families are the semaphorins (which bind the plexins and Nrp1), the ephrins (which bind Eph receptors) and the Slits (which bind Robo1/2) (reviewed in (O'Donnell, et al. 2009; Kaplan, et al. 2014). Furthermore, there exists extensive cross talk between pathways which increases the complexity of the system through synergistic and silencing effects of one molecular signal over another (Kundu, et al. 2013; Fothergill, et al. 2013; Kim, et al. 2014a; Sloan, et al. 2015). Netrin/DCC is especially well known for its interaction with Slit/Robo (Fothergill, et al. 2013; Kim, et al. 2014a). Many of these signaling pathways are crucial for CC development since disruption of any of the Netrin/DCC (Serafini, et al. 1996; Shu, et al. 2000), Slit2/Robo1 (Shu and Richards. 2001), Sema3c/Npn1(Niquille, et al. 2009; Piper, et al. 2009b) or ephrinB1/EphB (Hu, et al. 2003; Mendes, et al. 2006) pathways lead to agenesis of the CC in transgenic mice models.

These pioneering axons are guided by signals secreted from a group of transient support structures which form a corridor through the corticoseptal boundary (Figure 1-3) (Koester and O'Leary. 1994; Shu and Richards. 2001; Shu, et al. 2003a; Shu, et al. 2003b; Shu, et al. 2003c; Smith, et al. 2006; Niquille, et al. 2009). The glial wedge (GW) is composed of specialized radial glial cells that send out long processes extending toward the midline in a distinct triangle shape. This forms a ventral barrier for descending callosal axons through expression of Slit2 and other repulsive cues (Shu and Richards. 2001; Shu, et al. 2003c; Smith, et al. 2006). The indusium griseum (IG) is a composite structure, including both neurons and glia, located at the corticoseptal boundary directly above where axons cross (Shu and Richards. 2001; Shu, et al. 2003c; Smith, et al. 2006). The IG neurons are born E13.5-14.5 (Shu, et al. 2003c) and have a presumed role in axon guidance and CC formation due to their location, although they have not been functionally characterized. IG glia are born around E14.5 in the ventricular zone as part of the glial wedge and then migrate to the pia mater at the midline around E16.5 (Shu, et al. 2003c; Smith, et al. 2006). Here, they express repulsive cues such as Slit2 (Shu and Richards. 2001; Shu, et al. 2003c) to set the dorsal boundary of the CC. The IG and GW are crucial to CC formation as transgenic models which lack these structures fail to form a CC (Shu and Richards. 2001; Shu, et al. 2003a; Benadiba, et al. 2012).

A third cellular population, the guidepost neurons, migrate tangentially from the ventricular zone beginning at E16 (Shu, et al. 2003b; Niquille, et al. 2009). These neurons are presumed to be important in CC formation due to their location and their expression of Sema3c, an attractive cue to cingulate neurons (Niquille, et al. 2009), yet their precise function has not been characterized. Finally, the midline zipper glia are located below the CC between the halves of the septum and are involved in fusion of the two hemispheres (Shu, et al. 2003c).

Although Netrin has been well characterized in the spinal cord, its role in CC formation is less well understood. Netrin signaling is crucial to CC development since both Netrin and DCC knockout mice are acallosal (Serafini, et al. 1996; Shu, et al. 2000; Fothergill, et al. 2013). Netrin is expressed in the septum and in the glial component of the IG. Pioneering axons from the cingulate cortex are attracted to Netrin, while the directional growth of axons from the lateral cortex is unaffected (Fothergill, et al. 2013). In addition, Netrin/DCC signaling silences the Slit2/Robo1 mediated repulsion present at the midline, which allows axons to cross (Fothergill, et al. 2013)(merged). After crossing, axons downregulate DCC, which unmasks Slit2 repulsion and prevents axons from re-crossing or stalling at the midline, thus allowing them to continue to their final destination (Fothergill, et al. 2013).

Neuropilin-1 (Npn1) has been shown to be important in guiding tangential extension of callosal axons (Kitsukawa, et al. 1997; Gu, et al. 2003; Hatanaka, et al. 2009). Expression of a dominant negative form of Npn1 in lateral callosal neurons through *in utero* electroporation leads to axon defasciculation and re-entry of the electroporated axons into the ipsilateral cortex (Hatanaka, et al. 2009). This effect is thought to be primarily mediated through Sema signaling, most likely Sema3A (Polleux, et al. 1998; Zhao, et al. 2011), as defasciculation has been observed in both Npn1 (Kitsukawa, et al. 1997; Huber, et al. 2005) and Sema3A (Behar, et al. 1996; Catalano, et al. 1998) mutant mice. Defasciculation in Npn1 mutants in the sympathetic ganglion neurons was found to be dependent on Sema3A signaling (Kawasaki, et al. 2002). In addition to the classic Sema mediated signaling pathway, Npn1 has been shown to have homophillic adhesive activity (Shimizu, et al. 2000), and a mouse expressing a mutant form of Npn1 unable to bind Sema shows a milder phenotype than a full Npn-1 knock out (Gu, et al.

2003). It is therefore likely that some of the importance of Npn1 in axon fasciculation and guidance through the IZ is due to homophillic adhesive interactions between adjacent axons.

In the present study, we asked whether pocket proteins play a role in axon growth and guidance in the developing brain. We used a transgenic mouse deficient for both pRb and p107 to avoid compensatory upregulation of p107 in pRb deficient tissues (Marino, et al. 2003; Chen, et al. 2004; Berman, et al. 2009). An extreme CC defect was found in DKO embryos, with axon guidance errors detectable as early as E15.5, prior to when callosal axons cross the midline. Extensive defects were found in the midline support structures, namely in the GW and both the IG neurons and the IG glia, but these defects were predominantly found to develop at a later age than the primary axon guidance defect. pRb and p107 deficiency also leads to callosal axon defasciculation and re-entry of axons into the ipsilateral cortex independent from the midline. Furthermore, we show early deregulation of Netrin expression at the midline, already detectable at E15.5, which suggests a role of Netrin in development of the acallosal phenotype. Npn1 is also shown to be decreased starting at E15.5 and this may contribute to both callosal agenesis and axon re-entry into the ipsilateral cortex in DKO mice. Using cortical explant studies, we show *in vitro* defects in axon growth and a blunted response to Netrin stimulation. Overall we show that pocket proteins play an essential role in growth and guidance of callosal axons and CC formation through a combination of mechanisms including regulation of Netrin signaling.

Materials and Methods

Mice. pRb/p107 DKO mice were generated by crossing floxed Rb-F19 (Vooijs, et al. 1998; Marino, et al. 2000) with p107 germline knockout mice (LeCouter, et al. 1998). DKO mice were then crossed with Emx1-Cre mice (Jackson Laboratories) to delete pRb specifically in the dorsal

telencephalon. Mice were maintained on a mixed C57/Bl6/FVBN/Sv129 background and genotyped according to standard protocols with previously published primers for pRb (Jacks et al 1992) and p107 (LeCouter, et al. 1998). pRb f/f; p107 -/- females were crossed with pRb f/+; p107 +/-; Emx1-Cre+ males to generate wild type pRb f/+; p107 +/-; Emx1-Cre+ (WT), pRb f/f; p107 +/-; Emx1-Cre+ (RBKO), pRb f/+; p107 -/-; Emx1-Cre+ (p107KO) and double knock out pRb f/f; p107 -/-; Emx1-Cre+ (DKO) littermates. For embryonic time points, the time of plug identification was counted as embryonic day 0.5 (E0.5). Due to pRb autoregulation (Shan, et al. 1994), Rb expression in heterozygous mice is similar to that of wild-type controls. DKO-Bax-/- mice were bred by crossing pRb f/f; p107 -/- mice with Bax -/- mice (Jackson Laboratories) to generate pRb f/f; p107 -/-; Bax -/- females. These females were crossed with pRb f/+; p107 +/-; Bax +/-; Emx1-Cre+ males. These mice were also on a mixed C57/Bl6/FVBN/Sv129 background. All experiments were approved by the University of Ottawa's Animal Care ethics committee, adhering to the Guidelines of the Canadian Council on Animal Care.

Tissue fixation and cryoprotection. Pregnant female mice were euthanized with a lethal injection of sodium pentobarbitol. P0 pups were euthanized by decapitation. Embryo heads were removed and fixed overnight in 4% PFA in PBS, pH 7.4, and cryoprotected using a sucrose gradient of 10%, 15% and 20% sucrose in PBS. Electroporated brains were removed from the skull prior to fixation. Brains were frozen, and 14-µm coronal cryosections were collected on Superfrost Plus slides (12–550-15; Fisher Scientific).

Neural Precursor Cultures and Chromatin Immunoprecipitation (ChIP). Neural precursors were obtained by dissection of the ventral telencephalic tissue of developing embryos and neurosphere and *in vitro* differentiation assays were performed as previously described

(Vanderluit, et al. 2004; Julian, et al. 2013). ChIP analysis was performed as previously described (Andrusiak, et al. 2011; Julian, et al. 2013) in proliferating neurospheres. Each experiment was performed on at least three independent samples. ChIP-on-chip experiments were performed as previously described (Liu, et al. 2010; Julian, et al. 2013).

Immunohistochemistry and cell counts. All images were taken from tissue sections at equivalent anatomical locations along the rostro-caudal axis as determined by the presence of midline anatomical structures including the anterior commissure, hippocampal commissure, fused striatum, ventricle shape and external head structures including the sinus and retinae. Slides were treated with the Dako antigen retrieval protocol according to the manufacturer's protocol for 15-30 minutes depending on the epitope and treated with combinations of the following antibodies: Map2, L1, Neuropilin1, Calretinin, GFAP, Calbindin (CB), Ki67, Active-caspase 3 or Sox9. Antibody information is summarized in Table 4-1. Analysis of relative height of the corticoseptal boundary was done in Photoshop CS3 by performing three measurements; a = distance between the tip of the dorsal flexure and the dorsal edge of the region of CB+ cells, representing the top of the IG neurons; b = distance between the tip of the dorsal flexure and the ventral tip of the region of CB+ cells, representing the corticoseptal boundary; c = distance between the tip of the dorsal flexure and the bottom of the striatum, representing the height of the entire brain. The relative location of the corticoseptal boundary within the dorso-ventral axis was quantified by dividing a/c and b/c, and a one-way ANOVA with Bonferroni analysis was performed to assess significance of $p < 0.05$. Four or five animals were used for each genotype.

Table 4-1: Antibody and In Situ Probe Information

Immunohistochemistry				
Target Molecule	**Company (serial #)**	**Concentration**	**Antigen retrieval**	**Structure Marked**
Ki67	ThermoScientific (RM-9106-51)	1/500	DAKO or CA	Proliferating cells
Calretinin	Millipore (AB5054)	1/500	DAKO or CA	CR, guidepost, or IG neurons
Calbindin	Chemicon (AB1778)	1/500	DAKO or CA	IG neurons
GFP rabbit	Abcam (AB6556)	1/5000	CA	GFP
GFP Chicken	Abcam (AB13970)	1/5000	CA	GFP
Map2	Abcam (AB5392)	1/2000	None	Dendrites
L1		1/2000	None	Callosal axons
Neuropilin1	Calbiochem (PC343T)	1/500	None	Pioneer callosal axons
GFAP	DAKO (Z0334)	1/2000	DAKO or CA	Glial cells
Sox9	Millipore (AB5535)	1/1000	DAKO or CA	Glial cell nuclei
Active Caspase 3		1/250	DAKO or CA	Apoptosis
BIII-Tubulin	Millipore (MAB1864)	1/2000	None	Neural processes
In Situ Hybridization				
Probe	**Source**	**Concentration**	**Incubation Time**	**Structure Marked**
Netrin	Dr. Tito Serafini	1/1000	2 hours	Midline, GE
DCC	Dr. Tito Serafini	1/1000	3 hours	Cortical Neurons
Slit1	Dr. Tessier-Lavigne	1/1000	2 hours	GW, IG glia
Slit2	Dr. Tessier-Lavigne	1/1000	2 hours	IG glia, Guidepost Neurons
Robo1	Dr. Tessier-Lavigne	1/1000	1 hour	Cortical Neurons
Robo2	Dr. Tessier-Lavigne	1/1000	1 hour	Cortical Neurons
ephrinB2	Dr. Artur Kania	1/500	4 hours	Cortical Neurons
Gli3	Dr. Valerie Wallace	1/500	3 hours	VZ, IG glia
Western Blot				
Target Molecule	**Company (serial #)**	**Concentration**	**% Acrylamide**	**Mass (kDa)**
Netrin	Abcam (ab126729)	1/1000	10%	75
Neuropilin1	Calbiochem (PC343T)	1/1000	10%	130
N-Cadherin	Abcam (AB18203)	1/1000	10%	130
PSA-NCAM	Chemicon (MAB5324)	1/1000	10%	150-300
β-Actin	Sigma (A-5316)	1/3000	6%+	42

For Sox9 counts, all positive cells in the anatomical region of the corticoseptal boundary and IG, as defined by their proximity to the meninges and CB+ cells, were included. For Ki67 and AC3 counts, all cells within a defined area of 350µm by 150µm placed in the relevant anatomical area (IG, medial or lateral cortex) were counted.

***In Situ* Hybridization**. Nonradioactive *in situ* hybridization and digoxigenin probe labeling were performed according to previously described protocols (Wallace and Raff. 1999). Information on probes against Netrin, DCC, Slit1/2, Robo1/2, Gli3 ephrinB2, and BMP7 is summarized in Table 4-1. When performed in conjunction with Dab immunohistochemistry, the hybridization was performed first, followed by 48 hours in PBS, followed by a 10 minute treatment in 0.3% H2O2 and overnight exposure to the primary antibody. This was followed by a one hour exposure to the secondary antibody, treatment with an ABC kit (Vector Laboratories) and a Dab color reaction. All results are representative and were performed on a minimum of three independent animals.

Western Blots. Protein was isolated from the dorsal cortex or ganglionic eminence at E15.5 or E17.5 and western blot analyses performed as previously described (Ferguson, et al. 2005). Where applicable, the medial cortex was divided from the lateral cortex along the dorsal flexure for the entire length of the cortex. Nitrocellulose membranes were treated with antibodies as summarized in Table 4-1.

Cortical Explant Cultures. Cortical explants from the medial or lateral cortex (divided along the dorsal flexure) were dissected from E14.5 mouse embryos and cultured in three-dimensional

collagen gels for 24 or 48 hours (Bouchard, et al. 2004) at 37°C in Neurobasal media supplemented with 2% B27, 1% N2, 1X Glutamax and ABAM. Dissections were performed in DMEM. Netrin-1 was added to the medium at plating at a concentration of 200 ng/mL. Explants were fixed for 20 min in 4% PFA and stored in PBS. Explants were blocked with 10% Normal Donkey Serum in PBS for 2 hours and then incubated overnight at 4˚C with the BIII-Tubulin antibody in Tween-20/Triton X. They were then treated with a Cy3-conjugrated secondary IgG, Alexa488-conjugated phalloidin and Dapi for 2 hours. Z-stacks of 5 images evenly dispersed over 20 µm depth were obtained on a Zeiss confocal microscope and neurites were measured using ImageJ. The 100 longest neurites from each explant were measured, with a minimum of four explants per condition.

***In utero* electroporation**. *In utero* electroporation was performed as described in Chapter 3 (Svoboda, et al. 2015). In brief, animals were anesthetized using isoflurane gas and the embryos were exposed by removing the uterus from abdominal cavity (Figure 3-1). Previously prepared pulled glass pipettes, loaded with a plasmid solution were trimmed, with special attention to the quality of the tip, (Figure 3-1 J) and pups were injected in the lateral ventricle. Plasmids were prepped using the Qiagen Megaprep Kit, diluted to 2 µg/µl in sterile H_2O and mixed with trace amounts of Fast Green dye. The plasmid was injected into the lateral ventricle of the brain using an Eppendorf Femtojet Microinjector and the brain was electroporated using a BTX ECM 830 Square Wave Electroporator set to 40V.

For analysis of axon growth shown in Figure 4-14, pups of pregnant DKO females were electroporated at E14.5 into the lateral cortex with an empty pCig2 plasmid. Animals were sacrificed at E18.5, P0 and P10. Tissue sections were treated antibodies against GFP, Npn1 and

L1 and amplification was performed on the GFP signal. Images were taken by tile scanning on a fluorescent microscope.

Results

pRb/p107 deficiency leads to agenesis of the corpus callosum. Our lab and others have shown that the pRb/E2F pathway has numerous functions in the developing brain independent of its role in regulation of the cell cycle, including radial (Ferguson, et al. 2005; McClellan, et al. 2007; Andrusiak, et al. 2011; Svoboda, et al. 2013) and tangential migration (McClellan, et al. 2007; Andrusiak, et al. 2011) and terminal differentiation (Chen, et al. 2007a; Ghanem, et al. 2012b). Because pRb has recently been discovered to regulate these cell cycle independent processes, we hypothesized that this pathway has additional, currently unknown roles in neuron maturation. To better appreciate the multifaceted and complex role of pRb in neural development, a ChIP-on-chip screen was performed to obtain a genome wide list of E2F3 and E2F4 binding sites. A complete analysis of this screen has been published elsewhere (Julian, et al. 2015). The resulting list of E2F3 target genes is shown in Figure 4-1 and includes numerous genes with functions relating to synaptogenesis (Dasm1 and Gephrin), axon guidance (Fyn, Netrin, and Npn1), cytoskeleton dynamics (Dock7 and Elmo 1/2), adhesion (ALCAM and IGSF4), and neuritogenesis (Nogo). A selection of the genes listed were verified as being bound by E2F3 in wild type cortical tissue at E16.5 using a conventional non-quantitative ChIP assay (Figure 4-1 middle). These results support the hypothesis that pocket proteins regulate the expression of genes with cell cycle independent functions in neuron maturation and that the pRb/E2F pathway seems to have a much more complex role in neural development than previously appreciated.

Gene Name	Function
Dasm1	Synaptogenesis
Gephyrin	Synaptogenesis
Pea3	Dendritogenesis/Circuits
ER81	Dendritogenesis/Circuits
Plexin A3	Axon Guidance - Sema
Plexin B2	Axon Guidance - Sema
Nrp1	Axon Guidance - Sema
Sema5b	Axon Guidance - Sema
Fyn	Axon Guidance - Sema
Sema3d	Axon Guidance - Sema
Sema4c	Axon Guidance - Sema
Sema6a	Axon Guidance - Sema
Sema6c	Axon Guidance - Sema
CRMP2	Axon Guidance - Sema
Netrin 1	Axon Guidance – Netrin
Netrin G1	Axon Guidance – Netrin
UNC5	Axon Guidance – Netrin
EphA5	Axon Guidance – Ephrin
EphA7	Axon Guidance – Ephrin
EphB1	Axon Guidance – Ephrin
EphB2	Axon Guidance – Ephrin
CRPM5	Axon Guidance
Pax6	Patterning/Axon Guidance
LHX6	Patterning/Axon Guidance

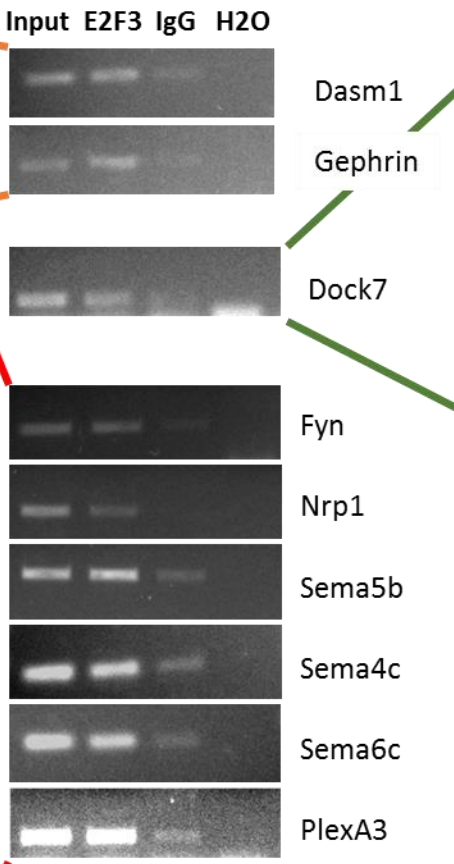

Gene Name	Function
Dab1	Migration
DOCK180	MT dynamics/Migration
Elmo1	Interacts with DOCK180
Elmo2	MT dynamics/dendrites
Nav1	MT dynamics/Neurites
Tiam1	MT dynamics/Ephrin B2
mDia2	MT dynamics/dendrites
Clf1	MT dynamics/dendrites
DOCK7	MT dynamics
Amigo1	Adhesion
Laminin B2	Adhesion
EMP	Adhesion
ALCAM	Adhesion
IGSF4	Adhesion
MDGA1	Adhesion
SOSC2	Neurite Formation/Electro
Nogo	Neurite formation
Ror2	Neurites/synaptogenesis
BzW2	Patterning/Differentiation
Raf1	Patterning/Differentiation
Zic1	Patterning/Differentiation
Calsenilin	Ca++ channels
NFATc1	Dendrite Maturation

Figure 4-1

Figure 4-1: E2F3 binding targets with functions related to neuron maturation. A ChIP-on-chip was performed on neurospheres to determine the targets of the E2F3 transcription factor. A selection of these targets with function important in neuron maturation are listed. Target genes are grouped according to functions in synaptogenesis (orange), axon guidance (red), cytoskeletal dynamics (green), adhesion (purple), neuritogenesis (yellow) or patterning/differentiation (blue). Targets from different functional categories were verified using a non-quantitative ChIP assay with an antibody specific to E2F3 on chromatin purified from wild type E16.5 cortex (middle). Input represents total chromatin and IgG represents immupoprecipitation with a normal rabbit IgG.

Axon guidance proteins represented the largest category of E2F3 target genes with functions in neuron maturation (Figure 4-1) and many of these targets were confirmed by ChIP. Since the roles of the pRb/E2F pathway in axon guidance is completely unknown, we sought to better understand the biological relevance of these target genes by investigating the role of pocket proteins in regulating axon growth and guidance in the developing brain. To evaluate the consequence of pRb/p107 deficiency on axon tract formation, WT, RBKO, and DKO brains were examined for evidence of anatomical defects at E17.5 (Figure 4-2) by staining for Map2, a dendritic marker, and L1, an axonal marker. Agenesis of the corpus callosum (CC) and formation of Probst bundles was observed in all DKO brains, accompanied by a distinct lengthening of the cingulate cortex and ventro-caudal shift of the corticoseptal boundary (quantified in Figure 4-6). A subset of RBKO brains showed an intermediate phenotype with partial crossing in the caudal portion of the CC (Figure 4-3). The axons within this caudal CC appear disorganized in comparison to the WT and unaffected RBKO brains and often formed small Probst bundles-like structures on the dorso-medial edges (Figure 4-3, arrows in inset).

To determine if this defect was due to the death of a population of cells expressing a crucial guidance factor, or due to apoptosis of the callosal neurons themselves, DKO mice additionally deficient in Bax expression (DKO-Bax) were included in this analysis (Figure 4-2). Increased cell death is a well-established effect of pocket protein deficiency and deletion of Bax in DKO mice has been shown to restore cell death to control levels in cortical neurons (Svoboda, et al. 2013). There was no difference in any aspect of this CC phenotype between DKO and DKO-Bax brains, indicating that this phenotype does not result from increased apoptosis (Figure 4-2).

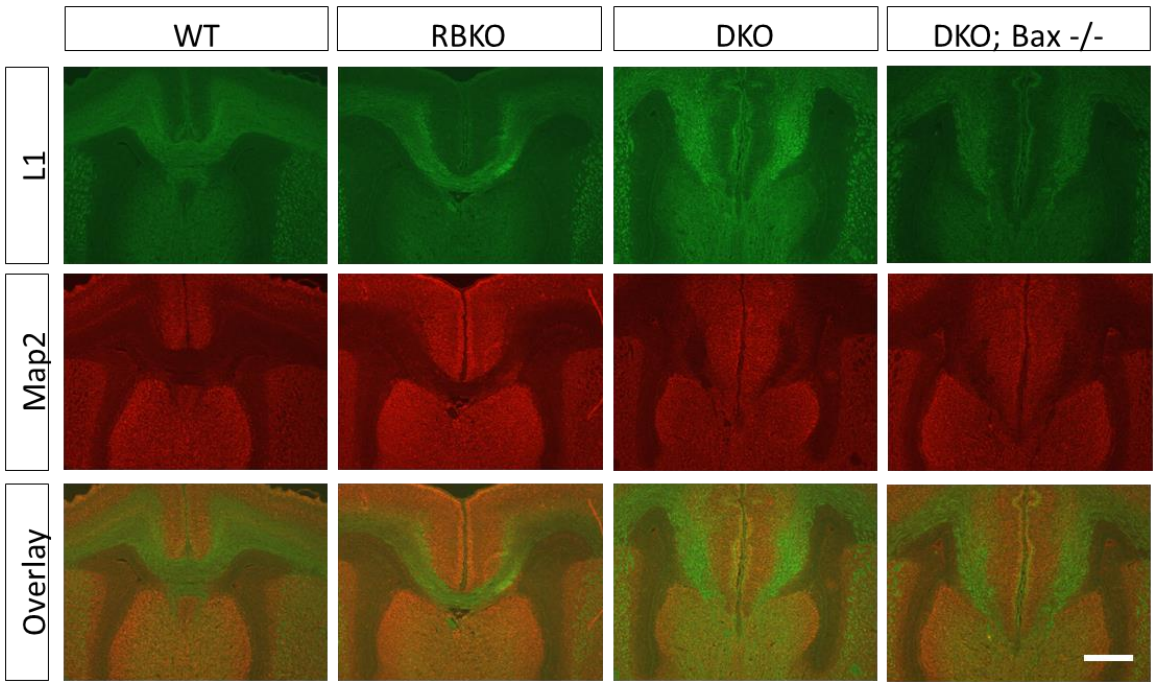

Figure 4-2: Defect in corpus callosum development in pRb;p107 double knock out brains. Representative images are shown of the developing corpus callosum of E17.5 brains from pRb f/+; p107-/+; Bax+/+ (WT), pRb f/f; p107+/-; Bax+/+ (RBKO), pRb f/f; p107-/-; Bax+/+ (DKO), and pRb f/f; p107-/-; Bax-/- (DKO;Bax-/-) embryos. Sections are stained with L1 (an axon marker - green) and Map2 (a dendritic marker - red). Scale bar = 200µm

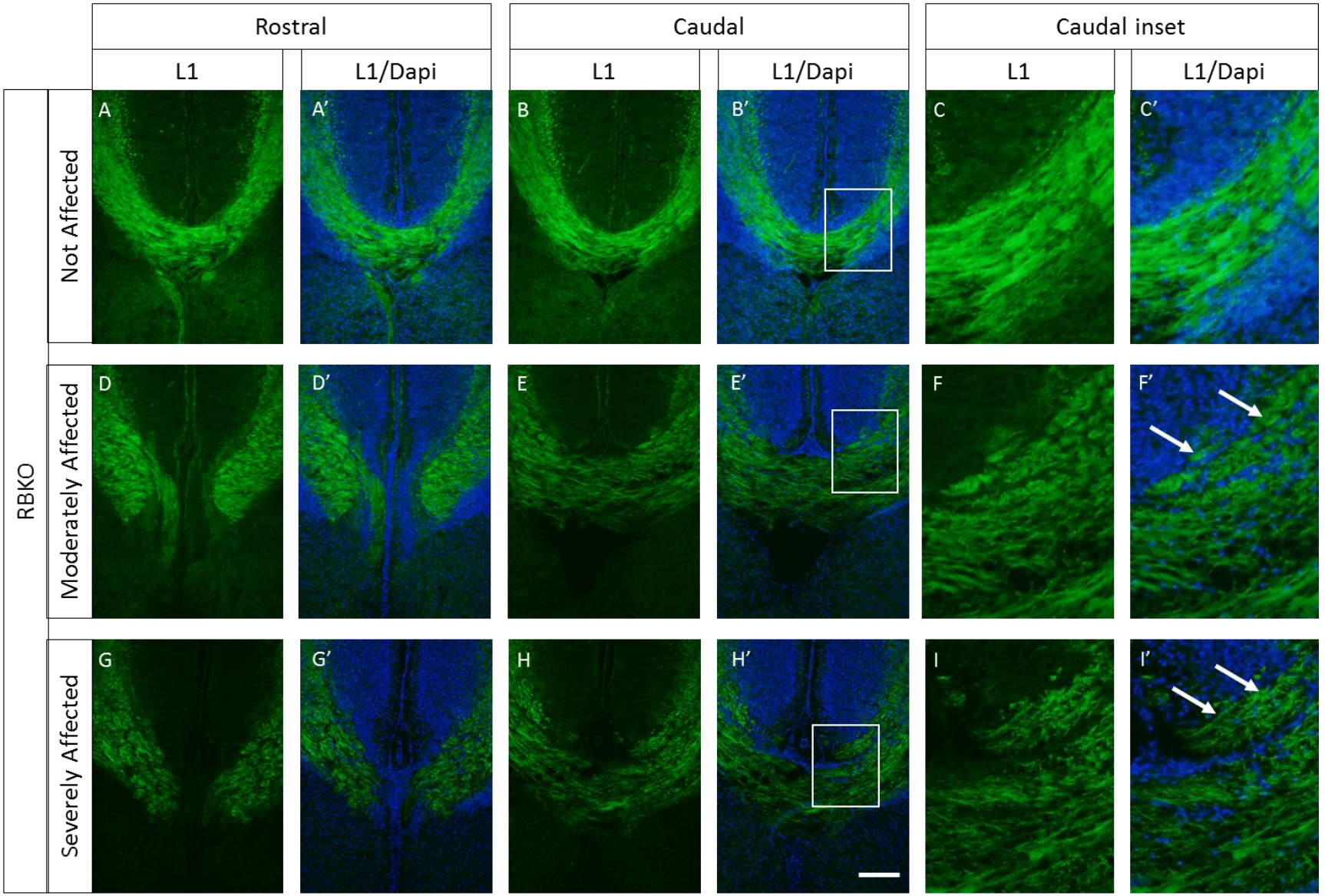
Rostral
Caudal
Caudal inset
L1
L1/Dapi
L1
L1/Dapi
L1
L1/Dapi
RBKO
Not Affected
Moderately Affected
Severely Affected
A
A'
B
B'
C
C'
D
D'
E
E'
F
F'
G
G'
H
H'
I
I'

Figure 4-3

Figure 4-3: Loss of pRb alone leads to minor CC formation defects in a subset of affected brains. Representative images of E17.5 pRb f/f; p107-/+; Emx1-Cre+ (RBKO) brains with normal development (unaffected – **A-C**), a moderate phenotype (**D-F**) and a more severe phenotype (**G-I**) are shown. Sections are shown from the rostral CC (**A, D, G**) and caudal CC (**B, E, H**), as well as an inset from the caudal image of each phenotype category showing axon disorganization and small Probst bundle-like formations oriented rostro-caudally at the dorso-medial aspect of the CC (arrows). Sections are stained for L1 (green) to mark callosal axons and for Dapi (blue) to show nuclei. Scale bar represents 150 μm.

Pioneering axons from the cingulate cortex cross the midline between E15.5 and E16.5 in the mouse and are found in the dorsal half of the mature CC; these axons serve as a necessary scaffold for later crossing axons from the lateral cortex (Koester and O'Leary. 1994; Rash and Richards. 2001b; Piper, et al. 2009b). To track the development and organization of pioneering axons in DKO embryos, brains were stained for Npn1, L1 and GFAP at E15.5, E17.7 and P0. At E15.5 (Figure 4-4A,B), WT brains showed intense staining and high axon density both in the IZ adjacent to the medial cortex and at the cortico-septal boundary, with lots of Npn1+ axons located at the midline. In DKO brains, axons traveling through the IZ showed signs of defasciculation as they were spread over a much larger area, with only a small portion of these axons reaching the midline. As axon density is much higher in the IZ than at the midline, this could indicate that axons are delayed in the IZ of DKO brains.

At E17.5 (Figure 4-4C,D), WT brains exhibited a clear segregation between the Npn1+ cingulate axons in the dorsal half of the CC and the Npn1-negative lateral axons in the ventral half of the CC. In DKO brains, this segregation is lost in the Probst bundles (Figure 4-4D), with most of the axons showing low levels of Npn1+ staining. At P0 (Figure 4-4E-H), the segregation is regained within the Probst bundles with a small portion of Npn1+ axons in the medial portion of a much larger axon bundle (Figure 4-4G). This developmental progression suggests a working model in which both the pioneering Npn1+ and the lateral Npn1-negative axons are progressively delayed in the DKO, with pioneering axons reaching the midline after E16.5 but before E17.5 and axons from the lateral cortex reaching the midline after E17.5, but before P0.

A partial caudal CC can be seen in a small subset of DKO brains at P0 (Figure 4-4H). In these brains, the crossing axons do not express Npn1, while the Npn1+ axons form small bundles

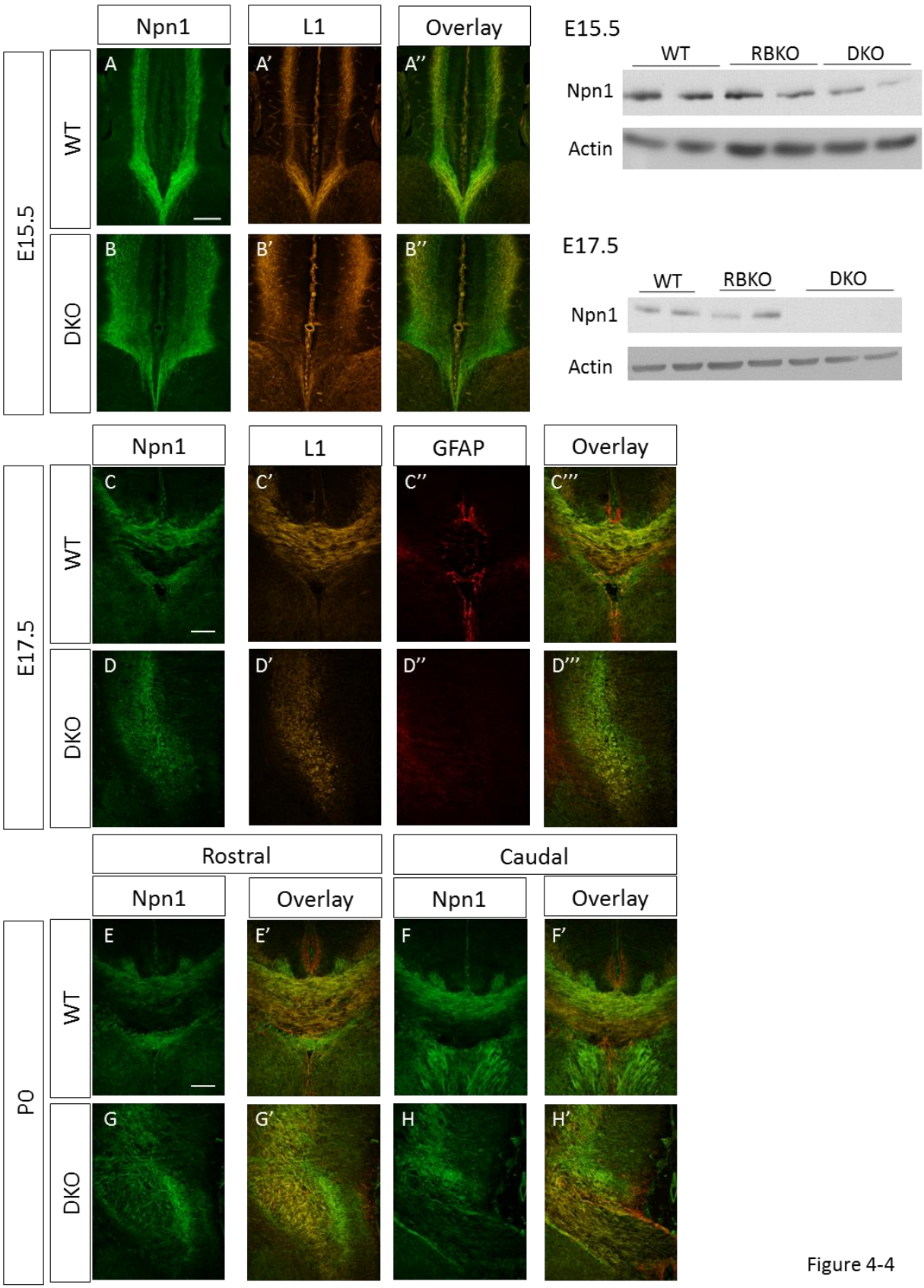
Npn1
L1
Overlay
E15.5
WT
DKO
A
A'
A''
B
B'
B''
E15.5
WT
RBKO
DKO
Npn1
Actin
E17.5
WT
RBKO
DKO
Npn1
Actin
Npn1
L1
GFAP
Overlay
E17.5
WT
DKO
C
C'
C''
C'''
D
D'
D''
D'''
Rostral
Caudal
Npn1
Overlay
Npn1
Overlay
P0
WT
DKO
E
E'
F
F'
G
G'
H
H'

Figure 4-4

Figure 4-4: Defect in pioneering axons and axon organization in DKO brains.
Representative images are shown of the developing corpus callosum of E15.5 (**A, B**), E17.5 (**C, D**) and P0 (**E, F**) brains from pRb f/+; p107-/+; Bax+/+ (WT) and pRb f/f; p107-/-; Bax+/+ (DKO) embryos. Sections are stained with L1 (green) to mark all callosal axons, Neuropilin-1 (Npn1, yellow) to mark the pioneering axons and GFAP (red) to mark the IG (not yet present at E15.5). **A,B:** At E15.5, DKO (**B**) axons show defasciculation and a decrease in Npn1+ axons at the corticoseptal boundary compared to WT (**A**) axons. **C,D:** At E17.5, the segregation between Npn+ and Npn- axons seen in the WT (**C**) CC is lost in the DKO (**D**) Probst bundles, along with a loss of the IG glia in this rostral section. **E-H:** At P0, some of the Npn+ and Npn-negative axon segregation is regained in DKO brains (**G, H**) and Npn-negative axons are able to cross the midline in caudal sections of some brains (**H**). All scale bars represent 100 μm.

on the medial aspects of the ipsilateral side of the corticoseptal boundary. These caudal Npn1-negative axons are sometimes able to cross the midline even though the Npn1+ were never observed to cross the midline in the DKO brain.

Defects in midline support structures in DKO brains are secondary to errors in axon crossing and organization. The commissural plate contains several glial and neuronal structures surrounding the corticoseptal boundary which express a variety of axon guidance cues to create a corridor for commissural axons (Koester and O'Leary. 1994; Shu and Richards. 2001; Shu, et al. 2003b; Shu, et al. 2003c; Niquille, et al. 2009; Magnani, et al. 2012a). As defects in the development or function of these structures represent a probable cause of the CC defects in DKO brains, the morphology of the GW and IG glia was examined through expression of GFAP, and the neuronal sling and IG neurons were examined using expression patterns of Calretinin (Figure 4-5). In WT brains, the GW formed a normal triangle shape under the CC with the IG just above the CC. In both DKO and DKO-Bax brains, the GW is present, although the GFAP+ staining intensity is weaker and the processes seem to be disorganized and elongated compared to those seen in WT brains. The glial component of the IG was found to be very inconsistent in DKO brains; these cells were consistently highly disorganized and shifted ventro-caudally, often below the corticoseptal boundary, yet in some DKO brains there was an increase in cell number compared to WT, and in other brains there was a decrease.

The number of calretinin (CR)+ cells was dramatically increased in DKO and DKO-Bax brains (Figure 4-5). In WT brains CR+ cells are found only at the midline just above the CC (the IG neurons) and under the CC (the guidepost neurons), while in the DKO brains there are numerous CR+ cells within the medial cortex, as well as among the descending axons and

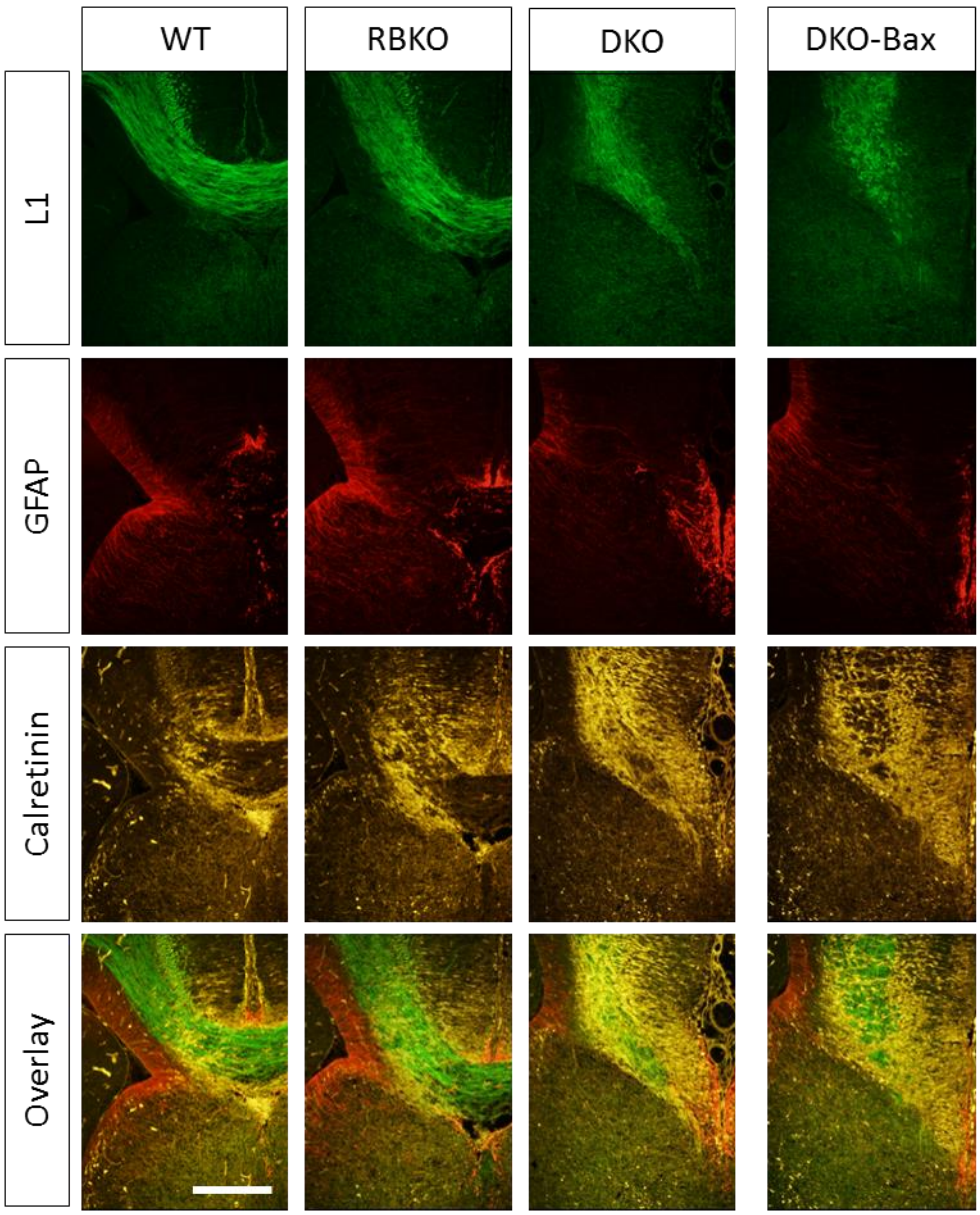

Figure 4-5

Figure 4-5: Defect in supporting midline glial structures in pRb;p107 double knock out brains. Representative images are shown of the developing corpus callosum of E17.5 brains from pRb f/+; p107-/+; Bax+/+ (WT), pRb f/f; p107+/-; Bax+/+ (RBKO), pRb f/f; p107-/-; Bax+/+ (DKO) and pRb f/f; p107-/-; Bax-/- (DKO-Bax) embryos. Sections are stained with L1 (an axon marker - green), GFAP (a glial marker, here showing the glial wedge and the indusium griseum - red) and Calretinin (a glial sling marker - yellow). Note the disorganization of the IG glia and overgrowth of the Calretinin+ cells in DKO and DKO-Bax brains. Scale bar = 60µm

between the axon bundles. To further determine the identity of these cells, brains were analyzed for calbindin (CB) expression, to mark the neural component of the IG (Figure 4-6). CB+ cells were found to be much more numerous and occupy a much larger area in DKO brains than in WT brains at E17.5 (Figure 4-6). As it was unclear whether the corticoseptal boundary was shifted downward due to specific over-proliferation of the CB+ neurons or an expansion of the entire cingulate cortex, the distance between the top of the brain and the top of the CB staining ("a" in the diagram in Figure 4-6) or the bottom of CB staining ("b" in the diagram in Figure 4-6) was measured at the rostral edge of the CC (or where the CC would have been in the DKO), middle of the CC, and caudal edge of the CC. These values were normalized against changes in size and shape of the entire brain by dividing by the entire height of the brain ("c" in the diagram in Figure 4-6). The greatest difference was seen in the rostral portion of the CC, where the distance between the top of the brain and top of the CB+ cells was increased by 1.5 fold in DKO brains compared to WT brains (1405±119 μm in DKO, 1159±94 μm in RBKO and 937±118 μm in WT), and the total length of the CB+ area was increased by 3.9 fold in DKO brains compared to WT brains (537±69 in DKO, 123±36 in RBKO and 138±32 in WT). Since the dorsal edge of the CB+ region was found to be shifted ventrally in DKO brains compared to WT brains, this indicates that displacement of the corticoseptal boundary is due to expansion of the entire cingulate cortex and is not specific to the IG neurons. Indeed, both proliferation and cell death were found to be more dramatically increased in the medial cortex than in the lateral cortex at E17.5, with only a 1.5 fold increase in proliferation in the lateral cortex of DKO brains as compared to WT brains (8.8±3.8 Ki67+ cells in .06mm^2 in WT lateral cortex to 13.5±8.2 Ki67+ cells in DKO lateral cortex), in contrast to a 5.6 fold increase in proliferation in the medial cortex (6.8±3.2 Ki67+ cells in WT medial cortex to 38.0±22.1 Ki67+ cells in DKO medial cortex)

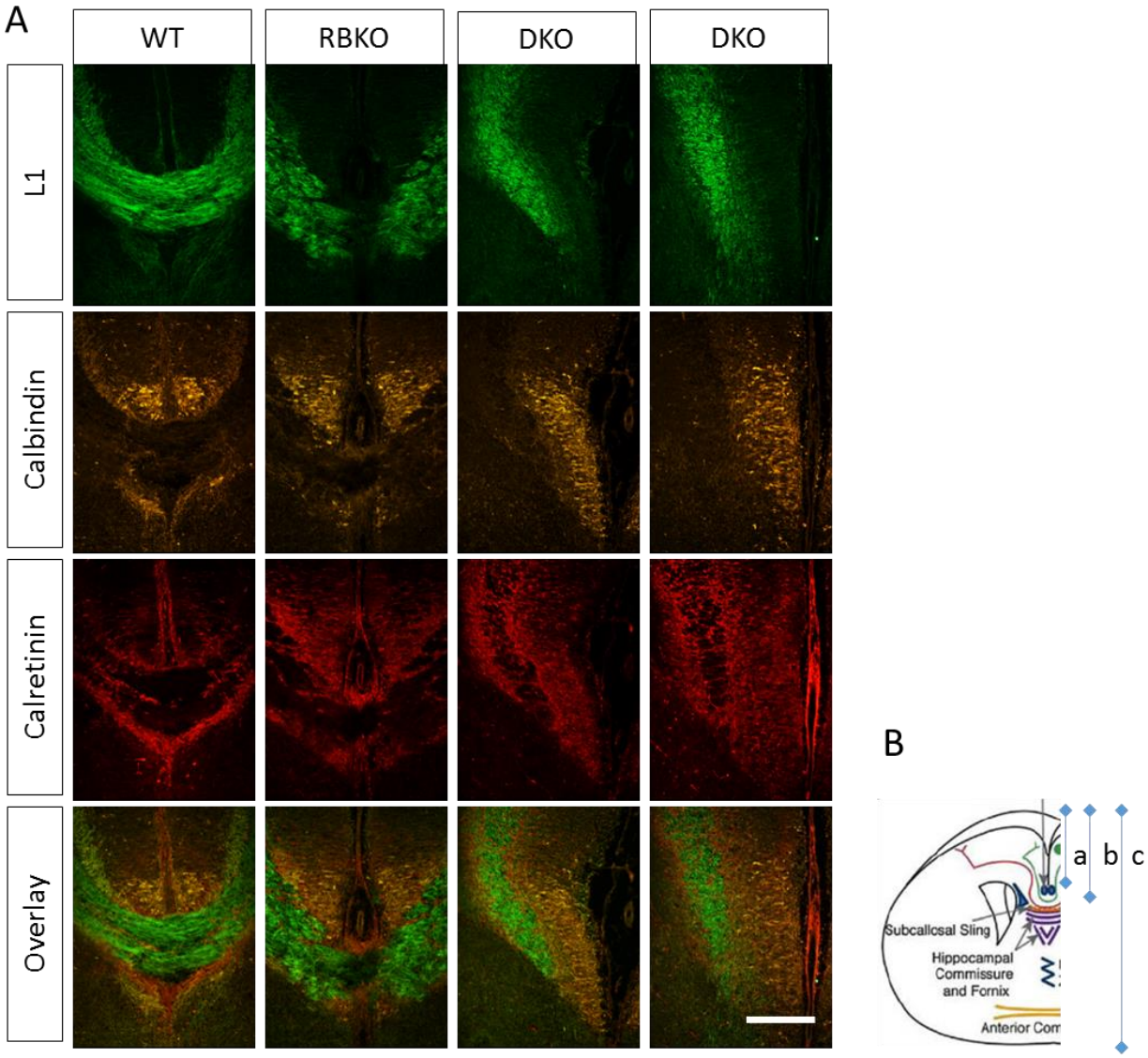
A
WT
RBKO
DKO
DKO
L1
Calbindin
Calretinin
Overlay
B
a
b
c
Subcallcsal Sling
Hippocampal
Commissure
and Fornix
C
Top of Calbindin
WT
RBKO
DKO
(a/c)x100
Rostral
Medial
Caudal
D
Bottom of Calbindin
WT
RBKO
DKO
(b/c)x100
ns
Rostral
Medial
Caudal

Figure 4-6

Figure 4-6: Corticoseptal boundary and indusium grisium neurons are shifted caudally in DKO brains. A) Representative images are shown of the developing corpus callosum of E17.5 brains from pRb f/+; p107-/+ (WT), pRb f/f; p107+/- (RBKO), pRb f/f; p107-/- (DKO) embryos. Sections are stained with L1 (axon marker - green), Calbindin (indusium grisium neural marker - yellow) and Calretinin (glial sling marker - red). Note the mild defect in the RBKO brain. Two DKO brains are shown to illustrate variations in severity of phenotype. To quantify the relative location of the calbindin+ (CB+) neurons, the distance between the top of the brain and the top of the CB staining (represented by line (a) in diagram **(B)**) or bottom of CB staining (line b) was measured and divided by the entire height of the brain (line c). Both the dorsal **(C)** and ventral **(D)** edges of the CB+ staining are shifted downwards in DKO brains. Measurements were made at E17.5 (not shown) and P0 (shown). Scale bar = 60µm $p<0.05$ = * $p<0.01$ = ** $p<0.005$ = *** ns = not significant

(Figure 4-7). A similar pattern was seen in quantification of cells expressing active caspase 3 to indicate apoptosis (Figure 4-7). This specific sensitivity of the medial cortex to loss of pRb and p107 could explain this midline dismorphia seen at later developmental stages in DKO brains.

Defects in axon organization and midline crossing can be observed in DKO brains as early as E15.5 and develop progressively to P0 (Figure 4-4). Therefore, if morphological abnormalities in the midline support structures are responsible for these axon guidance effects, these abnormalities must be present at or before E15.5, before the axon phenotype is visible. Since commissural axons cross the midline between E15.5 and E16.5 in the murine brain (Koester and O'Leary. 1994; Piper, et al. 2009b), CB and GFAP expression patterns relative to L1+ axons were analyzed in DKO brains at E15.5 and E16.5 (Figure 4-8A,B). At E15.5, the neural component of the IG appears slightly larger in DKO brains (Figure 4-8A), but grossly normal. However, the commissural axons in DKO brains which approach the midline are highly disorganized and, in contrast to the clear delineation between these descending axons and the CB+ region of the IG in WT brains, DKO axons mingle among the CB+ cells (insets Figure 4-8A). These observations suggest that either a repulsive signal between the CB+ cells and the pioneering axons has been lost or an attractive signal has been gained in DKO brains prior to midline crossing.

The glial portion of the IG was examined at E16.5, the earliest age at which strong GFAP expression can be detected (Figure 4-8B). In both WT and DKO brains, GFAP+ cells were found to make a normal GW at this age, showing that this structure develops normally initially and the abnormalities seen at later time points are due to distortion of the surrounding cortex. GFAP+ IG glial cells were also found at the midline in the correct location in both DKO and WT brains, with no significant difference at this age in the length of the medial cortex based on the

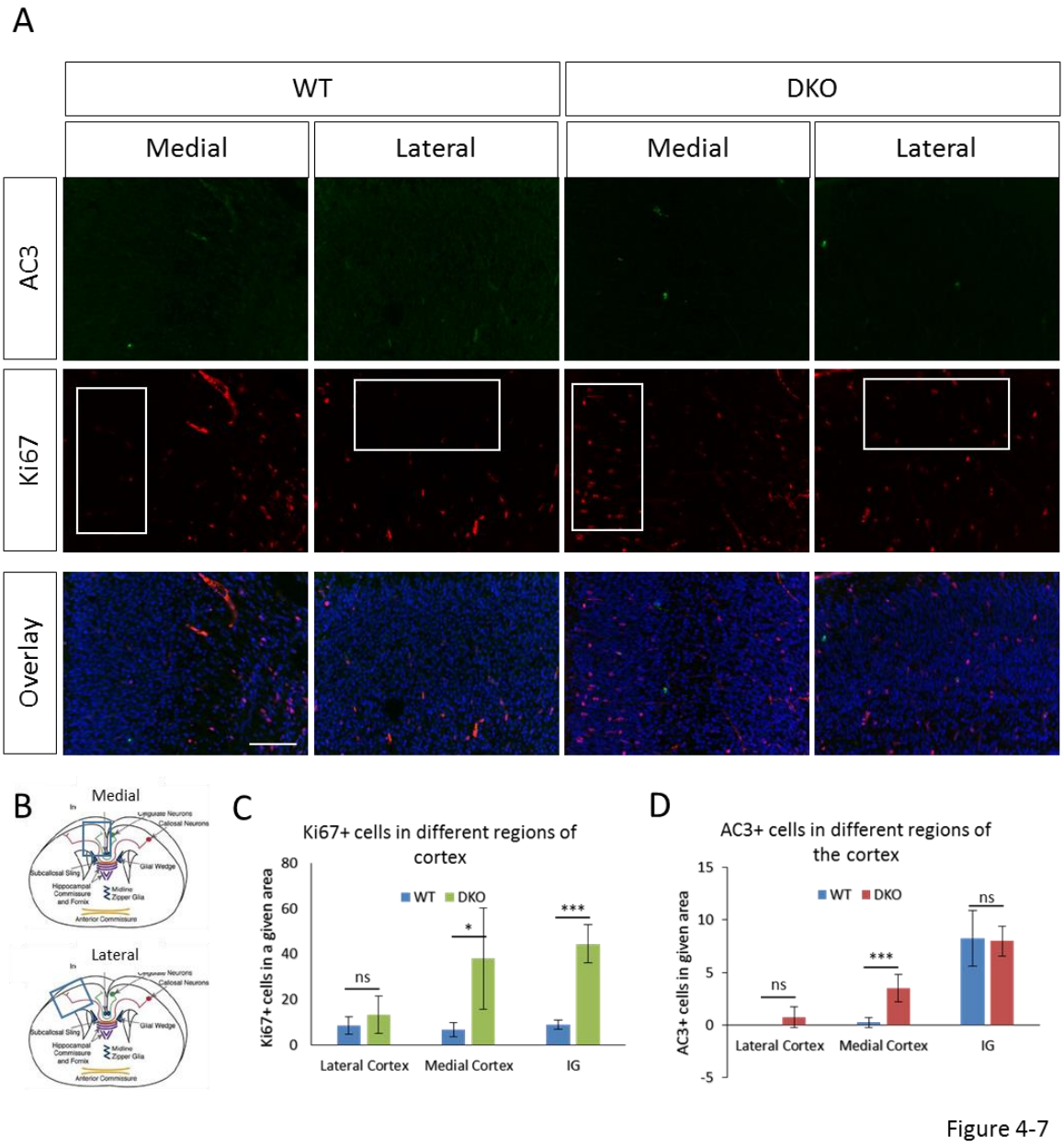

Figure 4-7

Figure 4-7: Increased proliferation and apoptosis in DKO brains is more pronounced in the medial cortex than in the lateral cortex. A) Representative images of WT and DKO medial and lateral cortex at E17.5 stained for Ki67 (red) to mark proliferating cells, and active caspase 3 (AC3, green) to mark cells undergoing apoptosis. Images and counts were done in the medial cortex (top diagram in **(B)**) and the lateral cortex (bottom diagram in **(B)**) as well as the IG (images not shown). Counts for Ki67+ cells **(C)** and AC3+ cells **(D)** were done by selecting a region of a defined area in the medial or lateral cortex (see white boxes on the Ki67 images). Scale bar represents 100 µm. $p<0.05$ = * $p<0.005$ = *** ns = not significant

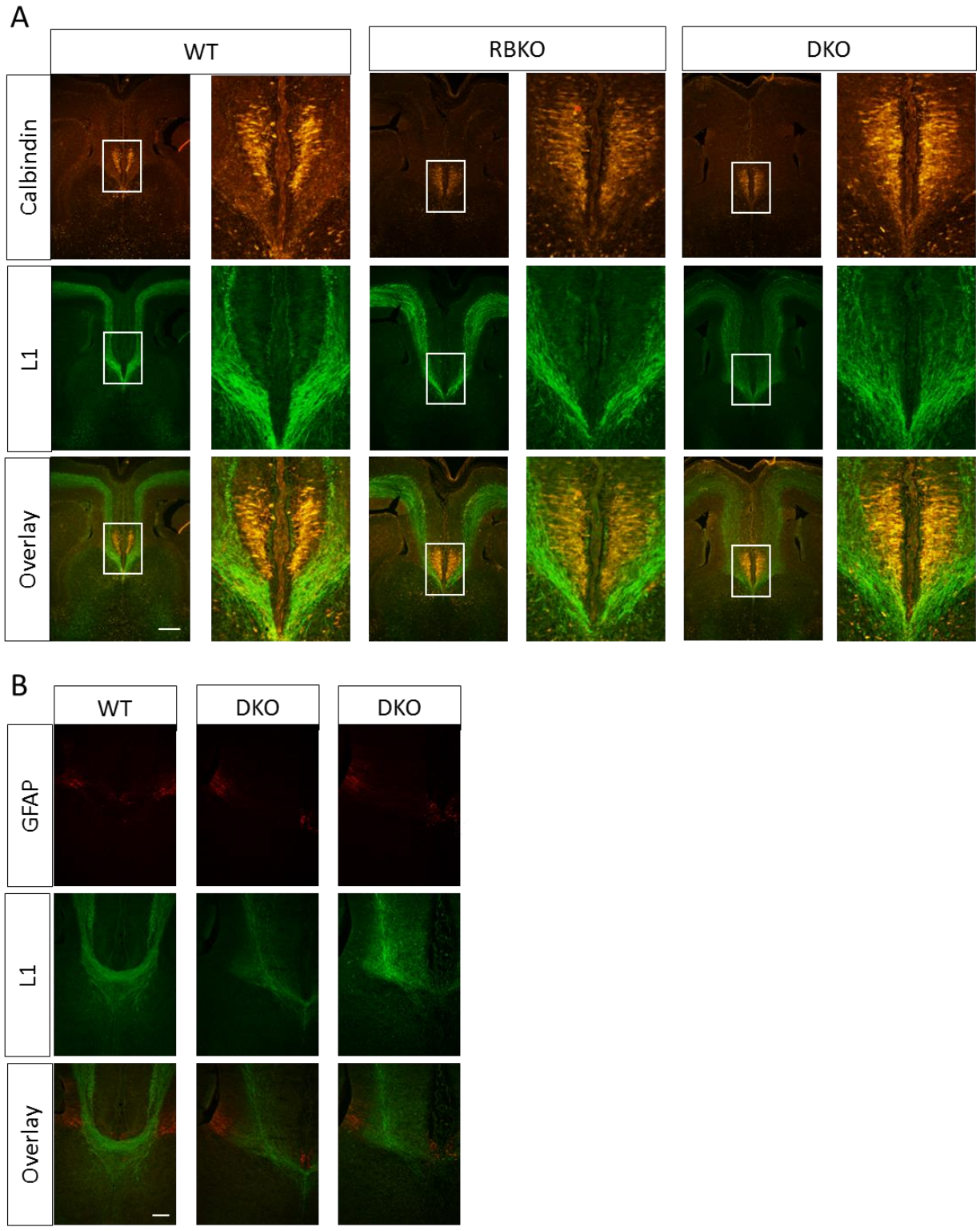
A
WT
RBKO
DKO
Calbindin
L1
Overlay
B
WT
DKO
DKO
GFAP
L1
Overlay

Figure 4-8

Figure 4-8: Defects in midline organization and axon guidance are present prior to axon crossing with a normal indusium griseum and glial wedge. Representative images are shown of the developing corpus callosum of E15.5 **(A)** and E16.5 **(B)** brains from pRb f/+; p107-/+ (WT), pRb f/f; p107+/- (RBKO), pRb f/f; p107-/- (DKO) embryos. To view the neural component of the IG **(A)**, sections are stained with L1 (axon marker - green) and calbindin (yellow). Note that there is a clear delineation between axons and CB+ neurons in WT brains, while the axons in DKO brains are disorganized and overlap with the CB staining. To view the glial component of the IG **(B)**, sections were stained for GFAP (red) and L1 (yellow). Note that glial cells can be found at the midline in all genotypes. **A)** Scale bar represents 200 µm. **B)** Scale bar represents 100 µm.

location of CB+ staining, with WT brains measuring 816.2±43.2 μm and DKO brains measuring 890±78.4 μm (data not shown). This indicates that IG glia cell number and migration from the glial wedge are normal in DKO brains. To confirm that that the IG is normal at the time of midline crossing, glial cell number was evaluated using the marker Sox9 at E15.5 and E17.5. At E15.5, there was no significant difference in the number or location of Sox9+ cells at the midline at the rostral and middle portions of the CC between DKO and WT animals (Figure 4-9A,B). At the middle portion of the CC, WT brains had 55±12 Sox9+ cells while DKO brains had 51±6 Sox9+ cells (represents total IG cells per section). At 17.5, Sox9+ cells were found to be decreased by 15 fold in DKO brain in the rostral CC (46±10 cells in WT brains and 3±3 cells in DKO brains) and then increased by 5 fold in the caudal CC in DKO animals (36±9 cells in WT and 188±81 cells in DKO brains), confirming the observation that IG glial cells distribution is normal at early time point but becomes shifted caudally at older developmental stages (Figure 4-9C,D). Because the GW and the IG are quantifiably normal at the crucial time of midline crossing, callosal agenesis is likely to be due to a failure in molecular communication between the axons and the midline structures or a defect in the axon themselves, rather than a defect in the formation or integrity of the midline support structures.

Expression of multiple classic axon guidance signaling proteins is disrupted in DKO brains: a focus on Netrin. Several axon guidance molecules are known to be required for development of a normal CC, including the Netrin/DCC (Serafini, et al. 1996; Fazeli, et al. 1997; Shu, et al. 2000; Fothergill, et al. 2013), Robo/Slit (Shu and Richards. 2001), Eph/ephrin (Mendes, et al. 2006; Bush and Soriano. 2009; Ho, et al. 2009) and Shh/Gli3 (Magnani, et al. 2012a; Magnani, et al. 2012b) pathways. To determine if expression of any of these molecules is

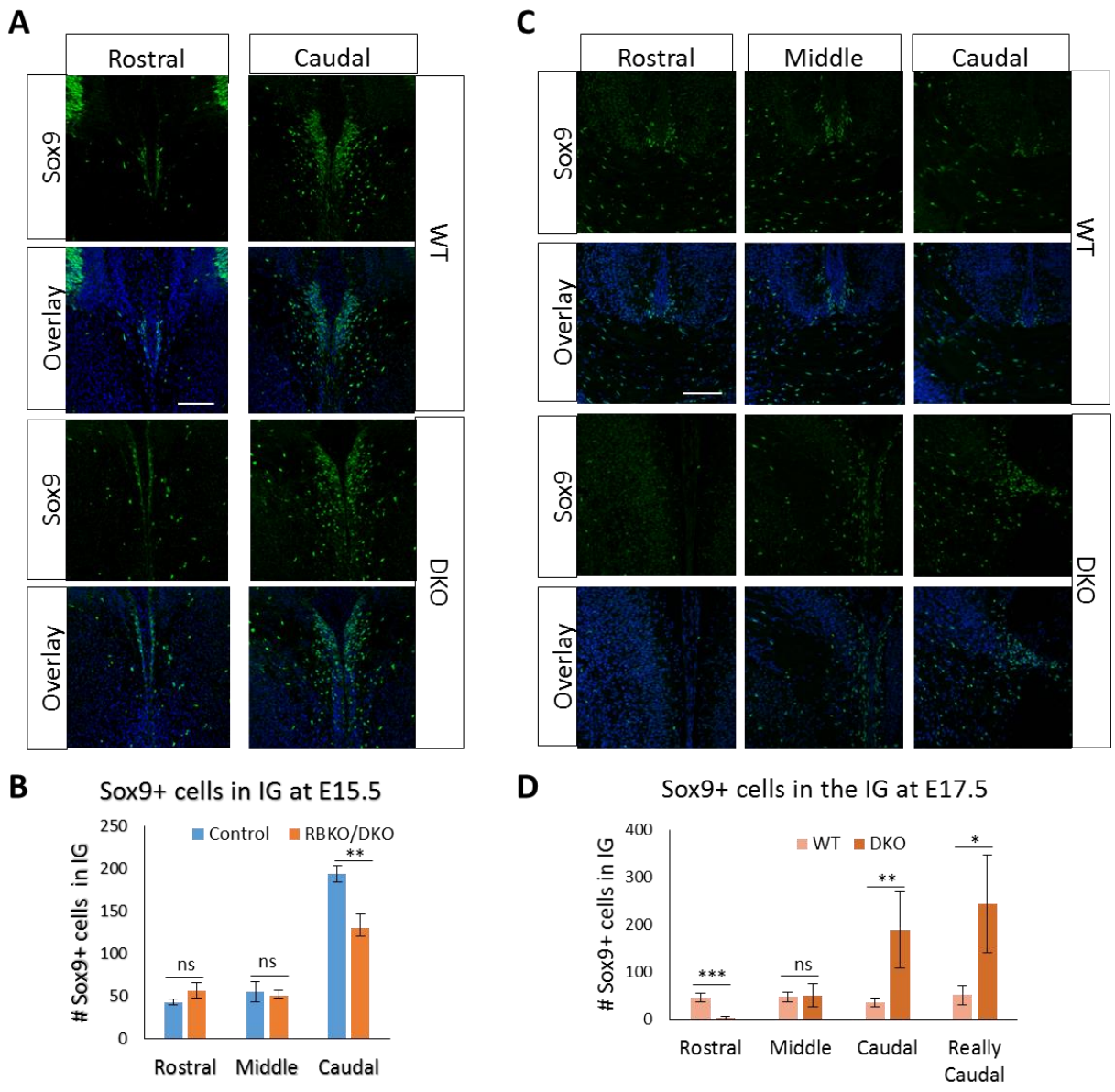

Figure 4-9

Figure 4-9: **IG glia cell numbers are normal at the time of axon crossing but become distorted later in development.** Representative images of Sox9 staining (green) overlaid with Dapi (blue) in the IG of pRb f/+; p107-/+ (WT) and pRb f/f; p107-/- (DKO) embryos are shown at E15.5 (**A**) and P0 (**C**). Sox9 is a glial cells nuclear marker. The number of Sox9+ cells in the region of the IG was counted at the rostral, middle and caudal levels of the corticoseptal boundary at E15.5 (**B**) and CC at P0 (**D**). Scale bars represent 100 µm. $p<0.05$ = * $p<0.01$ = ** $p<0.005$ = *** ns = not significant

abnormal at the midline of DKO brains, mRNA expression of a panel of classical axon guidance molecules was examined at E17.5 (Figure 4-10) and E15.5 (Figure 4-11) using ISH. At E17.5, two primary observations can be made. First, the cells occupying the space at the midline of DKO brains where the CC normally exists express various receptors commonly found in cingulate cortical neurons, including DCC and Robo1. Second, Netrin and Slit2, two secreted molecules expressed by the IG, are decreased in DKO brains. Since expression of both these molecules are expressed normally in other brain structures (data not shown), this specific loss at the midline could be due to either cell type specific downregulation or to absence of the cells which express these proteins.

Netrin expression was also found to be altered in DKO brains at E15.5 (Figure 4-11). In WT brains, there are two patches of Netrin expressing cells, one small population situated directly adjacent to the pre-crossing axons which is most likely IG glial cell precursors (Shu and Richards. 2001; Fothergill, et al. 2013), and one much larger population located higher in the cingulate cortex. In DKO brains, this dorsal patch of Netrin expression is gone, while the ventral population is expanded and often shifted caudally such that it was absent in rostral sections but expanded in caudal sections. In both WT and DKO brains, the IG glial precursors also express Slit1, Slit2 and Gli3 (Figure 4-11), with a small decrease in Slit2 and no change in Slit1 or Gli3 in DKO brains.

The location of the dorsal patch of Netrin expressing cells does not correlate with any known axon guidance structure in the developing commissural plate, although its location within the cingulate cortex suggests that this structure functions in guiding callosal axons. To determine if the Netrin-expressing cells are actually the IG neurons in WT brains, Netrin ISH was performed in conjunction with immunohistochemistry for CB at E15.5 and E17.5 (Figure 4-

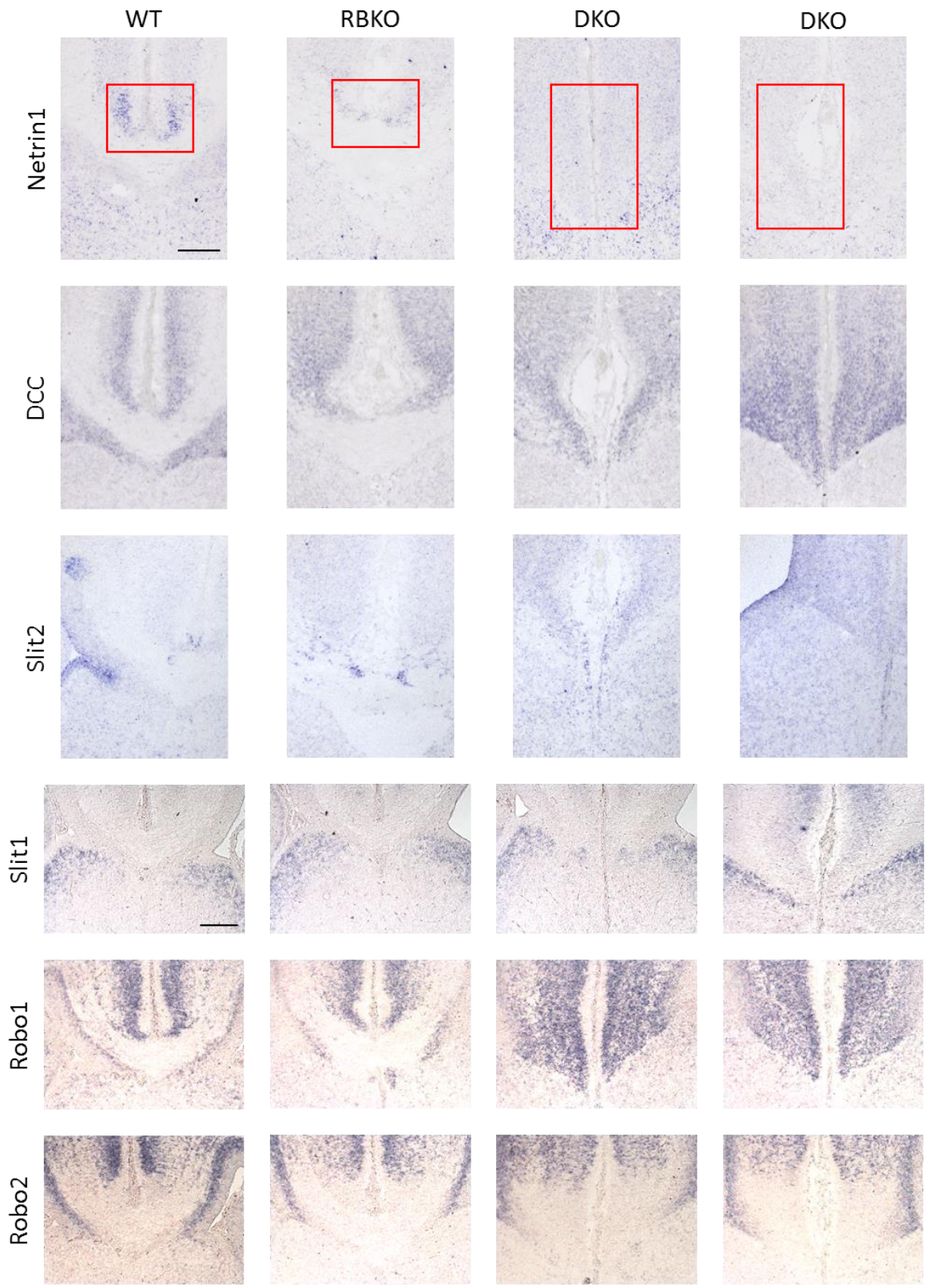

Figure 4-10

Figure 4-10: Expression of multiple axon guidance molecules are altered in the midline of DKO brains at E17.5. Patterns of mRNA expression of a panel of classic axon guidance molecules were analyzed at E17.5 using in situ hybridization in WT, RBKO and DKO brains. Note that Netrin1 is lost in DKO brains (red squares), the location of Slit2 expression is shifted ventrally and that Robo1 and DCC are increased. Scale bars represent 200 μm.

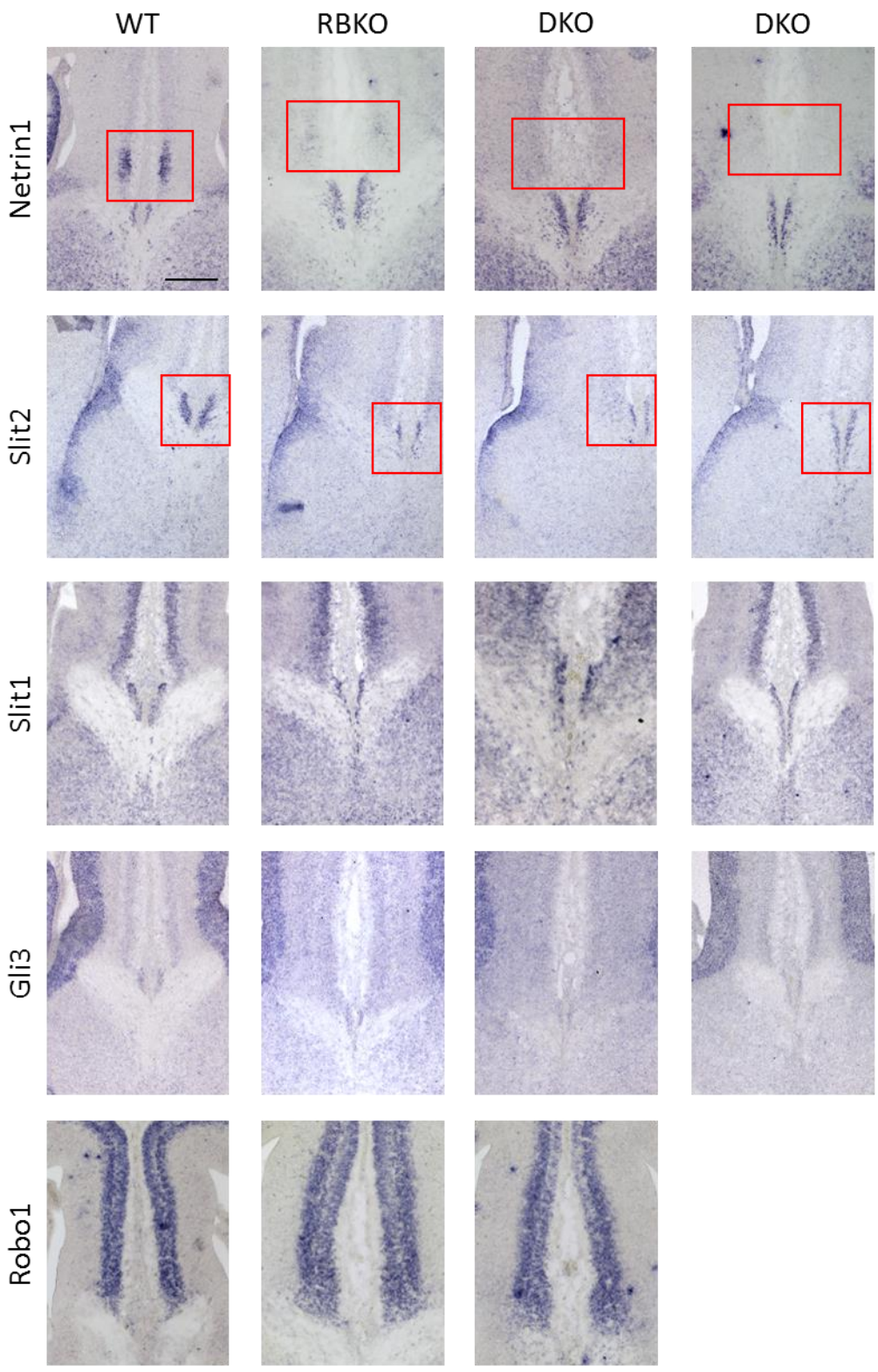

Figure 4-11

Figure 4-11: Expression of axon guidance molecules in the midline of DKO brains prior to callosal axon crossing. Patterns of mRNA expression of a panel of classic axon guidance molecules were analyzed at E15.5 using in situ hybridization in WT, RBKO and DKO brains. Note the two patches of Netrin expression in WT brains; the dorsal patch is lost in DKO and RBKO brains and the ventral patch is increased in size. Slit2 and Gli3 are slightly decreased specifically at the midline, while Slit1 is unchanged. Scale bar represents 200 μm.

12). Netrin and CB are expressed in distinct and separate cell populations with minimal overlap at both E17.5 (Figure 4-12A) and E15.5 (Figure 4-12B) in WT brains. At E15.5, the dorsal patch of Netrin expression is lost in DKO and RBKO brains despite the presence, and sometimes expansion, of CB+ cells (Figure 4-12B). Netrin protein levels were also found to be decreased in the medial cortex of DKO brains by Western blot analysis (Figure 4-12C) and Netrin was identified as an E2F3 target by ChIP (Figure 4-1). These results suggest that Netrin, which is a crucial attractive signal during CC formation (Fothergill, et al. 2013), may be secreted by two independent sources at the corticoseptal boundary, rather than only the IG glia as previously thought. Since loss of Netrin expression within these cells is correlated with callosal agenesis in DKO brains, this dorsal patch of Netrin expressing cells could represent a previously undescribed axon guidance structure necessary for CC formation.

Defects in axon growth and guidance in DKO brains begin prior to reaching the midline. Callosal axons originating in the lateral cortical plate must leave the cortex and then tangentially extend through the IZ as part of a fasciculated, cohesive tract before reaching the midline. (Hatanaka, et al. 2009; Leyva-Diaz and Lopez-Bendito. 2013). As described above, callosal axons were highly disorganized near the cingulate cortex in DKO brains at both E15.5 (Figures 4-4 and 4-8) and E17.5 (Figure 4-4). To determine if this disorganization was found throughout the length of these axons, the location and fasciculation of L1+ axons was examined in the IZ under the lateral cortex at E17.5 (data not shown) and P0 (Figure 4-13A). In DKO brains, axons within the IZ appear defasciculated and chaotic with clumps of L1+ staining seen throughout the cortex. At the dorsal flexure, where axons normally turn ventrally toward the commissural plate, clumps of axons appear to continue along a straight projection and re-enter the ipsilateral cortex

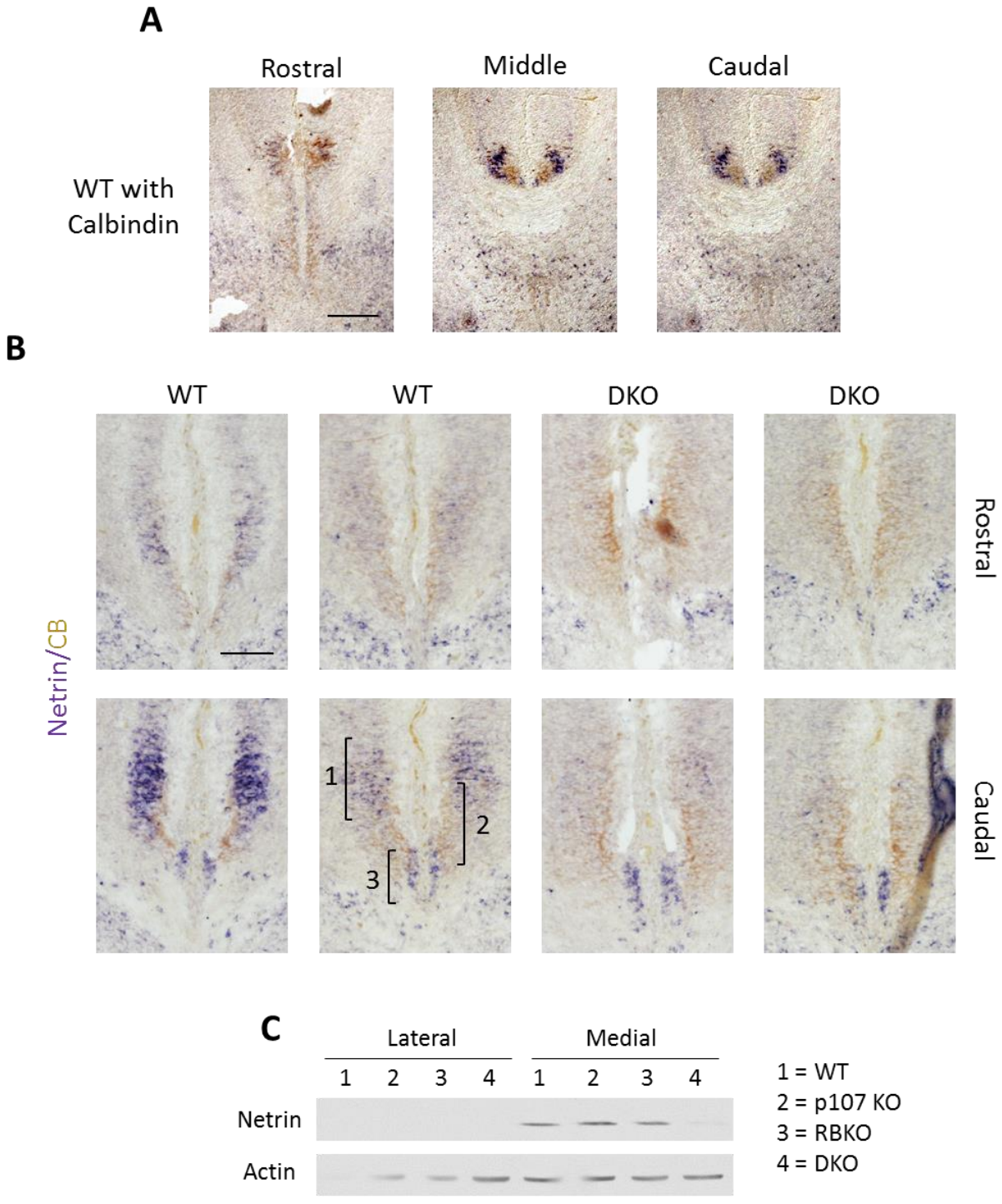
A
Rostral
Middle
Caudal
WT with
Calbindin
B
WT
WT
DKO
DKO
Netrin/CB
Rostral
Caudal
1
2
3
C
Lateral
Medial
1 2 3 4 1 2 3 4
Netrin
Actin
1 = WT
2 = p107 KO
3 = RBKO
4 = DKO

Figure 4-12

Figure 4-12: Netrin and Calbindin are expressed by separate populations of cells in the WT and DKO midline. To determine whether the neural portion of the IG is the source of Netrin in the midline of the WT brain, Netrin in situ hybridization was performed in conjunction with CB immunohistochemistry at E17.5 **(A)** and E15.5 **(B)**. Netrin and CB were found to be expressed in separate cell populations at both ages, indicating that the CB+ cells are not the source of Netrin in the WT brain. In the DKO brain **(B)** the CB population is present but the Netrin population is absent (or not expressing Netrin) as seen in previous figures, despite the presence of the CB expressing cells. There therefore seem to be three cell populations in the ventral cingulate cortex, the (1) dorsal Netrin expressing population, the (2) middle CB+ population, the IG neurons, and the (3) ventral Netrin expressing population, the IG glial precursors. **C)** Expression of Netrin in the medial and lateral cortex of WT, p107KO, RBKO and DKO brains was measured by Western blot at E17.5 (shown) and E15.5 (data not shown). Netrin was only detected in the medial cortex of control brains, but could not be detected in DKO medial cortex tissue. **A)** Scale bar represents 200 µm. **B)** Scale bar represents 100 µm.

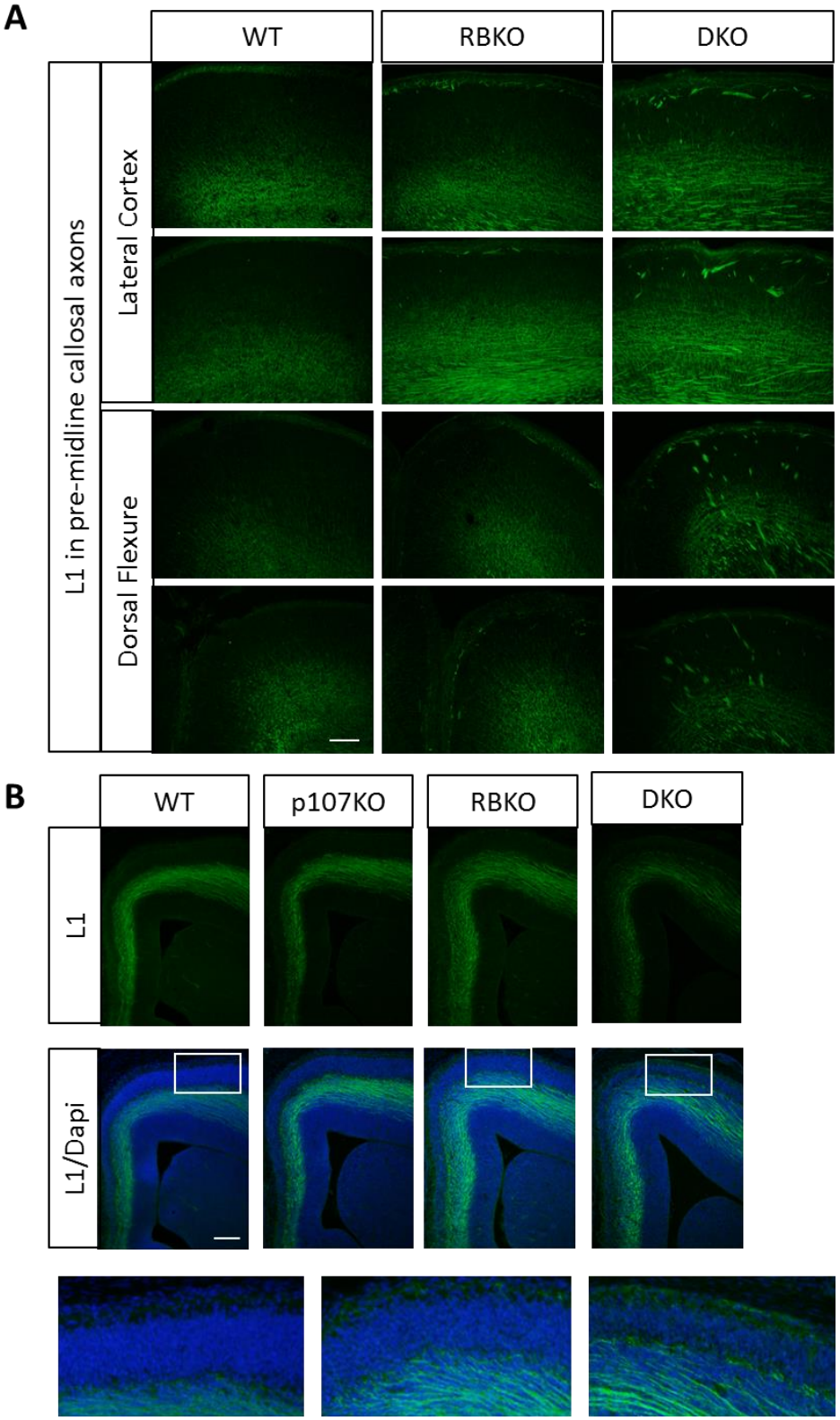
A
WT
RBKO
DKO
L1 in pre-midline callosal axons
Lateral Cortex
Dorsal Flexure
B
WT
p107KO
RBKO
DKO
L1
L1/Dapi

Figure 4-13

Figure 4-13: Callosal axons show defasciculation and disorganization prior to reaching the midline. To determine if axon disorganization is specific to the corticoseptal boundary, the morphology of the axon tract traveling through the intermediate zone below the lateral cortex was examined in WT, RBKO and DKO at P0 by staining for L1 (**A**). Extreme defasciculation and disorganization was observed in DKO brains, with clumps of axons present within and above the cortex. The same anatomical region was examined at E15.5 (**B**), and axons were found to be clumped with ectopic L1 visible staining above the cortex in RBKO (middle panel) and DKO brains (rightmost panel), but not WT brains (leftmost panel). Scale bars represent 100 μm.

in DKO brains (Figure 4-13A). Similar forms of axon disorganization and misguidance can be seen as early as E15.5 (Figure 4-13B), where L1 staining can be seen above the cortex in DKO but not WT brains, and DKO axons are spread out over a much larger area within the IZ.

To determine if these clumps of L1+ axons in the cortex resulted from premature expression of L1 prior to leaving the cortex or whether it was due to axons re-entering the cortex after reaching the IZ, the lateral cortices of DKO and WT embryos were electroporated with GFP (Figure 4-14) at E14.5 and examined 4 and 6 days later. GFP+ axons in DKO brains showed a dramatically shorter length compared to GFP+ axons in WT brains at both time points, suggesting that the rate of axon extension is decreased in the DKO neurons (Figure 4-14A). Furthermore, these axons leave the electroporated region of the cortex and turn medially normally, but then re-enter the cortex (arrows in Figure 4-14B). Together these observations show that DKO axons have defects in both growth and guidance independent of the midline.

The decrease in the rate of axonal growth could result from an either autonomous defect in axon extension in the DKO neurons or a difference in the balance of repulsive and attractive cues in the surrounding environment. To distinguish between these possibilities, explants from the medial and lateral cortex of DKO and WT brains were cultured in a collagen matrix and neurite length was measured after 24 or 48 hours. The results from a representative experiment are shown in Figure 4-15. A significant decrease in neurite length was found in DKO explants from both lateral (Figure 4-15I,K) and medial (Figure 4-15J,L) tissue at both time points, although the difference did not reach significance in all experiments until 48 hours. To determine if DKO axons are capable of responding to Netrin stimulation, explants were treated with a saturating dose of Netrin at the time of plating (Figure 4-15M-U). WT medial cortical explants were responsive to Netrin at 24 hours (Figure 4-15Q), whereas explants from WT

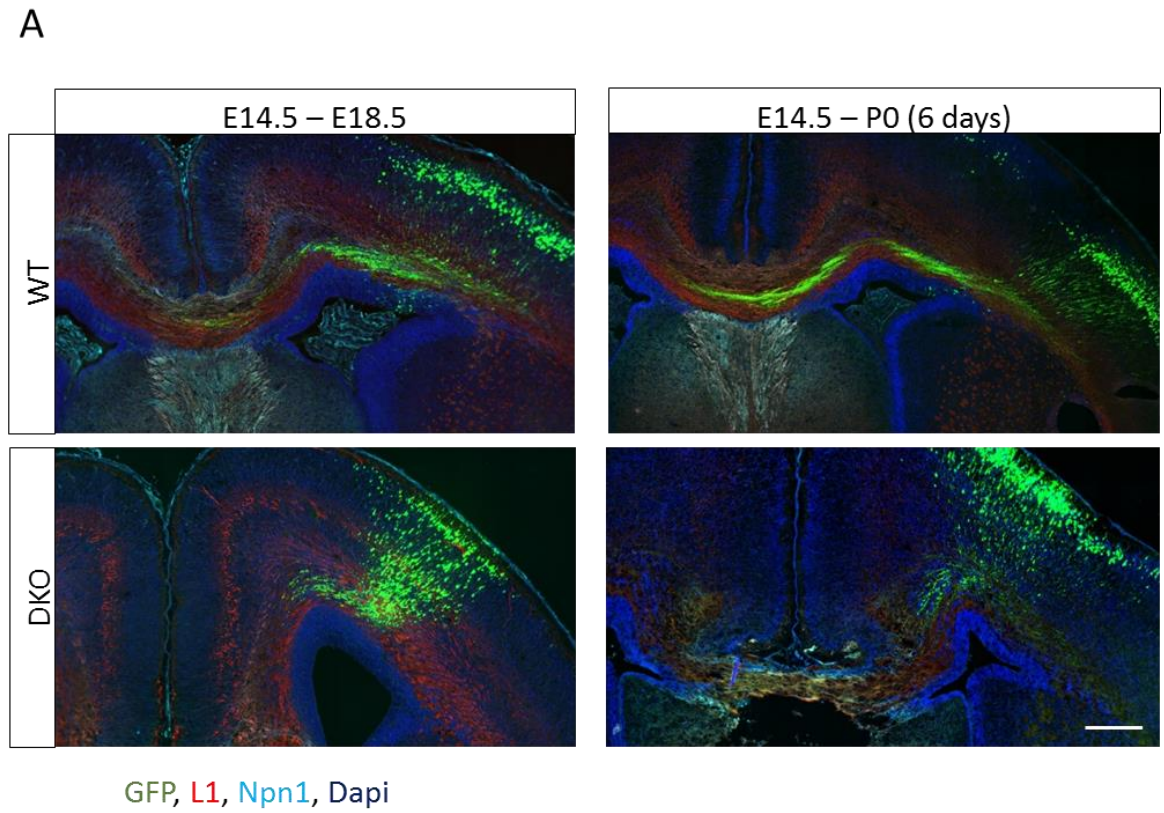
A
E14.5 – E18.5
E14.5 – P0 (6 days)
WT
DKO
GFP, L1, Npn1, Dapi
B
WT
DKO
GFP
Overlay w/Dapi

Figure 4-14

Figure 4-14: Slow growth and trajectory errors in DKO axons traveling through the intermediate zone. To better understand the growth and guidance of individual axons, the lateral cortex of DKO and WT embryos was electroporated at E14.5 and collected at E18.5 (**A left**) or P0 (**A right**). GFP+ axons in DKO brains had travelled a shorter distance compared to WT axons at both time points (**A**), and the axons showed signs of defasciculation and re-entering the cortex in DKO brains only (arrows in **B**). Scale bar represents 300 µm. **B**: Higher magnification of GFP+ axons at E18.5 to emphasize trajectory errors (arrows) in DKO brains. Scale bar represents 100 µm.

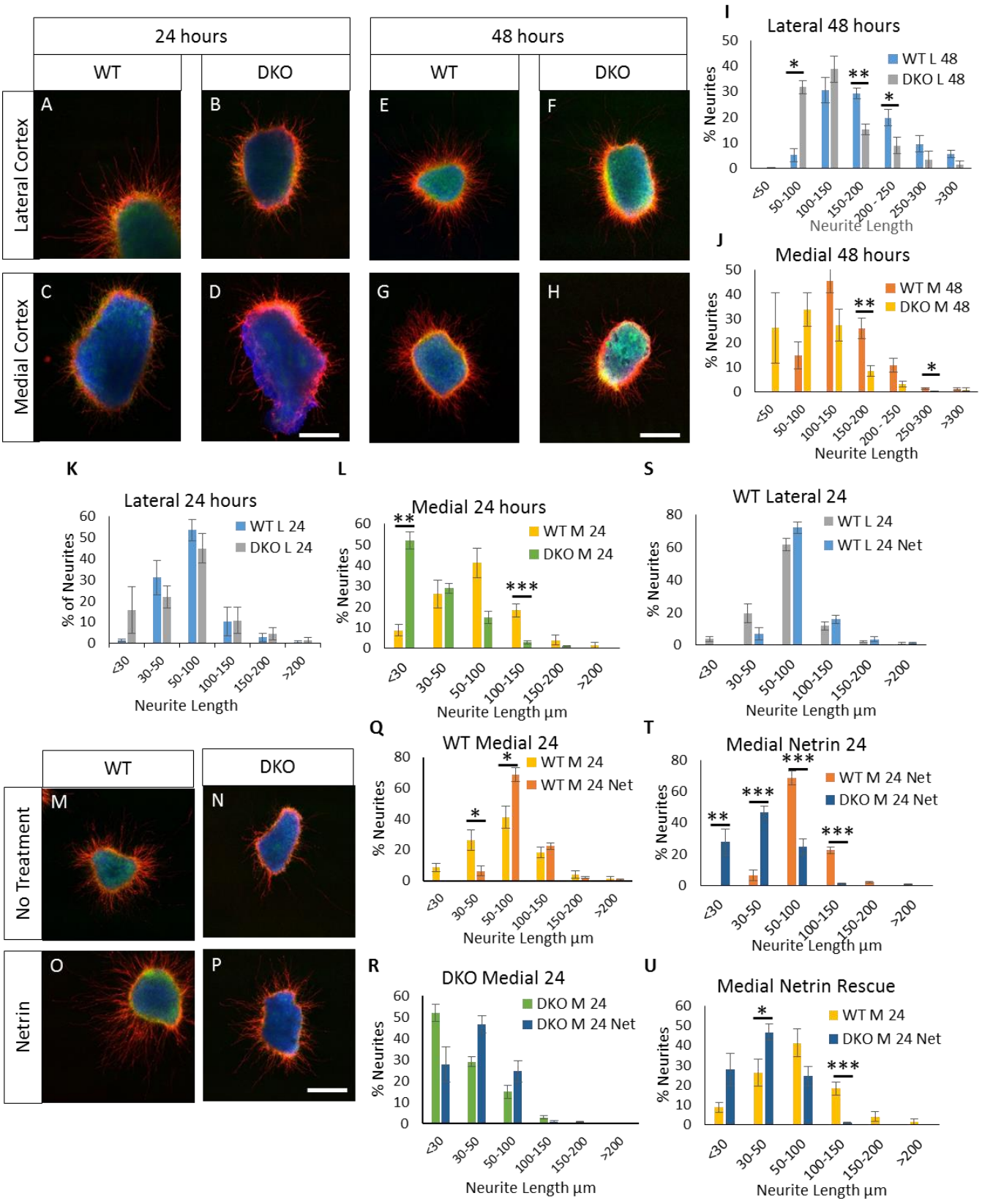
24 hours
48 hours
WT
DKO
WT
DKO
Lateral Cortex
Medial Cortex
A
B
C
D
E
F
G
H
I
Lateral 48 hours
% Neurites
WT L 48
DKO L 48
Neurite Length
J
Medial 48 hours
WT M 48
DKO M 48
Neurite Length
K
Lateral 24 hours
% of Neurites
WT L 24
DKO L 24
Neurite Length
L
Medial 24 hours
WT M 24
DKO M 24
Neurite Length µm
S
WT Lateral 24
WT L 24
WT L 24 Net
Neurite Length µm
WT
DKO
No Treatment
Netrin
M
N
O
P
Q
WT Medial 24
WT M 24
WT M 24 Net
Neurite Length µm
T
Medial Netrin 24
WT M 24 Net
DKO M 24 Net
Neurite Length µm
R
DKO Medial 24
DKO M 24
DKO M 24 Net
Neurite Length µm
U
Medial Netrin Rescue
WT M 24
DKO M 24 Net
Neurite Length µm

Figure 4-15

Figure 4-15: Decreased neurite outgrowth and blunted response to Netrin stimulation in DKO cortical explants. A-L: Explants from the lateral (**A, B, E, F**) or medial (**C, D, G, H**) cortex of WT (**A, C, E, G**) or DKO (**B, D, F, H**) brains were cultured for 24 (**A-D**) or 48 (**E-H**) hours and the 100 longest neurites were measured and binned according to length in micrometers (**I-L**). A significant decrease in neurite outgrowth was seen in DKO explants. **M-P:** Explants from the lateral (**S**) or medial cortex of WT (**M, O**) or DKO (**N, P**) brains were cultured in the absence (**M, N**) or presence of Netrin (**O, P**) for 24 hours. Neurite length was measured to determine if WT (**Q**) and DKO (**R**) neurites respond to Netrin growth stimulation and to determine whether this stimulation rescues the growth defect observed in **A-L**. Only WT neurites from the medial cortex were found to respond to Netrin (**Q, S**) and the response of DKO neurites was too small to be significant (**R**). Treatment with Netrin was unable to rescue the growth defect in DKO axons (**R, T, U**). All scale bars represent 250 μm. * = $p < 0.05$ ** = $p < 0.01$ ** = $p < 0.001$

lateral cortical explants showed no response to Netrin stimulation, as has been previously shown (Figure 4-15S) (Fothergill, et al. 2013). Similar results were seen for DKO medial (Figure 4-15R) and lateral (data not shown) explants, although the response was more modest than in WT and did not reach significance. Therefore, the difference in neurite length between DKO and WT medial explants achieved a much greater degree of divergence following Netrin treatment than when explants were untreated (compare level of significance in Figure 4-15 panel T to panel L). It is also of note that when Netrin treated DKO explants were compared to untreated WT explants, neurites from WT explants were still significantly longer, indicating that treatment with Netrin was unable to rescue the growth defect (Figure 4-15U). Together, these results show that DKO axons have an inherent defect in neurite extension and are capable of making only a blunted response to Netrin stimulation.

Axon growth through the IZ is dependent on both secreted axon guidance signals and direct adhesion to adjacent axons (Tables 1-3 and 1-4). To determine if axon defasciculation in DKO brains could be due to changes in the expression of adhesion molecules, protein levels of several well-known adhesive cues were analyzed by Western blot (Figure 4-16). DKO tissue was found to have decreased levels of Npn1 at both E15.5 and E17.5, which corresponds to the decreased Npn1 staining intensity observed using immunohistochemistry (Figure 4-4, 4-8A). As previously shown, Npn1 was confirmed as an E2F3 target gene on the ChIP on chip screen (Figure 4-1). As the Npn1/Sema3 pathway is very important in guiding callosal axons (Gu, et al. 2003; Huber, et al. 2005; Hatanaka, et al. 2009), deregulation of the Sema3 pathway could be responsible for the axon guidance defects in the IZ in DKO brains. These results support the hypothesis that axon defasciculation and cortex re-entry following loss of pRb and p107 could

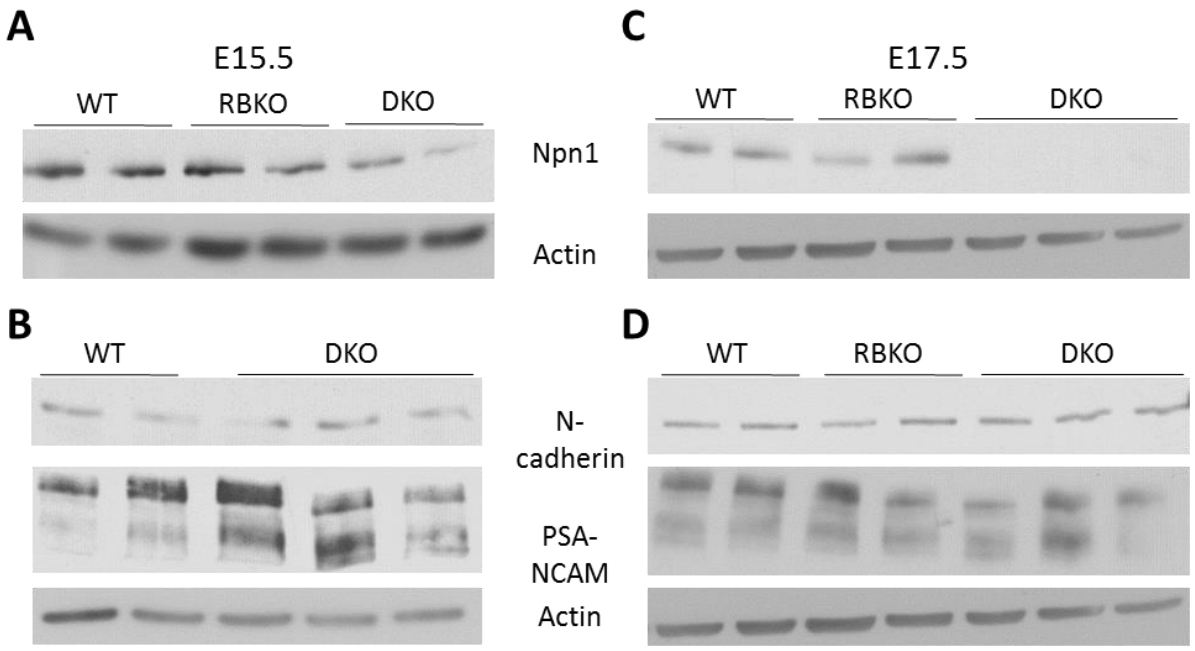

Figure 4-16

Figure 16: Decreased expression of Npn1 in DKO cortical tissue. To determine if regulation of adhesion proteins could be responsible for the axon defasciculation in DKO brains, the expression level of a panel of axonal adhesion proteins in cortical tissue was examined by Western blot at E15.5 (**A, B**) and E17.5 (**C, D**). Npn1 was found to be decreased in DKO brains at both ages (**A, C**) while no change was detected in all other proteins tested (**B, D).**

result from decreased Npn1 expression, possibly due to deregulation of E2F activity at the Npn1 promoter.

Discussion

In this study, we evaluated the role of pocket proteins pRb and p107 in the growth and guidance of callosal axons in the developing brain. Our results support a number of conclusions. First, we show that pocket proteins are necessary for the pioneering axons from the cingulate cortex to cross the midline, which is a crucial first step in CC formation. Second, we show that this callosal agenesis is due to a primary defect in axon growth and guidance, rather than resulting from the morphological defects in the GW and IG at the midline. In addition, several classical axon guidance molecules are deregulated in DKO brains and loss of Netrin expression following pocket protein loss could be responsible for the CC defect. We then demonstrate that there are defects in axon guidance independent from the midline, which are potentially due to decreased Npn1 expression. Finally, we provide evidence for an inherent axon growth defect following loss of pRb and p107 both *in vitro* and *in vivo*. Together, our results describe a novel function for pocket proteins in regulation of axon guidance and axon tract formation in the developing brain.

pRb and p107 are required for pioneer axon crossing. Here we show that pioneering cingulate axons, marked by high expression of Npn1, are unable to cross the midline following the loss of pRb and p107 expression (Figure 4-4). Rather than cross the midline, these axons form Probst bundles adjacent to the midline, as observed in numerous acallosal mouse models (Serafini, et al. 1996; Shu, et al. 2003a; Piper, et al. 2009b; Sanchez-Camacho, et al. 2011;

Fothergill, et al. 2013). Axons from the lateral cortex, which reach the midline after E16.5 (Price, et al. 2006b; Fothergill, et al. 2013), are unable to cross without the guidance normally provided by the pioneering axons and instead swirl and enlarge the Probst bundles. This is most obvious in the rostral and middle portions of the CC. In a subset of DKO brains, Npn1-negative axons in the caudal regions of the CC are able to cross the midline even though the Npn1+ axons form small Probst bundles at the midline (Figure 4-4H). This caudal crossing was observed in a subset of DKO at P0 and in about half of RBKO brains at E17.5 and P0; even in the RBKO brains which form a full CC, the CC is shifted caudally and shows signs of axon disorganization (Figure 4-3). Importantly, in all DKO brains with this partial caudal CC, all crossing axons were Npn1-negative. These observations emphasize the point that Npn1+ pioneering axons are unable to cross the midline in DKO brains. Furthermore, they suggest the possibility that the mechanisms governing axon crossing and the requirement for a scaffold of pioneering axons are fundamentally different between the rostral and caudal portions of the CC.

Analysis of the progressive development of the DKO phenotype in Figure 4-4 shows that axon bundling observed here is different than other acallosal phenotypes since the Probst bundles develop slowly; extensive axon swirling is not observed at E17.5 but only at P0. In fact, just before axon crossing at E15.5, when numerous pre-crossing Npn1+ pioneering axons have reached the midline in WT mice, visibly fewer axons have reached the midline in DKO mice. This is despite seemingly normal axon numbers within the IZ adjacent to the cingulate cortex. At E17.5, axons from the lateral cortex have joined the Npn1+ pioneering axons and now compose the ventral half of the CC in WT (Figure 4-4C), while in the DKO mice, the small Probst bundles still appear to be composed primarily of Npn1+ axons (Figure 4-4D). This suggests that the cingulate axons which were delayed at E15.5 have now reached the midline by

E17.5 in DKO mice. These axons have failed to cross, either (1) because they are unable to respond to existing guidance signals, (2) the appropriate guidance signals are not expressed, or (3) because the axons are too late and the responsible signals are expressed only during a short critical window. The observation that most of the axons still appear to express Npn1 at E17.5 could be because the Npn1-negative axons from the lateral cortex are delayed and have not yet reached the midline. These lateral axons continue to grow and reach the midline by P0, at which point the distinction between Npn1+ and Npn1-negative axons is regained in the now much larger Probst bundles in DKO brains. These observations suggest a model of progressive delay of first the pioneering axons from the cingulate cortex and then the axons from the lateral cortex in DKO mice.

Callosal agenesis is due to a primary axon defect defect rather than a defect in the midline support structures. Normal CC development is highly dependent on the axon guidance structures at the midline, primarily the GW (Shu and Richards. 2001; Shu, et al. 2003a; Shu, et al. 2003c; Sanchez-Camacho, et al. 2011; Lavado, et al. 2014; Chinn, et al. 2014), the IG neurons and glia (Shu and Richards. 2001; Magnani, et al. 2012a; Fothergill, et al. 2013), and the guidepost neurons (Niquille, et al. 2009). Disruption of these structures has been shown to result in acallosal phenotypes even when axons are otherwise normal (Shu, et al. 2003a; Piper, et al. 2009a; Sanchez-Camacho, et al. 2011; Magnani, et al. 2012a) and analysis of the integrity of these structures is an obvious first step in the evaluation of a novel CC defect. Indeed, we show here that at later developmental stages, the GW and both the neurons and glia of the IG are morphologically abnormal (Figure 4-5). Although this could easily contribute to the severity of the defect seen in the DKO embryos, these GW and IG defects do not seem to be the primary

cause of the callosal agenesis following pRb and p107 deficiency. This conclusion can be reached based on the following observations: (1) Axon guidance defects can be observed at the midline prior to the morphological defects in the GW and IG (Figure 4-8B), as seen in the axon disorganization and low axon number at the midline at E15.5 (Figure 4-4) and the overlap between the midline axons and the IG neurons (Figure 4-8A). Any potential mechanism explaining these axon guidance errors must be present at E15.5; (2) Axon guidance errors are not specific to the midline but occur throughout the IZ with defasciculation and ectopic re-entry into the ipsilateral cortex (Figure 13); (3) Multiple axon guidance molecules are deregulated (Figure 4-10 and 4-11), with special emphasis on Netrin (Figure 4-12) and Npn1 (Figures 4-4 and 4-16) since these molecules are deregulated as early as E15.5, while expression of axon guidance molecules in the GW and IG glia at E15.5 appear normal (Figure 4-11); (4) Decreased growth rates and blunted responses to Netrin stimulation occur *in vitro*, independent from the midline and therefore autonomous from any defects in the GW or IG (Figure 4-15). In conclusion, this evidence suggests that errors in axon guidance are visible prior to the defects visible in the GW and IG at the midline. These primary defects are most likely to be in the growth and guidance of the axons rather than in formation of the corticoseptal plate.

Loss of pRb and p107 lead to deregulation of multiple classic axon guidance pathways. The complicated process of guiding axon tips through multiple decision points to their distant final destinations is achieved through the combination of numerous well defined signaling pathways (Price, et al. 2006b). Due to the complexity and functional importance of the CC, members of every family of axon guidance molecule are expressed at the midline and necessary for callosal axon crossing (Edwards, et al. 2014) as has been shown through a combination of knockout

mouse models with acallosal phenotypes and *in vitro* growth cones guidance assays (Shu and Richards. 2001; Niquille, et al. 2009; Islam, et al. 2009; Piper, et al. 2009b; Fothergill, et al. 2013). To determine which of these required molecules displayed altered expression patterns, and was therefore a potential mediator of the DKO phenotype, mRNA expression of a panel of receptors and secreted molecules was examined at E17.5 (Figure 4-10) and E15.5 (Figure 4-11). At E17.5, expression patterns of almost every molecule examined appeared irregular in DKO brains. However, this result is difficult to interpret as by this late developmental stage, the medial cortex and corticoseptal boundary of DKO brains is highly deformed due to over-proliferation of the medial cortex (Figure 4-7). In some cases, such as for Robo1, it is difficult to evaluate whether regulation of the gene itself is effected or whether the apparent upregulation is actually due to an increase in the number of cells expressing the receptor. Although an increase in the number of cells expressing axon guidance genes could have an effect on axon guidance, only proteins which are misexpressed at E15.5 at the time that the primary axon guidance defect is first detected are likely to be involved in the mechanism responsible for the DKO phenotype. To identify genes whose expression is deregulated early, we examined expression profiles at E15.5 and found that most targets are normal at this age (Figure 4-11). A key exception to this is Netrin (Figure 4-12). Netrin expression is greatly decreased at both E15.5 and E17.5. At both ages there are two populations of Netrin expressing cells; the ventral population is the same cell group which expresses Slit1/2 and Gli3 and has previously been described as IG glial cell precursors, while the identity of the dorsal population of Netrin expressing cells remains unknown. These dorsal cells do not overlap with the CB+ IG neurons and these results raise the question as to the identity of this dorsal population. As no other axon guidance gene was found to have a similar expression pattern as Netrin, which is uncommon as most axon guidance genes

show considerable overlap, and no description of this cell population could be found in the literature, further research is needed to characterize the role of these cells in callosal axon guidance and to determine the function of Netrin in this location within the cingulate cortex. In addition, it remains unknown why Netrin expression is decreased in DKO brains. One possible explanation is that the Netrin expressing cells, regardless of their identity, are unable to differentiate without pRb and p107 and do not mature to the point that they activate Netrin synthesis. Another possibility is that pRb and p107 regulate Netrin expression directly through E2F binding to the promoter. Although additional research is needed to fully understand the role of pRb and p107 in regulation of Netrin expression and signaling during CC development, these results lend insight into the mechanisms controlling the expression of axon guidance molecules early in development.

pRb and p107 are required for normal axon growth and guidance independent from the midline. Axon guidance research has a tendency to focus on very clear decision points, such as when axons cross the midline of the CNS or make a distinct turn (Shu and Richards. 2001; Keeble, et al. 2006; Fothergill, et al. 2013), as these decision points can be highly informative when analyzing the mechanisms growth cones use to navigate their environment. However, axons must often travel considerable distances between these clear decision points and extension through these corridors is just as crucial to growth cones reaching their final destination and forming proper connections as the obvious turns. It was therefore important to determine whether axon growth and extension through the IZ was defective in DKO brains in order to fully understand the role of pRb and p107 in CC formation. When we examined axon growth through the IZ under the lateral cortex in DKO embryos at E17.5 and P0, we found clumps of L1+

staining within the cortex and in the marginal zone next to the pia mater in DKO brains, and to a lesser extent in RBKO brains (Figure 4-13A). This phenotype started as early as E15.5 (Figure 4-13B) and developed progressively to P0. Interestingly, the amount of ectopic L1+ signal was not related to the severity of the midline crossing phenotype in individual brains of the same genotype. To determine whether this ectopic staining was due to re-entry of axons into the cortex or pre-mature expression of L1 prior to axons reaching the IZ, DKO and WT embryos expressing Emx1-Cre throughout the entire cortex were *in utero* electroporated with GFP to track the axons of a small population of neurons. The results in Figure 4-14 conclusively show that axons from electroporated DKO neurons successfully reach the IZ but then re-enter the ipsilateral cortex as they tangentially extend towards the midline. Furthermore, Figure 4-14 shows that axon extension is much slower in DKO brains, as GFP axons were barely able to travel past the GFP patch in the lateral cortex in DKO brains yet were able to reach the midline and beyond in the same time in WT brains. This was at least partially due to a decreased rate in axon extension independent of environmental signals since neurite outgrowth from cortical explants made of DKO medial and lateral cortex was decreased in compared to outgrowth from WT explants (Figure 4-15). Although these results do not conclusively show a truly cell autonomous effect of pocket proteins on axon extension as this assay is done with large tissue explants that could have repressive intercellular signals, it can be concluded that decreased axon growth rates in DKO neurons is not dependent on the intact environment of the cortical plate and IZ but is most likely due to a mechanism working within the axon.

As described above, we hypothesize that the decreased number of pre-crossing axons at the corticoseptal boundary at E15.5 and E16.5 is due to a delay in these axons reaching the midline. This hypothesis is supported by the observations showing a decreased rate of extension

through the IZ. The idea that axon growth rates are decreased in the IZ near the cingulate cortex is complemented by the previously discussed data showing the loss of Netrin in the dorsal population of Netrin expressing cells in DKO brains (Figures 4-10 through 4-12). As Netrin is an attractive, growth promoting signal for callosal axons from the cingulate cortex, loss of Netrin could further contribute to slow axon extension in DKO brains, in addition to any cell autonomous mechanisms. In order to test this hypothesis it is necessary to determine if DKO axons have the ability to respond to Netrin. Here, we show using cortical explant cultures that medial cortical explants are capable of responding to Netrin, although this response is blunted compared to the response of WT explants (Figure 4-15). Since providing these explants with Netrin improved but did not completely normalize axon extension, this data suggests that the loss of Netrin attraction in the cingulate cortex of DKO brains combined with the already slow rates of axon extension would provide a plausible explanation for the delay in Npn1+ axons reaching the midline. It is tempting to hypothesize that the dorsal patch of Netrin expressing cells in the cingulate cortex help attract growth cones through the IZ and is possibly involved in guiding these pioneering axons through the ventral turn as they leave the cortex and enter the IZ .

Npn1 expression was also found to be decreased in DKO brains, seen both as decreased staining intensity (Figure 4-4) and by Western blot (Figure 4-16). Npn1 has been shown to be important in tangential extension of callosal axons through the IZ and loss of Npn1 activity in axons leads to defasciculation in the IZ and re-entry into the ipsilateral cortex (Hatanaka, et al. 2009), very similar to the phenotype observed here in DKO brains. This role of Npn1 is thought to be due to its function in mediating Sema3A signaling as well to its role in homophillic adhesion between axons, independent of Sema3A. Although these results are still preliminary, it is tempting to suggest that the axon disorganization seen in the lateral zone in DKO embryos is

due to decreases Npn1 expression following loss of pocket protein activity. This idea is supported by the observation that E2F3 binds the Npn1 promoter, implying the Npn1 is a directly target of pRb/E2F3 mediated transcriptional regulation (Figure 4-1). Although the mechanism through which pocket proteins influence Npn1 expression requires further clarification, it is encouraging to suggest that loss of pRb/p107 mediated regulation of E2F activity causes a decrease in Npn1 expression in DKO neurons. This may in turn influence the development of the phenotypes described in this work.

In conclusion, these results demonstrate that pocket proteins are required for CC formation. This is achieved through both regulation of growth rates of callosal axons and through regulation of key axon guidance molecules. These findings strongly support our hypothesis that pocket proteins control later stages of neuron maturation beyond their role in cell cycle progression and differentiation.

Acknowledgements

We thank Linda Jui, Alysen Lougheed, and Jason G. MacLaurin for excellent technical assistance. Special thanks to Joelle Azzi and Ruthann Duivesteyn for tissue sectioning and assistance with mouse colony maintenance. Equipment was supported by the Centre for Stroke Recovery.

This work was supported by a CIHR grant to R.S.S. and OGS and HSFO Doctoral Award to DSS.

CHAPTER 5

GENERAL DISCUSSION

5.1 Thesis Summary and Major Finding: Neuron maturation is a highly complex and tightly regulated process beginning with neurogenesis in the VZ and SVZ, proceeding through neural differentiation and migration, and culminating with axon extension and guidance, synaptogenesis and circuit formation. Regulation of these different phases of maturation are closely inter-coordinated to prevent the interference of mutually exclusive processes and to allow step-wise developmental programs to proceed (Ferguson and Slack. 2001; McClellan and Slack. 2006; Dehay and Kennedy. 2007; Cau and Blader. 2009; Gyda, et al. 2012). Understanding the mechanisms which coordinate and regulate the different phases of neuronal development is necessary both to our understanding of how the brain is formed and to our understanding of how the adult brain functions in health and disease. Increasing our knowledge of the role of cell cycle proteins in coordinating the transitions between proliferation, differentiation and maturation will broaden our understanding of neurodevelopmental and neuropsychiatric disorders. Furthermore, it will aid us in the development of regenerative therapies for treatment of traumatic or neurodegenerative injury.

The primary goal of this dissertation is to determine how two members of the pocket protein family, pRb and p107, are involved in regulating neuron maturation independently from their roles in controlling cell cycle exit. Previous publications from the Slack lab have shown the pRb-E2F pathway to have a role in neuron differentiation through the regulation of genes such as members of the Notch and Shh pathways (Vanderluit, et al. 2004; Vanderluit, et al. 2007), Sox2 (Julian, et al. 2013), Dlx1/2 (Ghanem, et al. 2012b) and Neogenin (Andrusiak, et al. 2011). pRb has also been shown to regulate cortical lamination and both radial and tangential migration (Ferguson, et al. 2005; McClellan, et al. 2007), showing a clear involvement in post-mitotic brain development. In addition, a recently published screen showed that E2F3 and E2F4

bind the promoters of many genes with roles in axon guidance, migration, cytoskeletal dynamics and synaptogenesis (Julian, et al. 2015). Here, we advance the field, first by showing a severe defect in radial migration in the pRb/p107 double knock out model (DKO) to be mediated through cell autonomous mechanisms, independent of ectopic apoptosis, as was previously thought. Furthermore, we show an entirely novel role of pRb and p107 in regulating multiple aspects of axon growth and guidance necessary for development of the corpus callosum.

In the pRb/p107 DKO, we show a specific role of pocket proteins in regulating radial migration in upper layer neurons independent of cell cycle defects. The neuroblasts which fail to enter the cortical plate were born at the appropriate age, as shown by BrdU incorporation (Figure 2-3), and have exited the cell cycle (Figure 2-4). In addition, DKO embryos exhibit a distinct thinning of the upper cortical layers (Figure 2-1 and 2-2), which could be due to retention of upper layer cortical neurons within the SVZ/IZ. Alternatively, loss of pRb and p107 could lead to changes in the rates of neurogenesis at different developmental ages. As the different cortical layers are formed in a progressive inside-out mechanism, changes in the rates of neuron production at different ages would affect the relative thickness of different cortical layers (Mairet-Coello, et al. 2012).

As many developmental defects resulting from pRb deficiency are due to increased cell death (Yoshikawa. 2000; Chen, et al. 2004; Maddika, et al. 2007; Ciavarra and Zacksenhaus. 2010b), we investigated the role of cell death in the pRb/p107-dependent regulation of radial migration. First, we show that rescuing the increased levels cell death seen in DKO embryos to control levels fails to rescue the radial migration phenotype (Figure 2-5). This supports the hypothesis that role of pRb and p107 in migration is independent of the role of pocket proteins in cell survival. This is especially significant since many *in vivo* differentiation defects resulting

from pocket protein deficiency have been attributed to ectopic cell death (Feddersen, et al. 1995; Chen, et al. 2004; MacPherson, et al. 2004; Maddika, et al. 2007; Ciavarra and Zacksenhaus. 2010b), including previous work from the Slack lab, which suggested that the migration defect in single pRb knockout brains is due to apoptosis in Cajal Retzius (CR) cells and the consequent loss of Reelin (Ferguson, et al. 2005). Our results imply that pocket proteins regulate radial migration through independent, yet unidentified mechanisms. Second, we show that the role of pRb in radial migration is due to a combination of cell autonomous and non-cell autonomous mechanisms. pRb deletion through *in utero* electroporation of Cre resulted in an intermediate radial migration defect in which affected neurons enter the cortex but are not able to reach the upper layers (Figure 2-6). This further supports the conclusion that pRb and p107 regulate radial migration through mechanisms alternative to CR cell death as CR cell numbers are normal in electroporated brains.

In this dissertation, we have also demonstrated a role in pocket proteins pRb and p107 in regulating axon growth and guidance during corpus callosum (CC) formation. In DKO brains, axons fail to cross the midline but instead swirl into complex Probst Bundles on either side of the corticoseptal boundary (Figure 4-2 and 4-4). Although the midline glial structures are morphologically disrupted at later ages (Figure 4-5), these structures appear to develop normally at E15.5-E16.5; the primary defect in this complex phenotype seems to involve the growth and guidance of callosal axons (Figure 4-8). Briefly, callosal axons show early signs of defasciculation and re-entry into the ipsilateral cortex both as they approach the corticoseptal boundary and in the IZ distant from the midline (Figure 4-13). There is a clear defect in the crossing of pioneering axons from the cingulate cortex in DKO brains (Figure 4-4), most likely due to a defect in axon guidance signaling at the corticoseptal boundary. In addition, DKO

neurons exhibit decreased rate of axon extension both *in vivo* (Figure 4-14) and *in vitro* (Figure 4-15), implying axon growth defects are at least partially caused by a cell autonomous mechanism within the neurite themselves, rather than due to a repulsive signal from an external source.

In search of the underlying mechanism, we show that expression of Netrin (Figure 4-12) and Npn1 (Figure 4-16) are both decreased in DKO cortical tissue. Netrin is found to be lost in a specific population of cells within the cingulate cortex which could have significant axon guidance functions (Figure 4-12). We hypothesize that the loss of Netrin expression in this strategic location could significantly contribute to the failure of pioneering axons to cross the midline in DKO mice. DKO axons from cingulate cortical explants exhibited a blunted response to Netrin *in vitro*, showing that pioneering axons are capable of responding to this attractive cue (Fothergill, et al. 2013). Similarly, the loss of Npn1 could also contribute to the failure of pioneering axons to cross the midline, as Npn1 is a receptors for the attractive signal Sema3c expressed by sling neurons (Niquille, et al. 2009). Furthermore, loss of Npn1 could explain the ectopic re-entry of callosal axons into the ipsilateral cortex through interaction with the repulsive cue Sema3a (Hatanaka, et al. 2009). I intend to continue to work toward understanding the mechanism through which pocket proteins regulate axon guidance in future studies.

Together these findings show that pRb and p107 have important roles in regulating diverse aspects of neuron maturation distinct from their roles in the cell cycle regulation.

5.2 The Role of pRb in Neurodevelopment – Significance and Mechanisms: The primary significance of the work presented in this dissertation is to determine how pocket proteins pRb and p107 are involved in neural development at much later stages of neuron maturation. A

common theme visible in recent publication on the developmental roles of cell cycle proteins is the hypothesis that pocket proteins, and cell cycle proteins in general, coordinate exit from the cell cycle with the initiation of neural differentiation and early development events (Ferguson, et al. 2005; McClellan and Slack. 2006; McClellan, et al. 2007; Chen, et al. 2007a; Chong, et al. 2009; Gyda, et al. 2012; Julian, et al. 2013). This role of pRb has been shown to occur through E2F-dependent mechanisms, as seen with the regulation of Dlx2 (Ghanem, et al. 2012b) and Neogenin (Andrusiak, et al. 2011), as well as E2F-independent mechanisms such as the activation of pro-differentiation genes via pRb interacting with PGC1α (Scime, et al. 2005) and RUNX2 (Lee, et al. 2006) in adipogenesis and osteogenesis, respectively. However, the generally accepted model of pRb activity during development currently ends with pRb regulating this transition from proliferation to differentiation, after which pocket proteins are thought to function mainly in long term gene repression (Andrusiak, et al. 2012a). By extending the role of pocket proteins to cell autonomous regulation of radial migration of upper layer neurons, rates of axon extension, axon guidance through the expression of classic axon guidance molecules and axon fasciculation, we have shown multiple completely novel functions of pocket proteins in these later stages of neuron maturation. Not only do these results support the hypothesis that pocket proteins have important developmental functions independent of the cell cycle, this work extends the instructive role of pRb to include events involved in later stages of neuron development taking place at a time when pRb was thought to be involved solely in long term repression of pro-proliferation genes.

Although we have shown that pocket proteins are involved in radial migration and axon guidance, the mechanisms through which pRb regulates these processes are still unknown. In the case of CC formation, we show a decrease in the protein levels of both Netrin and Npn1 and

suggest that pioneer axons fail to cross the midline at the corticoseptal boundary due to loss of these attractive cues. However, this hypothesis does not address the question of how pRb regulates expression of these potential target genes, both of which contain E2F responsive elements in their promoters (unpublished data from Slack lab). Several non-mutually exclusive possibilities exist:

First, axon guidance genes could be direct E2F targets regulated through the canonical pRb-E2F pathway. This would resemble pRb dependent regulation of pro-differentiation genes Hes1 and Dlx2 and the migration gene Neogenin. However, there is one important difference between the regulation of Neogenin and that of Npn1, which is that Neogenin was shown to increase following the loss of pRb (Andrusiak, et al. 2011), while Npn1 was shown to decrease (Figure 4-16). It follows that in wild type brains, pRb would repress transcription of Neogenin during G0, but would activate transcription of Npn1. As pRb is well established to be involved in gene repression in non-proliferating states (Andrusiak, et al. 2012a), downregulation of Neogenin following cell cycle exit could occur through the binding of repressive pRb-E2F4 complexes to the promoter and subsequence recruitment of LXCXE containing chromatin remodeling proteins. However, upregulation of Npn1 in post-mitotic neurons through this canonical pathway has less experimental support. Although definitely possible, it would require pRb-E2F complexes to activate transcription at the Npn1 promoter, possibly through the recruitment of co-activators. Should this mechanism be verified experimentally, it would add to the growing realization within the pRb-E2F field that the mechanism through which E2F proteins regulate transcription are much more complex that originally appreciated.

Second, pRb could regulate Npn1 expression through E2F-independent mechanisms through interaction with alternate binding partners. This would resemble interactions with PGC1α and

RUNX2 mentioned above. A similar situation has been seen in erythrogenesis in which pRb sequesters the transcription factor Id2 within differentiating macrophages and thus prevents Id2 repressing transcription of PU.1, a master regulator of macrophage differentiation (Iavarone, et al. 2004). In these examples, pRb has been shown to increase expression of a pro-differentiation gene in post-mitotic cells, reminiscent of the proposed regulation of Npn1.

Alternatively, the decrease in Npn1 expression in DKO embryos could result from indirect mechanisms. Although the promoters of both Netrin and Npn1 contain E2F responsive sequences and have been shown to bind E2F3 using ChIP experiment (Figure 4-1), this does not confirm that they are directly regulated by pRb *in vivo*. Disruption of pocket protein signaling early in development, as was done using the Emx1-Cre mouse model, has many complex and incompletely understood effects. The decrease in Npn1 expression in these embryos could be downstream of other yet unidentified pRb targets.

Finally, pRb could regulate Npn1 expression through alternative mechanisms completely independent from the previously described pathways, as is the case for other cell cycle proteins which have been shown to function in late stages of neuron maturation. p27 has been shown to regulate tangential migration of interneurons by acting as a microtubule binding protein and enabling neurite extension and nucleokinesis (Nguyen, et al. 2006). Another example of cell cycle proteins with cell cycle independent function in neuron maturation comes from CyclinE, which has been shown to be expressed in dendritic shafts of mature neurons *in vitro* and in the adult brain (Odajima, et al. 2011). CyclinE sequesters CDK5 into inactive complexes, and thus prevent CDK5 from entering the spine and phosphorylating synaptic proteins, such as gephryin and synapsin (Odajima, et al. 2011). This leads to decreases in synapse number and defects in synaptic function in adult mice (Odajima, et al. 2011; Kalbouneh, et al. 2014; Verstegen, et al.

2014). In both these cases, cell cycle proteins are acting outside of the nucleus through mechanisms unrelated to gene transcription. Although it may seem at first unnecessary to suggest the possibility of a completely unknown mechanism for pRb dependent regulation of Npn1, precedent exists for cell cycle proteins to be co-opted into alternative roles after their function in cell cycle regulation has been completed.

5.3 Implications of pRb as a regulator of Axon Guidance: Within the field of axon guidance research, a new class of axon guidance molecule, the morphogens, has emerged in recent years (Wallace and Raff. 1999; Sanchez-Camacho, et al. 2011; Magnani, et al. 2012a; Yam and Charron. 2013; Sloan, et al. 2015). Morphogens, originally known for their control of tissue patterning through sweeping concentration gradients, have been shown in recent work to be also function as axon guidance molecules (Wallace and Raff. 1999; Sanchez-Camacho, et al. 2011; Magnani, et al. 2012a; Yam and Charron. 2013; Sloan, et al. 2015). These proteins include Shh, Wnt and BMP family members. Additionally, Notch has been shown to be involved in radial migration through mediation of Reelin signaling (Hashimoto-Torii, et al. 2008b). Similar to cell cycle regulators, these proteins were originally discovered for their roles in stem cell proliferation and differentiation and have since been shown to have additional roles later in development mediated by both classical and non-canonical signaling pathways. This is highly relevant to the discovery that pocket proteins influence axon guidance for two reasons. First, the repurposing of both morphogens, such as Shh, and cell cycle regulators, like CyclinE and pRb, generates a consistent theme of molecules important in early development being reused in new roles later during neuron maturation. This pattern lends conceptual support to the idea that pRb can function as a regulator of radial migration and axon guidance. Second, pRb has been shown

to regulate transcription of members of the Shh, Wnt and Notch pathways during cell proliferation (Vanderluit, et al. 2004; Vanderluit, et al. 2007), which opens up the possibility that the pRb pathway also regulates these genes during axon guidance and is an important area for further research.

The functions of axon guidance molecules *in vivo* and the signaling pathways through which they regulate cytoskeletal dynamics, protein expression, and the presentation of receptors on the growth cone membrane are key areas of ongoing research. However, the mechanisms which control transcription of these signaling molecules have received much less attention. In particular, the elusive question of what controls expression of these proteins in specific, clearly defined locations remains unanswered. In order to be effective, axon guidance signals must be expressed in very precise and discrete patterns, otherwise the boundaries and interactions between these signals would become inaccurate and axons would be misrouted. An example of these discrete patterns is seen in the expression of Netrin at E15.5. The small patch of Netrin expressed within the cingulate cortex must be under tight regulation in order to achieve expression in such a precise location. Whether this is due to the interplay of combinations of external cues, or a result of a downstream signaling pathway consequent to the molecular identity of this small group of cells, these questions represent a level of regulatory control that has not been investigated in most axon guidance systems. By providing evidence that pRb is capable of regulating expression of Netrin and other axon guidance molecules, we provide insight into how these pathways are regulated.

5.4 Downstream Consequences of Cell-Cycle Deregulation: In this dissertation, pRb and p107 were shown to regulate both radial migration and axon growth through cell cycle independent

mechanisms. However, defects in cell cycle exit and NPC regulation are known to occur in these mice during neurogenesis (Ferguson, et al. 2002), and it is likely that these cell cycle defects contribute to the highly complex phenotypes observed in the cortex and commissural plate of DKO brains, despite the predominant importance of cell cycle independent mechanisms.

In the case of cortical lamination, the rate of cell cycle progression, in particular G1 length, have been shown to influence both the number of NPC divisions and the type of division (Caviness, et al. 1995; Shen, et al. 2006; Lange, et al. 2009). As discussed in section 2.3 of the introduction, the switch from proliferative to neurogenic divisions is associated with a lengthening of G1, and there is a general lengthening of G1 phase of neurogenic divisions as cortical development proceeds. This implies that divisions which generate upper layer neurons have longer G1 phases than divisions which generate lower layer neurons (Shen, et al. 2006). In the DKO mice, we observed a defect in lamination in which the upper cortical layers are thinner than lower layers, an effect which was most pronounced in the Cux1+ population at the very top of the cortical plate (Figure 2-1 and 2-2). This could result in an increase in the rate and therefore number of cell cycle progressions early in neurogenesis. This would generate adequate numbers lower layer neurons but then lead to stem cell exhaustion later in corticogenesis when layer II/III neurons are generated. Similarly, E2F3a/b isoforms have been shown to regulate the balance between neurogenic and proliferative divisions in NPCs (Julian, et al. 2013), and E2F3 upregulation is a common mediator of defects caused by deletion of pRb in the telencephalon (McClellan, et al. 2007). A shift toward neurogenic divisions at the expense of self-renewing divisions in the DKO embryos could similarly result in premature stem cell exhaustion and an imbalance between the different cortical layers as was observed.

In addition, data from our lab indicates that pRb deletion causes an increase in proliferation in the SVZ with a small effect on proliferation in the VZ (Ferguson, et al. 2002). As the lower cortical layers are derived from the VZ and the upper layers derived from the SVZ (see introduction section 2.2), this difference in the role of pRb in these different cell populations could explain the imbalance in the cortical layers. Furthermore, the state of NPCs has been shown to be very important in determining the identity of newly born neurons during neurogenesis (McConnell. 1988b; McConnell and Kaznowski. 1991; Shen, et al. 2006; Lange, et al. 2009). Changes in the cell cycle dynamics or chromatin remodeling within a specific population of NPCs, such as the IPs within the SVZ, could have unpredictable and long term downstream effects in differentiating neuroblasts. This enhanced sensitivity of NPCs within the SVZ to pRb deregulation could contribute to the cell autonomous defects in radial migration seen in the upper layer neurons of DKO brains. Similarly, errors in neural programming with long term effects on gene expression, could contribute to the defects in axon growth and the altered expression of axon guidance factors seen in the commissural plate of DKO embryos.

Another alternative that must be considered is the possibility of indirect, downstream consequences of cell cycle deregulation. This could occur of cell cycle deregulation led to errors in the relative timing of normally precisely coordinated events. Events which normally occur at the same time or in a precise sequence would became chronically disorganized, with significant consequences on cortical development. For example, deletion of pRb has been previously shown to cause defects in retinal ganglion neuron axons when exiting the retina in their journey to the optic chiasm in zebrafish (Gyda, et al. 2012). This was attributed to an error in coordination between extension of the growth cones and the expression of the signals that guided them to the exit point caused by a delay in cell cycle exit, although expression of these signals was not

examined. A similar possibility exists in CC formation in DKO embryos; a small delay in cell cycle exit may compound the already decreased rate of neurite growth and cause the pioneering axons to reach the midline at a time when the guidance signals are no longer expressed in the correct pattern. In the case of the migration defect, a delay in cell cycle exit could lead to a similar failure in signal coordination.

Another possible indirect consequence of cell cycle regulation is the increase in number of a specific cell type which secretes a migration or axon guidance molecule. This could lead to an increase in the levels of this protein and cause downstream migration or guidance errors. This possibility is suggested by the in situ data presented in Figure 4-10, which shows an apparent increase in the number of cells expressing DCC and Robo1 mRNA in DKO brain at E17.5.

This line of argument that cell cycle deregulation early in development can have lasting downstream consequences emphasizes the fact that early developmental defects can have extensive and unpredictable effects on later stages of brain development and on neurological function in the adult brain. This is especially relevant considering recent indications that adult onset diseases such as schizophrenia and bipolar disorder have developmental origins (Caruncho, et al. 2004; Uribe and Wix. 2012; Catts, et al. 2013; Olson. 2014). The long-term, cell autonomous effects of cell cycle deregulation therefore represent an interesting and highly relevant field of study.

5.5 The Big Picture: What are pocket proteins doing? Since their discovery two and a half decades ago, the role of pocket proteins in tissue development has been progressively expanded to include a multitude of different processes, raising the question as to what the real functions of these proteins might be. Although they were initially described as canonical cell cycle

regulators, pRb and p107 have been shown to regulate cell death, stem cell self-renewal and maintenance, differentiation, migration and, in this work, axon guidance, often through the downstream regulation of the E2F transcription factors. Within the limited context of development and differentiation, genomic studies have shown direct E2F binding to thousands of genes involved in a wide variety of processes, including cell cycle regulation, cell specific differentiation factors, stem cell maintenance, migration, cytoskeletal dynamics and metabolism. This begs the question of how two proteins with largely redundant functions, can possible regulate such a wide variety of cellular processes. Considering all the known functions of pRb and p107, is there a unifying theme which can cohesively and concisely describe the role pocket proteins during development?

One model that would explain the results presented in these studies as well as others (Chen, et al. 2004; Ferguson, et al. 2005; McClellan, et al. 2007; Andrusiak, et al. 2011; Ghanem, et al. 2012; Andrusiak, et al. 2012; Julian, et al. 2013; Julian, et al. 2015), is that pRb and p107 not only control cell division, but also regulate transitions between different cellular states, be it a transition from a slowly proliferating stem cell to a rapidly proliferating transit amplifying cell, or from a rapidly proliferating cell to a post-mitotic neuroblast. By controlling the simultaneous expression or repression of large gene networks of similarly related genes, pRb and p107 synchronize the simultaneous cessation of proliferation and the initiation of differentiation. As pRb/p107 are required for a smooth transition in all cell lineages examined thus far, pocket proteins do not control whether a stem cell becomes a myoblast or a neuroblast. Rather, they work within the context of the predefined lineages to control differentiation of a cell into whatever mature cell type it is genetically determined to be. In doing so, they function as master regulators, preparing the cell to fulfill the necessary functions of its lineage by

coordinating massive shifts in gene expression, presumably through interaction with cell type specific co-regulators. Evidence in support of this theory of pRb function is found in developmental defects following pRb deficiency in vivo and from genetic screens examining genes responsive to pRb/E2F regulation. As has been previously described in this dissertation, pRb deletion in the forebrain results in ectopic proliferation in the developing cortex and E2F3, a direct downstream mediator of pRb activity, was shown to regulate the transition from proliferating stem cell to differentiating neuroblast through transcriptional regulation of Sox2. The regulation of Sox2 suggests a mechanism through which the pRb/E2F pathway controls the switch from proliferation to differentiation in neural precursors, and the ectopic proliferation in the cortical plate of pRb-null brains indicates that when pRb is absent the transition between these two states, proliferation and differentiation, is aberrantly executed.

Furthermore, pRb-null brains show errors in cortical lamination manifested as disorganization between the cortical plate and the intermediate zone, and pRb has been shown to control interneuron migration through transcriptional regulation of Neogenin. This seems to result from errors in regulation of differentiation genes following deregulated E2F activity, as subsequent deletion of E2F1 or E2F3 rescues this phenotype. The ability of pRb to regulate these migration genes represents one aspect of its function in controlling the cohort of genes necessary to organize neuronal differentiation. Failure to turn off the proliferation genes causes incorrect cell cycle re-entry, while disorganized activation of genes necessary for migration, be it misexpression of receptors, disorganization of the cytoskeleton or other function necessary for movement into the cortex. Through deregulation of single genes or a cohort of related pathways, loss of pRb activity causes neural precursor cells to make a delayed or incomplete transition to a migrating neuroblast.

An alternative explanation of this phenotype is that these differentiation defects are consequences of cell cycle deregulation, however there is now strong evidence against this interpretation. ChIP-on-chip screens performed in neural precursor cells against E2F3 have revealed numerous pRb/E2F3 targets with specific roles in neural differentiation and maturation, including genes with roles in cell cycle regulation, stem cell maintenance, neural lineage specification, migration, cytoskeletal dynamics, axon guidance and metabolism. Each of these groups of genes represents some aspect of the magnificent and complex transition that must be undertaken when a neural precursor cell becomes a neuron. The conclusion of this study was not that pRb/E2F controls each of these processes individually or entirely, but rather that it modulates components of these pathways to coordinate groups of genes simultaneously. For example, this would ensure that the metabolism of the cell switches to oxidative phosphorylation at the same time that the energy demands of the cell are increased, and that the cytoskeleton is mobilized at the same time that axon guidance molecules are expressed.

In this dissertation, pRb and p107 were shown to be involved in several aspects of neuron maturation, namely radial migration and axon guidance. These functions fit with the view of pRb/p107 as transitional regulators, although in this case the transition is from differentiation to maturation. Unlike other cell types examined, in which early differentiation is severely compromised in the absence of pRb, neuroblasts are able to undergo basic differentiation in pRb deficient models, as shown by the expression of layer specific neural markers. Here, the transition which is dependent on pRb function is the switch to a more mature status, which involves more advanced, specialized processes such as neurite extension. Just as in previous examples, pRb organizes the simultaneous activation and repression of different cohorts of genes to prepare the neuron for the next stage of development. This theory explains the E2F-

responsive elements present in the promoters of genes involved in cytoskeletal dynamics, axon guidance and cell adhesion as shown in Figure 4-1 of this thesis in and Julian et al. 2015. Furthermore it explains the complex and multifaceted aspects of the pRb/p107 DKO brain described in Chapter 4; because the cohort of pro-maturation genes regulated by the pRb/E2F pathway as the immature neuron is prepared for the next stage of its development includes such a large number of genes involved in a variety of processes, many aspects of development are affected when pRb activity is lost.

Other examples have been found in non-neural tissues, as was described in detail in section 4.4 of the Introduction. In adipose tissue, pRb controls the transition between proliferation and differentiation through regulation of PGC1α, a pro-differentiation factor in adipogenesis (Scime, et al. 2005). Similarly, pRb regulates the transition from proliferation to differentiation in osteogenesis through interaction with the pro-osteogenic transcription factor Run-X2 (Thomas, et al. 2001; Lee, et al. 2006). The pRb/E2F pathway has also been shown to be very important in muscle development, and ChIP screen performed in differentiating myoblasts have revealed that pRb controls expression of both pro-proliferation genes, and a large number of muscle specific differentiation factors, similar to results from neural precursor cells. This indicates, not only that pRb controls both the cessation of proliferation and initiation of differentiation in muscle, similar to its role in neural cells, but that the specific genes regulated by the pRb pathway is dependent on the context of the cell type.

Although this view of pRb function was presented in the context of development, it also applies to the role of pRb in mature tissues. Recent work has shown that, in mature neurons, the primary function of pRb is to maintain the long-term repression of pro-proliferation genes and thus prevent ectopic cell cycle re-entry. Through the same mechanisms that pRb previously used

to achieve organized transitions between cell states, here pRb is actively preventing a transition to a proliferating cell.

In conclusion, pRb and p107 function to organize the transitions between different cellular states. Like a conductor of an orchestra cuing in the woodwinds while simultaneously signaling out the horns to achieve the perfect musical balance, pRb activates and inhibits large cohorts of related genes to ensure that the transitions from proliferation to differentiation to maturation occur smoothly and cohesively.

5.6 Conclusions: The studies presented herein provide new knowledge on functions of pRb and p107 as important regulators of multiple aspects of neuron maturation through cell-cycle independent mechanisms. We show a role of pRb/p107 in regulating radial migration of upper layer neurons through cell autonomous mechanisms, independent of the role this pathway is known to have in apoptosis. We show that pRb/p107 are required for normal development of the commissural plate and for normal growth of commissural axons. The role of these proteins in axon growth and guidance is multifaceted, with implication in regulating neurite extension, expression of guidance molecules and axon fasciculation. We go on to find the protein levels of guidance cues Netrin and Neuropilin1 are influenced by loss of pRb/p107 and suggest how this could be involved in the observed developmental defects. This work has revealed novel functions of the pocket proteins and supports the hypothesis that the pRb pathway is involved in coordinating cell cycle exit with later developmental stages through cell cycle independent mechanisms. Our results open new avenues of future research to understand basic developmental mechanisms as well as help explain causes behind developmental abnormalities in humans.

CHAPTER 5

REFERENCES CITED

References

Akil, M., Lewis, D.A., 1997. Cytoarchitecture of the Entorhinal Cortex in Schizophrenia. Am J Psychiatry 154, 1010-1012.

Alcamo, E.A., Chirivella, L., Dautzenberg, M., Dobreva, G., Farinas, I., Grosschedl, R., McConnell, S.K., 2008. Satb2 Regulates Callosal Projection Neuron Identity in the Developing Cerebral Cortex. Neuron 57, 364-377.

Alfano, C., Viola, L., Heng, J.I., Pirozzi, M., Clarkson, M., Flore, G., De Maio, A., Schedl, A., Guillemot, F., Studer, M., 2011. COUP-TFI Promotes Radial Migration and Proper Morphology of Callosal Projection Neurons by Repressing Rnd2 Expression. Development 138, 4685-4697.

Anderson, J.S., Druzgal, T.J., Froehlich, A., DuBray, M.B., Lange, N., Alexander, A.L., Abildskov, T., Nielsen, J.A., Cariello, A.N., Cooperrider, J.R., Bigler, E.D., Lainhart, J.E., 2011. Decreased Interhemispheric Functional Connectivity in Autism. Cereb Cortex 21, 1134-1146.

Anderson, S.A., Eisenstat, D.D., Shi, L., Rubenstein, J.L., 1997. Interneuron Migration from Basal Forebrain to Neocortex: Dependence on Dlx Genes. Science 278, 474-476.

Andrusiak, M.G., Vandenbosch, R., Park, D.S., Slack, R.S., 2012a. The Retinoblastoma Protein is Essential for Survival of Postmitotic Neurons. J Neurosci 32, 14809-14814.

Andrusiak, M.G., Vandenbosch, R., Park, D.S., Slack, R.S., 2012b. The Retinoblastoma Protein is Essential for Survival of Postmitotic Neurons. J Neurosci 32, 14809-14814.

Andrusiak, M.G., McClellan, K.A., Dugal-Tessier, D., Julian, L.M., Rodrigues, S.P., Park, D.S., Kennedy, T.E., Slack, R.S., 2011. Rb/E2F Regulates Expression of Neogenin during Neuronal Migration. Mol Cell Biol 31, 238-247.

Angevine, J.B.,Jr, Sidman, R.L., 1961. Autoradiographic Study of Cell Migration during Histogenesis of Cerebral Cortex in the Mouse. Nature 192, 766-768.

Antoine-Bertrand, J., Ghogha, A., Luangrath, V., Bedford, F.K., Lamarche-Vane, N., 2011. The Activation of Ezrin-Radixin-Moesin Proteins is Regulated by

Netrin-1 through Src Kinase and RhoA/Rho Kinase Activities and Mediates Netrin-1-Induced Axon Outgrowth. Mol Biol Cell 22, 3734-3746.

Arnold, S.E., Ruscheinsky, D.D., Han, L.Y., 1997. Further Evidence of Abnormal Cytoarchitecture of the Entorhinal Cortex in Schizophrenia using Spatial Point Pattern Analyses. Biol Psychiatry 42, 639-647.

Arnold, S.E., Hyman, B.T., Van Hoesen, G.W., Damasio, A.R., 1991. Some Cytoarchitectural Abnormalities of the Entorhinal Cortex in Schizophrenia. Arch Gen Psychiatry 48, 625-632.

Asp, P., Acosta-Alvear, D., Tsikitis, M., van Oevelen, C., Dynlacht, B.D., 2009. E2f3b Plays an Essential Role in Myogenic Differentiation through Isoform-Specific Gene Regulation. Genes Dev 23, 37-53.

Azzarelli, R., Kerloch, T., Pacary, E., 2015. Regulation of Cerebral Cortex Development by Rho GTPases: Insights from in Vivo Studies. Front Cell Neurosci 8, 445.

Bandara, L.R., Adamczewski, J.P., Hunt, T., La Thangue, N.B., 1991. Cyclin A and the Retinoblastoma Gene Product Complex with a Common Transcription Factor. Nature 352, 249-251.

Barry, J., Gu, Y., Gu, C., 2010. Polarized Targeting of L1-CAM Regulates Axonal and Dendritic Bundling in Vitro. Eur J Neurosci 32, 1618-1631.

Beckmann, H., Jakob, H., 1994. Prenatal Developmental Disorders of Brain Structures in Schizophrenic Psychoses. Nervenarzt 65, 454-463.

Behar, O., Golden, J.A., Mashimo, H., Schoen, F.J., Fishman, M.C., 1996. Semaphorin III is Needed for Normal Patterning and Growth of Nerves, Bones and Heart. Nature 383, 525-528.

Beijersbergen, R.L., Carlee, L., Kerkhoven, R.M., Bernards, R., 1995. Regulation of the Retinoblastoma Protein-Related p107 by G1 Cyclin Complexes. Genes Dev 9, 1340-1353.

Benadiba, C., Magnani, D., Niquille, M., Morle, L., Valloton, D., Nawabi, H., Ait-Lounis, A., Otsmane, B., Reith, W., Theil, T., Hornung, J.P., Lebrand, C., Durand, B., 2012. The Ciliogenic Transcription Factor RFX3 Regulates Early

Midline Distribution of Guidepost Neurons Required for Corpus Callosum Development. PLoS Genet 8, e1002606.

Berman, S.D., West, J.C., Danielian, P.S., Caron, A.M., Stone, J.R., Lees, J.A., 2009. Mutation of p107 Exacerbates the Consequences of Rb Loss in Embryonic Tissues and Causes Cardiac and Blood Vessel Defects. Proc Natl Acad Sci U S A 106, 14932-14936.

Berry, M., Rogers, A.W., 1965. The Migration of Neuroblasts in the Developing Cerebral Cortex. J Anat 99, 691-709.

Bhuiyan, M.I., Lee, J.H., Kim, S.Y., Cho, K.O., 2013. Expression of Exogenous LIN28 Contributes to Proliferation and Survival of Mouse Primary Cortical Neurons in Vitro. Neuroscience 248C, 448-458.

Blomen, V.A., Boonstra, J., 2007. Cell Fate Determination during G1 Phase Progression. Cell Mol Life Sci 64, 3084-3104.

Bock, H.H., Jossin, Y., May, P., Bergner, O., Herz, J., 2004. Apolipoprotein E Receptors are Required for Reelin-Induced Proteasomal Degradation of the Neuronal Adaptor Protein Disabled-1. J Biol Chem 279, 33471-33479.

Boitard, M., Bocchi, R., Egervari, K., Petrenko, V., Viale, B., Gremaud, S., Zgraggen, E., Salmon, P., Kiss, J.Z., 2015. Wnt Signaling Regulates Multipolar-to-Bipolar Transition of Migrating Neurons in the Cerebral Cortex. Cell Rep 10, 1349-1361.

Borello, U., Pierani, A., 2010. Patterning the Cerebral Cortex: Traveling with Morphogens. Curr Opin Genet Dev 20, 408-415.

Bouabe, H., Okkenhaug, K., 2013. Gene Targeting in Mice: A Review. Methods Mol Biol 1064, 315-336.

Bouchard, J.F., Moore, S.W., Tritsch, N.X., Roux, P.P., Shekarabi, M., Barker, P.A., Kennedy, T.E., 2004. Protein Kinase A Activation Promotes Plasma Membrane Insertion of DCC from an Intracellular Pool: A Novel Mechanism Regulating Commissural Axon Extension. J Neurosci 24, 3040-3050.

Bridgman, M.W., Brown, W.S., Spezio, M.L., Leonard, M.K., Adolphs, R., Paul, L.K., 2014. Facial Emotion Recognition in Agenesis of the Corpus Callosum. J Neurodev Disord 6, 32-1955-6-32. Epub 2014 Aug 14.

Britanova, O., de Juan Romero, C., Cheung, A., Kwan, K.Y., Schwark, M., Gyorgy, A., Vogel, T., Akopov, S., Mitkovski, M., Agoston, D., Sestan, N., Molnar, Z., Tarabykin, V., 2008. Satb2 is a Postmitotic Determinant for Upper-Layer Neuron Specification in the Neocortex. Neuron 57, 378-392.

Brown, W.S., Symingtion, M., VanLancker-Sidtis, D., Dietrich, R., Paul, L.K., 2005. Paralinguistic Processing in Children with Callosal Agenesis: Emergence of Neurolinguistic Deficits. Brain Lang 93, 135-139.

Burke, J.R., Hura, G.L., Rubin, S.M., 2012. Structures of Inactive Retinoblastoma Protein Reveal Multiple Mechanisms for Cell Cycle Control. Genes Dev 26, 1156-1166.

Burke, J.R., Deshong, A.J., Pelton, J.G., Rubin, S.M., 2010. Phosphorylation-Induced Conformational Changes in the Retinoblastoma Protein Inhibit E2F Transactivation Domain Binding. J Biol Chem 285, 16286-16293.

Burkhart, D.L., Wirt, S.E., Zmoos, A.F., Kareta, M.S., Sage, J., 2010. Tandem E2F Binding Sites in the Promoter of the p107 Cell Cycle Regulator Control p107 Expression and its Cellular Functions. PLoS Genet 6, e1001003.

Burkhart, D.L., Viatour, P., Ho, V.M., Sage, J., 2008. GFP Reporter Mice for the Retinoblastoma-Related Cell Cycle Regulator p107. Cell Cycle 7, 2544-2552.

Bush, J.O., Soriano, P., 2009. Ephrin-B1 Regulates Axon Guidance by Reverse Signaling through a PDZ-Dependent Mechanism. Genes Dev 23, 1586-1599.

Calegari, F., Haubensak, W., Haffner, C., Huttner, W.B., 2005. Selective Lengthening of the Cell Cycle in the Neurogenic Subpopulation of Neural Progenitor Cells during Mouse Brain Development. J Neurosci 25, 6533-6538.

Callaghan, D.A., Dong, L., Callaghan, S.M., Hou, Y.X., Dagnino, L., Slack, R.S., 1999. Neural Precursor Cells Differentiating in the Absence of Rb Exhibit Delayed Terminal Mitosis and Deregulated E2F 1 and 3 Activity. Dev Biol 207, 257-270.

Canty, A.J., Murphy, M., 2008. Molecular Mechanisms of Axon Guidance in the Developing Corticospinal Tract. Prog Neurobiol 85, 214-235.

Cao, L., Faha, B., Dembski, M., Tsai, L.H., Harlow, E., Dyson, N., 1992. Independent Binding of the Retinoblastoma Protein and p107 to the Transcription Factor E2F. Nature 355, 176-179.

Carper, R.A., Courchesne, E., 2005. Localized Enlargement of the Frontal Cortex in Early Autism. Biol Psychiatry 57, 126-133.

Carper, R.A., Moses, P., Tigue, Z.D., Courchesne, E., 2002. Cerebral Lobes in Autism: Early Hyperplasia and Abnormal Age Effects. Neuroimage 16, 1038-1051.

Caruncho, H.J., Dopeso-Reyes, I.G., Loza, M.I., Rodriguez, M.A., 2004. A GABA, Reelin, and the Neurodevelopmental Hypothesis of Schizophrenia. Crit Rev Neurobiol 16, 25-32.

Catalano, S.M., Messersmith, E.K., Goodman, C.S., Shatz, C.J., Chedotal, A., 1998. Many Major CNS Axon Projections Develop Normally in the Absence of Semaphorin III. Mol Cell Neurosci 11, 173-182.

Catarino, A., Andrade, A., Churches, O., Wagner, A.P., Baron-Cohen, S., Ring, H., 2013. Task-Related Functional Connectivity in Autism Spectrum Conditions: An EEG Study using Wavelet Transform Coherence. Mol Autism 4, 1-2392-4-1.

Catts, V.S., Fung, S.J., Long, L.E., Joshi, D., Vercammen, A., Allen, K.M., Fillman, S.G., Rothmond, D.A., Sinclair, D., Tiwari, Y., Tsai, S.Y., Weickert, T.W., Shannon Weickert, C., 2013. Rethinking Schizophrenia in the Context of Normal Neurodevelopment. Front Cell Neurosci 7, 60.

Cau, E., Blader, P., 2009. Notch Activity in the Nervous System: To Switch Or Not Switch? Neural Dev 4, 36.

Caviness, V.S.,Jr, Takahashi, T., Nowakowski, R.S., 1995. Numbers, Time and Neocortical Neuronogenesis: A General Developmental and Evolutionary Model. Trends Neurosci 18, 379-383.

Caviness, V.S.,Jr, 1982. Neocortical Histogenesis in Normal and Reeler Mice: A Developmental Study Based upon [3H]Thymidine Autoradiography. Brain Res 256, 293-302.

Chellappan, S.P., Hiebert, S., Mudryj, M., Horowitz, J.M., Nevins, J.R., 1991a. The E2F Transcription Factor is a Cellular Target for the RB Protein. Cell 65, 1053-1061.

Chellappan, S.P., Hiebert, S., Mudryj, M., Horowitz, J.M., Nevins, J.R., 1991b. The E2F Transcription Factor is a Cellular Target for the RB Protein. Cell 65, 1053-1061.

Chen, B., Schaevitz, L.R., McConnell, S.K., 2005. Fezl Regulates the Differentiation and Axon Targeting of Layer 5 Subcortical Projection Neurons in Cerebral Cortex. Proc Natl Acad Sci U S A 102, 17184-17189.

Chen, D., Chen, Y., Forrest, D., Bremner, R., 2013. E2f2 Induces Cone Photoreceptor Apoptosis Independent of E2f1 and E2f3. Cell Death Differ 20, 931-940.

Chen, D., Opavsky, R., Pacal, M., Tanimoto, N., Wenzel, P., Seeliger, M.W., Leone, G., Bremner, R., 2007a. Rb-Mediated Neuronal Differentiation through Cell-Cycle-Independent Regulation of E2f3a. PLoS Biol 5, e179.

Chen, D., Opavsky, R., Pacal, M., Tanimoto, N., Wenzel, P., Seeliger, M.W., Leone, G., Bremner, R., 2007b. Rb-Mediated Neuronal Differentiation through Cell-Cycle-Independent Regulation of E2f3a. PLoS Biol 5, e179.

Chen, D., Livne-bar, I., Vanderluit, J.L., Slack, R.S., Agochiya, M., Bremner, R., 2004. Cell-Specific Effects of RB Or RB/p107 Loss on Retinal Development Implicate an Intrinsically Death-Resistant Cell-of-Origin in Retinoblastoma. Cancer Cell 5, 539-551.

Chen, G., Sima, J., Jin, M., Wang, K.Y., Xue, X.J., Zheng, W., Ding, Y.Q., Yuan, X.B., 2008. Semaphorin-3A Guides Radial Migration of Cortical Neurons during Development. Nat Neurosci 11, 36-44.

Chen, G., Guy, C.T., Chen, H.W., Hu, N., Lee, E.Y., Lee, W.H., 1996. Molecular Cloning and Developmental Expression of Mouse p130, a Member of the Retinoblastoma Gene Family. J Biol Chem 271, 9567-9572.

Cheng, M., Olivier, P., Diehl, J.A., Fero, M., Roussel, M.F., Roberts, J.M., Sherr, C.J., 1999. The p21(Cip1) and p27(Kip1) CDK 'Inhibitors' are Essential Activators of Cyclin D-Dependent Kinases in Murine Fibroblasts. EMBO J 18, 1571-1583.

Chiang, C., Litingtung, Y., Lee, E., Young, K.E., Corden, J.L., Westphal, H., Beachy, P.A., 1996. Cyclopia and Defective Axial Patterning in Mice Lacking Sonic Hedgehog Gene Function. Nature 383, 407-413.

Chinn, G.A., Hirokawa, K.E., Chuang, T.M., Urbina, C., Patel, F., Fong, J., Funatsu, N., Monuki, E.S., 2014. Agenesis of the Corpus Callosum due to Defective Glial Wedge Formation in Lhx2 Mutant Mice. Cereb Cortex .

Chong, J.L., Wenzel, P.L., Saenz-Robles, M.T., Nair, V., Ferrey, A., Hagan, J.P., Gomez, Y.M., Sharma, N., Chen, H.Z., Ouseph, M., Wang, S.H., Trikha, P., Culp, B., Mezache, L., Winton, D.J., Sansom, O.J., Chen, D., Bremner, R., Cantalupo, P.G., Robinson, M.L., Pipas, J.M., Leone, G., 2009. E2f1-3 Switch from Activators in Progenitor Cells to Repressors in Differentiating Cells. Nature 462, 930-934.

Ciavarra, G., Zacksenhaus, E., 2010a. Rescue of Myogenic Defects in Rb-Deficient Cells by Inhibition of Autophagy Or by Hypoxia-Induced Glycolytic Shift. J Cell Biol 191, 291-301.

Ciavarra, G., Zacksenhaus, E., 2010b. Rescue of Myogenic Defects in Rb-Deficient Cells by Inhibition of Autophagy Or by Hypoxia-Induced Glycolytic Shift. J Cell Biol 191, 291-301.

Clarke, A.R., Maandag, E.R., van Roon, M., van der Lugt, N.M., van der Valk, M., Hooper, M.L., Berns, A., te Riele, H., 1992. Requirement for a Functional Rb-1 Gene in Murine Development. Nature 359, 328-330.

Classon, M., Dyson, N., 2001. P107 and P130: Versatile Proteins with Interesting Pockets. Exp Cell Res 264, 135-147.

Cobrinik, D., Lee, M.H., Hannon, G., Mulligan, G., Bronson, R.T., Dyson, N., Harlow, E., Beach, D., Weinberg, R.A., Jacks, T., 1996. Shared Role of the pRB-Related p130 and p107 Proteins in Limb Development. Genes Dev 10, 1633-1644.

Collinson, S.L., Gan, S.C., Woon, P.S., Kuswanto, C., Sum, M.Y., Yang, G.L., Lui, J.M., Sitoh, Y.Y., Nowinski, W.L., Sim, K., 2014. Corpus Callosum Morphology in First-Episode and Chronic Schizophrenia: Combined Magnetic Resonance and Diffusion Tensor Imaging Study of Chinese Singaporean Patients. Br J Psychiatry 204, 55-60.

Couly, G.F., Le Douarin, N.M., 1987. Mapping of the Early Neural Primordium in Quail-Chick Chimeras. II. the Prosencephalic Neural Plate and Neural Folds: Implications for the Genesis of Cephalic Human Congenital Abnormalities. Dev Biol 120, 198-214.

Crossley, P.H., Martinez, S., Ohkubo, Y., Rubenstein, J.L., 2001. Coordinate Expression of Fgf8, Otx2, Bmp4, and Shh in the Rostral Prosencephalon during Development of the Telencephalic and Optic Vesicles. Neuroscience 108, 183-206.

Dagnino, L., Zhu, L., Skorecki, K.L., Moses, H.L., 1995. E2F-Independent Transcriptional Repression by p107, a Member of the Retinoblastoma Family of Proteins. Cell Growth Differ 6, 191-198.

Dahiya, A., Gavin, M.R., Luo, R.X., Dean, D.C., 2000. Role of the LXCXE Binding Site in Rb Function. Mol Cell Biol 20, 6799-6805.

Dannenberg, J.H., te Riele, H.P., 2006. The Retinoblastoma Gene Family in Cell Cycle Regulation and Suppression of Tumorigenesis. Results Probl Cell Differ 42, 183-225.

de Bruin, A., Maiti, B., Jakoi, L., Timmers, C., Buerki, R., Leone, G., 2003a. Identification and Characterization of E2F7, a Novel Mammalian E2F Family Member Capable of Blocking Cellular Proliferation. J Biol Chem 278, 42041-42049.

de Bruin, A., Wu, L., Saavedra, H.I., Wilson, P., Yang, Y., Rosol, T.J., Weinstein, M., Robinson, M.L., Leone, G., 2003b. Rb Function in Extraembryonic Lineages Suppresses Apoptosis in the CNS of Rb-Deficient Mice. Proc Natl Acad Sci U S A 100, 6546-6551.

De Vry, J., Martinez-Martinez, P., Losen, M., Temel, Y., Steckler, T., Steinbusch, H.W., De Baets, M.H., Prickaerts, J., 2010. In Vivo Electroporation of the Central Nervous System: A Non-Viral Approach for Targeted Gene Delivery. Prog Neurobiol 92, 227-244.

de Wit, J., Verhaagen, J., 2003. Role of Semaphorins in the Adult Nervous System. Prog Neurobiol 71, 249-267.

DeGeer, J., Boudeau, J., Schmidt, S., Bedford, F., Lamarche-Vane, N., Debant, A., 2013. Tyrosine Phosphorylation of the Rho Guanine Nucleotide Exchange

Factor Trio Regulates Netrin-1/DCC-Mediated Cortical Axon Outgrowth. Mol Cell Biol 33, 739-751.

DeGregori, J., Johnson, D.G., 2006. Distinct and Overlapping Roles for E2F Family Members in Transcription, Proliferation and Apoptosis. Curr Mol Med 6, 739-748.

Dehay, C., Kennedy, H., 2007. Cell-Cycle Control and Cortical Development. Nat Rev Neurosci 8, 438-450.

Demopoulos, C., Arroyo, M.S., Dunn, W., Strominger, Z., Sherr, E.H., Marco, E., 2014. Individuals with Agenesis of the Corpus Callosum show Sensory Processing Differences as Measured by the Sensory Profile. Neuropsychology .

Deutsch, S.I., Burket, J.A., Katz, E., 2010. Does Subtle Disturbance of Neuronal Migration Contribute to Schizophrenia and Other Neurodevelopmental Disorders? Potential Genetic Mechanisms with Possible Treatment Implications. Eur Neuropsychopharmacol 20, 281-287.

Di Ieva, A., Fathalla, H., Cusimano, M.D., Tschabitscher, M., 2015. The Indusium Griseum and the Longitudinal Striae of the Corpus Callosum. Cortex 62, 34-40.

Dick, F.A., Rubin, S.M., 2013. Molecular Mechanisms Underlying RB Protein Function. Nat Rev Mol Cell Biol 14, 297-306.

Dick, F.A., 2007. Structure-Function Analysis of the Retinoblastoma Tumor Suppressor Protein - is the Whole a Sum of its Parts? Cell Div 2, 26.

Dixit, R., Lu, F., Cantrup, R., Gruenig, N., Langevin, L.M., Kurrasch, D.M., Schuurmans, C., 2011. Efficient Gene Delivery into Multiple CNS Territories using in Utero Electroporation. J Vis Exp (52). pii: 2957. doi, 10.3791/2957.

Drescher, U., 2000. Eph Receptor Tyrosine Kinases and their Ligands in Development. Ernst Schering Res Found Workshop (29), 151-164.

Edwards, T.J., Sherr, E.H., Barkovich, A.J., Richards, L.J., 2014. Clinical, Genetic and Imaging Findings Identify New Causes for Corpus Callosum Development Syndromes. Brain 137, 1579-1613.

Egea, J., Klein, R., 2007. Bidirectional Eph-Ephrin Signaling during Axon Guidance. Trends Cell Biol 17, 230-238.

Elias, G.M., Elias, L.A., Apostolides, P.F., Kriegstein, A.R., Nicoll, R.A., 2008. Differential Trafficking of AMPA and NMDA Receptors by SAP102 and PSD-95 Underlies Synapse Development. Proc Natl Acad Sci U S A 105, 20953-20958.

Evsyukova, I., Plestant, C., Anton, E.S., 2013. Integrative Mechanisms of Oriented Neuronal Migration in the Developing Brain. Annu Rev Cell Dev Biol 29, 299-353.

Ewen, M.E., Xing, Y.G., Lawrence, J.B., Livingston, D.M., 1991. Molecular Cloning, Chromosomal Mapping, and Expression of the cDNA for p107, a Retinoblastoma Gene Product-Related Protein. Cell 66, 1155-1164.

Fairchild, H.R., Fairchild, G., Tierney, K.M., McCartney, D.L., Cross, J.J., de Vries, P.J., 2011. Partial Agenesis of the Corpus Callosum, Hippocampal Atrophy, and Stable Intellectual Disability Associated with Roifman Syndrome. Am J Med Genet A 155A, 2560-2565.

Fame, R.M., MacDonald, J.L., Macklis, J.D., 2011. Development, Specification, and Diversity of Callosal Projection Neurons. Trends Neurosci 34, 41-50.

Fattaey, A., Helin, K., Harlow, E., 1993a. Transcriptional Inhibition by the Retinoblastoma Protein. Philos Trans R Soc Lond B Biol Sci 340, 333-336.

Fattaey, A.R., Helin, K., Dembski, M.S., Dyson, N., Harlow, E., Vuocolo, G.A., Hanobik, M.G., Haskell, K.M., Oliff, A., Defeo-Jones, D., 1993b. Characterization of the Retinoblastoma Binding Proteins RBP1 and RBP2. Oncogene 8, 3149-3156.

Fazeli, A., Dickinson, S.L., Hermiston, M.L., Tighe, R.V., Steen, R.G., Small, C.G., Stoeckli, E.T., Keino-Masu, K., Masu, M., Rayburn, H., Simons, J., Bronson, R.T., Gordon, J.I., Tessier-Lavigne, M., Weinberg, R.A., 1997. Phenotype of Mice Lacking Functional Deleted in Colorectal Cancer (Dcc) Gene. Nature 386, 796-804.

Feddersen, R.M., Clark, H.B., Yunis, W.S., Orr, H.T., 1995. In Vivo Viability of Postmitotic Purkinje Neurons Requires pRb Family Member Function. Mol Cell Neurosci 6, 153-167.

Ferguson, K.L., McClellan, K.A., Vanderluit, J.L., McIntosh, W.C., Schuurmans, C., Polleux, F., Slack, R.S., 2005. A Cell-Autonomous Requirement for the Cell Cycle Regulatory Protein, Rb, in Neuronal Migration. EMBO J 24, 4381-4391.

Ferguson, K.L., Vanderluit, J.L., Hebert, J.M., McIntosh, W.C., Tibbo, E., MacLaurin, J.G., Park, D.S., Wallace, V.A., Vooijs, M., McConnell, S.K., Slack, R.S., 2002. Telencephalon-Specific Rb Knockouts Reveal Enhanced Neurogenesis, Survival and Abnormal Cortical Development. EMBO J 21, 3337-3346.

Ferguson, K.L., Slack, R.S., 2001. The Rb Pathway in Neurogenesis. Neuroreport 12, A55-62.

Ferland, R.J., Cherry, T.J., Preware, P.O., Morrisey, E.E., Walsh, C.A., 2003. Characterization of Foxp2 and Foxp1 mRNA and Protein in the Developing and Mature Brain. J Comp Neurol 460, 266-279.

Ferreira, R., Magnaghi-Jaulin, L., Robin, P., Harel-Bellan, A., Trouche, D., 1998. The Three Members of the Pocket Proteins Family Share the Ability to Repress E2F Activity through Recruitment of a Histone Deacetylase. Proc Natl Acad Sci U S A 95, 10493-10498.

Fothergill, T., Donahoo, A.L., Douglass, A., Zalucki, O., Yuan, J., Shu, T., Goodhill, G.J., Richards, L.J., 2013. Netrin-DCC Signaling Regulates Corpus Callosum Formation through Attraction of Pioneering Axons and by Modulating Slit2-Mediated Repulsion. Cereb Cortex .

Frantz, G.D., McConnell, S.K., 1996. Restriction of Late Cerebral Cortical Progenitors to an Upper-Layer Fate. Neuron 17, 55-61.

Frolov, M.V., Dyson, N.J., 2004. Molecular Mechanisms of E2F-Dependent Activation and pRB-Mediated Repression. J Cell Sci 117, 2173-2181.

Frotscher, M., Chai, X., Bock, H.H., Haas, C.A., Forster, E., Zhao, S., 2009. Role of Reelin in the Development and Maintenance of Cortical Lamination. J Neural Transm 116, 1451-1455.

Fukuchi-Shimogori, T., Grove, E.A., 2001. Neocortex Patterning by the Secreted Signaling Molecule FGF8. Science 294, 1071-1074.

Garcia-Moreno, F., Lopez-Mascaraque, L., De Carlos, J.A., 2007. Origins and Migratory Routes of Murine Cajal-Retzius Cells. J Comp Neurol 500, 419-432.

Garriga, J., Limon, A., Mayol, X., Rane, S.G., Albrecht, J.H., Reddy, E.P., Andres, V., Grana, X., 1998. Differential Regulation of the Retinoblastoma Family of Proteins during Cell Proliferation and Differentiation. Biochem J 333 (Pt 3), 645-654.

Gavathiotis, E., Reyna, D.E., Bellairs, J.A., Leshchiner, E.S., Walensky, L.D., 2012. Direct and Selective Small-Molecule Activation of Proapoptotic BAX. Nat Chem Biol 8, 639-645.

Geraldo, S., Gordon-Weeks, P.R., 2009. Cytoskeletal Dynamics in Growth-Cone Steering. J Cell Sci 122, 3595-3604.

Ghanem, N., Andrusiak, M.G., Svoboda, D., Al Lafi, S.M., Julian, L.M., McClellan, K.A., De Repentigny, Y., Kothary, R., Ekker, M., Blais, A., Park, D.S., Slack, R.S., 2012a. The Rb/E2F Pathway Modulates Neurogenesis through Direct Regulation of the Dlx1/Dlx2 Bigene Cluster. J Neurosci 32, 8219-8230.

Ghanem, N., Andrusiak, M.G., Svoboda, D., Al Lafi, S.M., Julian, L.M., McClellan, K.A., De Repentigny, Y., Kothary, R., Ekker, M., Blais, A., Park, D.S., Slack, R.S., 2012b. The Rb/E2F Pathway Modulates Neurogenesis through Direct Regulation of the Dlx1/Dlx2 Bigene Cluster. J Neurosci 32, 8219-8230.

Giacinti, C., Giordano, A., 2006. RB and Cell Cycle Progression. Oncogene 25, 5220-5227.

Gongidi, V., Ring, C., Moody, M., Brekken, R., Sage, E.H., Rakic, P., Anton, E.S., 2004. SPARC-Like 1 Regulates the Terminal Phase of Radial Glia-Guided Migration in the Cerebral Cortex. Neuron 41, 57-69.

Gordon, G.M., Du, W., 2011. Conserved RB Functions in Development and Tumor Suppression. Protein Cell 2, 864-878.

Gotz, M., Huttner, W.B., 2005. The Cell Biology of Neurogenesis. Nat Rev Mol Cell Biol 6, 777-788.

Gotz, M., Hartfuss, E., Malatesta, P., 2002. Radial Glial Cells as Neuronal Precursors: A New Perspective on the Correlation of Morphology and Lineage Restriction in the Developing Cerebral Cortex of Mice. Brain Res Bull 57, 777-788.

Gu, C., Rodriguez, E.R., Reimert, D.V., Shu, T., Fritzsch, B., Richards, L.J., Kolodkin, A.L., Ginty, D.D., 2003. Neuropilin-1 Conveys Semaphorin and VEGF Signaling during Neural and Cardiovascular Development. Dev Cell 5, 45-57.

Guiley, K.Z., Liban, T.J., Felthousen, J.G., Ramanan, P., Litovchick, L., Rubin, S.M., 2015. Structural Mechanisms of DREAM Complex Assembly and Regulation. Genes Dev 29, 961-974.

Gyda, M., Wolman, M., Lorent, K., Granato, M., 2012. The Tumor Suppressor Gene Retinoblastoma-1 is Required for Retinotectal Development and Visual Function in Zebrafish. PLoS Genet 8, e1003106.

Hahamy, A., Behrmann, M., Malach, R., 2015. The Idiosyncratic Brain: Distortion of Spontaneous Connectivity Patterns in Autism Spectrum Disorder. Nat Neurosci 18, 302-309.

Haigis, K., Sage, J., Glickman, J., Shafer, S., Jacks, T., 2006. The Related Retinoblastoma (pRb) and p130 Proteins Cooperate to Regulate Homeostasis in the Intestinal Epithelium. J Biol Chem 281, 638-647.

Halbleib, J.M., Nelson, W.J., 2006. Cadherins in Development: Cell Adhesion, Sorting, and Tissue Morphogenesis. Genes Dev 20, 3199-3214.

Hannon, G.J., Demetrick, D., Beach, D., 1993. Isolation of the Rb-Related p130 through its Interaction with CDK2 and Cyclins. Genes Dev 7, 2378-2391.

Hashimoto-Torii, K., Torii, M., Sarkisian, M.R., Bartley, C.M., Shen, J., Radtke, F., Gridley, T., Sestan, N., Rakic, P., 2008a. Interaction between Reelin and Notch Signaling Regulates Neuronal Migration in the Cerebral Cortex. Neuron 60, 273-284.

Hashimoto-Torii, K., Torii, M., Sarkisian, M.R., Bartley, C.M., Shen, J., Radtke, F., Gridley, T., Sestan, N., Rakic, P., 2008b. Interaction between Reelin and Notch Signaling Regulates Neuronal Migration in the Cerebral Cortex. Neuron 60, 273-284.

Hatanaka, Y., Matsumoto, T., Yanagawa, Y., Fujisawa, H., Murakami, F., Masu, M., 2009. Distinct Roles of Neuropilin 1 Signaling for Radial and Tangential Extension of Callosal Axons. J Comp Neurol 514, 215-225.

Haubensak, W., Attardo, A., Denk, W., Huttner, W.B., 2004. Neurons Arise in the Basal Neuroepithelium of the Early Mammalian Telencephalon: A Major Site of Neurogenesis. Proc Natl Acad Sci U S A 101, 3196-3201.

Hayano, Y., Zhao, H., Kobayashi, H., Takeuchi, K., Norioka, S., Yamamoto, N., 2014. The Role of T-Cadherin in Axonal Pathway Formation in Neocortical Circuits. Development 141, 4784-4793.

Hazlett, H.C., Poe, M., Gerig, G., Smith, R.G., Provenzale, J., Ross, A., Gilmore, J., Piven, J., 2005. Magnetic Resonance Imaging and Head Circumference Study of Brain Size in Autism: Birth through Age 2 Years. Arch Gen Psychiatry 62, 1366-1376.

He, Y., Chen, Z., Evans, A., 2008. Structural Insights into Aberrant Topological Patterns of Large-Scale Cortical Networks in Alzheimer's Disease. J Neurosci 28, 4756-4766.

Heng, J.I., Nguyen, L., Castro, D.S., Zimmer, C., Wildner, H., Armant, O., Skowronska-Krawczyk, D., Bedogni, F., Matter, J.M., Hevner, R., Guillemot, F., 2008. Neurogenin 2 Controls Cortical Neuron Migration through Regulation of Rnd2. Nature 455, 114-118.

Hevner, R.F., Shi, L., Justice, N., Hsueh, Y., Sheng, M., Smiga, S., Bulfone, A., Goffinet, A.M., Campagnoni, A.T., Rubenstein, J.L., 2001. Tbr1 Regulates Differentiation of the Preplate and Layer 6. Neuron 29, 353-366.

Hiesberger, T., Trommsdorff, M., Howell, B.W., Goffinet, A., Mumby, M.C., Cooper, J.A., Herz, J., 1999. Direct Binding of Reelin to VLDL Receptor and ApoE Receptor 2 Induces Tyrosine Phosphorylation of Disabled-1 and Modulates Tau Phosphorylation. Neuron 24, 481-489.

Himanen, J.P., Yermekbayeva, L., Janes, P.W., Walker, J.R., Xu, K., Atapattu, L., Rajashankar, K.R., Mensinga, A., Lackmann, M., Nikolov, D.B., Dhe-Paganon, S., 2010. Architecture of Eph Receptor Clusters. Proc Natl Acad Sci U S A 107, 10860-10865.

Himanen, J.P., Saha, N., Nikolov, D.B., 2007. Cell-Cell Signaling Via Eph Receptors and Ephrins. Curr Opin Cell Biol 19, 534-542.

Hinds, P.W., Mittnacht, S., Dulic, V., Arnold, A., Reed, S.I., Weinberg, R.A., 1992. Regulation of Retinoblastoma Protein Functions by Ectopic Expression of Human Cyclins. Cell 70, 993-1006.

Hippenmeyer, S., 2014. Molecular Pathways Controlling the Sequential Steps of Cortical Projection Neuron Migration. Adv Exp Med Biol 800, 1-24.

Ho, S.K., Kovacevic, N., Henkelman, R.M., Boyd, A., Pawson, T., Henderson, J.T., 2009. EphB2 and EphA4 Receptors Regulate Formation of the Principal Inter-Hemispheric Tracts of the Mammalian Forebrain. Neuroscience 160, 784-795.

Honda, T., Kobayashi, K., Mikoshiba, K., Nakajima, K., 2011. Regulation of Cortical Neuron Migration by the Reelin Signaling Pathway. Neurochem Res 36, 1270-1279.

Hu, Z., Yue, X., Shi, G., Yue, Y., Crockett, D.P., Blair-Flynn, J., Reuhl, K., Tessarollo, L., Zhou, R., 2003. Corpus Callosum Deficiency in Transgenic Mice Expressing a Truncated Ephrin-A Receptor. J Neurosci 23, 10963-10970.

Huber, A.B., Kania, A., Tran, T.S., Gu, C., De Marco Garcia, N., Lieberam, I., Johnson, D., Jessell, T.M., Ginty, D.D., Kolodkin, A.L., 2005. Distinct Roles for Secreted Semaphorin Signaling in Spinal Motor Axon Guidance. Neuron 48, 949-964.

Hunter-Schaedle, K.E., 1997. Radial Glial Cell Development and Transformation are Disturbed in Reeler Forebrain. J Neurobiol 33, 459-472.

Huppi, K., Siwarski, D., Mock, B.A., Dosik, J., Hamel, P.A., 1996. Molecular Cloning, Chromosomal Mapping, and Expression of the Mouse p107 Gene. Mamm Genome 7, 353-355.

Hurford, R.K.,Jr, Cobrinik, D., Lee, M.H., Dyson, N., 1997. pRB and p107/p130 are Required for the Regulated Expression of Different Sets of E2F Responsive Genes. Genes Dev 11, 1447-1463.

Iavarone, A., King, E.R., Dai, X.M., Leone, G., Stanley, E.R., Lasorella, A., 2004. Retinoblastoma Promotes Definitive Erythropoiesis by Repressing Id2 in Fetal Liver Macrophages. Nature 432, 1040-1045.

Islam, S.M., Shinmyo, Y., Okafuji, T., Su, Y., Naser, I.B., Ahmed, G., Zhang, S., Chen, S., Ohta, K., Kiyonari, H., Abe, T., Tanaka, S., Nishinakamura, R., Terashima, T., Kitamura, T., Tanaka, H., 2009. Draxin, a Repulsive Guidance Protein for Spinal Cord and Forebrain Commissures. Science 323, 388-393.

Isler, J.R., Martien, K.M., Grieve, P.G., Stark, R.I., Herbert, M.R., 2010. Reduced Functional Connectivity in Visual Evoked Potentials in Children with Autism Spectrum Disorder. Clin Neurophysiol 121, 2035-2043.

Iyirhiaro, G.O., Zhang, Y., Estey, C., O'Hare, M.J., Safarpour, F., Parsanejad, M., Wang, S., Abdel-Messih, E., Callaghan, S.M., During, M.J., Slack, R.S., Park, D.S., 2014. Regulation of Ischemic Neuronal Death by E2F4-p130 Protein Complexes. J Biol Chem 289, 18202-18213.

Jacks, T., Fazeli, A., Schmitt, E.M., Bronson, R.T., Goodell, M.A., Weinberg, R.A., 1992. Effects of an Rb Mutation in the Mouse. Nature 359, 295-300.

Jakob, H., Beckmann, H., 1986. Prenatal Developmental Disturbances in the Limbic Allocortex in Schizophrenics. J Neural Transm 65, 303-326.

Jiang, H., Jiang, W., Zou, J., Wang, B., Yu, M., Pan, Y., Lin, Y., Mao, Y., Wang, Y., 2015. The GluN2B Subunit of N-Methy-D-Asparate Receptor Regulates the Radial Migration of Cortical Neurons in Vivo. Brain Res .

Jimenez, D., Rivera, R., Lopez-Mascaraque, L., De Carlos, J.A., 2003. Origin of the Cortical Layer I in Rodents. Dev Neurosci 25, 105-115.

Jossin, Y., Ignatova, N., Hiesberger, T., Herz, J., Lambert de Rouvroit, C., Goffinet, A.M., 2004. The Central Fragment of Reelin, Generated by Proteolytic Processing in Vivo, is Critical to its Function during Cortical Plate Development. J Neurosci 24, 514-521.

Jossin, Y., Bar, I., Ignatova, N., Tissir, F., De Rouvroit, C.L., Goffinet, A.M., 2003. The Reelin Signaling Pathway: Some Recent Developments. Cereb Cortex 13, 627-633.

Julian, L.M., Liu, Y., Pakenham, C.A., Dugal-Tessier, D., Ruzhynsky, V., Bae, S., Tsai, S.Y., Leone, G., Slack, R.S., Blais, A., 2015a. Tissue-Specific Targeting of Cell Fate Regulatory Genes by E2f Factors. Cell Death Differ .

Julian, L.M., Liu, Y., Pakenham, C.A., Dugal-Tessier, D., Ruzhynsky, V., Bae, S., Tsai, S.Y., Leone, G., Slack, R.S., Blais, A., 2015b. Tissue-Specific Targeting of Cell Fate Regulatory Genes by E2f Factors. Cell Death Differ .

Julian, L.M., Vandenbosch, R., Pakenham, C.A., Andrusiak, M.G., Nguyen, A.P., McClellan, K.A., Svoboda, D.S., Lagace, D.C., Park, D.S., Leone, G., Blais, A., Slack, R.S., 2013. Opposing Regulation of Sox2 by Cell-Cycle Effectors E2f3a and E2f3b in Neural Stem Cells. Cell Stem Cell 12, 440-452.

Kadison, S.R., Makinen, T., Klein, R., Henkemeyer, M., Kaprielian, Z., 2006. EphB Receptors and Ephrin-B3 Regulate Axon Guidance at the Ventral Midline of the Embryonic Mouse Spinal Cord. J Neurosci 26, 8909-8914.

Kalbouneh, H., Schlicksupp, A., Kirsch, J., Kuhse, J., 2014. Cyclin-Dependent Kinase 5 is Involved in the Phosphorylation of Gephyrin and Clustering of GABAA Receptors at Inhibitory Synapses of Hippocampal Neurons. PLoS One 9, e104256.

Kamb, A., Gruis, N.A., Weaver-Feldhaus, J., Liu, Q., Harshman, K., Tavtigian, S.V., Stockert, E., Day, R.S.,3rd, Johnson, B.E., Skolnick, M.H., 1994. A Cell Cycle Regulator Potentially Involved in Genesis of Many Tumor Types. Science 264, 436-440.

Kaplan, A., Kent, C.B., Charron, F., Fournier, A.E., 2014. Switching Responses: Spatial and Temporal Regulators of Axon Guidance. Mol Neurobiol 49, 1077-1086.

Kawasaki, T., Bekku, Y., Suto, F., Kitsukawa, T., Taniguchi, M., Nagatsu, I., Nagatsu, T., Itoh, K., Yagi, T., Fujisawa, H., 2002. Requirement of Neuropilin 1-Mediated Sema3A Signals in Patterning of the Sympathetic Nervous System. Development 129, 671-680.

Kawauchi, T., Chihama, K., Nabeshima, Y., Hoshino, M., 2003. The in Vivo Roles of STEF/Tiam1, Rac1 and JNK in Cortical Neuronal Migration. EMBO J 22, 4190-4201.

Keeble, T.R., Cooper, H.M., 2006. Ryk: A Novel Wnt Receptor Regulating Axon Pathfinding. Int J Biochem Cell Biol 38, 2011-2017.

Keeble, T.R., Halford, M.M., Seaman, C., Kee, N., Macheda, M., Anderson, R.B., Stacker, S.A., Cooper, H.M., 2006. The Wnt Receptor Ryk is Required for Wnt5a-Mediated Axon Guidance on the Contralateral Side of the Corpus Callosum. J Neurosci 26, 5840-5848.

Kennedy, T.E., Wang, H., Marshall, W., Tessier-Lavigne, M., 2006. Axon Guidance by Diffusible Chemoattractants: A Gradient of Netrin Protein in the Developing Spinal Cord. J Neurosci 26, 8866-8874.

Kennedy, T.E., Serafini, T., de la Torre, J.R., Tessier-Lavigne, M., 1994. Netrins are Diffusible Chemotropic Factors for Commissural Axons in the Embryonic Spinal Cord. Cell 78, 425-435.

Kern, J.K., Geier, D.A., King, P.G., Sykes, L.K., Mehta, J.A., Geier, M.R., 2015. Shared Brain Connectivity Issues, Symptoms, and Comorbidities in Autism Spectrum Disorder, Attention Deficit/Hyperactivity Disorder, and Tourette Syndrome. Brain Connect .

Kernie, S.G., Parent, J.M., 2010. Forebrain Neurogenesis After Focal Ischemic and Traumatic Brain Injury. Neurobiol Dis 37, 267-274.

Khidr, L., Chen, P.L., 2006. RB, the Conductor that Orchestrates Life, Death and Differentiation. Oncogene 25, 5210-5219.

Kiess, M., Gill, R.M., Hamel, P.A., 1995. Expression and Activity of the Retinoblastoma Protein (pRB)-Family Proteins, p107 and p130, during L6 Myoblast Differentiation. Cell Growth Differ 6, 1287-1298.

Kim, H.Y., Ahn, B.Y., Cho, Y., 2001. Structural Basis for the Inactivation of Retinoblastoma Tumor Suppressor by SV40 Large T Antigen. EMBO J 20, 295-304.

Kim, M., Farmer, W.T., Bjorke, B., McMahon, S.A., Fabre, P.J., Charron, F., Mastick, G.S., 2014a. Pioneer Midbrain Longitudinal Axons Navigate using a Balance of Netrin Attraction and Slit Repulsion. Neural Dev 9, 17-8104-9-17.

Kim, Y.U., Park, E.S., Jung, S., Suh, M., Choi, H.S., Rha, D.W., 2014b. Clinical Features and Associated Abnormalities in Children and Adolescents with Corpus Callosal Anomalies. Ann Rehabil Med 38, 138-143.

Kitsukawa, T., Shimizu, M., Sanbo, M., Hirata, T., Taniguchi, M., Bekku, Y., Yagi, T., Fujisawa, H., 1997. Neuropilin-Semaphorin III/D-Mediated Chemorepulsive Signals Play a Crucial Role in Peripheral Nerve Projection in Mice. Neuron 19, 995-1005.

Knudsen, E.S., Knudsen, K.E., 2008. Tailoring to RB: Tumour Suppressor Status and Therapeutic Response. Nat Rev Cancer 8, 714-724.

Knudsen, E.S., Wang, J.Y., 1997. Dual Mechanisms for the Inhibition of E2F Binding to RB by Cyclin-Dependent Kinase-Mediated RB Phosphorylation. Mol Cell Biol 17, 5771-5783.

Koester, S.E., O'Leary, D.D., 1994. Axons of Early Generated Neurons in Cingulate Cortex Pioneer the Corpus Callosum. J Neurosci 14, 6608-6620.

Konno, D., Yoshimura, S., Hori, K., Maruoka, H., Sobue, K., 2005. Involvement of the Phosphatidylinositol 3-Kinase/Rac1 and cdc42 Pathways in Radial Migration of Cortical Neurons. J Biol Chem 280, 5082-5088.

Korenjak, M., Brehm, A., 2005. E2F-Rb Complexes Regulating Transcription of Genes Important for Differentiation and Development. Curr Opin Genet Dev 15, 520-527.

Kriegstein, A., Noctor, S., Martinez-Cerdeno, V., 2006. Patterns of Neural Stem and Progenitor Cell Division may Underlie Evolutionary Cortical Expansion. Nat Rev Neurosci 7, 883-890.

Kriegstein, A.R., Gotz, M., 2003. Radial Glia Diversity: A Matter of Cell Fate. Glia 43, 37-43.

Kuge, A., Takemura, S., Kokubo, Y., Sato, S., Goto, K., Kayama, T., 2009. Temporal Profile of Neurogenesis in the Subventricular Zone, Dentate Gyrus and Cerebral Cortex Following Transient Focal Cerebral Ischemia. Neurol Res 31, 969-976.

Kuhla, A., Ludwig, S.C., Kuhla, B., Munch, G., Vollmar, B., 2015. Advanced Glycation End Products are Mitogenic Signals and Trigger Cell Cycle Reentry of Neurons in Alzheimer's Disease Brain. Neurobiol Aging 36, 753-761.

Kundu, A., Micholt, L., Friedrich, S., Rand, D.R., Bartic, C., Braeken, D., Levchenko, A., 2013. Superimposed Topographic and Chemical Cues Synergistically Guide Neurite Outgrowth. Lab Chip 13, 3070-3081.

Kusek, J.C., Greene, R.M., Pisano, M.M., 2001. Expression of the E2F and Retinoblastoma Families of Proteins during Neural Differentiation. Brain Res Bull 54, 187-198.

Lagace, D.C., Whitman, M.C., Noonan, M.A., Ables, J.L., DeCarolis, N.A., Arguello, A.A., Donovan, M.H., Fischer, S.J., Farnbauch, L.A., Beech, R.D., DiLeone, R.J., Greer, C.A., Mandyam, C.D., Eisch, A.J., 2007. Dynamic Contribution of Nestin-Expressing Stem Cells to Adult Neurogenesis. J Neurosci 27, 12623-12629.

Laguesse, S., Peyre, E., Nguyen, L., 2015. Progenitor Genealogy in the Developing Cerebral Cortex. Cell Tissue Res 359, 17-32.

Lammens, T., Li, J., Leone, G., De Veylder, L., 2009. Atypical E2Fs: New Players in the E2F Transcription Factor Family. Trends Cell Biol 19, 111-118.

Lange, C., Huttner, W.B., Calegari, F., 2009. Cdk4/cyclinD1 Overexpression in Neural Stem Cells Shortens G1, Delays Neurogenesis, and Promotes the Generation and Expansion of Basal Progenitors. Cell Stem Cell 5, 320-331.

Lavado, A., Ware, M., Pare, J., Cao, X., 2014. The Tumor Suppressor Nf2 Regulates Corpus Callosum Development by Inhibiting the Transcriptional Coactivator Yap. Development 141, 4182-4193.

Lazzerini Denchi, E., Helin, K., 2005. E2F1 is Crucial for E2F-Dependent Apoptosis. EMBO Rep 6, 661-668.

LeCouter, J.E., Kablar, B., Hardy, W.R., Ying, C., Megeney, L.A., May, L.L., Rudnicki, M.A., 1998. Strain-Dependent Myeloid Hyperplasia, Growth Deficiency, and Accelerated Cell Cycle in Mice Lacking the Rb-Related p107 Gene. Mol Cell Biol 18, 7455-7465.

Lee, B.K., Bhinge, A.A., Iyer, V.R., 2011. Wide-Ranging Functions of E2F4 in Transcriptional Activation and Repression Revealed by Genome-Wide Analysis. Nucleic Acids Res 39, 3558-3573.

Lee, E.Y., Hu, N., Yuan, S.S., Cox, L.A., Bradley, A., Lee, W.H., Herrup, K., 1994. Dual Roles of the Retinoblastoma Protein in Cell Cycle Regulation and Neuron Differentiation. Genes Dev 8, 2008-2021.

Lee, E.Y., Chang, C.Y., Hu, N., Wang, Y.C., Lai, C.C., Herrup, K., Lee, W.H., Bradley, A., 1992. Mice Deficient for Rb are Nonviable and show Defects in Neurogenesis and Haematopoiesis. Nature 359, 288-294.

Lee, J.O., Russo, A.A., Pavletich, N.P., 1998. Structure of the Retinoblastoma Tumour-Suppressor Pocket Domain Bound to a Peptide from HPV E7. Nature 391, 859-865.

Lee, J.S., Thomas, D.M., Gutierrez, G., Carty, S.A., Yanagawa, S., Hinds, P.W., 2006. HES1 Cooperates with pRb to Activate RUNX2-Dependent Transcription. J Bone Miner Res 21, 921-933.

Leyva-Diaz, E., Lopez-Bendito, G., 2013. In and Out from the Cortex: Development of Major Forebrain Connections. Neuroscience 254, 26-44.

Lipinski, M.M., Jacks, T., 1999. The Retinoblastoma Gene Family in Differentiation and Development. Oncogene 18, 7873-7882.

Litovchick, L., Florens, L.A., Swanson, S.K., Washburn, M.P., DeCaprio, J.A., 2011. DYRK1A Protein Kinase Promotes Quiescence and Senescence through DREAM Complex Assembly. Genes Dev 25, 801-813.

Litovchick, L., Sadasivam, S., Florens, L., Zhu, X., Swanson, S.K., Velmurugan, S., Chen, R., Washburn, M.P., Liu, X.S., DeCaprio, J.A., 2007. Evolutionarily Conserved Multisubunit RBL2/p130 and E2F4 Protein Complex Represses Human Cell Cycle-Dependent Genes in Quiescence. Mol Cell 26, 539-551.

Liu, Y., Chu, A., Chakroun, I., Islam, U., Blais, A., 2010. Cooperation between Myogenic Regulatory Factors and SIX Family Transcription Factors is Important for Myoblast Differentiation. Nucleic Acids Res 38, 6857-6871.

Lo, C.Y., Wang, P.N., Chou, K.H., Wang, J., He, Y., Lin, C.P., 2010. Diffusion Tensor Tractography Reveals Abnormal Topological Organization in

Structural Cortical Networks in Alzheimer's Disease. J Neurosci 30, 16876-16885.

LoTurco, J., Manent, J.B., Sidiqi, F., 2009. New and Improved Tools for in Utero Electroporation Studies of Developing Cerebral Cortex. Cereb Cortex 19 Suppl 1, i120-5.

Lowery, L.A., Van Vactor, D., 2009. The Trip of the Tip: Understanding the Growth Cone Machinery. Nat Rev Mol Cell Biol 10, 332-343.

Lukaszewicz, A., Savatier, P., Cortay, V., Kennedy, H., Dehay, C., 2002. Contrasting Effects of Basic Fibroblast Growth Factor and Neurotrophin 3 on Cell Cycle Kinetics of Mouse Cortical Stem Cells. J Neurosci 22, 6610-6622.

Lundberg, A.S., Weinberg, R.A., 1998. Functional Inactivation of the Retinoblastoma Protein Requires Sequential Modification by at Least Two Distinct Cyclin-Cdk Complexes. Mol Cell Biol 18, 753-761.

Ma, L., Li, X.W., Zhang, S.J., Yang, F., Zhu, G.M., Yuan, X.B., Jiang, W., 2014. Interleukin-1 Beta Guides the Migration of Cortical Neurons. J Neuroinflammation 11, 114-2094-11-114.

Macleod, K.F., Hu, Y., Jacks, T., 1996. Loss of Rb Activates both p53-Dependent and Independent Cell Death Pathways in the Developing Mouse Nervous System. EMBO J 15, 6178-6188.

MacPherson, D., Sage, J., Kim, T., Ho, D., McLaughlin, M.E., Jacks, T., 2004. Cell Type-Specific Effects of Rb Deletion in the Murine Retina. Genes Dev 18, 1681-1694.

Maddika, S., Ande, S.R., Panigrahi, S., Paranjothy, T., Weglarczyk, K., Zuse, A., Eshraghi, M., Manda, K.D., Wiechec, E., Los, M., 2007. Cell Survival, Cell Death and Cell Cycle Pathways are Interconnected: Implications for Cancer Therapy. Drug Resist Updat 10, 13-29.

Magdaleno, S., Keshvara, L., Curran, T., 2002. Rescue of Ataxia and Preplate Splitting by Ectopic Expression of Reelin in Reeler Mice. Neuron 33, 573-586.

Magnani, D., Hasenpusch-Theil, K., Benadiba, C., Yu, T., Basson, M.A., Price, D.J., Lebrand, C., Theil, T., 2012a. Gli3 Controls Corpus Callosum Formation

by Positioning Midline Guideposts during Telencephalic Patterning. Cereb Cortex .

Magnani, D., Hasenpusch-Theil, K., Theil, T., 2012b. Gli3 Controls Subplate Formation and Growth of Cortical Axons. Cereb Cortex .

Mairet-Coello, G., Tury, A., Van Buskirk, E., Robinson, K., Genestine, M., DiCicco-Bloom, E., 2012. p57(KIP2) Regulates Radial Glia and Intermediate Precursor Cell Cycle Dynamics and Lower Layer Neurogenesis in Developing Cerebral Cortex. Development 139, 475-487.

Malatesta, P., Hartfuss, E., Gotz, M., 2000. Isolation of Radial Glial Cells by Fluorescent-Activated Cell Sorting Reveals a Neuronal Lineage. Development 127, 5253-5263.

Manning, A.L., Dyson, N.J., 2012. RB: Mitotic Implications of a Tumour Suppressor. Nat Rev Cancer 12, 220-226.

Marin, O., Rubenstein, J.L., 2003. Cell Migration in the Forebrain. Annu Rev Neurosci 26, 441-483.

Marino, S., Hoogervoorst, D., Brandner, S., Berns, A., 2003. Rb and p107 are Required for Normal Cerebellar Development and Granule Cell Survival but Not for Purkinje Cell Persistence. Development 130, 3359-3368.

Marino, S., Vooijs, M., van Der Gulden, H., Jonkers, J., Berns, A., 2000. Induction of Medulloblastomas in p53-Null Mutant Mice by Somatic Inactivation of Rb in the External Granular Layer Cells of the Cerebellum. Genes Dev 14, 994-1004.

Martinez-Cerdeno, V., Noctor, S.C., Kriegstein, A.R., 2006. The Role of Intermediate Progenitor Cells in the Evolutionary Expansion of the Cerebral Cortex. Cereb Cortex 16 Suppl 1, i152-61.

Mayol, X., Grana, X., Baldi, A., Sang, N., Hu, Q., Giordano, A., 1993. Cloning of a New Member of the Retinoblastoma Gene Family (pRb2) which Binds to the E1A Transforming Domain. Oncogene 8, 2561-2566.

McClellan, K.A., Ruzhynsky, V.A., Douda, D.N., Vanderluit, J.L., Ferguson, K.L., Chen, D., Bremner, R., Park, D.S., Leone, G., Slack, R.S., 2007. Unique

Requirement for Rb/E2F3 in Neuronal Migration: Evidence for Cell Cycle-Independent Functions. Mol Cell Biol 27, 4825-4843.

McClellan, K.A., Slack, R.S., 2007. Specific in Vivo Roles for E2Fs in Differentiation and Development. Cell Cycle 6, 2917-2927.

McClellan, K.A., Slack, R.S., 2006. Novel Functions for Cell Cycle Genes in Nervous System Development. Cell Cycle 5, 1506-1513.

McConnell, S.K., 1995. Strategies for the Generation of Neuronal Diversity in the Developing Central Nervous System. J Neurosci 15, 6987-6998.

McConnell, S.K., Kaznowski, C.E., 1991. Cell Cycle Dependence of Laminar Determination in Developing Neocortex. Science 254, 282-285.

McConnell, S.K., 1988a. Fates of Visual Cortical Neurons in the Ferret After Isochronic and Heterochronic Transplantation. J Neurosci 8, 945-974.

McConnell, S.K., 1988b. Development and Decision-Making in the Mammalian Cerebral Cortex. Brain Res 472, 1-23.

McLear, J.A., Garcia-Fresco, G., Bhat, M.A., Van Dyke, T.A., 2006. In Vivo Inactivation of pRb, p107 and p130 in Murine Neuroprogenitor Cells Leads to Major CNS Developmental Defects and High Seizure Rates. Mol Cell Neurosci 33, 260-273.

McLone, D.G., Bondareff, W., 1975. Developmental Morphology of the Subarachnoid Space and Contiguous Structures in the Mouse. Am J Anat 142, 273-293.

Mendes, S.W., Henkemeyer, M., Liebl, D.J., 2006. Multiple Eph Receptors and B-Class Ephrins Regulate Midline Crossing of Corpus Callosum Fibers in the Developing Mouse Forebrain. J Neurosci 26, 882-892.

Merson, T.D., Bourne, J.A., 2014. Endogenous Neurogenesis Following Ischaemic Brain Injury: Insights for Therapeutic Strategies. Int J Biochem Cell Biol 56, 4-19.

Methot, L., Hermann, R., Tang, Y., Lo, R., Al-Jehani, H., Jhas, S., Svoboda, D., Slack, R.S., Barker, P.A., Stifani, S., 2013. Interaction and Antagonistic Roles

of NF-kappaB and Hes6 in the Regulation of Cortical Neurogenesis. Mol Cell Biol 33, 2797-2808.

Misson, J.P., Edwards, M.A., Yamamoto, M., Caviness, V.S.,Jr, 1988. Mitotic Cycling of Radial Glial Cells of the Fetal Murine Cerebral Wall: A Combined Autoradiographic and Immunohistochemical Study. Brain Res 466, 183-190.

Mitchell, B.D., Macklis, J.D., 2005. Large-Scale Maintenance of Dual Projections by Callosal and Frontal Cortical Projection Neurons in Adult Mice. J Comp Neurol 482, 17-32.

Miyagi, S., Saito, T., Mizutani, K., Masuyama, N., Gotoh, Y., Iwama, A., Nakauchi, H., Masui, S., Niwa, H., Nishimoto, M., Muramatsu, M., Okuda, A., 2004. The Sox-2 Regulatory Regions Display their Activities in Two Distinct Types of Multipotent Stem Cells. Mol Cell Biol 24, 4207-4220.

Miyata, T., Kawaguchi, A., Saito, K., Kawano, M., Muto, T., Ogawa, M., 2004. Asymmetric Production of Surface-Dividing and Non-Surface-Dividing Cortical Progenitor Cells. Development 131, 3133-3145.

Miyata, T., Kawaguchi, A., Okano, H., Ogawa, M., 2001. Asymmetric Inheritance of Radial Glial Fibers by Cortical Neurons. Neuron 31, 727-741.

Mizuno, H., Hirano, T., Tagawa, Y., 2010. Pre-Synaptic and Post-Synaptic Neuronal Activity Supports the Axon Development of Callosal Projection Neurons during Different Post-Natal Periods in the Mouse Cerebral Cortex. Eur J Neurosci 31, 410-424.

Moberg, K., Starz, M.A., Lees, J.A., 1996. E2F-4 Switches from p130 to p107 and pRB in Response to Cell Cycle Reentry. Mol Cell Biol 16, 1436-1449.

Moldrich, R.X., Gobius, I., Pollak, T., Zhang, J., Ren, T., Brown, L., Mori, S., De Juan Romero, C., Britanova, O., Tarabykin, V., Richards, L.J., 2010. Molecular Regulation of the Developing Commissural Plate. J Comp Neurol 518, 3645-3661.

Molyneaux, B.J., Arlotta, P., Fame, R.M., MacDonald, J.L., MacQuarrie, K.L., Macklis, J.D., 2009. Novel Subtype-Specific Genes Identify Distinct Subpopulations of Callosal Projection Neurons. J Neurosci 29, 12343-12354.

Morgenbesser, S.D., Williams, B.O., Jacks, T., DePinho, R.A., 1994. p53-Dependent Apoptosis Produced by Rb-Deficiency in the Developing Mouse Lens. Nature 371, 72-74.

Mulligan, G., Jacks, T., 1998. The Retinoblastoma Gene Family: Cousins with Overlapping Interests. Trends Genet 14, 223-229.

Nadarajah, B., Parnavelas, J.G., 2002. Modes of Neuronal Migration in the Developing Cerebral Cortex. Nat Rev Neurosci 3, 423-432.

Nadarajah, B., Brunstrom, J.E., Grutzendler, J., Wong, R.O., Pearlman, A.L., 2001. Two Modes of Radial Migration in Early Development of the Cerebral Cortex. Nat Neurosci 4, 143-150.

Nguyen, L., Besson, A., Heng, J.I., Schuurmans, C., Teboul, L., Parras, C., Philpott, A., Roberts, J.M., Guillemot, F., 2006. P27kip1 Independently Promotes Neuronal Differentiation and Migration in the Cerebral Cortex. Genes Dev 20, 1511-1524.

Nieto, M., Monuki, E.S., Tang, H., Imitola, J., Haubst, N., Khoury, S.J., Cunningham, J., Gotz, M., Walsh, C.A., 2004. Expression of Cux-1 and Cux-2 in the Subventricular Zone and Upper Layers II-IV of the Cerebral Cortex. J Comp Neurol 479, 168-180.

Niquille, M., Minocha, S., Hornung, J.P., Rufer, N., Valloton, D., Kessaris, N., Alfonsi, F., Vitalis, T., Yanagawa, Y., Devenoges, C., Dayer, A., Lebrand, C., 2013. Two Specific Populations of GABAergic Neurons Originating from the Medial and the Caudal Ganglionic Eminences Aid in Proper Navigation of Callosal Axons. Dev Neurobiol 73, 647-672.

Niquille, M., Garel, S., Mann, F., Hornung, J.P., Otsmane, B., Chevalley, S., Parras, C., Guillemot, F., Gaspar, P., Yanagawa, Y., Lebrand, C., 2009. Transient Neuronal Populations are Required to Guide Callosal Axons: A Role for Semaphorin 3C. PLoS Biol 7, e1000230.

Noctor, S.C., Martinez-Cerdeno, V., Ivic, L., Kriegstein, A.R., 2004. Cortical Neurons Arise in Symmetric and Asymmetric Division Zones and Migrate through Specific Phases. Nat Neurosci 7, 136-144.

Noctor, S.C., Flint, A.C., Weissman, T.A., Wong, W.S., Clinton, B.K., Kriegstein, A.R., 2002. Dividing Precursor Cells of the Embryonic Cortical Ventricular

Zone have Morphological and Molecular Characteristics of Radial Glia. J Neurosci 22, 3161-3173.

Noren, N.K., Pasquale, E.B., 2004. Eph Receptor-Ephrin Bidirectional Signals that Target Ras and Rho Proteins. Cell Signal 16, 655-666.

Novitch, B.G., Spicer, D.B., Kim, P.S., Cheung, W.L., Lassar, A.B., 1999. pRb is Required for MEF2-Dependent Gene Expression as Well as Cell-Cycle Arrest during Skeletal Muscle Differentiation. Curr Biol 9, 449-459.

Nowakowski, R.S., Caviness, V.S.,Jr, Takahashi, T., Hayes, N.L., 2002. Population Dynamics during Cell Proliferation and Neuronogenesis in the Developing Murine Neocortex. Results Probl Cell Differ 39, 1-25.

Obst-Pernberg, K., Medina, L., Redies, C., 2001. Expression of R-Cadherin and N-Cadherin by Cell Groups and Fiber Tracts in the Developing Mouse Forebrain: Relation to the Formation of Functional Circuits. Neuroscience 106, 505-533.

Odajima, J., Wills, Z.P., Ndassa, Y.M., Terunuma, M., Kretschmannova, K., Deeb, T.Z., Geng, Y., Gawrzak, S., Quadros, I.M., Newman, J., Das, M., Jecrois, M.E., Yu, Q., Li, N., Bienvenu, F., Moss, S.J., Greenberg, M.E., Marto, J.A., Sicinski, P., 2011. Cyclin E Constrains Cdk5 Activity to Regulate Synaptic Plasticity and Memory Formation. Dev Cell 21, 655-668.

O'Donnell, M., Chance, R.K., Bashaw, G.J., 2009. Axon Growth and Guidance: Receptor Regulation and Signal Transduction. Annu Rev Neurosci 32, 383-412.

Okada, A., Charron, F., Morin, S., Shin, D.S., Wong, K., Fabre, P.J., Tessier-Lavigne, M., McConnell, S.K., 2006. Boc is a Receptor for Sonic Hedgehog in the Guidance of Commissural Axons. Nature 444, 369-373.

Okada, T., Okumura, Y., Motoyama, J., Ogawa, M., 2008. FGF8 Signaling Patterns the Telencephalic Midline by Regulating Putative Key Factors of Midline Development. Dev Biol 320, 92-101.

Olson, E.C., 2014. Analysis of Preplate Splitting and Early Cortical Development Illuminates the Biology of Neurological Disease. Front Pediatr 2, 121.

Olson, E.C., Kim, S., Walsh, C.A., 2006. Impaired Neuronal Positioning and Dendritogenesis in the Neocortex After Cell-Autonomous Dab1 Suppression. J Neurosci 26, 1767-1775.

Ori-McKenney, K.M., Vallee, R.B., 2011. Neuronal Migration Defects in the Loa Dynein Mutant Mouse. Neural Dev 6, 26-8104-6-26.

O'Rourke, N.A., Dailey, M.E., Smith, S.J., McConnell, S.K., 1992. Diverse Migratory Pathways in the Developing Cerebral Cortex. Science 258, 299-302.

Ounkomol, C., Yamada, S., Heinrich, V., 2010. Single-Cell Adhesion Tests Against Functionalized Microspheres Arrayed on AFM Cantilevers Confirm Heterophilic E- and N-Cadherin Binding. Biophys J 99, L100-2.

Ozaki, H.S., Wahlsten, D., 1998. Timing and Origin of the First Cortical Axons to Project through the Corpus Callosum and the Subsequent Emergence of Callosal Projection Cells in Mouse. J Comp Neurol 400, 197-206.

Pacary, E., Heng, J., Azzarelli, R., Riou, P., Castro, D., Lebel-Potter, M., Parras, C., Bell, D.M., Ridley, A.J., Parsons, M., Guillemot, F., 2011. Proneural Transcription Factors Regulate Different Steps of Cortical Neuron Migration through Rnd-Mediated Inhibition of RhoA Signaling. Neuron 69, 1069-1084.

Padmanabhan, J., Park, D.S., Greene, L.A., Shelanski, M.L., 1999. Role of Cell Cycle Regulatory Proteins in Cerebellar Granule Neuron Apoptosis. J Neurosci 19, 8747-8756.

Palmer, A., Zimmer, M., Erdmann, K.S., Eulenburg, V., Porthin, A., Heumann, R., Deutsch, U., Klein, R., 2002. EphrinB Phosphorylation and Reverse Signaling: Regulation by Src Kinases and PTP-BL Phosphatase. Mol Cell 9, 725-737.

Papadimou, E., Menard, C., Grey, C., Puceat, M., 2005. Interplay between the Retinoblastoma Protein and LEK1 Specifies Stem Cells Toward the Cardiac Lineage. EMBO J 24, 1750-1761.

Park, D.S., Obeidat, A., Giovanni, A., Greene, L.A., 2000. Cell Cycle Regulators in Neuronal Death Evoked by Excitotoxic Stress: Implications for Neurodegeneration and its Treatment. Neurobiol Aging 21, 771-781.

Paul, L.K., Corsello, C., Kennedy, D.P., Adolphs, R., 2014. Agenesis of the Corpus Callosum and Autism: A Comprehensive Comparison. Brain 137, 1813-1829.

Paul, L.K., Brown, W.S., Adolphs, R., Tyszka, J.M., Richards, L.J., Mukherjee, P., Sherr, E.H., 2007. Agenesis of the Corpus Callosum: Genetic, Developmental and Functional Aspects of Connectivity. Nat Rev Neurosci 8, 287-299.

Paul, L.K., Schieffer, B., Brown, W.S., 2004. Social Processing Deficits in Agenesis of the Corpus Callosum: Narratives from the Thematic Appreciation Test. Arch Clin Neuropsychol 19, 215-225.

Paul, L.K., Van Lancker-Sidtis, D., Schieffer, B., Dietrich, R., Brown, W.S., 2003. Communicative Deficits in Agenesis of the Corpus Callosum: Nonliteral Language and Affective Prosody. Brain Lang 85, 313-324.

Pertile, P., Baldi, A., De Luca, A., Bagella, L., Virgilio, L., Pisano, M.M., Giordano, A., 1995. Molecular Cloning, Expression, and Developmental Characterization of the Murine Retinoblastoma-Related Gene Rb2/p130. Cell Growth Differ 6, 1659-1664.

Petreanu, L., Huber, D., Sobczyk, A., Svoboda, K., 2007. Channelrhodopsin-2-Assisted Circuit Mapping of Long-Range Callosal Projections. Nat Neurosci 10, 663-668.

Picard, M., Petrie, R.J., Antoine-Bertrand, J., Saint-Cyr-Proulx, E., Villemure, J.F., Lamarche-Vane, N., 2009. Spatial and Temporal Activation of the Small GTPases RhoA and Rac1 by the Netrin-1 Receptor UNC5a during Neurite Outgrowth. Cell Signal 21, 1961-1973.

Piper, M., Moldrich, R.X., Lindwall, C., Little, E., Barry, G., Mason, S., Sunn, N., Kurniawan, N.D., Gronostajski, R.M., Richards, L.J., 2009a. Multiple Non-Cell-Autonomous Defects Underlie Neocortical Callosal Dysgenesis in Nfib-Deficient Mice. Neural Dev 4, 43-8104-4-43.

Piper, M., Plachez, C., Zalucki, O., Fothergill, T., Goudreau, G., Erzurumlu, R., Gu, C., Richards, L.J., 2009b. Neuropilin 1-Sema Signaling Regulates Crossing of Cingulate Pioneering Axons during Development of the Corpus Callosum. Cereb Cortex 19 Suppl 1, i11-21.

Polleux, F., Giger, R.J., Ginty, D.D., Kolodkin, A.L., Ghosh, A., 1998. Patterning of Cortical Efferent Projections by Semaphorin-Neuropilin Interactions. Science 282, 1904-1906.

Polleux, F., Dehay, C., Kennedy, H., 1997a. The Timetable of Laminar Neurogenesis Contributes to the Specification of Cortical Areas in Mouse Isocortex. J Comp Neurol 385, 95-116.

Polleux, F., Dehay, C., Moraillon, B., Kennedy, H., 1997b. Regulation of Neuroblast Cell-Cycle Kinetics Plays a Crucial Role in the Generation of Unique Features of Neocortical Areas. J Neurosci 17, 7763-7783.

Pradhan, S., Kim, G.D., 2002. The Retinoblastoma Gene Product Interacts with Maintenance Human DNA (Cytosine-5) Methyltransferase and Modulates its Activity. EMBO J 21, 779-788.

Price, D.J., Kennedy, H., Dehay, C., Zhou, L., Mercier, M., Jossin, Y., Goffinet, A.M., Tissir, F., Blakey, D., Molnar, Z., 2006a. The Development of Cortical Connections. Eur J Neurosci 23, 910-920.

Price, D.J., Kennedy, H., Dehay, C., Zhou, L., Mercier, M., Jossin, Y., Goffinet, A.M., Tissir, F., Blakey, D., Molnar, Z., 2006b. The Development of Cortical Connections. Eur J Neurosci 23, 910-920.

Purohit, A.A., Li, W., Qu, C., Dwyer, T., Shao, Q., Guan, K.L., Liu, G., 2012. Down Syndrome Cell Adhesion Molecule (DSCAM) Associates with Uncoordinated-5C (UNC5C) in Netrin-1-Mediated Growth Cone Collapse. J Biol Chem 287, 27126-27138.

Qian, X., Shen, Q., Goderie, S.K., He, W., Capela, A., Davis, A.A., Temple, S., 2000. Timing of CNS Cell Generation: A Programmed Sequence of Neuron and Glial Cell Production from Isolated Murine Cortical Stem Cells. Neuron 28, 69-80.

Rakic, P., 1972. Mode of Cell Migration to the Superficial Layers of Fetal Monkey Neocortex. J Comp Neurol 145, 61-83.

Rakic, P., 1971. Guidance of Neurons Migrating to the Fetal Monkey Neocortex. Brain Res 33, 471-476.

Rash, B.G., Richards, L.J., 2001a. A Role for Cingulate Pioneering Axons in the Development of the Corpus Callosum. J Comp Neurol 434, 147-157.

Rash, B.G., Richards, L.J., 2001b. A Role for Cingulate Pioneering Axons in the Development of the Corpus Callosum. J Comp Neurol 434, 147-157.

Rice, H., Suth, S., Cavanaugh, W., Bai, J., Young-Pearse, T.L., 2010. In Utero Electroporation Followed by Primary Neuronal Culture for Studying Gene Function in Subset of Cortical Neurons. J Vis Exp (44). pii: 2103. doi, 10.3791/2103.

Richards, L.J., 2002. Axonal Pathfinding Mechanisms at the Cortical Midline and in the Development of the Corpus Callosum. Braz J Med Biol Res 35, 1431-1439.

Robertson, K.D., Ait-Si-Ali, S., Yokochi, T., Wade, P.A., Jones, P.L., Wolffe, A.P., 2000. DNMT1 Forms a Complex with Rb, E2F1 and HDAC1 and Represses Transcription from E2F-Responsive Promoters. Nat Genet 25, 338-342.

Sage, C., Huang, M., Vollrath, M.A., Brown, M.C., Hinds, P.W., Corey, D.P., Vetter, D.E., Chen, Z.Y., 2006. Essential Role of Retinoblastoma Protein in Mammalian Hair Cell Development and Hearing. Proc Natl Acad Sci U S A 103, 7345-7350.

Sage, J., Mulligan, G.J., Attardi, L.D., Miller, A., Chen, S., Williams, B., Theodorou, E., Jacks, T., 2000. Targeted Disruption of the Three Rb-Related Genes Leads to Loss of G(1) Control and Immortalization. Genes Dev 14, 3037-3050.

Saito, T., 2006. In Vivo Electroporation in the Embryonic Mouse Central Nervous System. Nat Protoc 1, 1552-1558.

Sanada, K., Gupta, A., Tsai, L.H., 2004. Disabled-1-Regulated Adhesion of Migrating Neurons to Radial Glial Fiber Contributes to Neuronal Positioning during Early Corticogenesis. Neuron 42, 197-211.

Sanchez-Camacho, C., Ortega, J.A., Ocana, I., Alcantara, S., Bovolenta, P., 2011. Appropriate Bmp7 Levels are Required for the Differentiation of Midline Guidepost Cells Involved in Corpus Callosum Formation. Dev Neurobiol 71, 337-350.

Santamaria, D., Ortega, S., 2006. Cyclins and CDKS in Development and Cancer: Lessons from Genetically Modified Mice. Front Biosci 11, 1164-1188.

Sato, M., Nagano, T., 2005. Involvement of Filamin A and Filamin A-Interacting Protein (FILIP) in Controlling the Start and Cell Shape of Radially Migrating Cortical Neurons. Anat Sci Int 80, 19-29.

Scime, A., Grenier, G., Huh, M.S., Gillespie, M.A., Bevilacqua, L., Harper, M.E., Rudnicki, M.A., 2005. Rb and p107 Regulate Preadipocyte Differentiation into White Versus Brown Fat through Repression of PGC-1alpha. Cell Metab 2, 283-295.

Sekine, K., Honda, T., Kawauchi, T., Kubo, K., Nakajima, K., 2011. The Outermost Region of the Developing Cortical Plate is Crucial for both the Switch of the Radial Migration Mode and the Dab1-Dependent "Inside-Out" Lamination in the Neocortex. J Neurosci 31, 9426-9439.

Senturk, A., Pfennig, S., Weiss, A., Burk, K., Acker-Palmer, A., 2011. Ephrin Bs are Essential Components of the Reelin Pathway to Regulate Neuronal Migration. Nature 472, 356-360.

Serafini, T., Colamarino, S.A., Leonardo, E.D., Wang, H., Beddington, R., Skarnes, W.C., Tessier-Lavigne, M., 1996. Netrin-1 is Required for Commissural Axon Guidance in the Developing Vertebrate Nervous System. Cell 87, 1001-1014.

Serrano, M., Hannon, G.J., Beach, D., 1993. A New Regulatory Motif in Cell-Cycle Control Causing Specific Inhibition of Cyclin D/CDK4. Nature 366, 704-707.

Shan, B., Chang, C.Y., Jones, D., Lee, W.H., 1994. The Transcription Factor E2F-1 Mediates the Autoregulation of RB Gene Expression. Mol Cell Biol 14, 299-309.

Shen, Q., Wang, Y., Dimos, J.T., Fasano, C.A., Phoenix, T.N., Lemischka, I.R., Ivanova, N.B., Stifani, S., Morrisey, E.E., Temple, S., 2006. The Timing of Cortical Neurogenesis is Encoded within Lineages of Individual Progenitor Cells. Nat Neurosci 9, 743-751.

Shimizu, M., Murakami, Y., Suto, F., Fujisawa, H., 2000. Determination of Cell Adhesion Sites of Neuropilin-1. J Cell Biol 148, 1283-1293.

Shimogori, T., Banuchi, V., Ng, H.Y., Strauss, J.B., Grove, E.A., 2004. Embryonic Signaling Centers Expressing BMP, WNT and FGF Proteins Interact to Pattern the Cerebral Cortex. Development 131, 5639-5647.

Shu, T., Butz, K.G., Plachez, C., Gronostajski, R.M., Richards, L.J., 2003a. Abnormal Development of Forebrain Midline Glia and Commissural Projections in Nfia Knock-Out Mice. J Neurosci 23, 203-212.

Shu, T., Li, Y., Keller, A., Richards, L.J., 2003b. The Glial Sling is a Migratory Population of Developing Neurons. Development 130, 2929-2937.

Shu, T., Puche, A.C., Richards, L.J., 2003c. Development of Midline Glial Populations at the Corticoseptal Boundary. J Neurobiol 57, 81-94.

Shu, T., Richards, L.J., 2001. Cortical Axon Guidance by the Glial Wedge during the Development of the Corpus Callosum. J Neurosci 21, 2749-2758.

Shu, T., Valentino, K.M., Seaman, C., Cooper, H.M., Richards, L.J., 2000. Expression of the Netrin-1 Receptor, Deleted in Colorectal Cancer (DCC), is Largely Confined to Projecting Neurons in the Developing Forebrain. J Comp Neurol 416, 201-212.

Siegenthaler, J.A., Pleasure, S.J., 2011. We have Got You 'Covered': How the Meninges Control Brain Development. Curr Opin Genet Dev 21, 249-255.

Silver, J., Edwards, M.A., Levitt, P., 1993. Immunocytochemical Demonstration of Early Appearing Astroglial Structures that Form Boundaries and Pathways Along Axon Tracts in the Fetal Brain. J Comp Neurol 328, 415-436.

Singh, M., Krajewski, M., Mikolajka, A., Holak, T.A., 2005. Molecular Determinants for the Complex Formation between the Retinoblastoma Protein and LXCXE Sequences. J Biol Chem 280, 37868-37876.

Sloan, T.F., Qasaimeh, M.A., Juncker, D., Yam, P.T., Charron, F., 2015. Integration of Shallow Gradients of Shh and Netrin-1 Guides Commissural Axons. PLoS Biol 13, e1002119.

Smith, K.M., Ohkubo, Y., Maragnoli, M.E., Rasin, M.R., Schwartz, M.L., Sestan, N., Vaccarino, F.M., 2006. Midline Radial Glia Translocation and Corpus Callosum Formation Require FGF Signaling. Nat Neurosci 9, 787-797.

Spear, P.C., Erickson, C.A., 2012. Apical Movement during Interkinetic Nuclear Migration is a Two-Step Process. Dev Biol 370, 33-41.

Stancik, E.K., Navarro-Quiroga, I., Sellke, R., Haydar, T.F., 2010a. Heterogeneity in Ventricular Zone Neural Precursors Contributes to Neuronal Fate Diversity in the Postnatal Neocortex. J Neurosci 30, 7028-7036.

Stancik, E.K., Navarro-Quiroga, I., Sellke, R., Haydar, T.F., 2010b. Heterogeneity in Ventricular Zone Neural Precursors Contributes to Neuronal Fate Diversity in the Postnatal Neocortex. J Neurosci 30, 7028-7036.

Stewart, G.R., Pearlman, A.L., 1987. Fibronectin-Like Immunoreactivity in the Developing Cerebral Cortex. J Neurosci 7, 3325-3333.

Sun, A., Bagella, L., Tutton, S., Romano, G., Giordano, A., 2007a. From G0 to S Phase: A View of the Roles Played by the Retinoblastoma (Rb) Family Members in the Rb-E2F Pathway. J Cell Biochem 102, 1400-1404.

Sun, A., Bagella, L., Tutton, S., Romano, G., Giordano, A., 2007b. From G0 to S Phase: A View of the Roles Played by the Retinoblastoma (Rb) Family Members in the Rb-E2F Pathway. J Cell Biochem 102, 1400-1404.

Sutcliffe, J.E., Brown, T.R., Allison, S.J., Scott, P.H., White, R.J., 2000. Retinoblastoma Protein Disrupts Interactions Required for RNA Polymerase III Transcription. Mol Cell Biol 20, 9192-9202.

Svoboda, D.S., Clark, A., Park, D.S., Slack, R.S., 2015. Induction of Protein Deletion through in Utero Electroporation to Define Deficits in Neuronal Migration in Transgenic Models. J Vis Exp (95):51983. doi, 51983.

Svoboda, D.S., Paquin, A., Park, D.S., Slack, R.S., 2013. Pocket Proteins pRb and p107 are Required for Cortical Lamination Independent of Apoptosis. Dev Biol 384, 101-113.

Szabo, N., Gergev, G., Kobor, J., Bereg, E., Turi, S., Sztriha, L., 2011. Corpus Callosum Anomalies: Birth Prevalence and Clinical Spectrum in Hungary. Pediatr Neurol 44, 420-426.

Takahashi, T., Nowakowski, R.S., Caviness, V.S.,Jr, 1996. Interkinetic and Migratory Behavior of a Cohort of Neocortical Neurons Arising in the Early Embryonic Murine Cerebral Wall. J Neurosci 16, 5762-5776.

Tamamaki, N., Fujimori, K.E., Takauji, R., 1997. Origin and Route of Tangentially Migrating Neurons in the Developing Neocortical Intermediate Zone. J Neurosci 17, 8313-8323.

Tamrakar, S., Rubin, E., Ludlow, J.W., 2000. Role of pRB Dephosphorylation in Cell Cycle Regulation. Front Biosci 5, D121-37.

Tarabykin, V., Stoykova, A., Usman, N., Gruss, P., 2001. Cortical Upper Layer Neurons Derive from the Subventricular Zone as Indicated by Svet1 Gene Expression. Development 128, 1983-1993.

Thomas, D.M., Carty, S.A., Piscopo, D.M., Lee, J.S., Wang, W.F., Forrester, W.C., Hinds, P.W., 2001. The Retinoblastoma Protein Acts as a Transcriptional Coactivator Required for Osteogenic Differentiation. Mol Cell 8, 303-316.

Thomas, N.S., Pizzey, A.R., Tiwari, S., Williams, C.D., Yang, J., 1998. p130, p107, and pRb are Differentially Regulated in Proliferating Cells and during Cell Cycle Arrest by Alpha-Interferon. J Biol Chem 273, 23659-23667.

Tissir, F., Goffinet, A.M., 2003. Reelin and Brain Development. Nat Rev Neurosci 4, 496-505.

Toyo-oka, K., Wachi, T., Hunt, R.F., Baraban, S.C., Taya, S., Ramshaw, H., Kaibuchi, K., Schwarz, Q.P., Lopez, A.F., Wynshaw-Boris, A., 2014. 14-3-3epsilon and Zeta Regulate Neurogenesis and Differentiation of Neuronal Progenitor Cells in the Developing Brain. J Neurosci 34, 12168-12181.

Treubert-Zimmermann, U., Heyers, D., Redies, C., 2002. Targeting Axons to Specific Fiber Tracts in Vivo by Altering Cadherin Expression. J Neurosci 22, 7617-7626.

Trikha, P., Sharma, N., Opavsky, R., Reyes, A., Pena, C., Ostrowski, M.C., Roussel, M.F., Leone, G., 2011. E2f1-3 are Critical for Myeloid Development. J Biol Chem 286, 4783-4795.

Trimarchi, J.M., Lees, J.A., 2002. Sibling Rivalry in the E2F Family. Nat Rev Mol Cell Biol 3, 11-20.

Tury, A., Mairet-Coello, G., DiCicco-Bloom, E., 2011. The Cyclin-Dependent Kinase Inhibitor p57Kip2 Regulates Cell Cycle Exit, Differentiation, and

Migration of Embryonic Cerebral Cortical Precursors. Cereb Cortex 21, 1840-1856.

Unni, D.K., Piper, M., Moldrich, R.X., Gobius, I., Liu, S., Fothergill, T., Donahoo, A.L., Baisden, J.M., Cooper, H.M., Richards, L.J., 2012. Multiple Slits Regulate the Development of Midline Glial Populations and the Corpus Callosum. Dev Biol 365, 36-49.

Uribe, E., Wix, R., 2012. Neuronal Migration, Apoptosis and Bipolar Disorder. Rev Psiquiatr Salud Ment 5, 127-133.

Vanderluit, J.L., Wylie, C.A., McClellan, K.A., Ghanem, N., Fortin, A., Callaghan, S., MacLaurin, J.G., Park, D.S., Slack, R.S., 2007. The Retinoblastoma Family Member p107 Regulates the Rate of Progenitor Commitment to a Neuronal Fate. J Cell Biol 178, 129-139.

Vanderluit, J.L., Ferguson, K.L., Nikoletopoulou, V., Parker, M., Ruzhynsky, V., Alexson, T., McNamara, S.M., Park, D.S., Rudnicki, M., Slack, R.S., 2004. P107 Regulates Neural Precursor Cells in the Mammalian Brain. J Cell Biol 166, 853-863.

Verstegen, A.M., Tagliatti, E., Lignani, G., Marte, A., Stolero, T., Atias, M., Corradi, A., Valtorta, F., Gitler, D., Onofri, F., Fassio, A., Benfenati, F., 2014. Phosphorylation of Synapsin I by Cyclin-Dependent Kinase-5 Sets the Ratio between the Resting and Recycling Pools of Synaptic Vesicles at Hippocampal Synapses. J Neurosci 34, 7266-7280.

Vietri, M., Bianchi, M., Ludlow, J.W., Mittnacht, S., Villa-Moruzzi, E., 2006. Direct Interaction between the Catalytic Subunit of Protein Phosphatase 1 and pRb. Cancer Cell Int 6, 3.

Vooijs, M., van der Valk, M., te Riele, H., Berns, A., 1998. Flp-Mediated Tissue-Specific Inactivation of the Retinoblastoma Tumor Suppressor Gene in the Mouse. Oncogene 17, 1-12.

Wakade, C.G., Mehta, S.H., Maeda, M., Webb, R.C., Chiu, F.C., 2013. Axonal Fasciculation and the Role of Polysialic Acid-Neural Cell Adhesion Molecule in Rat Cortical Neurons. J Neurosci Res 91, 1408-1418.

Wallace, V.A., Raff, M.C., 1999. A Role for Sonic Hedgehog in Axon-to-Astrocyte Signalling in the Rodent Optic Nerve. Development 126, 2901-2909.

Wang, C.L., Zhang, L., Zhou, Y., Zhou, J., Yang, X.J., Duan, S.M., Xiong, Z.Q., Ding, Y.Q., 2007a. Activity-Dependent Development of Callosal Projections in the Somatosensory Cortex. J Neurosci 27, 11334-11342.

Wang, H., Ge, G., Uchida, Y., Luu, B., Ahn, S., 2011. Gli3 is Required for Maintenance and Fate Specification of Cortical Progenitors. J Neurosci 31, 6440-6448.

Wang, X., Qiu, R., Tsark, W., Lu, Q., 2007b. Rapid Promoter Analysis in Developing Mouse Brain and Genetic Labeling of Young Neurons by Doublecortin-DsRed-Express. J Neurosci Res 85, 3567-3573.

Weinberg, R.A., 1991. Tumor Suppressor Genes. Science 254, 1138-1146.

Wenzel, P.L., Wu, L., de Bruin, A., Chong, J.L., Chen, W.Y., Dureska, G., Sites, E., Pan, T., Sharma, A., Huang, K., Ridgway, R., Mosaliganti, K., Sharp, R., Machiraju, R., Saltz, J., Yamamoto, H., Cross, J.C., Robinson, M.L., Leone, G., 2007. Rb is Critical in a Mammalian Tissue Stem Cell Population. Genes Dev 21, 85-97.

Wirt, S.E., Adler, A.S., Gebala, V., Weimann, J.M., Schaffer, B.E., Saddic, L.A., Viatour, P., Vogel, H., Chang, H.Y., Meissner, A., Sage, J., 2010. G1 Arrest and Differentiation can Occur Independently of Rb Family Function. J Cell Biol 191, 809-825.

Wirt, S.E., Sage, J., 2010. p107 in the Public Eye: An Rb Understudy and More. Cell Div 5, 9-1028-5-9.

Wolman, M.A., Regnery, A.M., Becker, T., Becker, C.G., Halloran, M.C., 2007. Semaphorin3D Regulates Axon Axon Interactions by Modulating Levels of L1 Cell Adhesion Molecule. J Neurosci 27, 9653-9663.

Wu, Q., Liu, J., Fang, A., Li, R., Bai, Y., Kriegstein, A.R., Wang, X., 2014. The Dynamics of Neuronal Migration. Adv Exp Med Biol 800, 25-36.

Wu, Z., Zheng, S., Yu, Q., 2009. The E2F Family and the Role of E2F1 in Apoptosis. Int J Biochem Cell Biol 41, 2389-2397.

Xu, X., Bieda, M., Jin, V.X., Rabinovich, A., Oberley, M.J., Green, R., Farnham, P.J., 2007. A Comprehensive ChIP-Chip Analysis of E2F1, E2F4, and E2F6 in

Normal and Tumor Cells Reveals Interchangeable Roles of E2F Family Members. Genome Res 17, 1550-1561.

Yam, P.T., Charron, F., 2013. Signaling Mechanisms of Non-Conventional Axon Guidance Cues: The Shh, BMP and Wnt Morphogens. Curr Opin Neurobiol 23, 965-973.

Yao, Z., Zhang, Y., Lin, L., Zhou, Y., Xu, C., Jiang, T., Alzheimer's Disease Neuroimaging Initiative, 2010. Abnormal Cortical Networks in Mild Cognitive Impairment and Alzheimer's Disease. PLoS Comput Biol 6, e1001006.

Yoshida, A., Yamaguchi, Y., Nonomura, K., Kawakami, K., Takahashi, Y., Miura, M., 2010. Simultaneous Expression of Different Transgenes in Neurons and Glia by Combining in Utero Electroporation with the Tol2 Transposon-Mediated Gene Transfer System. Genes Cells 15, 501-512.

Yoshida, M., Suda, Y., Matsuo, I., Miyamoto, N., Takeda, N., Kuratani, S., Aizawa, S., 1997. Emx1 and Emx2 Functions in Development of Dorsal Telencephalon. Development 124, 101-111.

Yoshikawa, K., 2000. Cell Cycle Regulators in Neural Stem Cells and Postmitotic Neurons. Neurosci Res 37, 1-14.

Yu, W., Wang, Y., McDonnell, K., Stephen, D., Bai, C.B., 2009. Patterning of Ventral Telencephalon Requires Positive Function of Gli Transcription Factors. Dev Biol 334, 264-275.

Zelina, P., Blockus, H., Zagar, Y., Peres, A., Friocourt, F., Wu, Z., Rama, N., Fouquet, C., Hohenester, E., Tessier-Lavigne, M., Schweitzer, J., Roest Crollius, H., Chedotal, A., 2014. Signaling Switch of the Axon Guidance Receptor Robo3 during Vertebrate Evolution. Neuron 84, 1258-1272.

Zhang, J., Gray, J., Wu, L., Leone, G., Rowan, S., Cepko, C.L., Zhu, X., Craft, C.M., Dyer, M.A., 2004. Rb Regulates Proliferation and Rod Photoreceptor Development in the Mouse Retina. Nat Genet 36, 351-360.

Zhang, L., Huang, Y., Chen, J.Y., Ding, Y.Q., Song, N.N., 2015. DSCAM and DSCAML1 Regulate the Radial Migration and Callosal Projection in Developing Cerebral Cortex. Brain Res 1594, 61-70.

Zhang, R.L., Zhang, Z.G., Zhang, L., Chopp, M., 2001. Proliferation and Differentiation of Progenitor Cells in the Cortex and the Subventricular Zone in the Adult Rat After Focal Cerebral Ischemia. Neuroscience 105, 33-41.

Zhao, H., Maruyama, T., Hattori, Y., Sugo, N., Takamatsu, H., Kumanogoh, A., Shirasaki, R., Yamamoto, N., 2011. A Molecular Mechanism that Regulates Medially Oriented Axonal Growth of Upper Layer Neurons in the Developing Neocortex. J Comp Neurol 519, 834-848.

Zheng, C., Heintz, N., Hatten, M.E., 1996. CNS Gene Encoding Astrotactin, which Supports Neuronal Migration Along Glial Fibers. Science 272, 417-419.

Zheng, W., Geng, A.Q., Li, P.F., Wang, Y., Yuan, X.B., 2012. Robo4 Regulates the Radial Migration of Newborn Neurons in Developing Neocortex. Cereb Cortex 22, 2587-2601.

Zhou, J., Wen, Y., She, L., Sui, Y.N., Liu, L., Richards, L.J., Poo, M.M., 2013. Axon Position within the Corpus Callosum Determines Contralateral Cortical Projection. Proc Natl Acad Sci U S A 110, E2714-23.

Ziebold, U., Lee, E.Y., Bronson, R.T., Lees, J.A., 2003. E2F3 Loss has Opposing Effects on Different pRB-Deficient Tumors, Resulting in Suppression of Pituitary Tumors but Metastasis of Medullary Thyroid Carcinomas. Mol Cell Biol 23, 6542-6552.

Zimmer, M., Palmer, A., Kohler, J., Klein, R., 2003. EphB-ephrinB Bi-Directional Endocytosis Terminates Adhesion Allowing Contact Mediated Repulsion. Nat Cell Biol 5, 869-878.

Appendix A

In Utero Electroporation Collaborations

At the beginning of PhD studies, I visited the lab of Freda Miller at the University of Toronto to learn how to perform in utero electroporation. I then returned to the University of Ottawa and proceeded to establish this procedure in the lab of Dr. Ruth Slack. Since then, I have entered into numerous collaborations with other members of the Slack lab, with other labs at the University of Ottawa, and with labs in other universities. In general, my part in these collaborations is to instruct my collaborators on plasmid preparation, perform the in utero electroporations, assist with tissue collection and harvesting and aid with data collection, analysis and interpretation. The figures in this this appendix represent the results of these collaborations, presented in chronological order.

The Rb/E2F Pathway Modulates Neurogenesis through Direct Regulation of the *Dlx1/Dlx2* Bigene Cluster

Noël Ghanem, Matthew G. Andrusiak, **Devon Svoboda**, Sawsan M. Al Lafi, Lisa M. Julian, Kelly A. McClellan, Yves De Repentigny, Rashmi Kothary, Marc Ekker, Alexandre Blais, David S. Park, and Ruth S. Slack.

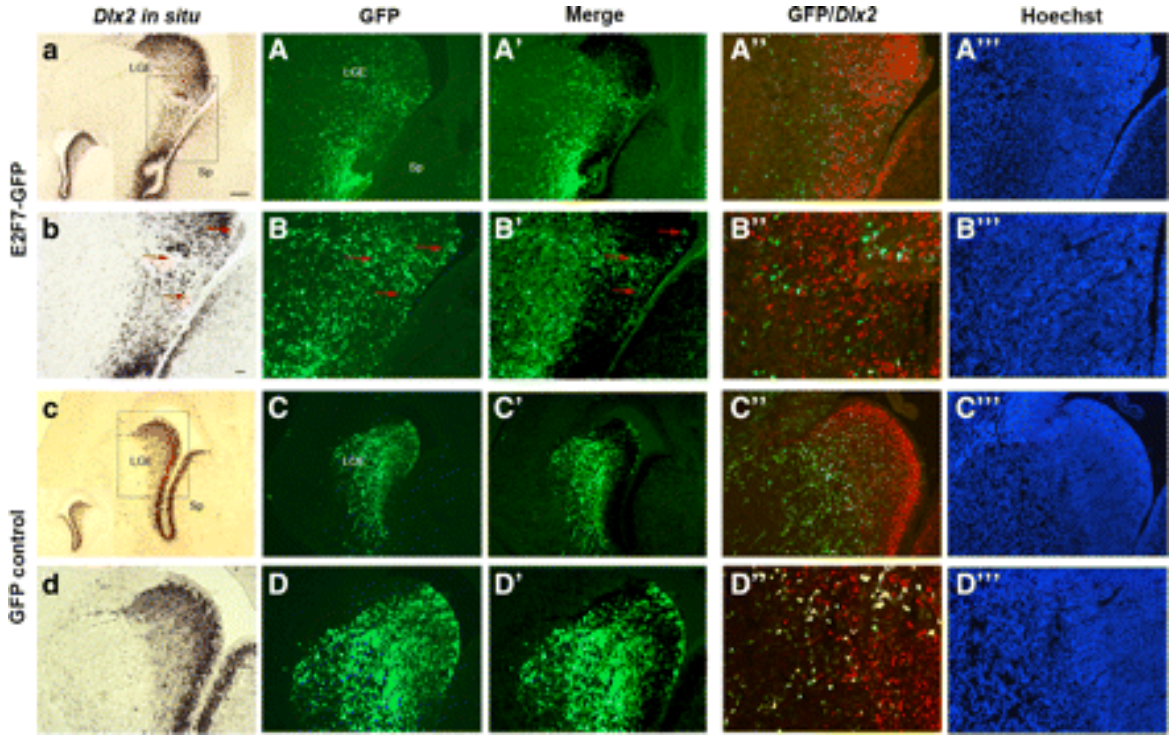

Figure A1-1: E2F7 represses *Dlx2* expression *in vivo.* *In utero* electroporation of a dual cassette containing both E2F7 and GFP, and an empty vector containing GFP alone in the ventral forebrain at E13.5. ***a–d***, *In situ* hybridization performed with a *Dlx2* probe on coronal sections at E15.5 and showing loss of *Dlx2* expression in E2F7-electroporated brains (***b***; arrows) compared with control brains (***c***, ***d***). Insets in ***a*** and ***c*** represent the non-electroporated contralateral side. ***A–D***, Anti-GFP staining of brains electroporated with E2F7-GFP (***A***, ***B***) and GFP alone (***C***, ***D***). ***A′–D′*** are merged images of ***a–d*** and ***A–D***, respectively. ***A″–D″***, Double immunostaining with anti-*Dlx2* (red) and anti-GFP (green) showing little colocalization of the two proteins in E2F7 electroporated brains (***B″***; inset) compared with GFP controls where many cells are *Dlx2*+/GFP+ (***D″***; inset).

The purpose of this experiment was to determine if E2F7 regulates Dlx2 expression. The decrease in Dlx2 indicates the E2F7 represses Dlx2 expression in ventral neural precursors. In this collaboration, I performed the in utero electroporations and harvested the tissue. I also aided in data collection, analysis and interpretation.

E2f3 Isoforms Differentially Regulate the Pluripotency Factor Sox2 to Balance Neural Precursor Maintenance and Neurogenesis.

Lisa Julian, Renaud Vandenbosch, Cathy Packenham, Matt Andrusiak, Angela Nguyen, Kelly McClellan, **Devon Svoboda**, David S Park, Gustavo Leone, Diane Lagace, Alexander Blais and Ruth S Slack.

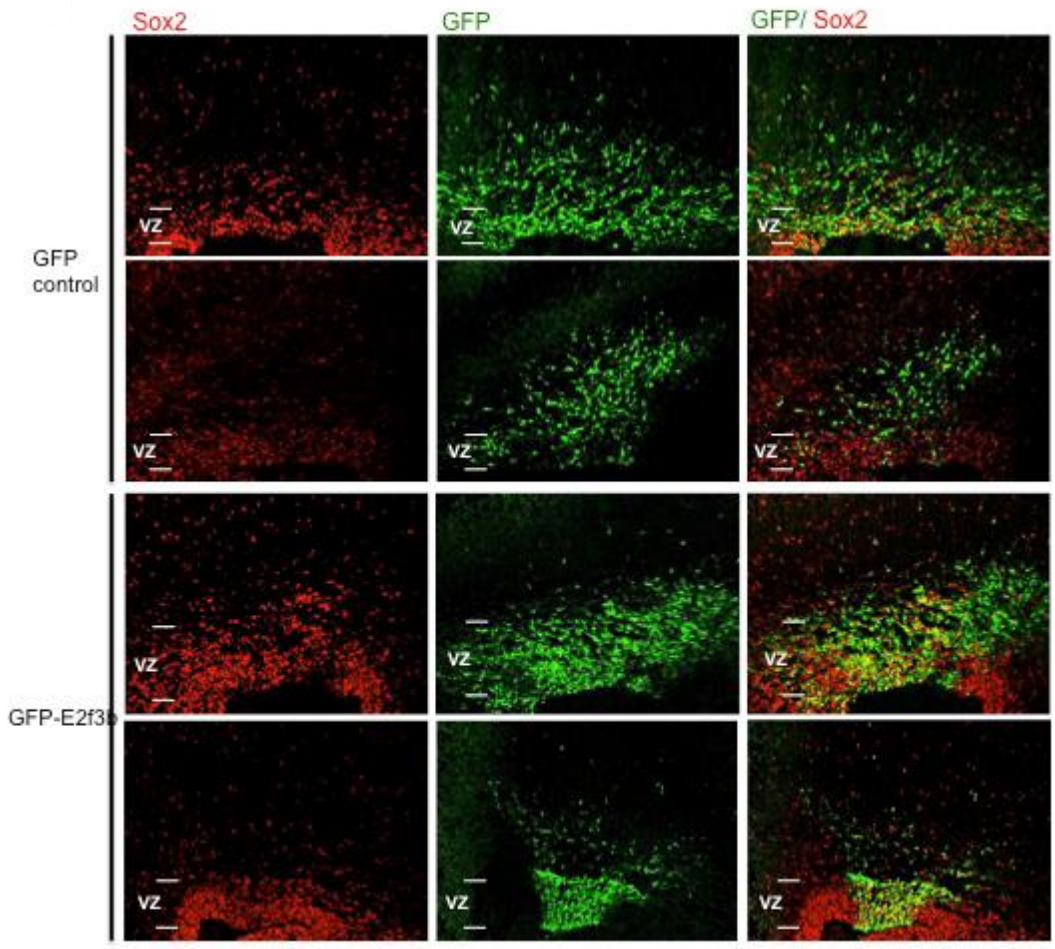

Figure A1-2: E2F3b promotes maintenance of stem cell identity in neural precursor cells. The lateral cortex of wild type mice was electroporated with pCig2 or pCig2-E2F3b at E13.5 and collected at E15.5. Brains were stained for GFP+ (green) to mark electroporated cells and Sox2 (red) to mark stem-like cells in the VZ. Yellow cells indicate co-labelled GFP/Sox2 cells. The increase in Sox2/GFP co-expression suggests that expression of E2F3b promotes the maintenance of stem-like characteristics at the expense of neural differentiation in electroporated cells.

The purpose of this experiment was to determine expression of E2F3a/b isoforms alter NPC cell fate. The increase in Sox2/GFP co-labelling in E2F3b electroporated brain indicates the E2F3b promotes maintenance of the stem cell identity. In this collaboration, I performed the in utero electroporations and harvested the tissue. I also aided in data collection, analysis and interpretation. These results were not included in the final paper.

Interaction and Antagonistic Roles of NF-κB and Hes6 in the Regulation of Cortical Neurogenesis.

Laurent Methot, Robert Hermann, Yeman Tang, Rita Lo, Hosam Al-Jehani, Sumit Jhas, **Devon Svoboda**, Ruth S. Slack, Philip A. Barker and Stefano Stifani.

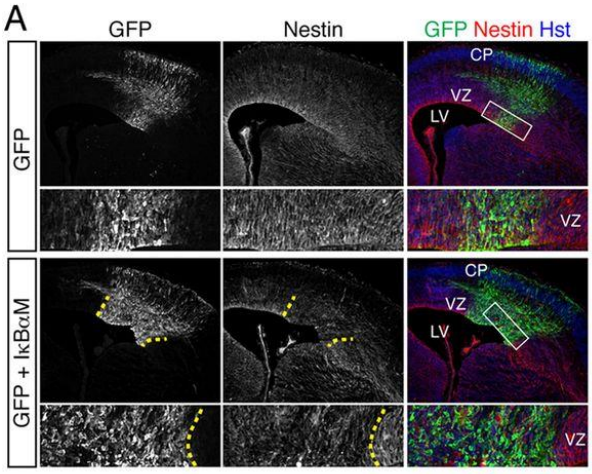

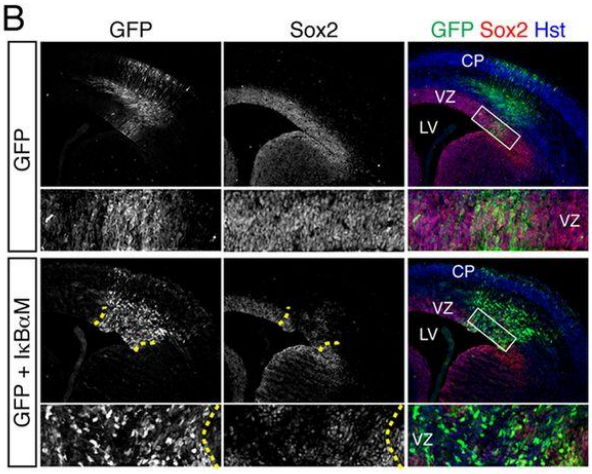

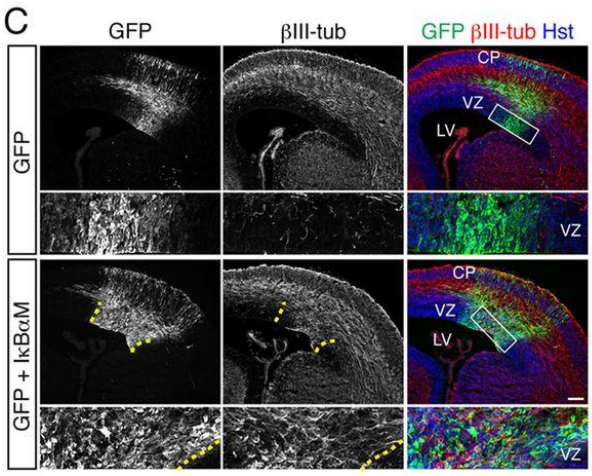

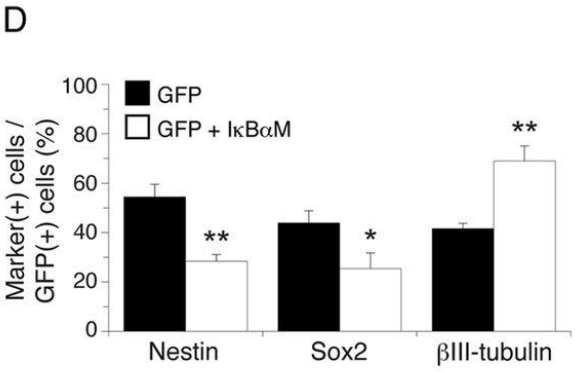

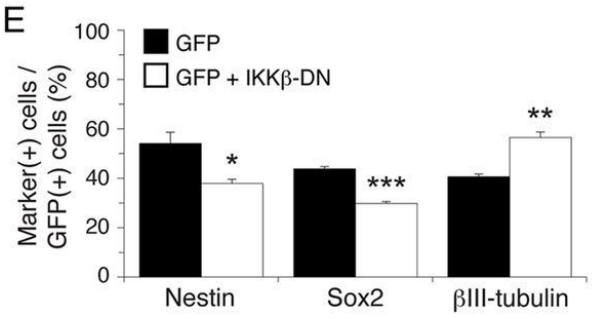

Figure A1-3: NF-κB signaling is important to prevent premature neuronal differentiation in the developing neocortex *in vivo*. (A to C) Double-label immunofluorescence analysis of GFP and either nestin (A), Sox2 (B), or βIII-tubulin (βIII-tub) (C) expression 48 h after *in utero* electroporation of E13.5 mouse embryos with either a bicistronic plasmid expressing both IκBαM and GFP or the empty vector expressing GFP alone. Bottom rows, high-magnification views of the areas indicated by rectangles in the right-hand panels. Where shown (when IκBαM was used), dotted lines roughly demarcate the GFP^+ electroporated area in the VZ. Hst, Hoechst. Scale bar, 100 μm. (D) Quantification of the fraction of GFP^+ cells coexpressing nestin, Sox2, or βIII-tubulin. Results are shown as the means ± standard errors of the means (SEM) (*, $P < 0.05$; **, $P < 0.01$; $n = 5$ electroporated embryos per condition; *t* test). (E) Quantification of the fraction of GFP^+ cells coexpressing nestin, Sox2, or βIII-tubulin 48 h after *in utero* electroporation of E13.5 embryos with either a bicistronic plasmid expressing both IKKβ-DN and GFP or the empty vector expressing GFP alone. Results are shown as the means ± SEM (***, $P < 0.001$; $n = 3$ electroporated embryos per condition; *t* test).

The purpose of this experiment was to determine if electroporation of IκBαM, in inhibitor of NF- κB influences neural differentiation as determined by co-expression of GFP with βIII-Tubulin or Sox2. Ectopic expression of βIII-Tubulin and loss of Sox2 in the ventricular zone indicate premature differentiation in brains electroporated with pCig2- IκBαM compared to an empty pCig2 plasmid. In this collaboration, I performed the *in utero* electroporations and harvested the tissue. I also taught Laurent Method, from the lab of Stefano Stifani in the Montreal Neuroscience Institute at McGill University, how to perform *in utero* electroporation.

Phosphorylation of Jip1 on residue Thr 205 regulates radial migration during brain development.

Dianbo Qu, Doo Soo Im, **Devon Svoboda**, Roger Davis, Ruth S Slack and David S Park.

The following represents two of several experiments in an unpublished study designed to investigate the effect of JNK-interacting protein (Jip1) on neural migration. The activity of Jip1 on CDK5 is dependent on phosphorylation of Jip1 on threonine residue 205. The Jip1-T205D mutant represents a constitutively active form of Jip1, while the Jip1-T205A mutant represents a dominant negative form of Jip1. In this collaboration, I performed the in utero electroporations, instructed by collaborators in plasmid preparation, tissue collection and immunostaining, and aided in data analysis and interpretation.

Figure A1-4: Jip1 phosphorylation regulates radial migration. The lateral cortex of wild type mouse embryos was electroporated at E14.5 with an empty p-Cig2 plasmid (GFP only), pCig2-Jip1 (Jip1 WT), pCig2-Jip1-T205A mutant (T205A) or pCig2-Jip1-T205D mutant (T205D). Brains were collected at E16.5 **(A)** or E18.5 **(B)**. Sections were stained for GFP+ (green) and Tbr1 (red) to mark the lower cortical layers to provide reference for the location of GFP+ cells. For E16.5 brains **(A)** the number of GFP+ cells located in the intermediate zone (IZ, below Tbr2 staining) and within the cortical plate (CP – within Tbr1 layer) were quantified. For E18.5 brains **(B)**, GFP+ cells were defined as being located in the IZ, in the lower cortical layers (within Tbr1) or in the upper cortical layers (above Tbr1). At both timepoints, expression of Jip1-T205A was found to delay neuroblast migration. * = $p < 0.05$.

A

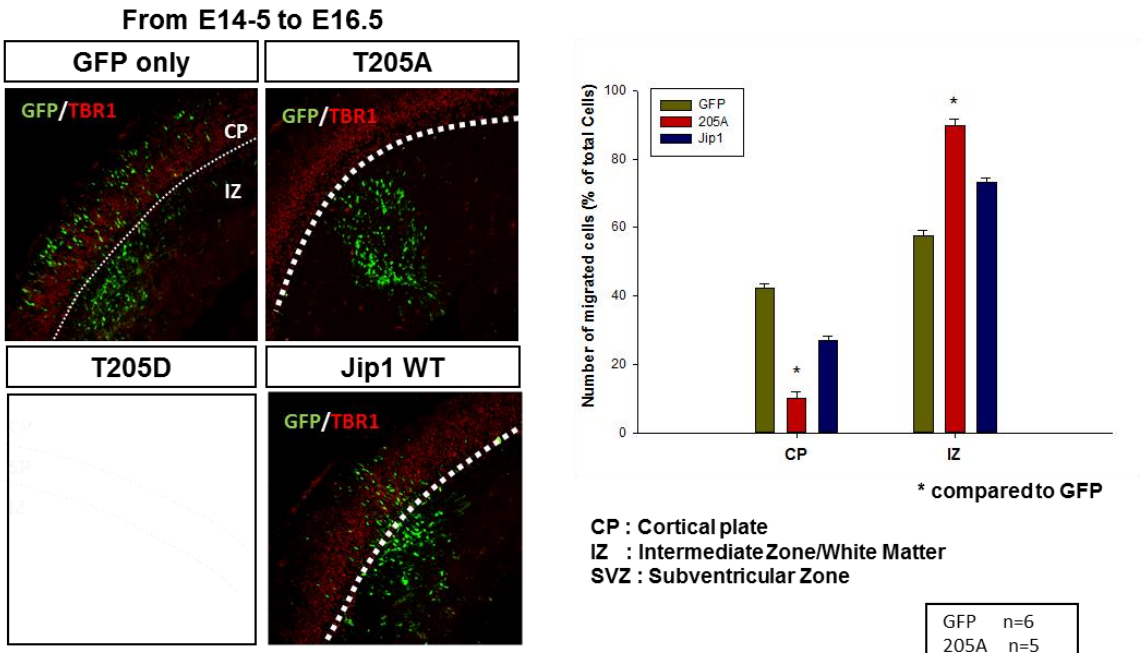

CP : Cortical plate
IZ : Intermediate Zone/White Matter
SVZ : Subventricular Zone

GFP	n=6
205A	n=5
WT	n=6

T205 A : Jip1 alanine mutant on residue Thr 205
T205 D : Jip1 aspartic acid mutant on residue Thr 205 (Phosphomimics)
Jip1 WT : expression of wild type Jip1

B

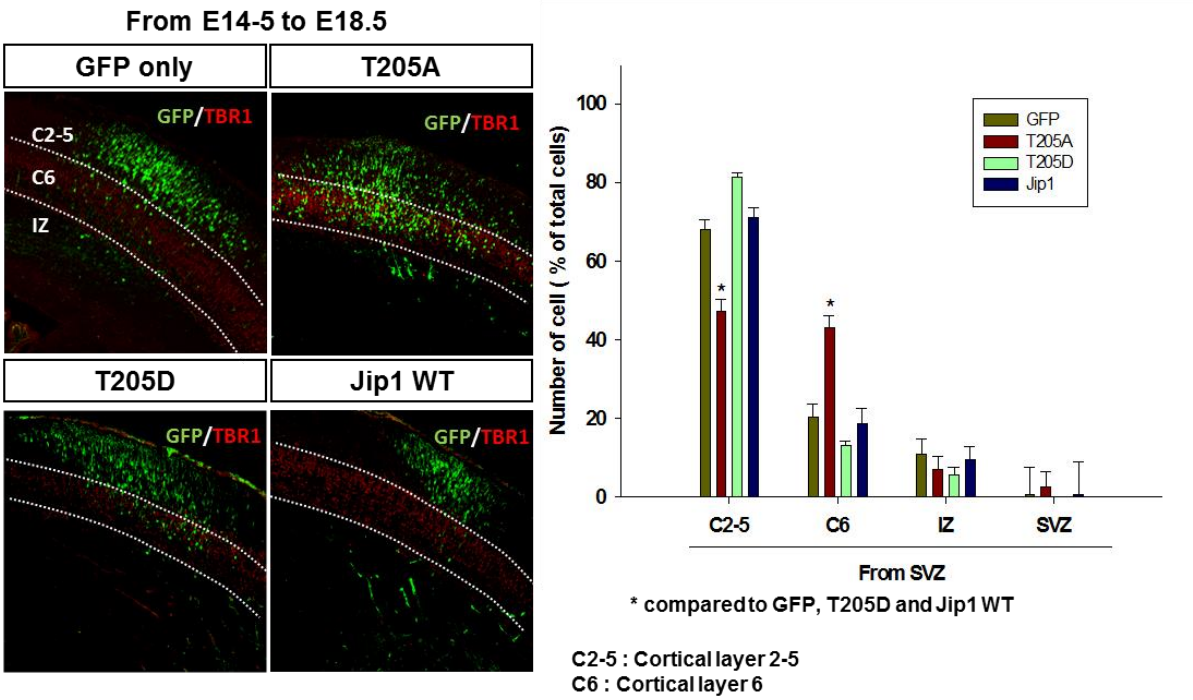

C2-5 : Cortical layer 2-5
C6 : Cortical layer 6
IZ : Intermediate Zone/white matter
SVZ : Subventricular Zone

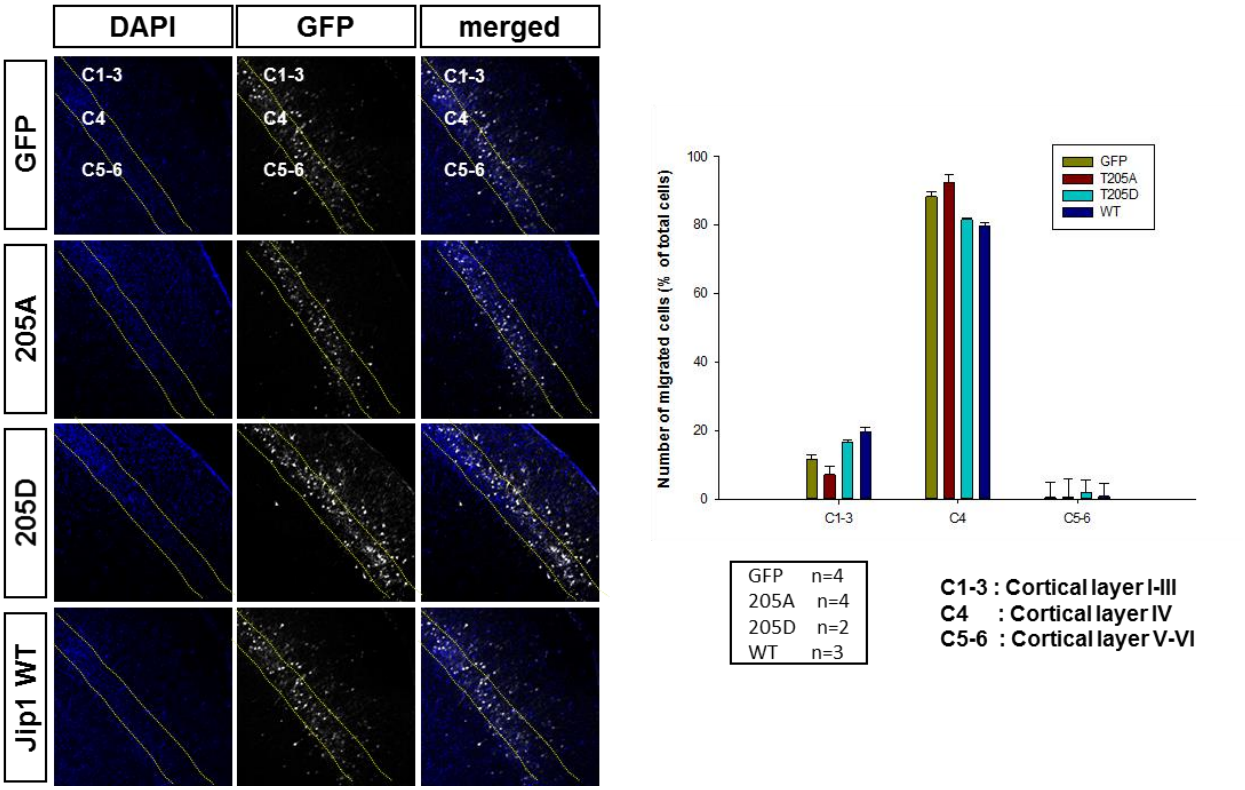

Figure A1-5: Jip1 phosphorylation does not regulate cortical lamination and final neuron location. The lateral cortex of wild type mouse embryos was electroporated at E14.5 with an empty p-Cig2 plasmid (GFP only), pCig2-Jip1 (Jip1 WT), pCig2-Jip1-T205A mutant (T205A) or pCig2-Jip1-T205D mutant (T205D). Brains were collected 7 days after electroporation. The percentage of GFP+ cells in upper cortical layers (C1-3), layer IV (C4) and lower cortical layers (C5-6) were quantified. No difference in the location of GFP+ cells electroporated with different Jip1 constructs was detected. This suggests that the defects in radial migration shown at earlier time points represent delays in migration which are corrected with time.

Pocket proteins p107 and p130 regulate neural differentiation through the DREAM complex.

Devon S Svoboda, Joelle Azzi, Mireille Khacho, Ruthann Duivesteyn, David S Park and Ruth S Slack.

In addition to the work presented in this dissertation, I have led the in vivo portion of a study aimed at determining the role of DREAM in neural stem cell maintenance, neurogenesis and differentiation in the developing and adult mouse brains. DREAM is a repressive transcriptional complex composed of p107/p130, E2F4/5, DP and the MuvB core. Formation of DREAM is regulated by phosphorylation of Lin52, a member of the MuvB core, by DYRK1A. When Lin52 is unphosphorylated, the DREAM complex cannot form. Instead, the MuvB core binds with B-Myb and FoxM1 and promotes the transcription of pro-proliferation genes. Alternatively, when Lin52 is phosphorylated by DYRK1A, it binds to p130 or p107 (but not pRb) and E2F/DP to form the DREAM complex. The DREAM complex then binds to E2F responsive elements in gene promotors of pro-proliferation genes and represses transcription through the recruitment of chromatin remodeling proteins. The DREAM complex is an evolutionarily conserved complex present in all cell types investigated in mammals and invertebrates.

In this project, DSS performed all electroporations and managed the mouse colony. DSS also advised MSc candidate JA and honors student RD. Immunohistochemistry, data collection and data analysis for the electroporation studies was performed by DSS and JA. Other parts of this project not shown here include characterization of the p107/p130 double knock out embryonic brain, performed by RD and DSS, and in vitro experiments, performed by JA, MK and DSS.

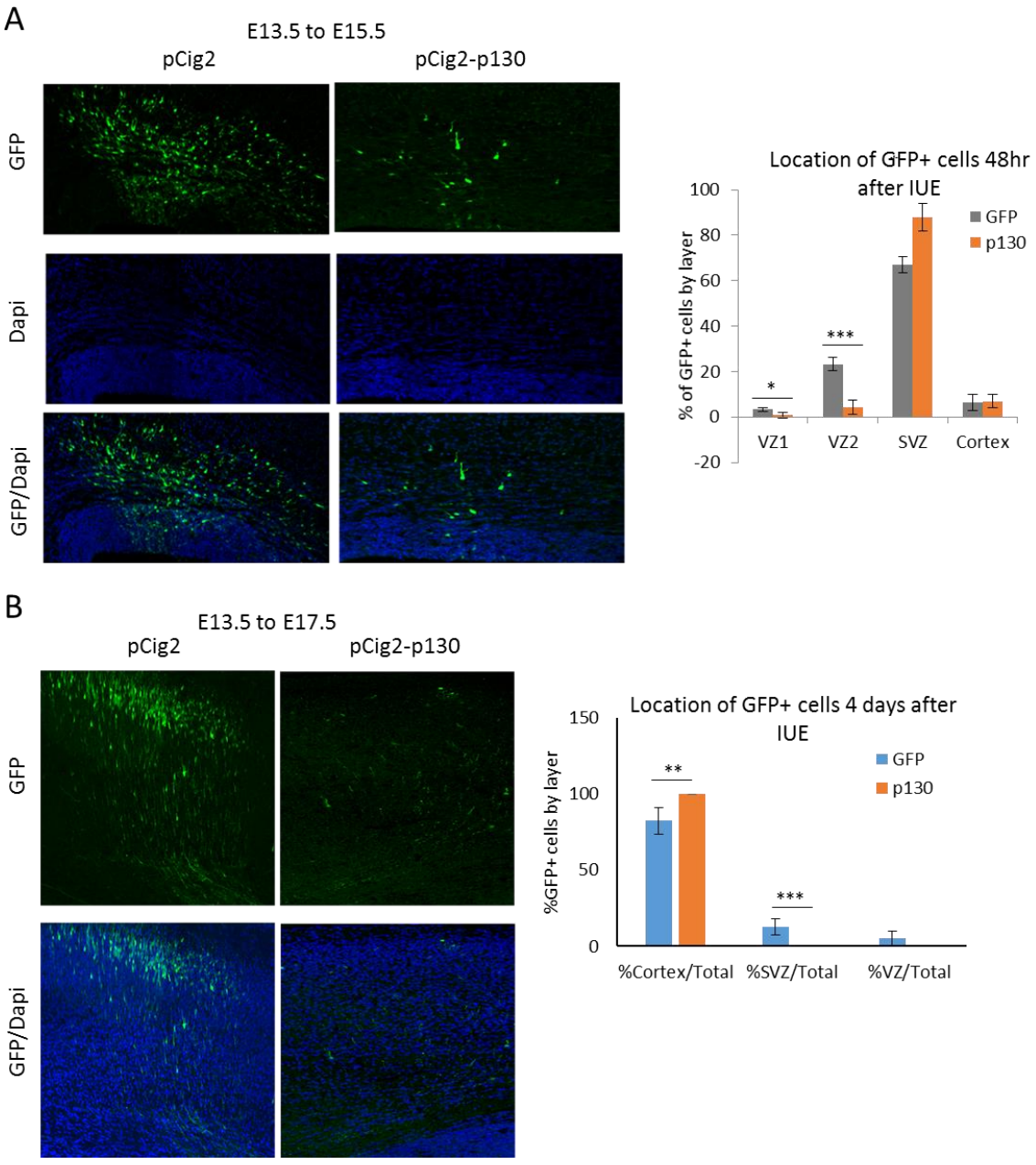
A
E13.5 to E15.5
pCig2
pCig2-p130
GFP
Dapi
GFP/Dapi
Location of GFP+ cells 48hr after IUE
% of GFP+ cells by layer
100
80
60
40
20
0
-20
GFP
p130
*
***
VZ1
VZ2
SVZ
Cortex
B
E13.5 to E17.5
pCig2
pCig2-p130
GFP
GFP/Dapi
Location of GFP+ cells 4 days after IUE
%GFP+ cells by layer
150
100
50
0
GFP
p130
**
***
%Cortex/Total
%SVZ/Total
%VZ/Total

Figure A1-6: Electroporation of p130 promotes neural migration or differentiation. The lateral cortex of wild type mouse embryos was electroporated at E13.5 with an empty p-Cig2 plasmid (GFP only) or pCig2-p130. Brains were collected at E15.5 **(A)** or E17.5 **(B)**. Sections were stained for GFP+ (green) and Dapi (blue) to distinguish the ventricular zone (VZ) subventricular zone (SVZ) and cortex based on cell density. For E15.5 brains **(A)** the VZ was subdivided into VZ1 adjacent to the ventricle and VZ2 adjacent to the SVZ according to Sox2 staining (not shown). The percentage of GFP+ cells in each layer was quantified. At both time points, expression of p130 was found to promote the progression of neuroblasts towards the cortical plate. It is not yet known whether this is due to promoting neurogenesis and neural differentiation or increasing the rate of neural migration. * = $p < 0.05$; ** = $p < 0.01$; *** = $p < 0.001$

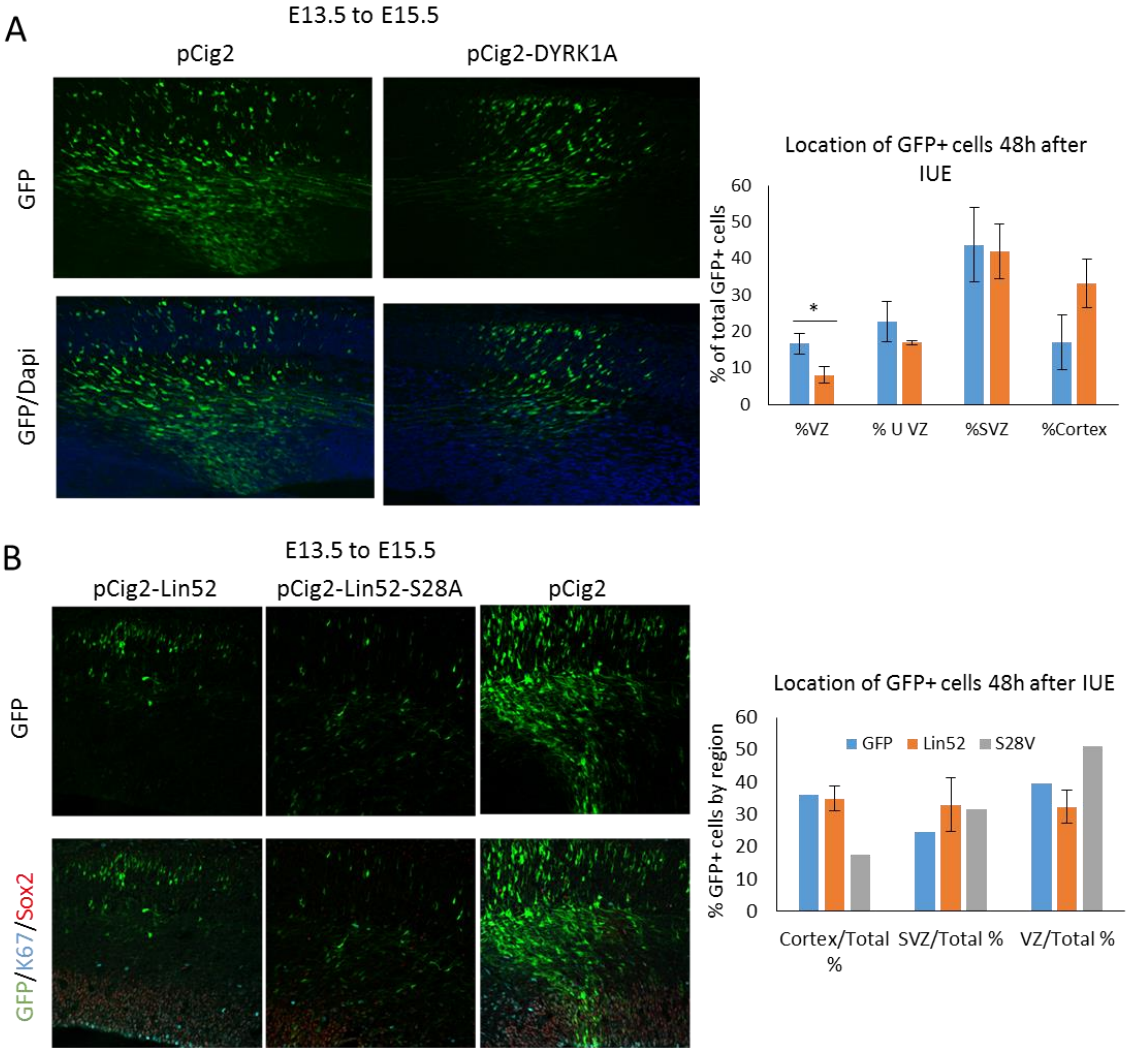
A
E13.5 to E15.5
pCig2
pCig2-DYRK1A
GFP
GFP/Dapi
Location of GFP+ cells 48h after IUE
% of total GFP+ cells
60
50
40
30
20
10
0
*
%VZ
% U VZ
%SVZ
%Cortex
B
E13.5 to E15.5
pCig2-Lin52
pCig2-Lin52-S28A
pCig2
GFP
GFP/K67/Sox2
Location of GFP+ cells 48h after IUE
% GFP+ cells by region
GFP
Lin52
S28V
60
50
40
30
20
10
0
Cortex/Total %
SVZ/Total %
VZ/Total %

Figure A1-7: Electroporation of DREAM pathway proteins regulates neural migration or differentiation. A) The lateral cortex of wild type mouse embryos was electroporated at E13.5 with an empty p-Cig2 plasmid (GFP only) or pCig2-DYRK1A. Brains were collected at E15.5 and stained for GFP+ (green) and Dapi (blue) to distinguish the ventricular zone (VZ) subventricular zone (SVZ) and cortex based on cell density. The VZ was subdivided into VZ adjacent to the ventricle and upper VZ (UVZ) adjacent to the SVZ according to Sox2 staining (not shown). Quantification of the percentage of GFP+ cells in each layer shows that expression of DYRK1A, which promotes phosphorylation of Lin52 and formation of the DREAM complex, promotes progression of neuroblasts out of the VZ. **B)** The lateral cortex of wild type mouse embryos was electroporated at E13.5 with an empty p-Cig2 plasmid (GFP only), pCig2-Lin52 or pCig2-Lin52-S28A, a phospho-incompetent mutant. Brains were collected at E15.5 and stained for GFP+ (green), Ki67 (blue) and Sox2 (red) and Dapi (not shown) to distinguish the ventricular zone (VZ) subventricular zone (SVZ) and cortex. Although this is preliminary data with only one animal per plasmid so far, electroporation the dominant negative form of Lin52 seems to prevent the progression of neuroblasts into the cortical plate. It is not yet known whether this is due to promoting neurogenesis and neural differentiation or increasing the rate of neural migration. * = $p < 0.05$

Appendix B

Curriculum Vitae

DEVON S SVOBODA

Snapshot

- PhD Candidate at the University of Ottawa
- 5 peer reviewed publications
- 10 Academic Honors

Education

2009 – present **Doctorate of Philosophy**
University of Ottawa, Department of Neuroscience
Thesis Supervisor: Dr. Ruth S Slack
Title of Project: The Unique Role of Pocket Proteins in Cortical Migration and Axon Guidance.

2007 – 9 **Master's of Science**
Queen's University, Department: Anatomy and Cell Biology GPA: 88.8
Thesis Supervisor: Dr. Michael D Kawaja
Title of Project: Proteomic Analysis of the Superior Mesenteric Ganglion and Liver of Spontaneously Hypertensive Rats

2003 – 7 **Bachelor's of Science**
Cornell University, Department of Animal Science
GPA: 4.05 Cuma Sum Lauda

2002 – 3 **The Clarkson School**
Clarkson University, Department of Biology
GPA: 4.0 President's List
Program Description - bridging program at Clarkson University combining senior year of high school and freshman year of college

Research Experience

2009-Present **PhD Candidate**
Supervisor: Dr. RS Slack
Research Project: I am analyzing the role of pocket proteins pRb and p107 in brain development and neural maturation. This project is aimed at improving our understanding of how these proteins are required cortical migration and axon tract development.
Techniques used: In utero electroporation, cortical explants, cortical slice cultures, mouse colony maintenance, chromatin immunoprecipitation, in situ hysbridization, immunohistochemistry, Western blotting.

2007-9 **Master's Student**
Supervisor: Dr. MD Kawaja

Research Project: I analyzed changes in global protein expression in the autonomic nervous system and liver in a genetic model of primary hypertension. This project improved our understanding of how these tissues are affected by the stresses of hypertension.
Techniques Used: Two-dimension gel electrophoresis, MALDI-TOF Mass Spectrometry, Quantitative Protein Expression Analysis, Western blotting, Immunohistochemistry.

2004-7 **Research Scholar**
Supervisor: Dr. John Hermanson and Dr. Norman Ducharme
Research Project: I analyzed the muscle fiber composition and axon myelination of the primary tissues affected in the equine neuromuscular pathology, Idiopathic Laryngeal Hemiplegia. This analysis was part of a larger project to develop pacemaker implants to regulate laryngeal function in racehorses.
Techniques Used: Myosin ATPase Stain, Immunohistochemistry, Anatomical data analysis.

2006 **Research Assistant**
Supervisor: Dr. Lisa Fortier
Animal Experience: I performed health checks, surgical prep and post-operative care for horses used in research experiment. I also was responsible for training and socializing horses for use in experiments.

2005 **Research Assistant**
Supervisor: Dr. Maria Viveiros
Techniques Used: In vitro fertilization and in vitro maturation of oocytes, mouse colony maintenance.

Awards

2013-14	**Heart and Stroke Doctoral Award**	$21,000
2013-14	**Ontario Graduate Scholarship**	$10,000
2010-13	**University of Ottawa International Student Tuition Award**	$15,000/year
2007-9	**Queen's University International Student Tuition Award**	$15,000/year
2003-7	**Cornell Presidential Research Scholarship**	$10,000

Award given to top 3% of incoming undergraduate class for research excellence potential. Students begin research in a lab of their choosing starting in second year of university.

2005-7 **Morrison Award**

Given by Cornell University Animal Science department for academic excellence.

2005-7	**Animal Science Excellence Award** Given by Cornell University Animal Science department for academic excellence.	
2004-7	**Dean's List at Cornell University**	
2006	**Golden Key Honor Society Membership**	
2003	**Augsbury North-Country Scholarship** – DECLINED	$15,000/year
2003	**Carl Michael Award** Given by Clarkson University for writing skills	
2003	**The Clarkson School's Highest Academic Honor**	

Tutoring Experience

2010-2011 Tutored a student for ANP1105 and ANP1107, 4 hours per week for the academic year
2010-2012 Tutored various students in high school science and math. Approximate total of 40 hours.

Leadership and Community Involvement

2009-2012 **Vice President of Academics on the CMM/NSC Student Council**
Responsibilities: On this committee, I organized workshops and seminars to meet the academic needs of the graduate student body. These workshops included:
Statistics for Biologists Seminar Series
Comprehensive Exam Workshop
Scientific Poster Design Workshop
Public Speaking for Scientists
Learn to Use Photoshop for Scientists

Publications

Svoboda DS, Clark A, Park DS, and Slack RS. Induction of Protein Deletion Through *In Utero* Electroporation to Define Deficits in Neuronal Migration in Transgenic Models. *J of Vis Exp.* 2015:(95), e51983, doi:10.3791/51983.

Svoboda DS, Paquin A, Park DS, Slack RS. Pocket proteins pRb and p107 are required for cortical lamination independent of apoptosis. *Dev. Biol.* 2013: 384(1):101-13.

Svoboda DS, Kawaja MD. Changes in Hepatic Protein Expression in Spontaneously Hypertensive Rats Suggest Early Stages of Non-Alcoholic Fatty Liver Disease. *J Prot* 2012;75(6):1752-63.

Ghanem N, Andrusiak MG, Svoboda D, Al Lafi SM, Julian LM, McClellan KA, De Repentigny Y, Kothary R, Ekker M, Blais A, Park DS, Slack RS. The Rb/E2F pathway modulates neurogenesis through direct regulation of the Dlx1/Dlx2 bigene cluster. J Neurosci. 2012;32(24):8219-30.

Julian LM, Vandenbosch R, **Pakenham** CA, Andrusiak MA, Nguyen AP, McClellan KA, **Svoboda DS**, Park DS, Leone G, Lagace D, Blais A, and Slack RS. E2f3 Isoforms Differentially Regulate the Pluripotency Factor Sox2 to Balance Neural Precursor Maintenance and Neurogenesis. *Cell Stem Cell*. 2013:12(4):440-52.

Methot L, Hermann R, Tang Y, Lo R, Al-Jehani H, Jhas S, **Svoboda D**, Slack RS, Barker PA and Stifani S. Interaction and Antagonistic Roles of NF-kappaB and Hes6 in the Regulation of Cortical Neurogenesis. Mol Cell Biol. 2013;33(14):2797-808.

Abstracts and Presentations

Svoboda DS, Kennedy TE, Park DS and RS Slack. Role of the pRb family proteins in axon growth and guidance. *Canadian Student Health Research Forum* in Winnipeg, Canada, 2015. (forthcoming)

Svoboda DS, Park DS, Kennedy TE and RS Slack. Cell cycle regulators and Netrin in axon growth and guidance. *Wiring the Brain* in Cold Spring Harbor, USA, 2015.

Svoboda DS, Park DS and RS Slack. Role of the pRb family proteins in interhemispheric axon tract formation. *Third International Rb Meeting* in Monterey, USA, 2013.

Svoboda DS, Park DS and RS Slack. Role of the pRb family proteins in interhemispheric axon tract formation. *BSDB: Axon Guidance and Regeneration* in Aberdeen Scotland, 2013.

Svoboda D, Julian LM, Park DS and RS Slack. Role of the pRb family proteins in neuronal differentiation and axon tract formation. *International Rb Meeting* in Toronto, Canada, 2011.

Svoboda D, Julian LM, Sage J, Park DS and RS Slack. The Role of Rb Family Proteins in Neuronal Differentiation and Synaptogenesis. *University of Ottawa Brain Health Research Day* in Ottawa, Canda, 2011.

Svoboda D, Julian LM, Sage J, Park DS and RS Slack. The Role of Rb Family Proteins in Neuronal Differentiation and Synaptogenesis. *Wiring the Brain International Conference* in Powerscourt, Ireland, 2011.

Svoboda D, Vendenbosch R, Ghanem N, Park DS and RS Slack. A requirement for pRb during olfactory bulb and hippocampal neurogenesis. *Meeting for the International Society of Developmental Neuroscience* in Estoril, Portugal, 2010.

Svoboda D, McDonald T and MD Kawaja. Proteomic Analysis of the Superior Mesenteric Ganglion in Spontaneously Hypertensive Rats. *Queen's Cardiovascular Conference* in Kingston, Canada, 2009.

Appendix C

Permission to reprint published manuscripts.

ELSEVIER LICENSE
TERMS AND CONDITIONS

May 13, 2015

This is a License Agreement between University of Ottawa ("You") and Elsevier ("Elsevier") provided by Copyright Clearance Center ("CCC"). The license consists of your order details, the terms and conditions provided by Elsevier, and the payment terms and conditions.

All payments must be made in full to CCC. For payment instructions, please see information listed at the bottom of this form.

Supplier	Elsevier Limited The Boulevard,Langford Lane Kidlington,Oxford,OX5 1GB,UK
Registered Company Number	1982084
Customer name	University of Ottawa
Customer address	451 Smyth Rd Ottawa, ON K1H8M5
License number	3627201390279
License date	May 13, 2015
Licensed content publisher	Elsevier
Licensed content publication	Developmental Biology
Licensed content title	Pocket proteins pRb and p107 are required for cortical lamination independent of apoptosis
Licensed content author	D.S. Svoboda,A. Paquin,D.S. Park,R.S. Slack
Licensed content date	1 December 2013
Licensed content volume number	384
Licensed content issue number	1
Number of pages	13
Start Page	101
End Page	113
Type of Use	reuse in a thesis/dissertation
Portion	full article
Format	both print and electronic
Are you the author of this Elsevier article?	Yes
Will you be translating?	No
Title of your thesis/dissertation	The Role of Pocket Proteins pRb and p107 in Neuron Maturation and Brain Development.

Expected completion date	May 2015
Estimated size (number of pages)	300
Elsevier VAT number	GB 494 6272 12
Permissions price	0.00 CAD
VAT/Local Sales Tax	0.00 CAD / 0.00 GBP
Total	0.00 CAD
Terms and Conditions	

INTRODUCTION

1. The publisher for this copyrighted material is Elsevier. By clicking "accept" in connection with completing this licensing transaction, you agree that the following terms and conditions apply to this transaction (along with the Billing and Payment terms and conditions established by Copyright Clearance Center, Inc. ("CCC"), at the time that you opened your Rightslink account and that are available at any time at http://myaccount.copyright.com).

GENERAL TERMS

2. Elsevier hereby grants you permission to reproduce the aforementioned material subject to the terms and conditions indicated.

3. Acknowledgement: If any part of the material to be used (for example, figures) has appeared in our publication with credit or acknowledgement to another source, permission must also be sought from that source. If such permission is not obtained then that material may not be included in your publication/copies. Suitable acknowledgement to the source must be made, either as a footnote or in a reference list at the end of your publication, as follows:

"Reprinted from Publication title, Vol /edition number, Author(s), Title of article / title of chapter, Pages No., Copyright (Year), with permission from Elsevier [OR APPLICABLE SOCIETY COPYRIGHT OWNER]." Also Lancet special credit - "Reprinted from The Lancet, Vol. number, Author(s), Title of article, Pages No., Copyright (Year), with permission from Elsevier."

4. Reproduction of this material is confined to the purpose and/or media for which permission is hereby given.

5. Altering/Modifying Material: Not Permitted. However figures and illustrations may be altered/adapted minimally to serve your work. Any other abbreviations, additions, deletions and/or any other alterations shall be made only with prior written authorization of Elsevier Ltd. (Please contact Elsevier at permissions@elsevier.com)

6. If the permission fee for the requested use of our material is waived in this instance, please be advised that your future requests for Elsevier materials may attract a fee.

7. Reservation of Rights: Publisher reserves all rights not specifically granted in the

combination of (i) the license details provided by you and accepted in the course of this licensing transaction, (ii) these terms and conditions and (iii) CCC's Billing and Payment terms and conditions.

8. License Contingent Upon Payment: While you may exercise the rights licensed immediately upon issuance of the license at the end of the licensing process for the transaction, provided that you have disclosed complete and accurate details of your proposed use, no license is finally effective unless and until full payment is received from you (either by publisher or by CCC) as provided in CCC's Billing and Payment terms and conditions. If full payment is not received on a timely basis, then any license preliminarily granted shall be deemed automatically revoked and shall be void as if never granted. Further, in the event that you breach any of these terms and conditions or any of CCC's Billing and Payment terms and conditions, the license is automatically revoked and shall be void as if never granted. Use of materials as described in a revoked license, as well as any use of the materials beyond the scope of an unrevoked license, may constitute copyright infringement and publisher reserves the right to take any and all action to protect its copyright in the materials.

9. Warranties: Publisher makes no representations or warranties with respect to the licensed material.

10. Indemnity: You hereby indemnify and agree to hold harmless publisher and CCC, and their respective officers, directors, employees and agents, from and against any and all claims arising out of your use of the licensed material other than as specifically authorized pursuant to this license.

11. No Transfer of License: This license is personal to you and may not be sublicensed, assigned, or transferred by you to any other person without publisher's written permission.

12. No Amendment Except in Writing: This license may not be amended except in a writing signed by both parties (or, in the case of publisher, by CCC on publisher's behalf).

13. Objection to Contrary Terms: Publisher hereby objects to any terms contained in any purchase order, acknowledgment, check endorsement or other writing prepared by you, which terms are inconsistent with these terms and conditions or CCC's Billing and Payment terms and conditions. These terms and conditions, together with CCC's Billing and Payment terms and conditions (which are incorporated herein), comprise the entire agreement between you and publisher (and CCC) concerning this licensing transaction. In the event of any conflict between your obligations established by these terms and conditions and those established by CCC's Billing and Payment terms and conditions, these terms and conditions shall control.

14. Revocation: Elsevier or Copyright Clearance Center may deny the permissions described in this License at their sole discretion, for any reason or no reason, with a full refund payable to you. Notice of such denial will be made using the contact information provided by you. Failure to receive such notice will not alter or invalidate the denial. In no event will Elsevier or Copyright Clearance Center be responsible or liable for any costs, expenses or damage incurred by you as a result of a denial of your permission request, other than a refund of the

amount(s) paid by you to Elsevier and/or Copyright Clearance Center for denied permissions.

LIMITED LICENSE

The following terms and conditions apply only to specific license types:

15. **Translation**: This permission is granted for non-exclusive world **English** rights only unless your license was granted for translation rights. If you licensed translation rights you may only translate this content into the languages you requested. A professional translator must perform all translations and reproduce the content word for word preserving the integrity of the article. If this license is to re-use 1 or 2 figures then permission is granted for non-exclusive world rights in all languages.

16. **Posting licensed content on any Website**: The following terms and conditions apply as follows: Licensing material from an Elsevier journal: All content posted to the web site must maintain the copyright information line on the bottom of each image; A hyper-text must be included to the Homepage of the journal from which you are licensing at http://www.sciencedirect.com/science/journal/xxxxx or the Elsevier homepage for books at http://www.elsevier.com; Central Storage: This license does not include permission for a scanned version of the material to be stored in a central repository such as that provided by Heron/XanEdu.

Licensing material from an Elsevier book: A hyper-text link must be included to the Elsevier homepage at http://www.elsevier.com . All content posted to the web site must maintain the copyright information line on the bottom of each image.

Posting licensed content on Electronic reserve: In addition to the above the following clauses are applicable: The web site must be password-protected and made available only to bona fide students registered on a relevant course. This permission is granted for 1 year only. You may obtain a new license for future website posting.

17. **For journal authors:** the following clauses are applicable in addition to the above:

Preprints:

A preprint is an author's own write-up of research results and analysis, it has not been peer-reviewed, nor has it had any other value added to it by a publisher (such as formatting, copyright, technical enhancement etc.).

Authors can share their preprints anywhere at any time. Preprints should not be added to or enhanced in any way in order to appear more like, or to substitute for, the final versions of articles however authors can update their preprints on arXiv or RePEc with their Accepted Author Manuscript (see below).

If accepted for publication, we encourage authors to link from the preprint to their formal publication via its DOI. Millions of researchers have access to the formal publications on ScienceDirect, and so links will help users to find, access, cite and use the best available

version. Please note that Cell Press, The Lancet and some society-owned have different preprint policies. Information on these policies is available on the journal homepage.

Accepted Author Manuscripts: An accepted author manuscript is the manuscript of an article that has been accepted for publication and which typically includes author-incorporated changes suggested during submission, peer review and editor-author communications.

Authors can share their accepted author manuscript:

- immediately
    - via their non-commercial person homepage or blog
    - by updating a preprint in arXiv or RePEc with the accepted manuscript
    - via their research institute or institutional repository for internal institutional uses or as part of an invitation-only research collaboration work-group
    - directly by providing copies to their students or to research collaborators for their personal use
    - for private scholarly sharing as part of an invitation-only work group on commercial sites with which Elsevier has an agreement
- after the embargo period
    - via non-commercial hosting platforms such as their institutional repository
    - via commercial sites with which Elsevier has an agreement

In all cases accepted manuscripts should:

- link to the formal publication via its DOI
- bear a CC-BY-NC-ND license - this is easy to do
- if aggregated with other manuscripts, for example in a repository or other site, be shared in alignment with our hosting policy not be added to or enhanced in any way to appear more like, or to substitute for, the published journal article.

Published journal article (JPA): A published journal article (PJA) is the definitive final record of published research that appears or will appear in the journal and embodies all value-adding publishing activities including peer review co-ordination, copy-editing, formatting, (if relevant) pagination and online enrichment.

Policies for sharing publishing journal articles differ for subscription and gold open access articles:

Subscription Articles: If you are an author, please share a link to your article rather than the

full-text. Millions of researchers have access to the formal publications on ScienceDirect, and so links will help your users to find, access, cite, and use the best available version.

Theses and dissertations which contain embedded PJAs as part of the formal submission can be posted publicly by the awarding institution with DOI links back to the formal publications on ScienceDirect.

If you are affiliated with a library that subscribes to ScienceDirect you have additional private sharing rights for others' research accessed under that agreement. This includes use for classroom teaching and internal training at the institution (including use in course packs and courseware programs), and inclusion of the article for grant funding purposes.

Gold Open Access Articles: May be shared according to the author-selected end-user license and should contain a CrossMark logo, the end user license, and a DOI link to the formal publication on ScienceDirect.

Please refer to Elsevier's posting policy for further information.

18. **For book authors** the following clauses are applicable in addition to the above: Authors are permitted to place a brief summary of their work online only. You are not allowed to download and post the published electronic version of your chapter, nor may you scan the printed edition to create an electronic version. **Posting to a repository:** Authors are permitted to post a summary of their chapter only in their institution's repository.

19. **Thesis/Dissertation**: If your license is for use in a thesis/dissertation your thesis may be submitted to your institution in either print or electronic form. Should your thesis be published commercially, please reapply for permission. These requirements include permission for the Library and Archives of Canada to supply single copies, on demand, of the complete thesis and include permission for Proquest/UMI to supply single copies, on demand, of the complete thesis. Should your thesis be published commercially, please reapply for permission. Theses and dissertations which contain embedded PJAs as part of the formal submission can be posted publicly by the awarding institution with DOI links back to the formal publications on ScienceDirect.

Elsevier Open Access Terms and Conditions

You can publish open access with Elsevier in hundreds of open access journals or in nearly 2000 established subscription journals that support open access publishing. Permitted third party re-use of these open access articles is defined by the author's choice of Creative Commons user license. See our open access license policy for more information.

Terms & Conditions applicable to all Open Access articles published with Elsevier:

Any reuse of the article must not represent the author as endorsing the adaptation of the article nor should the article be modified in such a way as to damage the author's honour or reputation. If any changes have been made, such changes must be clearly indicated.

The author(s) must be appropriately credited and we ask that you include the end user license and a DOI link to the formal publication on ScienceDirect.

If any part of the material to be used (for example, figures) has appeared in our publication with credit or acknowledgement to another source it is the responsibility of the user to ensure their reuse complies with the terms and conditions determined by the rights holder.

Additional Terms & Conditions applicable to each Creative Commons user license:

CC BY: The CC-BY license allows users to copy, to create extracts, abstracts and new works from the Article, to alter and revise the Article and to make commercial use of the Article (including reuse and/or resale of the Article by commercial entities), provided the user gives appropriate credit (with a link to the formal publication through the relevant DOI), provides a link to the license, indicates if changes were made and the licensor is not represented as endorsing the use made of the work. The full details of the license are available at http://creativecommons.org/licenses/by/4.0.

CC BY NC SA: The CC BY-NC-SA license allows users to copy, to create extracts, abstracts and new works from the Article, to alter and revise the Article, provided this is not done for commercial purposes, and that the user gives appropriate credit (with a link to the formal publication through the relevant DOI), provides a link to the license, indicates if changes were made and the licensor is not represented as endorsing the use made of the work. Further, any new works must be made available on the same conditions. The full details of the license are available at http://creativecommons.org/licenses/by-nc-sa/4.0.

CC BY NC ND: The CC BY-NC-ND license allows users to copy and distribute the Article, provided this is not done for commercial purposes and further does not permit distribution of the Article if it is changed or edited in any way, and provided the user gives appropriate credit (with a link to the formal publication through the relevant DOI), provides a link to the license, and that the licensor is not represented as endorsing the use made of the work. The full details of the license are available at http://creativecommons.org/licenses/by-nc-nd/4.0. Any commercial reuse of Open Access articles published with a CC BY NC SA or CC BY NC ND license requires permission from Elsevier and will be subject to a fee.

Commercial reuse includes:

- Associating advertising with the full text of the Article
- Charging fees for document delivery or access
- Article aggregation
- Systematic distribution via e-mail lists or share buttons

Posting or linking by commercial companies for use by customers of those companies.

20. **Other Conditions**:

v1.7

Questions? customercare@copyright.com or +1-855-239-3415 (toll free in the US) or +1-978-646-2777.

Gratis licenses (referencing $0 in the Total field) are free. Please retain this printable license for your reference. No payment is required.

Re: Author Dissertation Request

1 message

Michelle Kinahan <michelle.kinahan@jove.com> Wed, May 13, 2015 at 3:17 PM

Dear Devon,

You have our permission to print part or all of your JoVE article "Svoboda, D. S., Clark, A., Park, D. S., Slack, R. S. Induction of Protein Deletion Through In UteroElectroporation to Define Deficits in Neuronal Migration in Transgenic Models. *J. Vis. Exp.* (95), e51983, doi:10.3791/51983 (2015)." in your dissertation as requested.

Please be sure to cite the JoVE article as applicable. Please consider this email as approval.

Best,

Michelle

Michelle E. Kinahan, Ph.D.
Deputy Director of Editorial - Review
JoVE
1 Alewife Center, Suite 200, Cambridge, MA 02140
tel: 617-674-1888

On Wed, May 13, 2015 at 3:14 PM, Chris Macdonald <chris.macdonald@jove.com> wrote:

> Hello Michelle,
>
> Could you please help this author out? Thanks.
>
> **Devon Svoboda**
> May 13, 15:01
> Message: I need permission to reprint this article in full for my PhD thesis.
> Name: Devon Svoboda
> Email:
> Page: http://www.jove.com/video/51983/induction-protein-deletion-through-utero-electroporation-to-define
>
> Chris Macdonald
> Deputy Director of Information Technology
> JoVE
> 1 Alewife Center, Suite 200, Cambridge, MA 02140
> tel: 617-945-9051

Appendix D

First author publication reprints

Developmental Biology 384 (2013) 101–113

Contents lists available at ScienceDirect

Developmental Biology

journal homepage: www.elsevier.com/locate/developmentalbiology

Pocket proteins pRb and p107 are required for cortical lamination independent of apoptosis

D.S. Svoboda [a], A. Paquin [b,c,1], D.S. Park [a], R.S. Slack [a,*]

[a] Department of Cellular and Molecular Medicine, Faculty of Medicine, University of Ottawa, 451 Smyth Road, Ottawa, Ont., Canada K1H 8M5
[b] Developmental & Stem Cell Biology, Hospital for Sick Children, Toronto, Ont., Canada M5G 1L7
[c] Institute of Medical Science, University of Toronto, Toronto, Ont., Canada M5G 1L7

ARTICLE INFO

Article history:
Received 9 July 2013
Received in revised form
6 September 2013
Accepted 9 September 2013
Available online 19 September 2013

Keywords:
Retinoblastoma
Cell cycle
Radial migration
Pocket proteins

ABSTRACT

Pocket proteins (pRb, p107 and p130) are well studied in their role of regulating cell cycle progression. Increasing evidence suggests that these proteins also control early differentiation and even later stages of cell maturation, such as migration. However, pocket proteins also regulate apoptosis, and many of the developmental defects in knock out models have been attributed to increased cell death. Here, we eliminate ectopic apoptosis in the developing brain through the deletion of Bax, and show that pocket proteins are required for radial migration independent of their role in cell death regulation. Following loss of pRb and p107, a population of cortical neurons fails to pass through the intermediate zone into the cortical plate. Importantly, these neurons are born at the appropriate time and this migration defect cannot be rescued by eliminating ectopic cell death. In addition, we show that pRb and p107 regulate radial migration through a cell autonomous mechanism since pRb/p107 deficient neurons fail to migrate to the correct cortical layer within a wild type brain. These results define a novel role of pocket proteins in regulating cortical lamination through a cell autonomous mechanism independent of their role in apoptosis.

Introduction

Activating neurogenesis is a promising strategy for rehabilitating damage following traumatic injury or neurodegenerative disease. However, to use this therapeutic tool effectively it is crucial to understand the mechanisms which regulate neuronal birth and maturation. The retinoblastoma protein (pRb), together with its two family members p107 and p130, controls cell cycle progression and terminal mitosis (Ferguson and Slack, 2001; Giacinti and Giordano, 2006). However, it remains unclear whether the pocket protein family plays additional roles in later stages of neuron maturation, such as terminal differentiation and migration.

During normal brain development, proliferating neural precursor cells in the ventricular and subventricular zones exit the cell cycle and migrate dorsally through the intermediate zone, into the cortical plate (Nowakowski et al., 2002). The first neurons born are the Cajal Retzuis cells of layer I (Garcia-Moreno et al., 2007), which guide later born migrating neurons through secretion of Reelin (Honda et al, 2011). These neurons migrate radially to the top of the cortical plate and reside in an "inside-out" pattern with the youngest neurons in the uppermost layers.

It is now well established that pocket proteins regulate both proliferation and cell death. In addition, increasing evidence suggests that cell cycle proteins also influence later stages of brain development (Nguyen et al., 2006; Tury et al., 2011), such as cortical plate formation (Ferguson et al., 2005; McClellan et al., 2007). Understanding developmental phenotypes in knockout models is complicated by increased apoptosis following pRb deletion through the E2F1/p53 pathway; thus it is often unknown whether a defect in cell maturation is due to a novel function of pRb or is an indirect result of this ectopic cell death. For example, Ciavarra and colleagues found a defect in pRb-null cardiomyocyte maturation, yet were able to completely rescue the phenotype by preventing apoptosis through expression of the anti-apoptotic protein Bcl2 (Ciavarra and Zacksenhaus, 2010). In contrast, Chen et al. found that rescuing cell death and through E2F1 deletion does not rescue maturation defects in amacrine cells in the developing retina (Chen et al., 2007). Cell death has been shown to cause severe developmental defects in pRb null animals in the retina (Chen et al., 2004), cerebellum, (Feddersen et al., 1995; Padmanabhan et al., 1999; Marino et al., 2003), and the Organ of Corti (Sage et al., 2006). Similarly, in cases where morphological or functional defects were reported in pRb-null cells (Lee et al., 1994; Sage et al., 2006), it was often not possible to determine whether these differentiation defects were a secondary result of the increased cell death or represented a separate Rb function. Finally, we have previously shown that pRb deletion led to a defect in

* Corresponding author. Fax: +1 613 562 5434.
E-mail addresses: rslack@uottawa.ca, jmaclaur@uottawa.ca (R.S. Slack).
[1] Current address: VisualSonics Inc, Toronto, Ont., Canada M4N 3N1.

0012-1606/$ - see front matter © 2013 Elsevier Inc. All rights reserved.
http://dx.doi.org/10.1016/j.ydbio.2013.09.015

cortical lamination, where the delineation between the cortical plate and the intermediate zone was obscured; we were unable to determine whether this phenotype resulted from the established role of pocket proteins in cell death (Ferguson et al., 2005; McClellan et al., 2007). As examples of cell death dependent and independent developmental defects have been reported following loss of pocket proteins, the role of pRb and p107 in neuron maturation independent of cell death therefore remains an unanswered question in the field.

In the present study, we asked whether radial migration in the developing cortex is modulated by pocket proteins, independently from their role in cell death regulation. The pRb/p107 double mutants were used to avoid compensatory effects of p107 in pRb deficient tissues (Marino et al., 2003; Chen et al., 2004; Berman et al., 2009). The contribution of apoptosis in the cortical migration phenotype observed in pRb/p107 double mutants, was evaluated by crossing these mice with animals carrying a null allele for Bax, a key apoptotic protein (Gavathiotis et al., 2012). Here we show a defect in the migration of cortical neurons lacking pocket proteins pRb and p107, which could not be attributed to failed cell cycle exit or unchecked apoptosis. Notably, deletion of Bax did not rescue the defect in radial migration, despite the fact that apoptosis was returned to wild type levels. Furthermore, we show that pocket proteins regulate radial migration through cell autonomous mechanisms since *in utero* electroporation of Cre leads to migration defects in p107/pRb deficient neurons in the context of an otherwise healthy brain. Overall, we show that pRb and p107 play an essential role in the regulation of radial migration, independent of their role in apoptosis.

Materials and methods

Mice

pRb/p107 DKO mice were generated by crossing floxed Rb-F19 (Vooijs et al., 1998; Marino et al., 2000) with p107 germline knockout mice (LeCouter et al., 1998). DKO mice were then crossed with Emx1-cre mice (Jackson Laboratories) to delete pRb specifically in the dorsal telencephalon. Mice were maintained on a mixed C57/Bl6/FVBN/Sv129 background and genotyped according to standard protocols with previously published primers for Rb (Jacks et al., 1992) and p107 (LeCouter et al., 1998). pRb f/f; p107 −/− females were crossed with pRb f/+; p107 +/−; Emx1-Cre+ males to generate wild type pRb f/+; p107 +/−; Emx1-Cre+ (WT), pRb f/f; p107 +/−; Emx1-Cre+ (RBKO), pRb f/+; p107 −/−; Emx1-Cre+ (p107KO) and double knock out pRb f/f; p107 −/−; Emx1-Cre+ (DKO) littermates. For embryonic time points, the time of plug identification was counted as embryonic day 0.5 (E0.5). Due to pRb autoregulation (Shan et al., 1994), pRb expression in heterozygous mice is similar to that of wild-type controls. DKO-Bax−/− mice were bred by crossing pRb f/f; p107 −/− mice with Bax −/− mice (Jackson Laboratories) to generate pRb f/f; p107 −/−; Bax −/− females. These females were crossed with pRb f/+; p107 +/−; Bax +/−; Emx1-Cre+ males. These mice were also on a mixed C57/Bl6/FVBN/Sv129 background. All experiments were approved by the University of Ottawa's Animal Care ethics committee, adhering to the Guidelines of the Canadian Council on Animal Care.

Tissue fixation and cryoprotection

Pregnant female mice were killed with a lethal injection of sodium pentobarbitol. P0 pups were killed by decapitation. Embryos were dissected and fixed overnight in 4% PFA in PBS, pH 7.4, and cryoprotected using a sucrose gradient of 10%, 15% and 20% in PBS. Brains were frozen, and 14-μm coronal cryosections were collected on Superfrost Plus slides (12–550-15; Fisher Scientific).

BrdU labeling and immunohistochemistry

To mark neurons born at E13.5, a single intraperitoneal injection of BrdU (dissolved in 0.007 N/NaOH in 0.9% NaCl; 50 mg/kg body mass) was given to timed pregnant females at E13.5. Injected females were euthanized at E17.5 or pups were collected on the morning after birth (P0).

For all cell counts, images were taken from matching tissue sections, cut at equivalent locations along the rostro-caudal axis of the brain on the first section where a complete anterior commissure was visible crossing the midline. Images were taken from a portion of the cortex in between the dorsomedial and ventrolateral cortex, just as the cortex begins to slope downwards. For total cell counts, slides were treated with the Dako antigen retrieval protocol according to the manufacturer's protocol for 30 min and treated with combinations of the following antibodies: Cux1 (layers II–IV (Nieto et al., 2004); 1/100; Santa Cruz), FoxP1 (layers III/IV (Ferland et al., 2003); 1/750; Abcam), Ki67 (1/100; Cell Marque), Nestin (1/500; Abcam), SatB2 (layers II–IV (Britanova et al., 2008); 1/500; Abcam), Tbr1 (layer V/VI (Hevner et al., 2001); 1/1000; Abcam). Once equivalent sections of the cortex were identified and imaged, a 200 μm wide column of cortical tissue (450 μm for FoxP1 counts) was delineated within the image, extending vertically from the top of the cortical plate down through the ventricular zone. All cells expressing the marker of interest within this column were counted and binned according to their anatomical layer. Cortical layers were identified as follows: layer II was defined as being marked by Cux1 and/or Satb2, but not by FoxP1. Layer III/IV was identified as expressing FoxP1 but not Tbr1. Layers V/VI were defined as expressing Tbr1. For total cell counts, cells were counted as being located either in the upper layers (II–IV) or lower layers (V/VI). For BrdU counts, BrdU detection was performed according to Ferguson et al. (2002), followed by Dako treatment for 15 min. Slides were then treated with combinations of the same antibodies, colabeling with anti-BrdU (1/250; Accurate Chemical and Scientific Corporation). All cells labeled with BrdU+, and with Foxp1 or SatB2 for co-labeling studies, were counted in 150 μm column of the cortex extending vertically from the top of the cortical plate through the ventricular zone, as described above. One-way ANOVA with Bonferroni was performed for all graphs in every figure. Significant differences were assessed at values of $p < 0.05$. Four or five animals were used for each genotype at each age.

For Cajal Retzius cell counts, equivalent rostro-caudal sections were stained with Reelin (1/1000; Abcam) and Calretinin (1/500; Swant), two markers of Cajal Retzius cells. Six images of layer I of the cortex were taken from three different brain sections at 40×, covering a total distance of 1400 μm for each embryo. Only cells positive for both Reelin and Calretinin were counted. Cells from the six images were totaled for each animal, and totals for animals of the same genotype were averaged. Four to six animals were used for each genotype.

TUNEL staining

Apoptotic cells were detected in equivalent rostro-caudal brain sections at E17.5 by TUNEL using the Terminal Transferase Recombinant Kit (Roche Applied Science) together with dUTP-16-Biotin (Roche Applied Science) according to the manufacturer's protocol. In each brain, 6 fields of view were counted at 20× and the total number of TUNEL positive cells was totaled for each animal. Fields of view were located in the same part of the cortex in each animal to ensure consistency. One-way ANOVA with Bonferroni was

performed to compare the mean numbers of TUNEL-positive cells and significant differences were assessed at values of $p < 0.05$.

Western blots

Protein was isolated from the dorsal cortex or ganglionic eminence at E15.5 and western blot analyses performed as previously described (Ferguson et al. 2002) with antibodies directed toward pRb (1/1000; PharMingen), p107 (1/1000; Santa Cruz), Bax (1/1000; Santa Cruz) and β-actin (1/5000; Sigma).

In utero electroporation

Pups of pregnant DKO females were electroporated at E13.5 with a plasmid containing Cre fused to GFP under control of the pCAAG promoter. The fused Cre was used so that GFP would be localized to the nucleus to facilitate image analysis. Plasmids were prepped using the Qiagen Megaprep Kit, diluted to 2 μg/μl in sterile H_2O and mixed with trace amounts of Trypan Blue dye. The plasmid was injected into the lateral ventricle of the brain using an Eppendorf Femtojet Microinjector and electroporated into the dorsolateral cortex using a BTX ECM 830 Square Wave Electroporator. Animals were sacrificed 4 days later at E17.5. For analysis, electroporated sections at equivalent rostro-caudal levels of the brain, relative to the corpus callosum and anterior commissure, were selected. Tissue sections were treated with hot, non-boiling citric acid for 15 min and then stained with antibodies against GFP (1/4000; Abcam), FoxP1 (1/750) and Tbr1 (1/500). Amplification was performed on the GFP signal using the Avidin–Biotin Complex (ABC) kit according to the manufacturer's protocol (Vector Laboratories). Briefly, following binding of secondary IgG, slides were treated with 3% H_2O_2 for 30 min, followed by incubation with ABC complex for 1 h. Finally slides were exposed to the Fluorescein Tyramide Reagent (Perkin Elmer) for 10 min. For counts, all GFP+ neurons which had reached the cortex were counted in two sections per brain. Neurons were binned according to whether they were found in layers II, (defined as being dorsal to FoxP1 staining), layer III/IV (within the Foxp1+ layer) or layer V/VI (within the Tbr1+ layer). GFP+ cells below the cortex were counted but not included in calculations since there was no difference between genotypes.

Results

pRb/p107 double knock out (DKO) embryos exhibit a defect in cortical lamination in vivo

We have previously described minor defects in cortical lamination following loss of pRb in the developing brain (Ferguson et al., 2005; McClellan et al., 2007). However, members of the pocket protein family are known to compensate for each other in knock out models (Chen et al., 2004; Haigis et al., 2006; Berman et al., 2009), so the full role of pocket proteins in radial migration has never been defined. To characterize the role of pRb and p107 in establishment of the cortical plate, we examined the cortical layers of pRb f/f; p107−/−; Emx1-Cre+ double knockout (DKO), pRb f/f; p107+/−; Emx1-Cre+ single knock out (RBKO), pRb f/+;p107−/−; Emx1-Cre+ (p107KO) and pRb+/f; p107+/−; Emx1-Cre+ wild type (WT) brains at E17.5, with the use of cortical layer-specific markers. Deletion of pRb and p107 was confirmed via Western blot at E15.5 (Fig. 1A, B). Cortical layers were defined according to the following method: the delineation between the intermediate zone and the cortical plate was defined as the clear line between high cell density and low density according to Dapi staining (Fig. 1C, D white and red lines), while the delineation between upper and lower layers was defined as the top of Tbr1 staining. Where relevant, layer II was defined as expressing Cux1 but not FoxP1, while layer III/IV was defined as expressing FoxP1 but not Tbr1. In DKO animals, where low levels of Tbr1 staining sometimes extended into the upper cortical layers, or there was a scattering of Tbr1+ cells in the upper layers, the delineation between layers was defined as the top of intense, high cell density Tbr1 staining. In WT, p107KO and RBKO brains, upper layer markers FoxP1 (layers III/IV) and SatB2 (layers II–IV) (data not shown) were confined to their expected locations. In DKO brains, however, a population of cells expressing these upper layer markers was found below the cortical plate in the intermediate zone, with a corresponding 34.4% decrease in the average number of FoxP1+ neurons in the upper layers of the cortical plate (Fig. 1C, F). Note that FoxP1 is normally only expressed in mature neurons which have reached their final location (Ferland et al., 2003). Cortical lamination in p107KO brains was indistinguishable from that in WT brains (data not shown). These observations suggest that pRb and p107 play a necessary role in radial migration and cortical lamination.

As FoxP1 cell numbers were decreased in the DKO cortical plate, we further investigated whether pocket proteins have a specific role in the development of the upper cortical layers. To test this, we asked whether layer II formed normally, using a more comprehensive upper layer marker CuxI (layers II–IV), which in our wild type mice is found above FoxP1 staining. Our results revealed a 50% decrease in the number of Cux1 cells in layers II–IV of DKO brains compared to WT animals (Fig. 1C, E). Cux1 counts could not be done in layers V/VI since recently born neurons migrating through this area express Cux1 (Nieto et al., 2004) and could not be differentiated from misplaced neurons, which failed to migrate correctly.

Interestingly, there was no difference in the number of Tbr1+ neurons in layers V/VI (defined by Dapi staining), although there was an increase in the number of Tbr1+ neurons in the IZ and the Tbr1 layer appeared disorganized in DKO brains (Fig. 1C, G). Consistent with the layer specific changes in neuron number, the thickness of the upper layers is reduced in DKO brains relative to WT brains, with no change in the thickness of the lower layers (Fig. 1D, H). The total thickness of the cortical plate was not different between WT and DKO brains since there was a non-significant increase in the thickness of the subventricular zone in the DKO to compensate for the decrease in thickness of layers II–IV (Fig. 1D, H). As the upper layer neurons are visibly split into two populations, with an associated drop in the number of layer II neurons reaching the cortical plate, the migration phenotype in these later born neurons in DKO brains is much more striking and severe than in the early born neurons in the layer V/VI. For this reason, we chose to focus our studies on the formation of layers II–IV. These findings suggest that the pocket proteins pRb and p107 are required for the proper migration or specification of upper cortical layer neurons.

One potential explanation for this defect in lamination is that radial migration is delayed due to a delay in cell cycle exit. If neurons migrate normally following a delayed cell cycle exit, the defect should be corrected with further development. To determine if these migrating neurons reach their layer II/IV destination at a later age, we examined cortical lamination two days later at P0. At this later time point, misplaced FoxP1+ neurons were still found in the intermediate zone of DKO, but not RBKO or WT brains (Fig. 2A, D). Importantly, the numbers of FoxP1+ cells in the intermediate zone at P0 and at E17.5 were similar, with 256 ± 40 FoxP1+ cells in DKO brains at E17.5, and 293 ± 43 FoxP1+ cells in this same region at P0, indicating that there is not even a small rescue of this phenotype. Furthermore, there was still a 33% decrease in the number of FoxP1 neurons (Fig. 2D) and a 41%

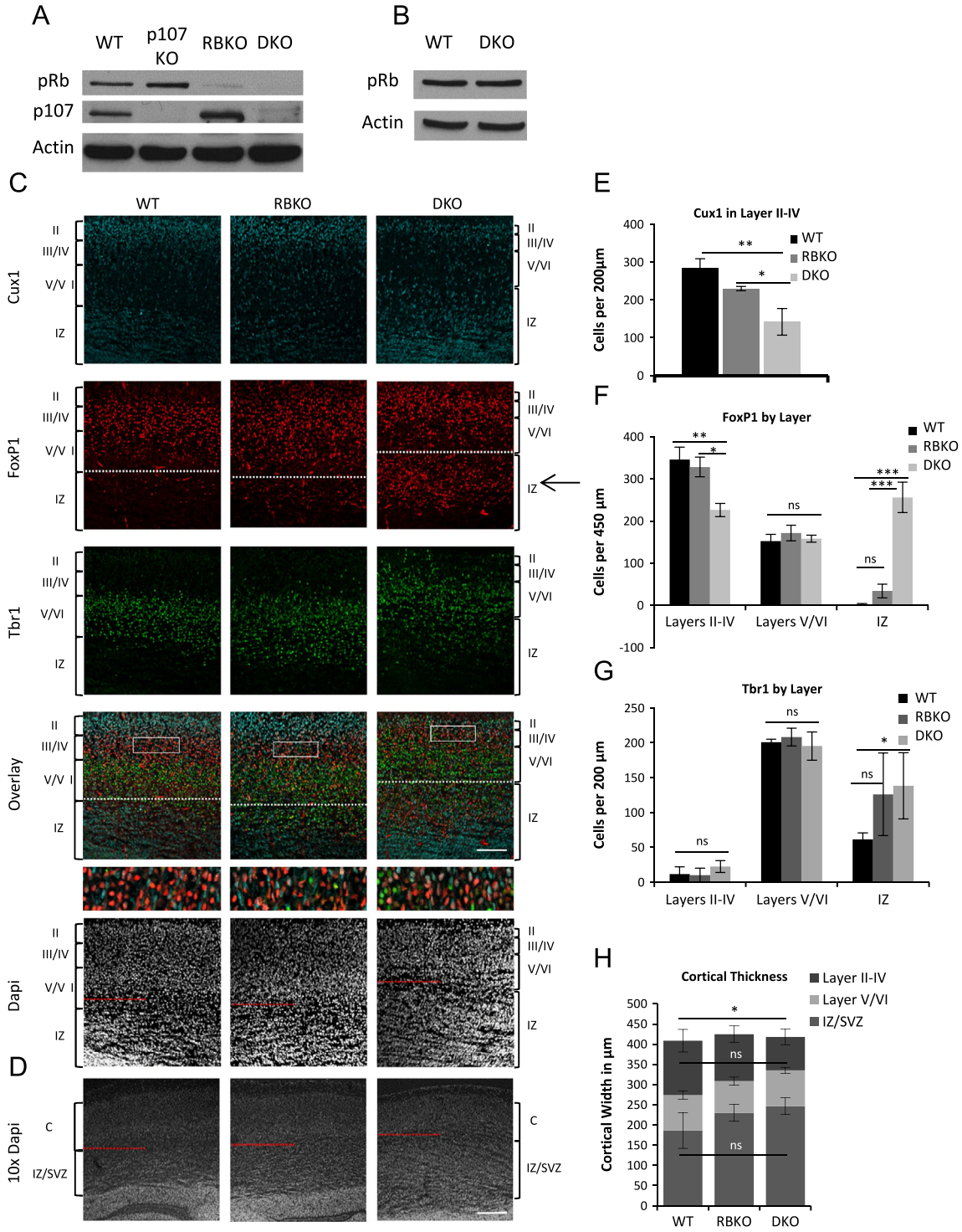

Fig. 1. Cortical neurons are mislocalized in Rb/p107 double knock out (DKO) mice. (A–E) Expression of cortical layer markers was examined in pRb f/+; p107 +/− (WT), pRb f/f; p107 +/− (RBKO) and pRb f/f; p107 −/− (DKO) brains at E17.5. Deletion of pRb and p107 expression in the E15.5 cortex was confirmed in the Emx1-cre model by Western blot (A). pRb deletion was specific to the dorsal telencephalon as expected, since it was not deleted in tissue collected for the ventral telencephalon (B). (C) Brains were stained for Cux1 (blue; marker of layer II), FoxP1 (red; marker of layer III/IV), Tbr1 (green; marker of layer V/VI) and Dapi (gray; nuclear stain). Low power Dapi images are provided to illustrate gross anatomy of the cortical plate (D). We observed a population of cells expressing FoxP1 in the intermediate zone of DKO embryos (arrow), but not WT or RBKO embryos, with a concurrent decrease in the number of FoxP1+ neurons in layers II–IV of the cortex in DKO brains relative to both RBKO and WT brains (F) (layers II–IV were defined as being above the Tbr1+ layers; layers V/VI were defined as expressing Tbr1). Cells were counted in a 450 μm wide (FoxP1) or 200 μm wide (Cux1 and Tbr1) column of cortex extending from the top of the cortical plate to the ventricular zone. The delineation between the cortical plate and intermediate zone, defined using Dapi staining, is shown with a white line (red line in the Dapi panel). An inset is provided below the merged images to show nuclear staining in greater detail. There was a similar decrease in the number of cells expressing Cux1 in DKO brains compared to both WT and RBKO brains (E). Tbr1 cells were found to be disorganized and increased in the intermediate zone but there was no change in the number of Tbr1 cells in the cortical plate (G). Thickness of the upper cortical layers was found to be decreased in DKO brains compared to WT brains (H) with no difference in thickness of lower layers. Three to five embryos were used for each phenotype. C=Cortex IZ=Intermediate Zone SVZ=Subventricular Zone Error bars show standard deviation. ***$p < 0.001$; **$p < 0.01$; *$p < 0.05$. (A) Scale bar=100 μm and (B) scale bar=200 μm.

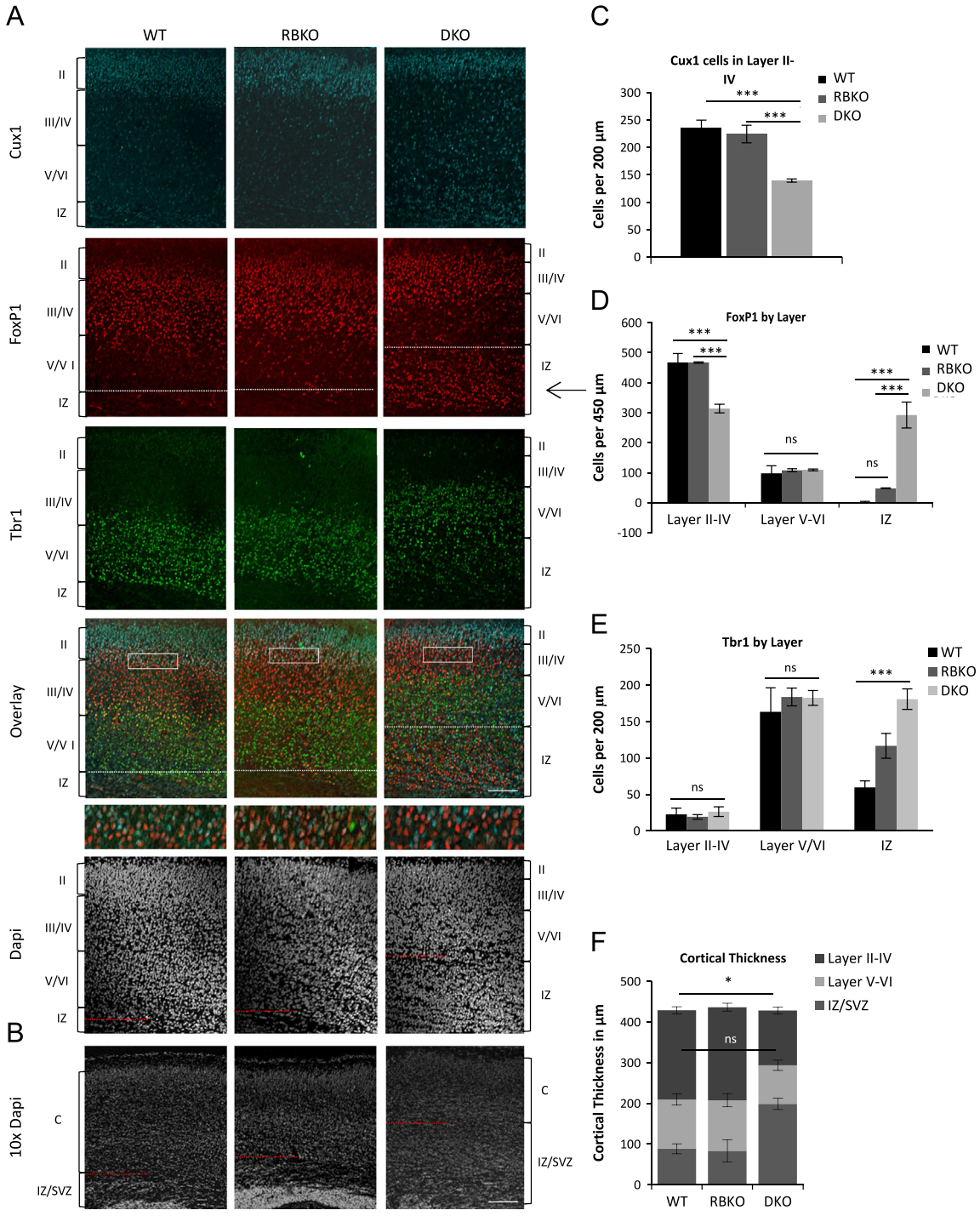

Fig. 2. Cortical neuron mislocalization is not corrected. To determine whether the migration defect was due to a delay in migration, expression of cortical layer markers was examined at P0. Brains were stained for Cux1 (blue; marker of layer II), FoxP1 (red; marker of layer III/IV), Tbr1 (green; marker of layer V/VI) and Dapi (gray; nuclear stain) (A). Low power Dapi images are provided to illustrate gross anatomy of the cortical plate (B). The population of FoxP1+ cells in the intermediate zone of DKO embryos seen at E17.5 (Fig. 1) was still present at P0 (arrow), and there was still a decrease in FoxP1+ cells (D) and Cux 1+ cells (C) within the cortical plate. Cells were counted in a 450 μm wide (FoxP1) or 200 μm wide (Cux1 and Tbr1) column of cortex extending from the top of the cortical plate to the ventricular zone. The delineation between the cortical plate and intermediate zone, defined using Dapi staining, is shown with a white line (red line in the Dapi panel). An inset is provided below the merged images to show nuclear staining. Thickness of the upper cortical layers was found to be decreased in DKO brains compared to WT brains (F) as shown at a lower magnification (10x) Dapi image (B). C=Cortex IZ=Intermediate Zone SVZ=Subventricular Zone Three to five embryos were used for each phenotype. Error bars show standard deviation. $^{***}p < 0.001$; $^{**}p < 0.01$; $^{*}p < 0.05$. (A) Scale bar=100 μm and (B) scale bar=200 μm.

decrease in the number of Cux1 neurons (Fig. 2C) in the upper layers of DKO brains relative to WT brains, as well as a 40% decrease in thickness of the upper layers (Fig. 2F). As seen at E17.5, there was an increase in the thickness of the subventricular zone in DKO brains to compensate for this decrease in the thickness if the upper layers. Again, there was no detectable decrease in the number of Tbr1 neurons within layer V/VI, although there was an increase in Tbr1+ neurons in the intermediate zone (Fig. 2E). Although it would have been useful to determine if cortical lamination was corrected at P7, when migration is complete in the mouse, this was not possible due to neonatal lethality of the DKO pups. Together, these findings show that the misplacement of

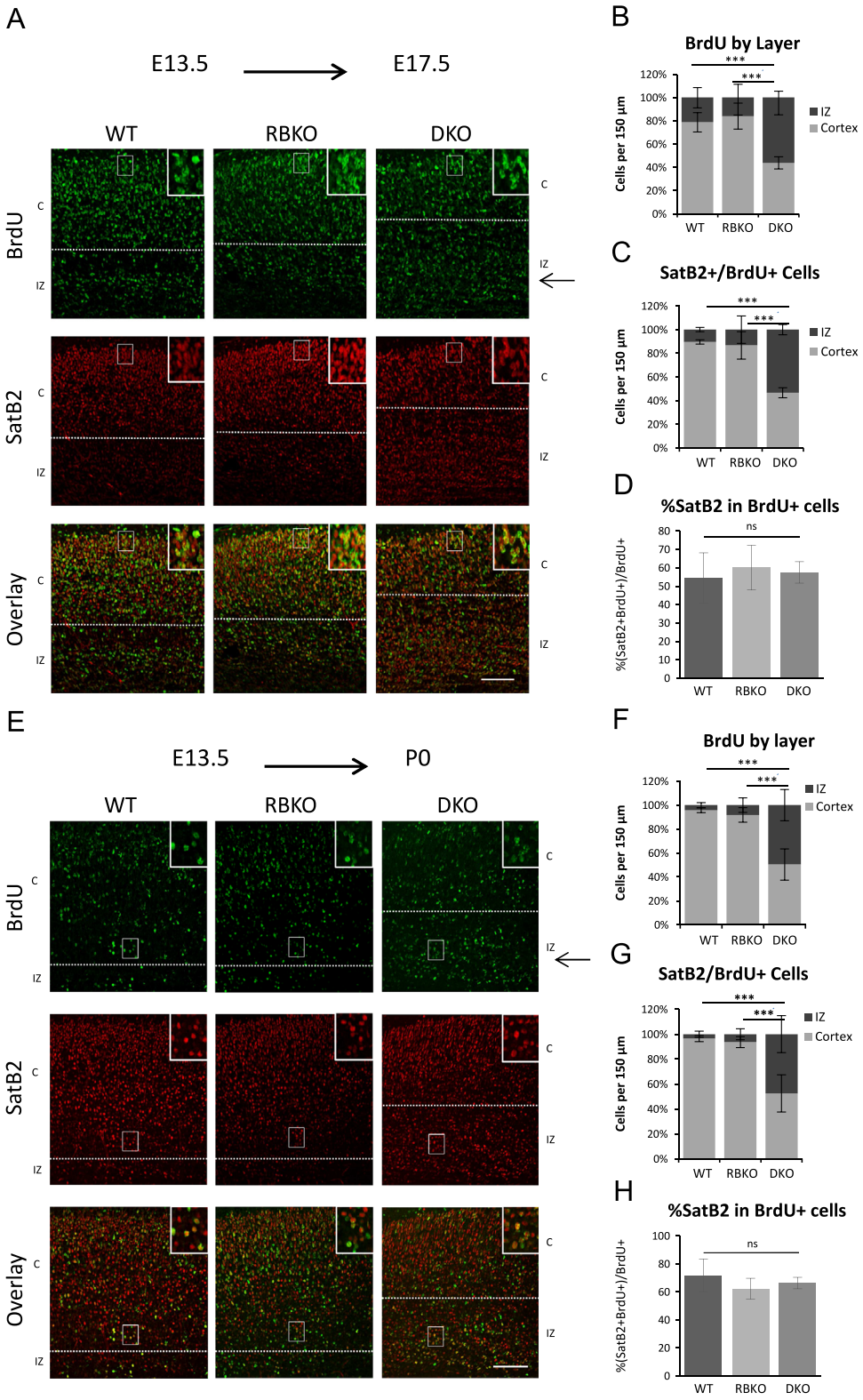

Fig. 3. Misplaced neurons exhibit a defect in radial migration. (A,E) To determine if cells born 4 days previous were located in the correct layer and expressed the correct cortical layer markers, pregnant females were injected with BrdU at E13.5 and pups collected at either E17.5 (A) or P0 (E). The delineation between the cortical plate and intermediate zone, defined using Dapi staining, is shown with a white line. Brains were stained for BrdU incorporation (green) and SatB2 (red), a marker for layers II–IV. An inset is provided to show double labeling. Cells were counted in a 150 μm wide strip of cortex extending from the top of the cortical plate to the ventricular zone. Approximately 50% of the BrdU+ neurons remain in the intermediate zone in DKO brains at both ages, while only 5–20% of these BrdU+ cells stay in the intermediate zone in RBKO and WT brains (see text for exact percentages) (B,F). Arrows (A,E) indicate the increase in BrdU staining in the intermediate zone of DKO brains. Similar values were obtained at both E17.5 and P0 for the percentage of BrdU+/SatB2+ (C,G) in the intermediate zone and cortical plate. There is no difference in the percentage of BrdU+ cells which double label with SatB2 between DKO and WT brains at either timepoint (D,H). Three to five embryos were used for each phenotype. Error bars show standard deviation. $^{***}p < 0.001$; $^{**}p < 0.01$; $^{*}p < 0.05$. Scale bars = 100 μm.

the cortical neurons in DKO brains is not due to a delay in migration. Again, since delayed migration due to delayed cell cycle exit would have been corrected, this data also indicates that the errors in migration in the DKO are unlikely to result simply from delayed cell cycle dynamics in affected cells.

Pocket proteins are required for radial migration of upper layer neurons

To resolve whether the Foxp1+ cells in the DKO intermediate zone were fated for the cortical plate, we performed a birthdating assay to determine if these neurons had exited the cell cycle at a time appropriate for neurons of the upper cortical layers. Pregnant mothers were injected with BrdU at E13.5 and embryos were collected at E17.5 or P0. BrdU injection was done at E13.5 because, on our mouse background strain, this time point revealed the highest level of colocalization with upper layer markers, while later injections at E15.5 targeted neurons still migrating through the intermediate zone. We then analyzed the location of neurons born at E13.5 to determine whether these neurons had migrated into the cortex or remained stalled in the intermediate zone. In WT and RBKO brains, 78.6 ± 8% and 83.9 ± 11% of the BrdU+ cells were found in the cortical plate, respectively, while only 43.7 ± 5% of the BrdU+ cells reached the cortical plate in the DKO brains (Fig. 3A, B). Due to variation in BrdU labeling between litters, total BrdU+ cell counts for all layers ranged from 248 ± 46 (average ± SD) cells in DKO brains, 186 ± 74 in RBKO, and 250 ± 102 in WT. At P0, 97.6 ± 2% of BrdU+ cells reached the cortical plate in WT brains, but only 51.8 ± 1% of BrdU+ cells reached the same destination in DKO brains (Fig. 3E, F). Total cell counts ranged between 208 ± 24 in DKO, 177 ± 27 in RBKO and 149 ± 40 in WT. Similar results were found when the locations of double stained BrdU+/SatB2+ (Fig. 3C, G) or BrdU+/FoxP1+ (data not shown) cells were quantified, with 91 ± 33 FoxP1+/BrdU+ and 133 ± 43 SatB2+/BrdU+ total cells counted per brain regardless of genotype or age. There was no difference in the percentage of BrdU+ cells which co-labeled with SatB2 at either E17.5 or P0, indicating that the identity of the cells born at E13.5 is similar in WT and DKO brains (Fig. 3D, H). These results show that the misplaced Foxp1+ cells in the intermediate zone of DKO brains were born at the correct time for upper layer cortical neurons, but were unable to migrate to the correct location. This evidence supports the hypothesis that pocket proteins play a direct role in regulating radial migration.

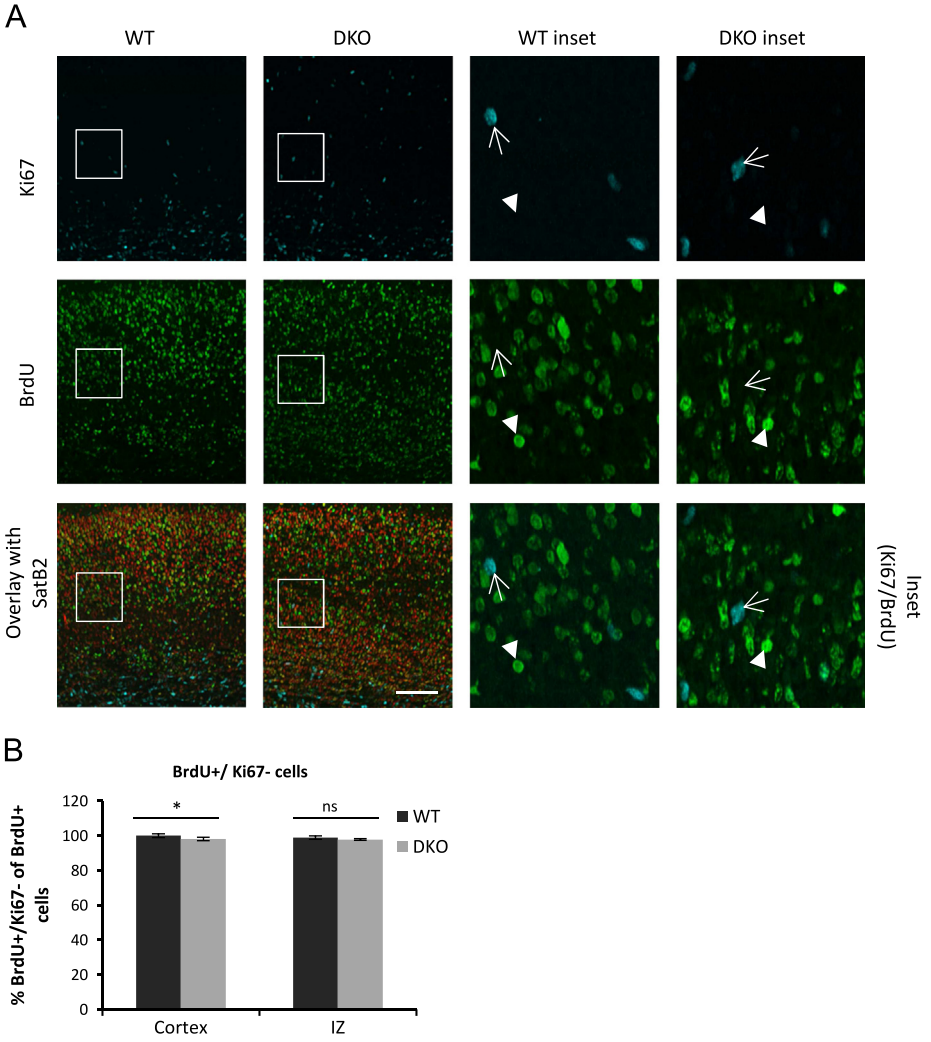

Fig. 4. Assessment of cell cycle exit in misplaced neurons of DKO brains. (A) To determine if misplaced neurons in the intermediate zone inappropriately express the cell cycle marker Ki67, pregnant females were injected at E13.5 and pups collected at E17.5. Sections were stained for BrdU incorporation (green), Ki67 (blue) and SatB2 (red). The percentage of BrdU+ cells, born 4 days prior to tissue collection, which do not stain for Ki67 were quantified (B). Cells were counted in a 450 μm wide strip of cortex extending from the top of the cortical plate to just above the subventricular zone. In both WT and DKO brains, at least 97% of the BrdU+ neurons did not express Ki67, indicating that they have left the cell cycle. High magnification insets (right side of A) show examples of a BrdU+/Ki67- neurons (arrowheads) and BrdU−/Ki67+ neurons (arrows). Overlay is shown with SatB2 staining to show the location of the layers. Three to five embryos were used for each phenotype. Error bars show standard deviation. *$p < 0.05$. Scale bars = 100 μm.

Misplaced neurons in the DKO intermediate zone have exited the cell cycle

Many of the developmental phenotypes described in pRb mutants result from defects in cell cycle exit, even in cells expressing markers normally associated with terminal differentiation (Chen et al., 2004; Haigis et al., 2006; Berman et al., 2009). To determine whether the migration defect in DKO embryos results from misplaced neurons having failed to exit the cell cycle, we injected pregnant mothers with BrdU at E13.5 and collected brains at E17.5, as described above, and examined whether BrdU+ neurons expressed the cell cycle progression marker Ki67. We found that 98 ± 0.4% of BrdU+ cells in DKO brains no longer expressed Ki67 (Fig. 4), compared to 99.8 ± 0.1% of BrdU+ cells in

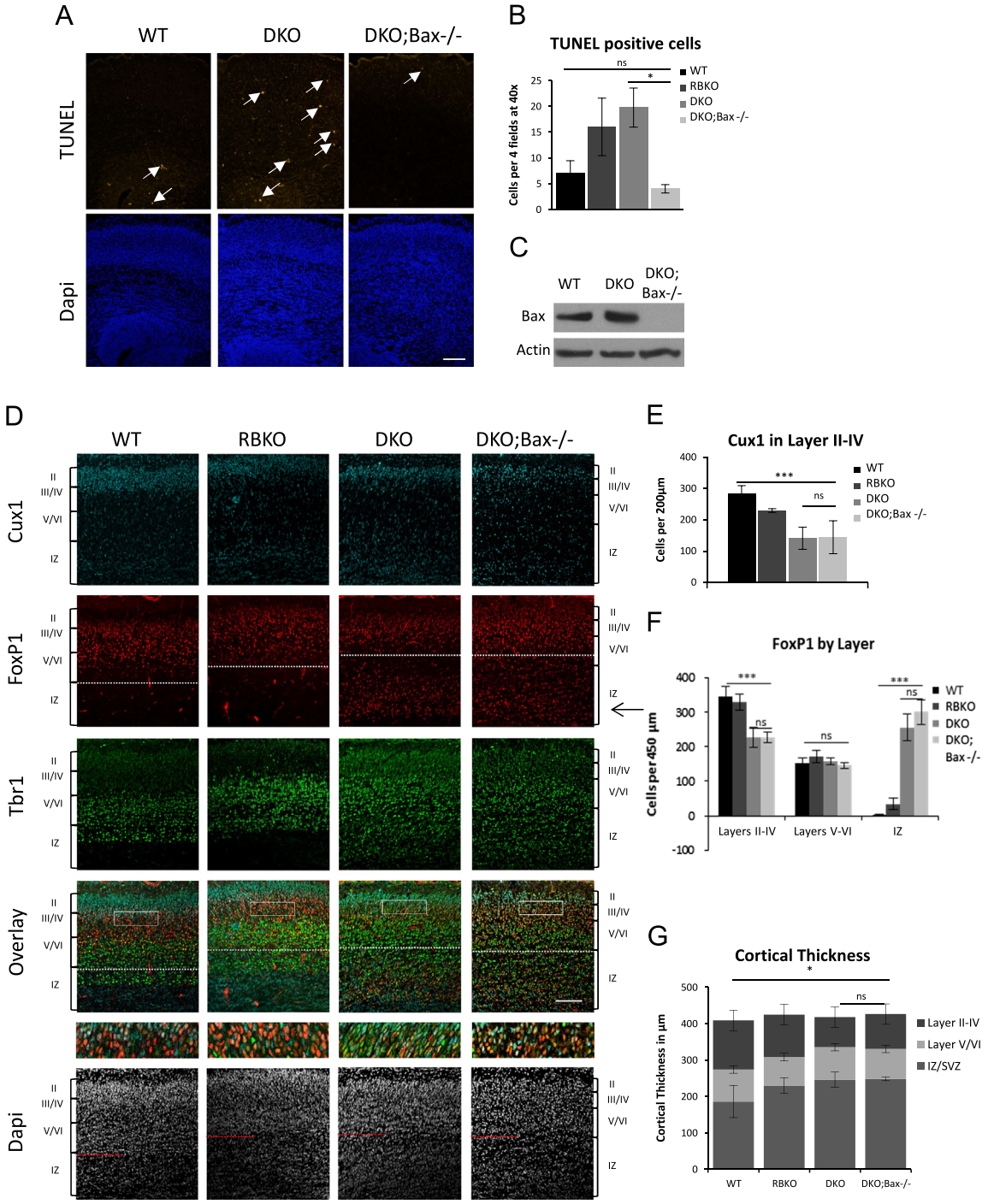

Fig. 5. The migration defect in DKO brains is not due to increased cell death. To determine if the migration defect is due to increased apoptosis, cortical lamination was examined in DKO;Bax−/− brains at E17.5. (A,B) TUNEL staining was used to confirm that the increase in cell death seen in DKO brains was returned to wild type levels in DKO;Bax−/− brains. (C) Deletion of Bax in cortical tissue was confirmed by Western blot at E17.5. (D) Cortical lamination was examined by staining for Cux1 (blue; marker of layer II–IV), FoxP1 (red; marker of layer III/IV), Tbr1 (green; marker of layer V/VI) and Dapi (gray; nuclear stain). The delineation between the cortical plate and intermediate zone, defined using Dapi staining, is shown with a white line (red line in the Dapi panel). The population of FoxP1+ cells in the intermediate zone of DKO brains is maintained in DKO;Bax−/− brains (arrow). Quantification of FoxP1 cells (F), Cux1+ cells (E), and cortical thickness (G) showed no difference between DKO and DKO;Bax brains, indicating that rescuing cell death failed to rescue these phenotypes. Quantifications were done the same way as those described in Fig. 1. Error bars show standard deviation. $^{***}p < 0.001$; $^{**}p < 0.01$; $^{*}p < 0.05$. Scale bars = 100 µm.

WT brains (203 ± 55 cells counted per brain). Although there are significantly more Ki67+/BrdU+ cells in DKO brains, these cells represent such a small percentage of the total BrdU+ cells that they could not account for the observed migration phenotype. Furthermore, the 2% of BrdU+ cells which do express Ki67 were evenly distributed throughout the cortex and intermediate zone, rather than concentrated in the intermediate zone like the misplaced FoxP1+ neurons. Together, the observations that radial migration does not correct with time and that misplaced neurons have exited the cell cycle by E17.5, suggest that the defect in migration in DKO brains is not due to ectopic proliferation or a failure to exit the cell cycle.

Inhibition of cell death does not rescue the migration defect in DKO neurons

pRb loss has been shown to lead to increased apoptosis which may cause or accentuate many of the phenotypes described in RBKO mutants (Lee et al., 1994; Feddersen et al., 1995; Chen et al., 2004; MacPherson et al., 2004; Berman et al., 2009; Wu et al., 2009; Ciavarra and Zacksenhaus, 2010), while in other cases maturation defects are cell death independent (Chen et al., 2007). It remains an outstanding question whether pocket proteins regulate post-mitotic cell maturation directly or if this role is attributable to the role of pRb in apoptosis. We have previously shown that the defect in radial migration in the RBKO mutant coincides with a decrease in Cajal Retzius cells (Ferguson et al., 2005; McClellan et al., 2007). However, it remains unknown whether the defect in radial migration shown in Figs. 1 and 2 is a result of deregulated apoptosis following loss of pRb and p107, or whether these pocket proteins regulate radial migration directly. To determine whether migration is impaired in DKO brains due to increased apoptosis and subsequent loss of a crucial migratory signal, we crossed the pRb/p107 DKO mice with Bax −/− mice to generate DKO;Bax −/− mice and examined cortical lamination at E17.5. First, we used TUNEL staining to confirm that the increased

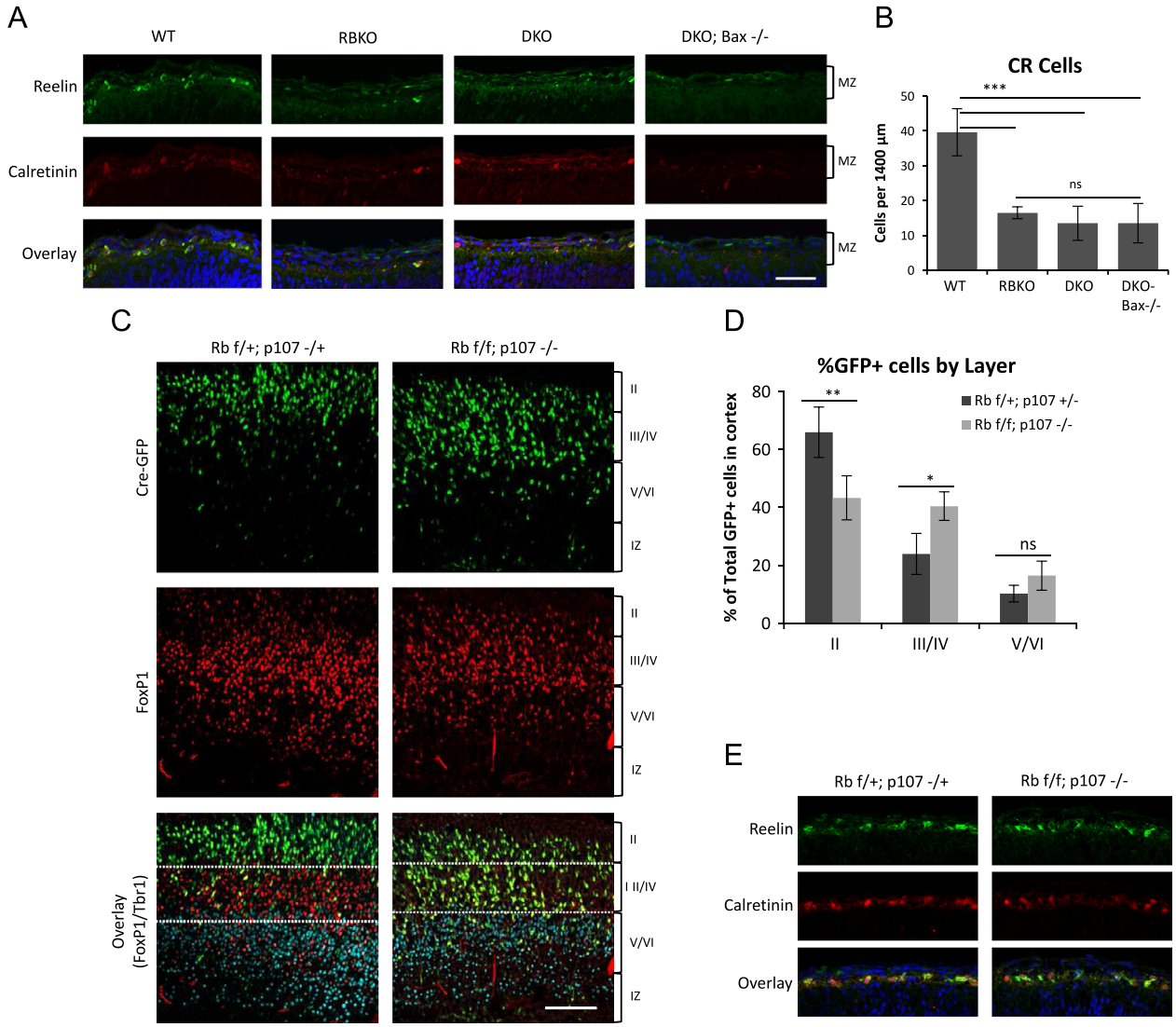

Fig. 6. Pocket proteins regulate radial migration through a cell autonomous mechanism. (A,B) To determine if the migration defect correlated with a decrease in Cajal Retzius cells, WT, RBKO, DKO and DKO;Bax−/− brains were stained for Reelin (green) and Calretinin (red) at E17.5. All double labeled cells in the marginal zone (MZ) were counted in a total of 1400 μm per brain (B). Scale bars=50 μm. (C) To determine if pocket proteins regulate radial migration cell autonomously, pRb f/f;p107−/− and pRb f/+; p107−/+ embryos were electroporated *in utero* at E13.5 and brains were collected at E17.5. The location of GFP+ neurons was quantified according to cortical layer. Layer II was defined as being above FoxP1 staining (red), layer III/IV was defined as within FoxP1+ staining, above Tbr1+ (blue) and layer V/VI was defined as within the Tbr1+ layer (D). We show that a portion pRb/p107 deficient neurons fail to reach layer II but instead remain in layer III/IV. (E) Cajal Retzius cells were normal in all electroporated brains, which emphasizes that Reelin signaling is not involved in this migration defect. $^{***}p < 0.001$; $^{**}p < 0.01$; $^{*}p < 0.05$. Scale bars=100 μm.

levels of cell death seen in DKO brains was rescued to wild type levels following deletion of Bax (Fig. 5A–C). We then asked if cortical migration was rescued in DKO;Bax−/− brains by staining for layer specific markers. Deletion of Bax did not rescue the migration defect, as no differences in cortical lamination or layer specific cell counts could be found between DKO and DKO;Bax−/− embryos (Fig. 5D–G) (counts were performed as described for Fig. 1). Specifically, DKO;Bax−/− brains have an average of 302 ± 36 FoxP1+ neurons stalled in the intermediate zone, with a corresponding 35% decrease in the number of FoxP1+ neurons in layers II–IV compared to WT. There is a 50% decrease in the number of Cux1+ cells in the upper layers and a 30% decrease in cortical thickness compared to WT, as seen in absence of pRb/p107 alone. Loss of Bax alone could therefore not account for these phenotypes, as there was no difference in FoxP1 or Cux1 cell number or localization, or cortical thickness between Bax+/+ and Bax−/− brains (these brains were wild type for pRb and p107) (Fig. S1). This evidence indicates that apoptosis cannot account for the migration defect in DKO embryos and that pocket proteins influence cortical lamination and neuron migration through a mechanism that is independent from its role in regulating neuron survival.

Pocket proteins regulate cortical migration through a combination of cell autonomous and environmental mechanisms

Given that the migration defect could not be rescued by inhibition of apoptosis, we next asked whether pocket proteins regulate radial migration through a cell autonomous mechanism, or whether the migration defect is the result of a failing environment. We have previously shown a decrease in Cajal Retzius cells in pRb mutants (Ferguson et al., 2005; McClellan et al., 2007). As we had hypothesized that loss of the migratory signal Reelin from these Cajal Retzius cells might account for the lamination defect in RBKO brains, we asked whether there was a further decrease in Cajal Retzius cells in DKO and DKO-Bax−/− brains. Surprisingly, Cajal Retzius cells were similarly decreased in both RBKO and DKO embryos, but the migration defect is specific to DKO brains. Staining with two markers of Cajal Retzius cells, Reelin and Calretinin, revealed a 65% and 58% decrease in DKO and RBKO, respectively, which was not rescued by Bax deficiency (also a 65% decrease in DKO;Bax−/− brains) (Fig. 6A, B). These results show that Cajal Retzius cell loss cannot explain the migration phenotype and that pocket proteins regulate migration through an alternative mechanism.

The radial glial scaffold provides structural support for migrating neurons. To determine whether defects in this scaffold are responsible for the migration phenotype in DKO brains, we asked whether this scaffold is intact in DKO brains by staining for Nestin. We found that the glial scaffold appeared normal in both DKO and WT brains (Fig. S2), indicating that these cells are unlikely to be involved in the migration defect in DKO brains.

Cortical migration depends on a complex array of environmental factors, such as secreted migratory cues (e.g. Reelin), intact radial glial scaffolding, as well as cell autonomous factors, such as migratory cue receptors and regulation of cytoskeletal dynamics. To further pursue the mechanism by which pocket proteins modulate cortical migration, we asked whether their role in migration was cell autonomous. To address this question, we performed *in utero* electroporation to track the migration of Rb/p107 deficient neuroblasts in the context of a healthy environment, where migratory cues remain intact. Embryos (Rbf/f; p107−/− and Rbf/+; p107+/−) were electroporated with Cre-GFP at E13.5, and brains were collected 4 days later at E17.5. The efficiency of Cre mediated recombination was confirmed both *in vivo* and *in vitro* (data not shown). The location of GFP+ neurons relative to cortical layer markers FoxP1 and Tbr1 was analyzed. In WT brains, 65.8 ± 8.7% GFP+ neurons migrated to layer II, and 23.9 ± 7.1% were found in layer III/IV (Fig. 6C, D). In DKO brains, however, only 43.2 ± 7.6% of GFP+ neurons reached layer II, with 40.4 ± 4.9% of GFP+ neurons scattered throughout layers III/IV. A minimum of 250 cells were counted for each brain. Layer II was defined as being above the FoxP1+ layer, while layer III/IV was defined as being within the FoxP1+ layer, above the Tbr1+ layer. There was no difference in the number of GFP+ neurons in the intermediate zone between the two phenotypes, and no defect was seen in electroporated RBKO brains (data not shown). Unlike in conditional knockouts (Fig. 6A), here there was no difference in the number of Cajal Retzius cells between pRb f/f; p107−/− and wild type electroporated brains (Fig. 6E). Given that pRb/p107 deficient neurons failed to migrate correctly in a healthy environment, we conclude that pocket proteins are essential to modulate radial migration through a cell autonomous mechanism.

Discussion

In this study, we evaluated the role of pocket proteins pRb and p107 in the regulation of radial migration in the developing cortex. Our results support a number of conclusions. First, we present a novel defect in radial migration which is specific to the pRb/p107 DKO brains. We then show that this defect is not due to unchecked cell death, despite the importance of pocket proteins in regulating apoptosis. Finally, we show that pRb and p107 regulate radial migration through a combination of cell autonomous and non-cell autonomous mechanisms. These results are summarized in Table 1. Together, our results describe a novel function of pocket proteins in regulating cortical plate formation in the developing brain.

pRb and p107 are required for radial migration in the developing cortex

pRb is known to play a variety of roles during brain development, namely control of cell cycle progression, apoptosis and early fate specification (Jacks et al., 1992; Ferguson and Slack, 2001; MacPherson et al., 2004; Vanderluit et al., 2004; McClellan and Slack, 2006; Wu et al., 2009; Ghanem et al., 2012). Indeed, we have shown that pRb regulates early differentiation factors and tangential migration in ventrally derived neurons (Ferguson et al., 2005; Andrusiak et al., 2011; Ghanem et al., 2012), independently of its role in proliferation. pRb was also shown to be involved in cortical lamination as deletion of pRb caused the normally well-organized delineation between cortical plate and intermediate zone to become indistinct (McClellan et al., 2007). However, p107 has been shown to compensate for loss of pRb in various models (Marino et al., 2003; Chen et al., 2004; Haigis et al., 2006; Berman et al., 2009). Pocket proteins may therefore have additional roles in neuron maturation which could not be detected in single knock-out models. To address

Table 1
Phenotype Summary.

	WT	RBKO	DKO	DKO;Bax−/−
FoxP1+ neurons in IZ	−	−	++	++
Thinning of Cux+ layer	−	+	++	++
BrdU+ cells in IZ	−	−	++	ND
Loss of CR cells	−	+	+	+
GFP+ neurons in layer III/IV following IUE	−	−	+	ND

Negative sign indicates not observed, + indicates mild phenotype, and ++ indicates severe phenotype.
IZ=Intermediate Zone, CR=Cajal Retzius, ND=Not done, IUE=in utero Electroporation.

this issue, we used the pRb/p107 double knock out (DKO) mouse to test the hypothesis that pocket proteins have more extensive roles in radial migration in the developing brain.

Here we show a defect in radial migration in DKO brains with a concurrent decrease in the number of upper layer neurons within the cortical plate. Our data implies that the phenotype in DKO brains is due to a primary defect in migration rather than the result of a delay in cell cycle exit for two reasons. First, if the misplaced neurons were migrating normally but were delayed because they exited the cell cycle late, they would continue migration and approach their destination at P0 (Fig. 2), which does not occur. Second, the misplaced neurons do not express the cell cycle marker, Ki67 (Fig. 4); at E17.5, only 2% of the migrating population exhibited ectopic proliferation. Together, these findings suggest that the defect in radial migration does not result from failed cell cycle exit. Whether this migration defect results from other cell cycle related mechanisms, such as delayed exit, disruption of polarity or impaired precursor differentiation cannot be determined at this time and requires further investigation.

In this study we have focused on the migration defect in the upper layers neurons of DKO brains. However, there is also a defect in lamination in the lower layers as seen by the increased Tbr1+ neurons in the IZ of RBKO and DKO at E17.5 (Fig. 1). Interestingly, this defect appears to be distinct from that seen in the upper layers, since there is no decrease in the number of Tbr1+ neurons which reach the cortical plate in DKO brains, as is seen with FoxP1+ and Cux1+ neurons. Likewise there is no difference in the thickness of the lower cortical layers between DKO and WT brains. For these reasons, the defect in formation of layers V/VI cannot result solely from Tbr1+ neurons failing to migrate through the intermediate zone. An alternate possibility is that pocket proteins control the relative rates of proliferation during development such that neurogenesis is increased early when layers V/VI are formed, but later slows when layers II–IV are formed. This increase in neurogenesis would then account for the increased Tbr1+ neurons in the intermediate zone, rather than, or in addition to, a defect in migration of these neurons. At this point it is only possible to conclude that pocket proteins regulate formation of upper cortical layers differently than the formation of lower cortical layers and further analysis is required to understand the responsible mechanisms.

Pocket protein regulation of radial migration does not depend on cell death

pRb was first identified as a tumor suppressor and has been extensively studied in its role in regulation of cell division and apoptosis (Chen et al., 2004; Lazzerini Denchi and Helin, 2005; Giacinti and Giordano, 2006; Ciavarra and Zacksenhaus, 2010; Gordon and Du, 2011; Manning and Dyson, 2012). Ectopic cell death has been shown to contribute to many developmental phenotypes in pRb knockout models (Feddersen et al., 1995; Marino et al., 2003; Chen et al., 2004; MacPherson et al., 2004; Sage et al., 2006; Berman et al., 2009; Ciavarra and Zacksenhaus, 2010). Increased apoptosis found in pocket protein knock out models is primarily due to deregulated E2F1 activity and subsequent activation of the p53 pathway (Macleod et al., 1996; Lazzerini Denchi and Helin, 2005; Wu et al., 2009), although increased apoptosis has been found to sometimes be p53 and even E2F1 independent in the retina (MacPherson et al., 2004; Chen et al., 2013). pRb has also been shown to be crucial for survival in post-mitotic neurons (Andrusiak et al., 2012). This dual role of Rb in regulating both cell proliferation and death has obscured our understanding of other important developmental roles of pocket proteins. It was therefore unclear whether the migration phenotype in the DKO brains was due to death of cells providing regulatory signals necessary for radial migration, or whether it represented a primary migratory function of pocket proteins. To resolve this question, we eliminated this ectopic apoptosis through deletion of the apoptotic regulator Bax (Gavathiotis et al., 2012) in the DKO and determine whether the defect radial migration persisted. Surprisingly, despite the fact that cell death was successfully restored to wild type levels in the DKO; Bax−/− brains (Fig. 5A), none of the migratory phenotypes described in DKO brains were rescued by Bax deletion (Fig. 5D–G; Table 1). The FoxP1+ cells are still present in the intermediate zone of these DKO;Bax−/− brains and the upper cortical layers were still thinner, indicating that this migration defect does not result from apoptosis. Furthermore, a migration defect was observed in GFP+ neurons following *in utero* electroporation of Cre (see below); because these neurons migrate in a healthy environment, and have clearly survived, cell death does not seem to be involved. This shows that, in the developing brain, pocket proteins regulate migration and apoptosis through separate, independent mechanisms.

Pocket proteins have a cell autonomous role in radial migration

We have previously shown that Cajal Retzius cells are decreased in the RBKO mouse and hypothesized first, that these cells were lost to apoptosis, and second that their loss was responsible for the minor defect in radial migration. However, we show here that deletion of Bax fails to rescue these Cajal Retzius cells (Fig. 6A) and that there was no difference in the number Cajal Retzius cells between RBKO and DKO mice (Fig. 6B). There are two possible explanations for the absence of Cajal Retzius cells in DKO brains; these cells could either be lost through an alternative apoptotic pathway or there could be a defect in their differentiation following loss of pRb and p107. Further experimentation is necessary in order to distinguish between these scenarios. More importantly, the fact that both RBKO and DKO brains show the same decrease in Cajal Retzius cell number while only DKO brains have a migration defect implies that the loss of Cajal Retzius cells cannot explain why a subset of DKO neurons fails to pass through the intermediate zone.

Radial migration is dependent on numerous factors which can be categorized as being either cell autonomous or non-cell autonomous. Here we show that pocket proteins control radial migration through a cell autonomous mechanism independent of environmental factors through the use of *in utero* electroporation, as the pRb and p107 deficient neurons failed to migrate correctly through a healthy cortical plate. It should be noted that these animals are genome knockouts for p107. However, since there is no migration phenotype following p107 deletion (data not shown) and there is no apparent defect in cortical lamination in non-electroporated regions of the pRb flox/flox;p107−/− electroporated brains, we conclude that the defect requires the loss of both pRb and p107 in GFP+ neurons.

Following pRb deletion in electroporated pRb flox/flox;p107−/− brains, GFP+ neurons reach the cortical plate but are highly disorganized, while in DKO Emx1-Cre brains the misplaced neurons fail to migrate past the intermediate zone. One possible explanation for this difference is that pRb and p107 regulate migration through a combination of cell autonomous and non-cell autonomous mechanisms. In electroporated brains, the pRb/p107 deficient neurons may have been able to reach the cortex since environmental support was still intact, while in the full cortex knockout both environmental and cell autonomous mechanisms were compromised. For example, it is possible that, in the DKO;Emx1-Cre+ cortex, the cell autonomous defect makes these neurons more sensitive to the drop in Reelin and this contributes to their failure to migrate through the intermediate

zone, while in the RBKO cortex the low levels of Reelin are sufficient. Another possibility is that the time required for Cre to be expressed, excise pRb and for pRb target genes to become deregulated, allows neurons electroporated at E13.5 have time to pass through the intermediate zone and into the cortical plate before migration is disrupted. Further experimentation is required to fully understand the mechanism through which pocket proteins regulate cortical migration.

These results represent the first description of a cell autonomous role of pRb in radial migration in the developing cortex. We have shown in previous work that pRb is involved in tangential migration of ventrally derived immature interneurons, also in a cell autonomous manner through regulation of the Netrin receptor Neogenin (Ferguson et al., 2005; McClellan et al., 2007; Andrusiak et al., 2011). When considered together, these studies suggest that neither phenotype is a single phenomenon but that pRb may regulate migration in a wide variety of cell types. It remains to be determined whether pocket proteins control migration in non-neural cells, or whether migration is regulated through similar mechanisms in different cell types. Further exploration into the mechanisms through which pocket proteins regulate cell migration in various tissues will greatly increase our understanding of how this protein family influences both normal development and tumor formation.

In conclusion, these results demonstrate that pocket proteins are required for radial migration. This is achieved through a combination of cell autonomous and environmental factors which are independent of cell death. These finding strongly support our hypothesis that pocket proteins are important in later stages of neuron maturation through mechanisms independent of their role in cell cycle progression or apoptosis.

Acknowledgments

We are indebted to Pierre Mattar and Freda Miller for their assistance with the *in utero* electroporation. We thank Linda Jui, Angela Nguyen, and Jason G. MacLaurin for excellent technical assistance. Equipment was supported by the Centre for Stroke Recovery.

This work was supported by a CIHR grant to R.S.S.

Appendix A. Supporting information

Supplementary data associated with this article can be found in the online version at http://dx.doi.org/10.1016/j.ydbio.2013.09.015.

References

Andrusiak, M.G., McClellan, K.A., Dugal-Tessier, D., Julian, L.M., Rodrigues, S.P., Park, D.S., Kennedy, T.E., Slack, R.S., 2011. Rb/E2F regulates expression of neogenin during neuronal migration. Mol. Cell. Biol. 31, 238–247.

Andrusiak, M.G., Vandenbosch, R., Park, D.S., Slack, R.S., 2012. The retinoblastoma protein is essential for survival of postmitotic neurons. J. Neurosci. 32, 14809–14814.

Berman, S.D., West, J.C., Danielian, P.S., Caron, A.M., Stone, J.R., Lees, J.A., 2009. Mutation of p107 exacerbates the consequences of Rb Loss in embryonic tissues and causes cardiac and blood vessel defects. Proc. Natl. Acad. Sci. U. S. A. 106, 14932–14936.

Britanova, O., de Juan Romero, C., Cheung, A., Kwan, K.Y., Schwark, M., Gyorgy, A., Vogel, T., Akopov, S., Mitkovski, M., Agoston, D., Sestan, N., Molnar, Z., Tarabykin, V., 2008. Satb2 is a postmitotic determinant for upper-layer neuron specification in the neocortex. Neuron 57, 378–392.

Chen, D., Chen, Y., Forrest, D., Bremner, R., 2013. E2f2 induces cone photoreceptor apoptosis independent of E2f1 and E2f3. Cell Death. Differ. 20, 931–940.

Chen, D., Livne-bar, I., Vanderluit, J.L., Slack, R.S., Agochiya, M., Bremner, R., 2004. Cell-specific effects of RB Or RB/p107 loss on retinal development implicate an intrinsically death-resistant cell-of-origin in retinoblastoma. Cancer Cell 5, 539–551.

Chen, D., Opavsky, R., Pacal, M., Tanimoto, N., Wenzel, P., Seeliger, M.W., Leone, G., Bremner, R., 2007. Rb-mediated neuronal differentiation through cell-cycle-independent regulation of E2f3a. PLoS Biol. 5, e179.

Ciavarra, G., Zacksenhaus, E., 2010. Rescue of myogenic defects in Rb-deficient cells by inhibition of autophagy or by hypoxia-induced glycolytic shift. J. Cell Biol. 191, 291–301.

Feddersen, R.M., Clark, H.B., Yunis, W.S., Orr, H.T., 1995. In vivo viability of postmitotic purkinje neurons requires pRb family member function. Mol. Cell. Neurosci. 6, 153–167.

Ferguson, K.L., McClellan, K.A., Vanderluit, J.L., McIntosh, W.C., Schuurmans, C., Polleux, F., Slack, R.S., 2005. A cell-autonomous requirement for the cell cycle regulatory protein, Rb, in neuronal migration. EMBO J. 24, 4381–4391.

Ferguson, K.L., Slack, R.S., 2001. The Rb pathway in neurogenesis. Neuroreport 12, A55–62.

Ferguson, K.L., Vanderluit, J.L., Hebert, J.M., McIntosh, W.C., Tibbo, E., MacLaurin, J. G., Park, D.S., Wallace, V.A., Vooijs, M., McConnell, S.K., Slack, R.S., 2002. Telencephalon-specific Rb knockouts reveal enhanced neurogenesis, survival and abnormal cortical development, EMBO J. 21, 3337–3346.

Ferland, R.J., Cherry, T.J., Preware, P.O., Morrisey, E.E., Walsh, C.A., 2003. Characterization of Foxp2 and Foxp1 mRNA and protein in the developing and mature brain. J. Comp. Neurol. 460, 266–279.

Garcia-Moreno, F., Lopez-Mascaraque, L., De Carlos, J.A., 2007. Origins and migratory routes of murine cajal-retzius cells. J. Comp. Neurol. 500, 419–432.

Gavathiotis, E., Reyna, D.E., Bellairs, J.A., Leshchiner, E.S., Walensky, L.D., 2012. Direct and selective small-molecule activation of proapoptotic BAX. Nat. Chem. Biol. 8, 639–645.

Ghanem, N., Andrusiak, M.G., Svoboda, D., Al Lafi, S.M., Julian, L.M., McClellan, K.A., De Repentigny, Y., Kothary, R., Ekker, M., Blais, A., Park, D.S., Slack, R.S., 2012. The Rb/E2F pathway modulates neurogenesis through direct regulation of the Dlx1/Dlx2 bigene cluster. J. Neurosci. 32, 8219–8230.

Giacinti, C., Giordano, A., 2006. RB and cell cycle progression. Oncogene 25, 5220–5227.

Gordon, G.M., Du, W., 2011. Conserved RB functions in development and tumor suppression. Protein Cell 2, 864–878.

Haigis, K., Sage, J., Glickman, J., Shafer, S., Jacks, T., 2006. The related retinoblastoma (pRb) and p130 proteins cooperate to regulate homeostasis in the intestinal epithelium. J. Biol. Chem. 281, 638–647.

Hevner, R.F., Shi, L., Justice, N., Hsueh, Y., Sheng, M., Smiga, S., Bulfone, A., Goffinet, A.M., Campagnoni, A.T., Rubenstein, J.L., 2001. Tbr1 regulates differentiation of the preplate and layer 6. Neuron 29, 353–366.

Honda, T., Kobayashi, K., Mikoshiba, K., Nakajima, K., 2011. Regulation of cortical neuron migration by the reelin signaling Pathway. Neurochem. Res. 36, 1270–1279.

Jacks, T., Fazeli, A., Schmitt, E.M., Bronson, R.T., Goodell, M.A., Weinberg, R.A., 1992. Effects of an Rb mutation in the mouse. Nature 359, 295–300.

Lazzerini Denchi, E., Helin, K., 2005. E2F1 is crucial for E2F-dependent apoptosis. EMBO Rep. 6, 661–668.

LeCouter, J.E., Kablar, B., Hardy, W.R., Ying, C., Megeney, L.A., May, L.L., Rudnicki, M.A., 1998. Strain-dependent myeloid hyperplasia, growth deficiency, and accelerated cell cycle in mice lacking the Rb-related p107 gene. Mol. Cell. Biol. 18, 7455–7465.

Lee, E.Y., Hu, N., Yuan, S.S., Cox, L.A., Bradley, A., Lee, W.H., Herrup, K., 1994. Dual roles of the retinoblastoma protein in cell cycle regulation and neuron differentiation. Genes Dev. 8, 2008–2021.

Macleod, K.F., Hu, Y., Jacks, T., 1996. Loss of Rb activates both p53-dependent and independent cell death pathways in the developing mouse nervous system. EMBO J. 15, 6178–6188.

MacPherson, D., Sage, J., Kim, T., Ho, D., McLaughlin, M.E., Jacks, T., 2004. Cell type-specific effects of Rb deletion in the murine retina. Genes Dev. 18, 1681–1694.

Manning, A.L., Dyson, N.J., 2012. RB: Mitotic implications of a tumour suppressor. Nat. Rev. Cancer 12, 220–226.

Marino, S., Hoogervoorst, D., Brandner, S., Berns, A., 2003. Rb and p107 are required for normal cerebellar development and granule Cell Survival but not for purkinje cell persistence. Development 130, 3359–3368.

Marino, S., Vooijs, M., van Der Gulden, H., Jonkers, J., Berns, A., 2000. Induction of medulloblastomas in p53-null mutant mice by somatic inactivation of Rb in the external granular layer cells of the cerebellum. Genes Dev. 14, 994–1004.

McClellan, K.A., Ruzhynsky, V.A., Douda, D.N., Vanderluit, J.L., Ferguson, K.L., Chen, D., Bremner, R., Park, D.S., Leone, G., Slack, R.S., 2007. Unique requirement for Rb/E2F3 in neuronal migration: evidence for cell cycle-independent functions. Mol. Cell. Biol. 27, 4825–4843.

McClellan, K.A., Slack, R.S., 2006. Novel functions for cell cycle genes in nervous system development. Cell Cycle 5, 1506–1513.

Nguyen, L., Besson, A., Heng, J.I., Schuurmans, C., Teboul, L., Parras, C., Philpott, A., Roberts, J.M., Guillemot, F., 2006. P27kip1 independently promotes neuronal differentiation and migration in the cerebral cortex. Genes Dev. 20, 1511–1524.

Nieto, M., Monuki, E.S., Tang, H., Imitola, J., Haubst, N., Khoury, S.J., Cunningham, J., Gotz, M., Walsh, C.A., 2004. Expression of Cux-1 and Cux-2 in the subventricular zone and upper layers II–IV of the cerebral cortex. J. Comp. Neurol. 479, 168–180.

Nowakowski, R.S., Caviness Jr, V.S., Takahashi, T., Hayes, N.L., 2002. Population dynamics during cell proliferation and neuronogenesis in the developing murine neocortex. Results Probl. Cell Differ. 39, 1–25.

Padmanabhan, J., Park, D.S., Greene, L.A., Shelanski, M.L., 1999. Role of cell cycle regulatory proteins in cerebellar granule neuron apoptosis. J. Neurosci. 19, 8747–8756.

Sage, C., Huang, M., Vollrath, M.A., Brown, M.C., Hinds, P.W., Corey, D.P., Vetter, D.E., Chen, Z.Y., 2006. Essential role of retinoblastoma protein in mammalian hair cell development and hearing. Proc. Natl. Acad. Sci. U. S. A. 103, 7345–7350.
Shan, B., Chang, C.Y., Jones, D., Lee, W.H., 1994. The transcription factor E2F-1 mediates the autoregulation of rb gene expression. Mol. Cell. Biol. 14, 299–309.
Tury, A., Mairet-Coello, G., DiCicco-Bloom, E., 2011. The cyclin-dependent kinase inhibitor p57Kip2 regulates cell cycle exit, differentiation, and migration of embryonic cerebral cortical precursors. Cereb. Cortex 21, 1840–1856.
Vanderluit, J.L., Ferguson, K.L., Nikoletopoulou, V., Parker, M., Ruzhynsky, V., Alexson, T., McNamara, S.M., Park, D.S., Rudnicki, M., Slack, R.S., 2004. P107 Regulates neural precursor cells in the mammalian brain. J Cell Biol 166, 853–863.
Vooijs, M., van der Valk, M., te Riele, H., Berns, A., 1998. Flp-mediated tissue-specific inactivation of the retinoblastoma tumor suppressor gene in the mouse. Oncogene 17, 1–12.
Wu, Z., Zheng, S., Yu, Q., 2009. The E2F family and the role of E2F1 in apoptosis. Int. J. Biochem. Cell Biol. 41, 2389–2397.

jove Journal of Visualized Experiments www.jove.com

Video Article

Induction of Protein Deletion Through *In Utero* Electroporation to Define Deficits in Neuronal Migration in Transgenic Models

Devon S. Svoboda[1], Alysen Clark[1], David S. Park[1], Ruth S. Slack[1]

[1]Department of Cellular and Molecular Medicine, University of Ottawa

Correspondence to: Devon S. Svoboda or Ruth S. Slack

URL: http://www.jove.com/video/51983
DOI: doi:10.3791/51983

Keywords: Developmental Biology, Issue 95, *In utero* electroporation, brain development, neural migration, transgenic, cell autonomous, mouse model

Date Published: 1/12/2015

Citation: Svoboda, D.S., Clark, A., Park, D.S., Slack, R.S. Induction of Protein Deletion Through *In Utero* Electroporation to Define Deficits in Neuronal Migration in Transgenic Models. *J. Vis. Exp.* (95), e51983, doi:10.3791/51983 (2015).

Abstract

Genetic deletion using the Cre-Lox system in transgenic mouse lines is a powerful tool used to study protein function. However, except in very specific Cre models, deletion of a protein throughout a tissue or cell population often leads to complex phenotypes resulting from multiple interacting mechanisms. Determining whether a phenotype results from disruption of a cell autonomous mechanism, which is intrinsic to the cell in question, or from a non-cell autonomous mechanism, which would result from impairment of that cell's environment, can be difficult to discern. To gain insight into protein function in an *in vivo* context, *in utero* electroporation (IUE) enables gene deletion in a small subset of cells within the developing cortex or some other selected brain region. IUE can be used to target specific brain areas, including the dorsal telencephalon, medial telencephalon, hippocampus, or ganglionic eminence. This facilitates observation of the consequences of cell autonomous gene deletion in the context of a healthy environment. The goal of this protocol is to show how IUE can be used to analyze a defect in radial migration in a floxed transgenic mouse line, with an emphasis on distinguishing between the cell autonomous and non-cell autonomous effects of protein deletion. By comparing the phenotype resulting from gene deletion within the entire cortex versus IUE-mediated gene deletion in a limited cell population, greater insight into protein function in brain development can be obtained than by using either technique in isolation.

Video Link

The video component of this article can be found at http://www.jove.com/video/51983/

Introduction

Radial migration is a central process to early cortical development. It depends on a variety of cell autonomous factors, such as correct mitotic exit and neuronal differentiation, cell polarity, regulation of cytoskeletal dynamics and expression of transmembrane receptors, as well as non-cell autonomous factors, such as formation of the radial glial scaffold and secretion of migratory guidance molecules[1-3]. Since disruption of any of these mechanisms can impair neuronal migration in a transgenic mouse model[4-8], determining the underlying cause of a defect in migration can be a complex and difficult process. *In utero* electroporation (IUE) can be used to complement and simplify interpretation of the phenotype of a genetic knock-out model and thereby elucidate important mechanisms required for radial migration[7,9-11].

In utero electroporation (IUE) is the process by which a plasmid carrying both a gene of interest and a reporter is injected into the ventricle in the brain of a mouse or rat embryo and then drawn into the cells lining the ventricle through use of an electric current[12-14]. This allows the investigator to analyze the effect of up or down regulation of a gene of interest in development or function of electroporated neurons. Following IUE, brains can be processed for immunohistochemistry [7,9-11], electrophysiology [15] or cell culture [16,17]. The major advantage of IUE is that is allows for highly specific manipulation of gene expression. Furthermore, IUE can be used to target a specific region of the developing brain through a directed current (**Figure 2**). IUE can also be used to target a specific cell type through injection of plasmids carrying genes under control of various promoters or plasmid activation systems (tetracycline induced gene expression is an example) [10,18-21].

IUE can be used in conjunction with the Cre-Lox mediated gene excision system [7-9,11,22]. A plasmid containing a gene encoding the message for the Cre protein can be electroporated into an embryo homozygous for the floxed allele (in which the gene or specific DNA regions are flanked by two *loxP* sites for Cre mediated DNA recombination). Cre will then induce recombination of the gene of interest specifically in electroporated neural precursors, generating a knock-out of the floxed allele.The effect of protein knockdown on neural migration and development within individual neurons can then be studied. Electroporation of Cre induces recombination in only a small population of affected cells, leaving the supporting environment intact. In contrast, tissue specific expression of Cre under control of a cell type specific promoter, occurs throughout the entire tissue so that both migrating neuroblasts and the surrounding environment could be affected. Thus, juxtaposition of these two approaches can determine whether a given migration defect is due to cell autonomous or cell non-autonomous mechanisms. Defective migration in both experimental systems suggests that the observed phenotype results from a cell autonomous mechanism; normal migration following electroporation of Cre with defective migration in a tissue specific Cre model indicates that the gene of interest is acting through a non-cell autonomous mechanism.

IUE can also be used to perform rescue experiments by electroporating potential interacting genes into knock out animals [7,9,10]. For example, an investigator could attempt to rescue a migration phenotype in a transgenic model by electroporating a downstream target and determining if the migration defect is corrected in the electroporated neurons. This has the additional benefit that a successful rescue indicates that normal migration can be restored by manipulating protein expression in a specific neuron, even though the surrounding environment is still deficient for the targeted gene. Again, this approach is more time and cost effective than crossing or generating transgenic lines, with the added benefit of determining whether the defective mechanism is cell autonomous.

IUE can be used to track migrating neurons through electroporation of a reporter plasmid into knock out embryos (**Figure 4C**). As only the neurons lining the ventricle at the time of surgery are electroporated [17], IUE can be used to follow the neurons born at a specific time with the advantage of visualization of their morphology *in vivo*.

Finally, it is possible to use IUE to target brain regions such as the medial or dorsal telencephalon, hippocampus or ganglionic eminence (**Figure 2**). This gives researchers the power to investigate gene function in a specific area independent of complications resulting from protein knockdown in neighboring structures.

Retinoblastoma protein (pRb), p107 and p130 comprise the pocket protein family and are well established regulators of cell cycle exit. However, there is increasing evidence that these proteins also regulate cell cycle independent aspects of neural development. As we have previously shown, pRb and p107 play a crucial role in both tangential [4,23] and radial migration [6]. Here, we demonstrate the role of pocket protein family members pRb and p107 on neural migration [6] to exemplify the use of *in utero* electroporation of Cre in a transgenic model. In summary, IUE provides a powerful way of analyzing cell autonomous effects of gene deletion (or overexpression). When combined with tissue specific knock out models, IUE can provide additional information regarding the mechanisms controlling neural migration.

Protocol

NOTE: All experiments were approved by the University of Ottawa's Animal Care ethics committee, adhering to the Guidelines of the Canadian Council on Animal Care.

1. Pre-surgical Preparation and Materials

1. Plasmid Preparation:
    1. Prepare plasmids using the Qiagen MegaPrep according to the manufacturer's protocol. Innoculate at least 400 ml of LB broth with transformed bacteria to ensure a high DNA yield and incubate overnight.
    2. Resuspend plasmid in 100-200 µl TE to a final concentration of at least 5 µg/µl. Aliquot DNA and store at -20 °C. If the concentration is too low, do not precipitate and resuspend as this can add impurities. Start over with a new preparation.
    3. Before surgery, dilute a single plasmid (Cre-GFP for example) to 2 µg/µl in sterile water with 1 µl of 0.1% (w/v) Fast Green dye per 10 or 20 µl of diluted plasmid solution. If GFP and the gene of interest are to be co-electroporated on separate plasmids, inject the GFP plasmid and the plasmid carrying the gene of interest at a ratio of 1:4 to maximize the likelihood that all cells marked with GFP are co-electroporated with both plasmids.
2. Pull glass microcapillary tubes (1 mm outer diameter - hereafter referred to as needles) on a standard needle puller, using a single step pull at 62 °C.
3. Autoclave a surgical pack containing the following: needle holders, wound retractor, forceps, scissors for surgery, scissors for needles, stapler, staples, gauze, wound covers, surgical drapes (**Figure 1A, B**; **Materials Table**).
4. Collect other required tools: Electroporator, Femtojet Microinjecter, Tweezertrodes (5 or 7 mm), saline, suture, 5 ml syringe (**Materials Table**).

2. Prepare Mouse for Surgery

1. For pain management, inject a timed-pregnant mouse with Buprenorphine (0.05 mg/kg body weight) one hour before surgery. Apply this protocol to mice timed anywhere from embryonic day 12.5 (E12.5) to E17.5.
2. Use microloader pipette tips to back-load pulled needles with the plasmid solution. Do not fill all the way into the tip of needle yet as this will cause the needle to become clogged.
3. Anaesthetize mouse using 2-5% isoflurane gas with 1 L/min O_2. Once immobile, place in face mask and apply ointment to eyes to prevent drying. Inject with 1 ml saline (0.9% NaCl) subcutaneously in back.
   NOTE: When working with isoflurane gas, use a gas scavenger to recapture excess gas and prevent it from escaping into the room.
4. Shave abdomen. Wash abdomen with Chlorohexadine scrub, rinse with water, and apply a final prep solution of chlorohexadine and 70% ethanol. Cover mouse with sterile drape or gauze to cover fur but leave abdomen exposed (**Figure 1C, D**).

3. *In utero* Electroporation

1. Make an incision in the skin over the abdomen between the lower teats. Pull the skin away from the underlying muscle layer by tearing the connective tissue, then cut through the peritoneum into the abdominal cavity along the linea alba. Insert the wound retractor to pull the edges of the wound apart.
2. Remove the uterus from the abdominal cavity and lay it out as shown (**Figure 1E**).
    1. If different pups are to be injected with different plasmids (such as GFP *vs.* GFP with the gene of interest), count the pups on each side and decide which ones and how many to inject with each plasmid. Replace one side of the uterus back into the abdomen to keep the embryos warm and lubricated. Immediately moisten the exposed uterus with saline (preferably warmed to body temperature).

2. If injecting all pups with the same plasmid (such as when injecting Cre-GFP into transgenic embryos) only remove one horn of the uterus at a time.

3. Put a loaded needle in the grip head of the injection wand and carefully cut the tip with a pair of small surgical scissors or fine forceps. Cut the tip so the needle stays as long as possible while still allowing fluid to pass through (**Figure 1Ji-iv**).
    1. Adjust length of injection (in seconds) and injection pressure on the microinjector so that a small yet easily visible droplet of 0.1-0.2 µl appears on the tip of the needle when the foot paddle is pressed. Keep the volume of this droplet as consistent as possible between different needles.
    NOTE: this step is crucial for embryo survival (see discussion).
    2. Use the following injection parameters for the Femtojet: injecting pressure (pi) = 250-300 hPa; injection time (ti) = 0.8-1.2 sec; compensation pressure = 10-50 hPa. If required, adjust these parameters to accommodate variation between needles.

4. Select an embryo and gently position it on its back, head tilted upward (**Figure 1F**).
NOTE: This may require turning or shifting the embryo; be careful not to apply too much pressure and avoid rupture of the amniotic sac while manipulating the embryo.
5. Once the embryo is in place, locate the ventricle, which presents as a crescent shaped shadow parallel to the sagittal sinus. Touch the tip of the needle to the uterus above the ventricle at a slight angle and guide the needle through the uterine wall. The amount of pressure required depends on the sharpness of the needle. Push the needle through the cortex into the ventricle.
NOTE: Although there is rarely any additional detectable resistance, the embryo's head is often pushed away slightly and then recoils as the needle passes through the cortex into the ventricle.
6. Pump the foot paddle to inject the plasmid solution. Continue to pump until a green area is visible and conforms to the arc shape of the ventricle (**Figure 1G**). In young embryos (E12.5 to E14.5) the dye will often diffuse into the contralateral ventricle.
NOTE: The number of pumps depends on the diameter of the needle tip, the age of the embryo (and resulting size of the ventricle) and the desired injection volume. Keep volume injected as consistent as possible between embryos.
7. Inject three or four embryos. Keep all exposed embryos moist with saline throughout procedure.
8. Go back to the first embryos injected and place the paddles such that the positive electrode will draw the plasmid into the desired region of the brain (**Figure 1H**). Angle the negative electrode so that the shortest path between the electrodes passes directly through the structure targeted for electroporation (**Figure 2**).
9. Once the paddles are in place, apply the shock. Depending on the age and size of the embryos, use 5 pulses of 35-50 V (see **Table 1**). Use the following electroporation parameters: pulse length of 5 msec with a pulse interval of 950 msec. Repeat with all injected embryos.
10. Cut the tip of new pre-loaded needle as in step 3.3 as the last needle likely dried and clogged during step 3.9. Inject the next set of three or four embryos with either the same plasmid or a different plasmid and then apply the shock as in step 3.9. When all the pups in one side of the uterus are injected, remove the second side of the uterus from the female's abdomen and then replace the completed side to keep it warm.
11. Return both sides of the uterus to the female being careful to keep the surface moist with saline and not to apply too much pressure to prevent trauma to the amniotic sacs. Suture the muscle layer closed using a simple continuous stitch. Staple the skin closed. If staples are not available, suture the skin with a simple interrupted stitch. (**Figure 1I**)
12. While suturing, progressively turn down the isoflurane to allow the pregnant female's anesthesia to lighten.
NOTE: This will expedite arousal of the dam after the surgery is complete; keeping the female anesthetized for as short a time as possible will improve embryo survival. Total surgery time, starting from when the female is first anaesthetized, should be approximately 30 min.

4. Aftercare

1. Place the sutured female in an incubator or on a heating pad to recover from anesthesia. Bed her on clean bedding and place a standard recovery gel in the cage maintain hydration. For pain management following surgery, give the female three doses of Buprenorphine (0.05 mg/kg body weight) at 8 hr intervals following surgery, then four additional doses at 12 hr intervals.

5. Harvesting Brains

NOTE: Brains can be harvested at any age up to adulthood. The following applies for collecting brains prior to birth. Note that once pups are born, the order within the uterus is lost, so either every pup in the litter must be injected with the same plasmid, or another method of differentiating between control and experimental animals must be devised.

1. Prepare cold (4 °C), filtered 4% paraformaldehyde (PFA) prior to euthanizing female.
2. Euthanize the female using an intraperitoneal injection of a lethal dose of sodium pentobarbital (100 mg/kg body weight) and cut open abdomen. Pull out both sides of the uterus and lay out as when pups were initially injected.
    1. In the case where all pups received the same plasmid, such as when injecting Cre into a transgenic litter, embryo order is not important, therefore cut the uterus out of the female and place in PBS.
    2. If pups were injected with different plasmids, be sure to locate each pup, noting any dead pups, and determine which ones were injected with control and experimental plasmids before removing the uterus from the female. Be careful to keep track of which pup belongs to which group after the uterus is in PBS.

3. Remove each pup individually, decapitate with sharp scissors or a razor blade and place the head in PBS. In the case of transgenic mice, collect tissue samples for genotyping and keep each head separate, such as in a 12-well plate.
4. Under a dissecting scope, remove the brain from the skull, being careful not to nick the cortex or tear the midline. Using a fluorescent microscope, check to see if brains have a GFP+ patch, indicating that they were electroporated successfully.
5. Fix brains by immersion in PFA at 4 °C overnight.
NOTE: Check brains for expression of GFP prior to fixation since PFA often quenches the signal.

6. Cryoprotect brains through immersion in 20% sucrose for at least three days prior to freezing. Use a sucrose gradient of 10%, 15% and 20% (24 hr in each solution) to prevent tissue damage due to osmotic pressure. Store frozen brains at -80 °C and cut on a cryostat at 10-14 µm thick sections.

6. Co-staining with anti-GFP

NOTE: If antigen retrieval is necessary in order to co-stain with anti-GFP, it is important to use a gentle antigen retrieval protocol that does not compromise the GFP signal. Some antigen retrieval protocols are too harsh to use in conjunction with GFP staining (even with an antibody against GFP). A basic citric acid pre-treatment prior to application of the primary antibody is successful for most epitopes [24].

1. Make a 0.01 M solution of citric acid in ddH_2O. pH to 6 using a calibrated pH meter.
2. Heat citric acid in staining chamber in microwave or water bath until citric acids reaches 75-80 °C. Put slides in staining chamber for 10-15 min. Maintain temperature as stable as possible.
3. Wash slides in PBS 3x for 3 min at room temperature. Apply the primary antibody and proceed with immunostaining according to a standard protocol.
4. Validate Cre mediated excision by co-labelling for GFP and the gene of interest to confirm knock down (**Figure 3A**).

Representative Results

Different regions of the brain can be targeted for electroporation by varying the orientation of the paddle electrodes over the embryo's head (**Figure 2**). For all parts of the forebrain, the plasmid is injected into the lateral ventricle (the hind brain can be targeted by injecting into the fourth ventricle). In general, place the electrodes so that the straight line between them passes through the region of interest, with DNA being drawn toward the positive electrode. To target the lateral cortex (**Figure 2A**), place the positive electrode on top of the green crescent, with a slight rostral angle. For the medial cortex (**Figure 2B**), switch the orientation so that the positive electrode is over the contralateral non-injected ventricle, this time with an even larger forward angle. To target the hippocampus (**Figure 2C**), place the positive electrode over the contralateral side, but instead angle the positive electrode caudally (electroporations must be done at an age when the neural precursors are still part of the cortical hem, prior to migration to the final location of the hippocampus). To target the ganglionic eminence (**Figure 2D**) place the paddles on the embryo in line with the ears, with the positive electrode slightly lower than the negative electrode. Representative images of these electroporated regions are shown in **Figure 2**.

It is important to validate Cre-mediated excision in electroporated brains. The ideal approach is to perform in situ hybridization or immunohistochemistry against the transcript or protein in question. Unfortunately, as is the case for pRb, reliable probes or antibodies are not always available against the deleted gene. In these cases, alternative approaches, such as staining for a downstream target regulated by the deleted gene (**Figure 3A**) or confirming excision of the targeted allele in electroporated sections by PCR (**Figure 3B**), can be used. For example, **Figure 3A** confirms Cre mediated excision by reproducing a well-documented effect of pRb/p107/p130 gene deletion in electroporated neurons. Following electroporation of pRb f/f; p107 -/-; p130 f/f neurons with the pCig2-Cre plasmid, these triple knock out GFP+ cells continue to express the cell cycle progression marker Ki67, which is a known effect following excision of pocket proteins[25]. Control GFP+ neurons electroporated with the empty pCig2 plasmid do not express Ki67. The Cre plasmid should also be tested *in vitro* through co-transfection with a plasmid carrying a reporter gene behind a floxed stop codon, such as the NL-dsRed plasmid (**Figure 3C**) in a cell line, but this should only be used in combination with other *in vivo* techniques.

Due to the variation between electroporated brains, analysis of electroporated neurons requires calculating the percentage of total GFP+ neurons that portray a specific characteristic, such as expression of a protein marker or location within a given cortical layer. It is crucial to compare electroporated sections from similar anatomical locations within the brain relative to known landmarks. For example, images for **Figure 4** were taken at the level of the anterior commissure. Furthermore, due to horizontal migration, images taken near the edge of the electroporated regions have a higher proportion of mature neurons that have reached the cortex, while images taken near the middle of the electroporated region have both mature and immature GFP+ cells. To insure consistency, it is important to quantify images selected from similar places within the electroporated patch.

Following Emx1-Cre mediated deletion of pRb and p107 in pyramidal neurons in the dorsal telencephalon, a population of neurons expressing the upper cortical layer marker FoxP1 were mislocalized to the intermediate zone (IZ) (**Figure 4A**). There are significantly more FoxP1+ cells in the IZ of double knock out (DKO) brains compared to control brains with a corresponding decrease in the number of FoxP1+ cells in the upper cortical layers (above layer IV) of DKO brains than found in the upper layers of control brains (**Figure 4B**). There was no corresponding defect in the radial glial scaffold (Figure S2 of Svoboda *et al.*, 2012)[6]. Here we compare expression of cortical layer markers Tbr1, FoxP1 and Cux1 in pRb f/+; p017 +/-; Emx1-Cre + (wild type (WT)) brains to expression of these same markers pRb f/f; p107 -/-; Emx1-Cre + (DKO) brains. Heterozygote embryos can be used as controls since pocket proteins exhibit autoregulation at the protein level and heterozygote animals are aphenotypic [26].

It was unclear whether these FoxP1+ cells were found in the IZ because these cells were immature neurons inappropriately expressing FoxP1, or whether they were earlier born neurons that had failed to migrate. To distinguish between these possibilities, we electroporated GFP into the wild type (WT) and double knock out (DKO) embryos at E14.5 and tracked the progress of these neurons over 4 days. Although this technique does not conclusively identify the final cell division, as with BrdU birthdating, it does allow the tracking of newborn neurons since it marks the discrete set of neurons derived from cells lining the ventricle at the time of electroporation [17]. As shown in **Figure 4C**, all of the GFP+ neurons reach the uppermost cortical layer in the WT brains, but only a subset of these neurons reach the top of the cortex in DKO brains, indicating that there is in fact a defect in the migration of upper layer neurons, rather than improper expression of neuronal markers (similar results were obtained through traditional BrdU birthdating [6]).

Neuronal migration is a highly complex process that is regulated by a multitude of interconnected mechanisms [1-3]. As it is very difficult to identify the mechanism underlying a migration defect in an uncharacterized transgenic model, distinguishing cell autonomous versus non-

cell autonomous defects can facilitate phenotype characterization. If following electroporation of Cre-GFP, GFP+ neurons fail to migrate in an otherwise wild type brain, this indicates that the mechanism disrupted by gene deletion is specific to the electroporated cell. Alternatively, if the electroporated neurons migrate normally in the wild type brain, this suggests that the cause of aberrant migration in the transgenic embryo is due to an environmental defect. Following electroporation of Cre-GFP in control pRb f/+; p107 +/- and double knock out pRb f/f; p107 -/- embryos, GFP+ neurons were found to migrate into the cortex in pRb f/f; p107 -/- brains, but many of these neurons failed reach the upper cortical layers as they did in control brains (**Figure 4D**) [6]. There were significantly lower percentage of GFP+ neurons within the layer III/IV, marked by expression of FoxP1[27], in pRbf/f; p107 -/- electroporated brains than in control brains (**Figure 4E**). A Cre-GFP fusion protein was used to limit GFP fluorescence to the cell body and facilitate localization of the neuron to a specific cortical layer. Since the phenotype following electroporation of Cre is less severe than the phenotype following gene deletion throughout the cortex, this suggests that the original phenotype shown in **Figure 4A** is a combination of multiple mechanisms, both cell autonomous and not cell autonomous. Alternatively, it is possible that the time delay following electroporation, during which Cre is expressed, DNA recombination is performed, pRb is downregulated and the effects are manifested, is long enough to allow the electroporated neurons to reach the cortex before a migration defect becomes apparent.

It should be noted that the distinction between cell autonomous and non-cell autonomous mechanisms should be interpreted with caution in brains with high electroporation efficiencies, where 100-200 or more neurons are electroporated in a single 14 µm thick section.If a high enough proportion of neurons are electroporated, GFP+ neurons may influence each other and create a small microenvironment. To be truly cell autonomous, migration defects must be detected even when electroporation efficiency is very low (10-30 GFP+ neurons per section). If necessary, the number of transfected cells can be lowered by decreasing voltage, pulse number or DNA concentration. All of these factors must be taken into consideration when analyzing the results following electroporation of Cre in a transgenic model.

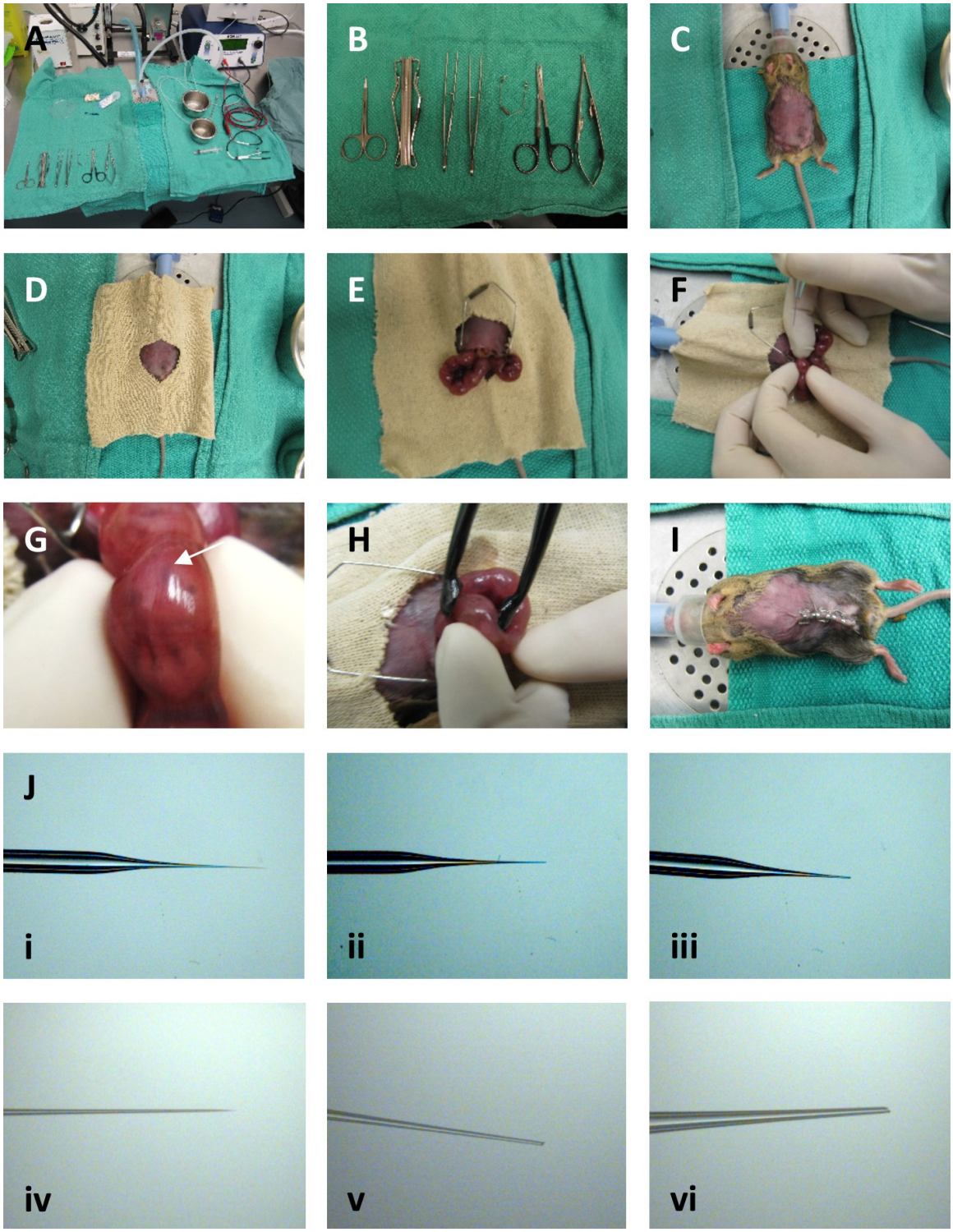

Figure 1: Performing *In utero* electroporation. (A) Sterile surgical set up. **(B)** Surgical tools from left: fine scissors for cutting needle tips; stapler; forceps; wound retractor; surgical scissors; needle holder. **(C)** Prepped pregnant mouse with shaved and disinfected abdomen. **(D)** Mouse covered with sterile drape prior to incision. **(E)** Uterus with E13.5 embryos removed from abdominal cavity. **(F)** Injecting pups in the ventricle. **(G)** Close up of injected pup; note the blue crescent on the embryo's head indicating that the ventricle was successfully injected with the plasmid solution (arrow). **(H)** Paddles are placed to electroporate the lateral cortex. **(I)** Mouse post-surgery. **(J)** Preparing sharp needles is a crucial part of *in utero* electroporation. Examples of uncut needles **(i, iv)**, good needles **(ii, v)** and poor needles **(iii, vi)** are shown at low **(i-iii)** and high **(iv-vi)** magnification. Please click here to view a larger version of this figure.

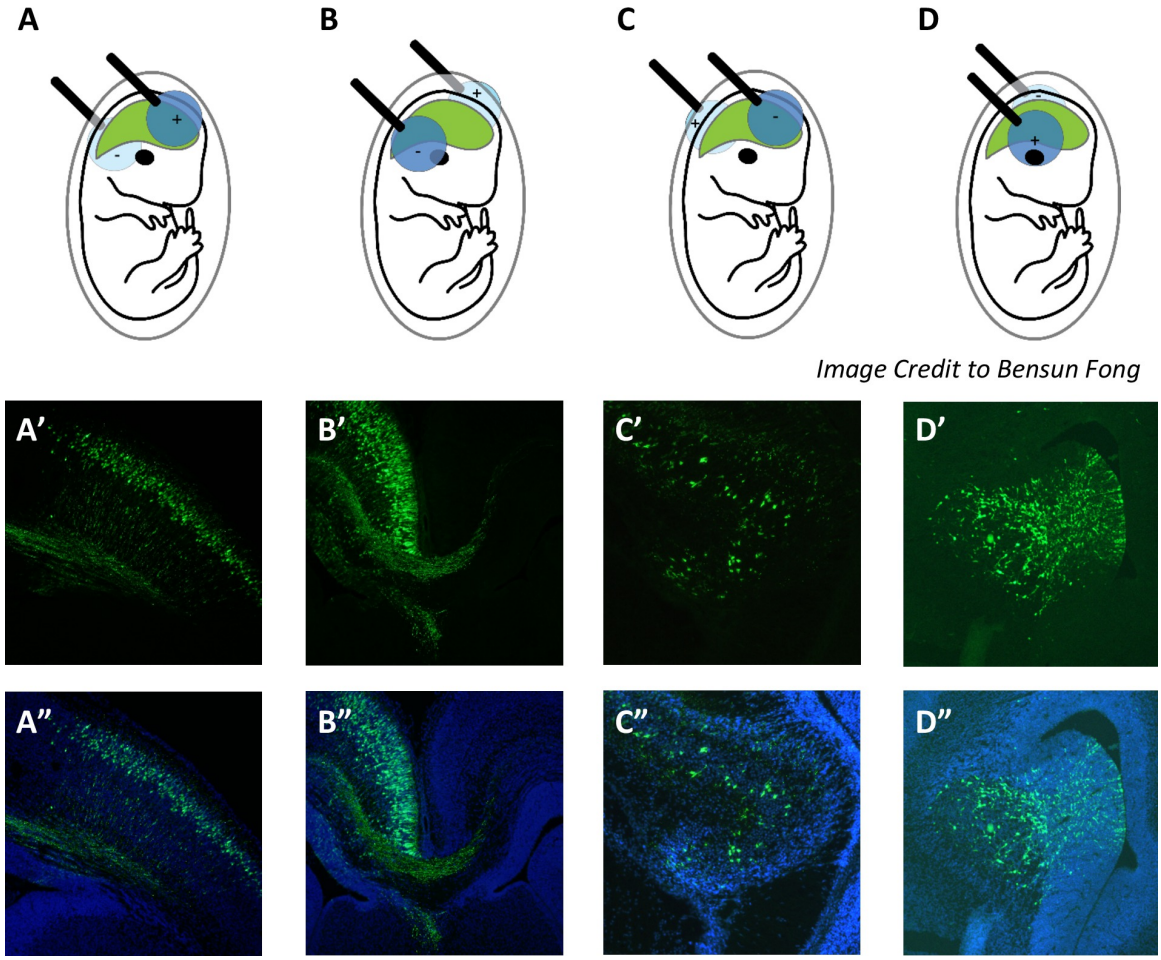

Figure 2: Targeting different brain regions. Diagrams A-D show paddle placement for targeting different regions of the forebrains. The dark blue circle represents the paddle in front of the embryo while the light blue circle represents the paddle behind the embryo. Positive and negative electrodes are indicated with the appropriate sign. **(A)** Electrodes angled to target the lateral cortex. **(A', A")** Example of electroporation of the lateral cortex, three days after surgery. **(B)** Electrodes angled to target the medial cortex. **(B', B")** Example of electroporation of the medial cortex. **(C)** Electrodes angled to target the hippocampus. **(C', C")** Example of electroporation of the hippocampus. **(D)** Electrodes angled to target the ganglionic eminence (GE). **(D', D")** Example of electroporation of the GE. Please click here to view a larger version of this figure.

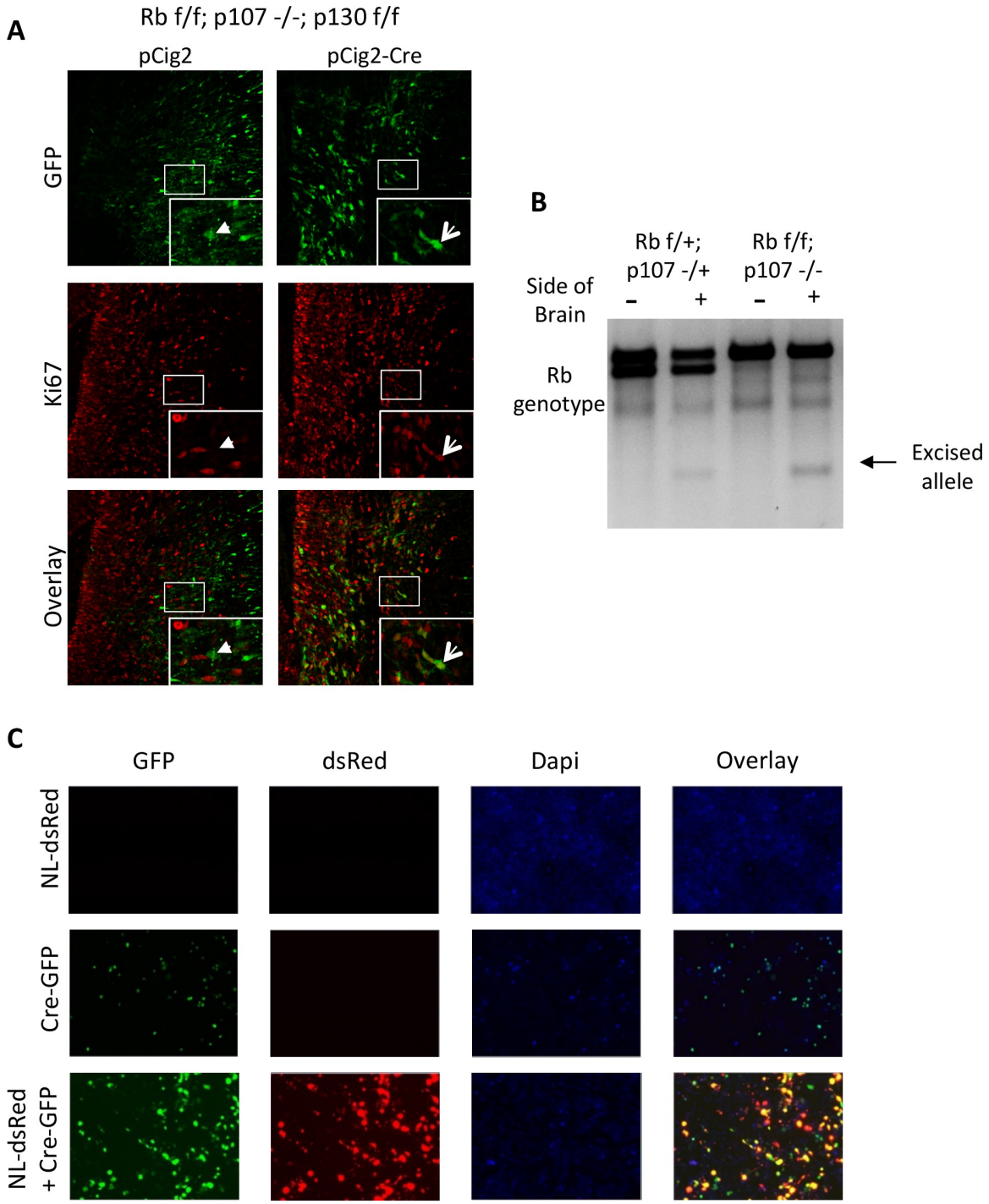

Figure 3: Confirming Cre-mediated gene excision in electroporated neurons. (A) Cre mediated excision can be confirmed by co-staining for a downstream target of the deleted gene. pRb f/f; p107 -/-; p130 f/f embryos were electroporated with either the empty pCig2 plasmid or the pCig2-Cre plasmid and stained for GFP and Ki67, a marker of cell cycle entry. Double stained cells were seen in neurons electroporated with Cre (arrows in inset) but not in neurons electroporated with pCig2 alone (arrowheads). **(B)** Excision of pRb was also confirmed by performing PCR with genotyping primers on DNA extracted from the tissue sections removed from the slides. Sections were divided down the midline and the electroporated side of the section was pooled. The upper band represents the floxed allele and the lower band represents the wild type allele. The arrow indicates the excised allele in the electroporated side of the brain only. Because pRb f/+; p107 +/- heterozygotes were used as controls, an excised allele can be seen in the electroporated side of the brain in both the control and knockout brains. **(C)** Cre-mediated excision can also be confirmed *in vitro* using plasmids with floxed stop codons upstream of RFP, such as NL-dsRed. RFP is only expressed in HEK cells when co-transfected with Cre-GFP in Hek293 cells (bottom row), indicating that excision was successful. Please click here to view a larger version of this figure.

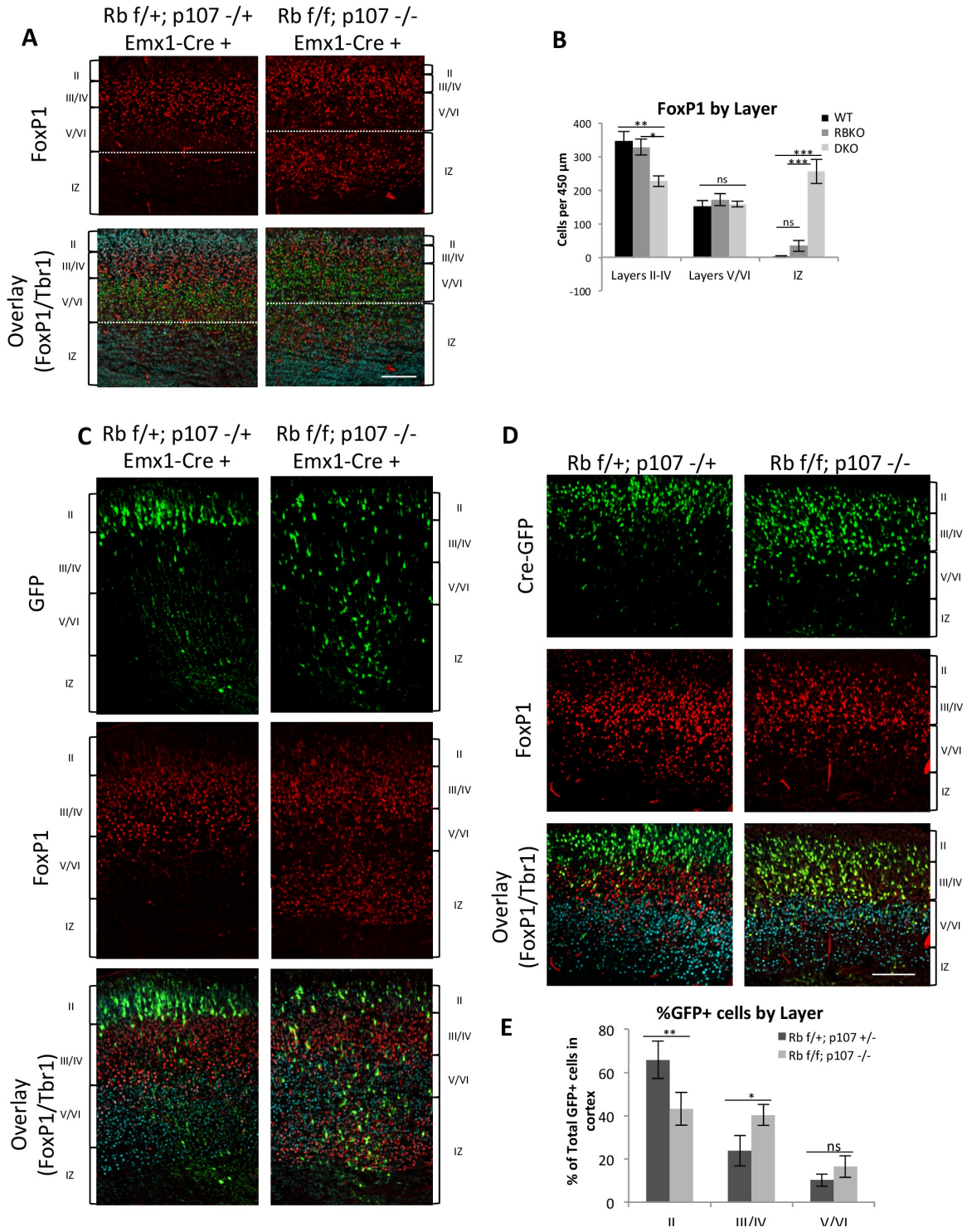

Figure 4: Using IUE to study migration in transgenic mouse models. (A) Expression of FoxP1, a marker for layer III/IV cortical neurons, was examined in pRb f/+; p107 +/-; Emx1-Cre + (WT), and pRb f/f; p107 -/-; Emx1-Cre + (DKO) brains at E17.5. Overlay includes Cux1 (blue - marker for layers II-IV) and Tbr1 (green - marker for layers V/VI). A population of cells expressing FoxP1 was observed in the intermediate zone of DKO embryos (arrow), but not WT embryos, with a concurrent decrease in the number of FoxP1+ neurons in layers II-IV of the cortex in DKO brains relative to WT brains **(B)**. The white line indicates the delineation between the cortical plate and intermediate zone, which was determined using DAPI staining (not shown). **(C)** To trace the migration of a discrete population of late born neurons, WT and DKO embryos were electroporated with GFP at E14.5 and collected the brains at E18.5. Brains were co-stained with FoxP1 (red) and Tbr1 (blue) to show that GFP+ neurons are found almost exclusively in layer II in the WT brain but are delayed in the intermediate zone (IZ) and lower cortical layers in the DKO. **(D)** To determine if pRb and p107 regulate radial migration cell autonomously, pRb f/f; p107-/- and pRb f/+; p107-/+ embryos were electroporated with Cre-GFP at E13.5 and brains were collected at E17.5. The location of GFP+ neurons was quantified according to cortical layer. Layer II was defined as being above FoxP1 staining (red), layer III/IV was defined as within FoxP1 staining, above Tbr1 (blue) and layer V/VI was defined as within the Tbr1 positive layer **(E)**. We show that a portion pRb and p107 deficient neurons fail to reach layer II but instead remain in layer III/IV. The figure has been modified from Svoboda *et al*., 2012. Please click here to view a larger version of this figure.

Embryo Age	Voltage
E12.5 – E13.5	35V
E14.5 – E15.5	40V
E16.5	45V
E17.5	50V

Table 1: Electroporation voltage by embryo age.

Discussion

Two of the primary challenges in performing *in utero* electroporations are 1) preventing embryo lethality and 2) decreasing variability between electroporations. One of the most important factors in preventing lethality is needle quality, as blunt needles inflict more damage to the embryo. When cutting the needle, keep the tip as long as possible while still allowing a visible droplet of 0.1-0.2 µl of fluid to appear following a pump of the foot paddle **(Figure 1J)**. If the needle is too dull or the shaft too short, the resulting tissue damage could kill the embryo. Conversely, if the tip of the needle is too fine, it will take too long to inject sufficient plasmid volume; leaving the needle in the brain for too long causes damage due to unavoidable vibrations of the investigator's hands and slight rotations of the embryo. Furthermore, use a microbeveler to make needles with a sharp, beveled tips to allow injections into younger, more fragile embryos, although this should not be necessary for embryos E13.5 and older.

The stress level of the pregnant female is another key factor affecting embryo survival. The higher the dam's stress level, the more likely she will abort the litter. For this reason it is important to minimize anesthesia time and change housing as little as possible before and after surgery. The background strain can also affect stress level and it may be necessary to outcross colonies prone to anxiety onto a strain such as CD1, assuming that the phenotype under investigation is maintained across different background strains.

The single biggest limitation to IUE is the inherent variability between electroporations. Each electroporated brain is different due to variations in injection volume, paddle placement, paddle contact and embryo age. Since needles are variable, it is not possible to inject a fixed volume – rather the investigator must approximate the size of the green patch to deliver similar amounts to all embryos. Similarly, because the embryo is floating in a fluid filled sac, it is not possible to systematically measure the location and orientation of the paddles over the embryo's head, as is done for stereotactic injections. Finally, slight differences in embryonic age can have significant effects on experimental results. For this reason, comparison between littermates is recommended.

Disclosures

The authors have nothing to disclose

Acknowledgements

We are indebted to Pierre Mattar and Freda Miller for their assistance with the *in utero* electroporation and to Noel Ghanem and Bensun Fong for creating diagrams. We thank Linda Jui and Jason G. MacLaurin for excellent technical assistance. Equipment was supported by the Centre for Stroke Recovery.

This work was supported by a scholarship from HSFO and OGS to D.S.S. and a CIHR grant to R.S.S.

References

1. Hippenmeyer,S. Molecular pathways controlling the sequential steps of cortical projection neuron migration. *Adv.Exp.Med.Biol.* **800** 1-24, 10.1007/978-94-007-7687-6_1; 10.1007/978-94-007-7687-6_1, (2014).
2. Evsyukova,I., Plestant,C. and Anton,E.S. Integrative mechanisms of oriented neuronal migration in the developing brain. *Annu.Rev.Cell Dev.Biol.* **29** 299-353, 10.1146/annurev-cellbio-101512-122400; 10.1146/annurev-cellbio-101512-122400, (2013).
3. Wu,Q.*, et al*. The dynamics of neuronal migration. *Adv.Exp.Med.Biol.* **800** 25-36, 10.1007/978-94-007-7687-6_2; 10.1007/978-94-007-7687-6_2, (2014).
4. McClellan,K.A.*, et al*. Unique requirement for Rb/E2F3 in neuronal migration: evidence for cell cycle-independent functions. *Mol.Cell.Biol.* **27** (13), 4825-4843, 10.1128/MCB.02100-06, (2007).
5. Nguyen,L.*, et al*. P27kip1 Independently Promotes Neuronal Differentiation and Migration in the Cerebral Cortex. *Genes Dev.* **20** (11), 1511-1524, 10.1101/gad.377106, (2006).
6. Svoboda,D.S., Paquin,A., Park,D.S. and Slack,R.S. Pocket proteins pRb and p107 are required for cortical lamination independent of apoptosis. *Dev.Biol.* **384** (1), 101-113, 10.1016/j.ydbio.2013.09.015; 10.1016/j.ydbio.2013.09.015, (2013).
7. Hashimoto-Torii,K.*, et al*. Interaction between Reelin and Notch signaling regulates neuronal migration in the cerebral cortex. *Neuron.* **60** (2), 273-284, 10.1016/j.neuron.2008.09.026; 10.1016/j.neuron.2008.09.026, (2008).
8. Ori-McKenney,K.M. and Vallee,R.B. Neuronal migration defects in the Loa dynein mutant mouse. *Neural Dev.* **6** 26-8104-6-26, 10.1186/1749-8104-6-26; 10.1186/1749-8104-6-26, (2011).
9. Wang,H., Ge,G., Uchida,Y., Luu,B. and Ahn,S. Gli3 is required for maintenance and fate specification of cortical progenitors. *J.Neurosci.* **31** (17), 6440-6448, 10.1523/JNEUROSCI.4892-10.2011; 10.1523/JNEUROSCI.4892-10.2011, (2011).
10. Heng,J.I.*, et al*. Neurogenin 2 controls cortical neuron migration through regulation of Rnd2. *Nature.* **455** (7209), 114-118, 10.1038/nature07198; 10.1038/nature07198, (2008).

11. Alfano,C., *et al*. COUP-TFI promotes radial migration and proper morphology of callosal projection neurons by repressing Rnd2 expression. *Development.* **138** (21), 4685-4697, 10.1242/dev.068031; 10.1242/dev.068031, (2011).
12. De Vry,J., *et al*. In vivo electroporation of the central nervous system: a non-viral approach for targeted gene delivery. *Prog.Neurobiol.* **92** (3), 227-244, 10.1016/j.pneurobio.2010.10.001; 10.1016/j.pneurobio.2010.10.001, (2010).
13. Dixit,R. *et al*. Efficient gene delivery into multiple CNS territories using in utero electroporation. *J.Vis.Exp.* **(52)**. pii: 2957. doi (52), 10.3791/2957, 10.3791/2957; 10.3791/2957, (2011).
14. Saito,T. In vivo electroporation in the embryonic mouse central nervous system. *Nat.Protoc.* **1** (3), 1552-1558, 10.1038/nprot.2006.276, (2006).
15. Elias,G.M., Elias,L.A., Apostolides,P.F., Kriegstein,A.R. and Nicoll,R.A. Differential trafficking of AMPA and NMDA receptors by SAP102 and PSD-95 underlies synapse development. *Proc.Natl.Acad.Sci.U.S.A.* **105** (52), 20953-20958, 10.1073/pnas.0811025106; 10.1073/pnas.0811025106, (2008).
16. Bhuiyan,M.I., Lee,J.H., Kim,S.Y. and Cho,K.O. Expression of exogenous LIN28 contributes to proliferation and survival of mouse primary cortical neurons in vitro. *Neuroscience.* **248C** 448-458, 10.1016/j.neuroscience.2013.06.023; 10.1016/j.neuroscience.2013.06.023, (2013).
17. Rice,H., Suth,S., Cavanaugh,W., Bai,J. and Young-Pearse,T.L. In utero electroporation followed by primary neuronal culture for studying gene function in subset of cortical neurons. *J.Vis.Exp.* **(44).** pii: 2103. doi (44), 10.3791/2103, 10.3791/2103; 10.3791/2103, (2010).
18. Yoshida,A., Yamaguchi,Y., Nonomura,K., Kawakami,K., Takahashi,Y. and Miura,M. Simultaneous expression of different transgenes in neurons and glia by combining in utero electroporation with the Tol2 transposon-mediated gene transfer system. *Genes Cells.* **15** (5), 501-512, 10.1111/j.1365-2443.2010.01397.x; 10.1111/j.1365-2443.2010.01397.x, (2010).
19. Miyagi,S., *et al*. The Sox-2 regulatory regions display their activities in two distinct types of multipotent stem cells. *Mol.Cell.Biol.* **24** (10), 4207-4220,(2004).
20. Wang,X., Qiu,R., Tsark,W. and Lu,Q. Rapid promoter analysis in developing mouse brain and genetic labeling of young neurons by doublecortin-DsRed-express. *J.Neurosci.Res.* **85** (16), 3567-3573, 10.1002/jnr.21440, (2007).
21. LoTurco,J., Manent,J.B. and Sidiqi,F. New and improved tools for in utero electroporation studies of developing cerebral cortex. *Cereb.Cortex.* **19 Suppl 1** i120-5, 10.1093/cercor/bhp033; 10.1093/cercor/bhp033, (2009).
22. Bouabe,H. and Okkenhaug,K. Gene targeting in mice: a review. *Methods Mol.Biol.* **1064** 315-336, 10.1007/978-1-62703-601-6_23; 10.1007/978-1-62703-601-6_23, (2013).
23. Ferguson,K.L., *et al*. A cell-autonomous requirement for the cell cycle regulatory protein, Rb, in neuronal migration. *EMBO J.* **24** (24), 4381-4391, 10.1038/sj.emboj.7600887, (2005).
24. Lagace,D.C., *et al*. Dynamic contribution of nestin-expressing stem cells to adult neurogenesis. *J.Neurosci.* **27** (46), 12623-12629, 10.1523/JNEUROSCI.3812-07.2007, (2007).
25. Andrusiak,M.G., Vandenbosch,R., Park,D.S. and Slack,R.S. The retinoblastoma protein is essential for survival of postmitotic neurons. *J.Neurosci.* **32** (42), 14809-14814, 10.1523/JNEUROSCI.1912-12.2012; 10.1523/JNEUROSCI.1912-12.2012, (2012).
26. Shan,B., Chang,C.Y., Jones,D. and Lee,W.H. The transcription factor E2F-1 mediates the autoregulation of RB gene expression. *Mol.Cell.Biol.* **14** (1), 299-309,(1994).
27. Ferland,R.J., Cherry,T.J., Preware,P.O., Morrisey,E.E. and Walsh,C.A. Characterization of Foxp2 and Foxp1 mRNA and protein in the developing and mature brain. *J.Comp.Neurol.* **460** (2), 266-279, 10.1002/cne.10654, (2003).

Appendix E

Co-author publication reprints – first page

The Journal of Neuroscience, June 13, 2012 • 32(24):8219–8230 • 8219

Development/Plasticity/Repair

The Rb/E2F Pathway Modulates Neurogenesis through Direct Regulation of the *Dlx1/Dlx2* Bigene Cluster

Noël Ghanem,[1,4] Matthew G. Andrusiak,[1] Devon Svoboda,[1] Sawsan M. Al Lafi,[4] Lisa M. Julian,[1] Kelly A. McClellan,[1] Yves De Repentigny,[5] Rashmi Kothary,[5] Marc Ekker,[2] Alexandre Blais,[3] David S. Park,[1] and Ruth S. Slack[1]

Departments of [1]Cellular and Molecular Medicine, [2]Biology, and [3]Biochemistry, Microbiology and Immunology, University of Ottawa, Ottawa, Ontario K1H 8M5, Canada, [4]Department of Biology, American University of Beirut, Beirut 1107 2020, Lebanon, and [5]Ottawa Hospital Research Institute, Regenerative Medicine Program, Ottawa, Ontario K1Y 4E9, Canada

During brain morphogenesis, the mechanisms through which the cell cycle machinery integrates with differentiation signals remain elusive. Here we show that the Rb/E2F pathway regulates key aspects of differentiation and migration through direct control of the Dlx1 and Dlx2 homeodomain proteins, required for interneuron specification. Rb deficiency results in a dramatic reduction of *Dlx1* and *Dlx2* gene expression manifested by loss of interneuron subtypes and severe migration defects in the mouse brain. The Rb/E2F pathway modulates *Dlx1/Dlx2* regulation through direct interaction with a *Dlx* forebrain-specific enhancer, I12b, and the *Dlx1/Dlx2* proximal promoter regions, through repressor E2F sites both *in vitro* and *in vivo*. In the absence of Rb, we demonstrate that repressor E2Fs inhibit *Dlx* transcription at the *Dlx1/Dlx2* promoters and *Dlx1/2*-I12b enhancer to suppress differentiation. Our findings support a model whereby the cell cycle machinery not only controls cell division but also modulates neuronal differentiation and migration through direct regulation of the *Dlx1/Dlx2* bigene cluster during embryonic development.

Introduction

During brain development, cell cycle regulation and differentiation are tightly coordinated developmental programs. Cross talk exists between the cell cycle machinery and differentiation pathways to ensure that progenitor populations are maintained and that differentiation is induced at the time of terminal mitosis (McConnell and Kaznowski, 1991; Nguyen et al., 2006; Farkas and Huttner, 2008; Frank and Tsai, 2009). Despite the importance of the precise coordination of these events, the mechanisms by which the cell cycle machinery integrates with differentiation signals remain poorly understood.

The retinoblastoma protein, pRb, is a tumor suppressor gene that controls the G_1-S phase checkpoint during cell cycle regulation (McClellan and Slack, 2006; Chen et al., 2009; Freedman et al., 2009). Rb regulates the transcription of genes that are required for DNA replication and cell cycle progression by binding and inhibiting E2F transcription factors (Burkhart and Sage, 2008). There are eight E2Fs, five of which can bind Rb (E2F1–5) and are considered among the classical Rb partners while E2F6–8 are Rb-independent repressors (Dick and Dyson, 2006; Chen et al., 2009; Lammens et al., 2009). E2F1, 2, and 3 are primarily transcriptional activators while E2F4 and 5 repress transcription and induce gene silencing through pocket protein binding (Dick and Dyson, 2006). E2F7 and E2F8, two atypical E2Fs (Lammens et al., 2009), can form homo and heterodimers which, in the absence of pocket proteins, bind and repress E2F target genes. The expression of E2F7 and 8 is induced by activating E2Fs and are believed to serve as a fine tuning mechanism to modulate E2F target gene regulation (Di Stefano et al., 2003; Christensen et al., 2005; Lammens et al., 2009).

It has been proposed that the Rb pathway may have novel function(s) that extend beyond cell cycle control (McClellan and Slack, 2006, 2007). Conditional knock-out studies have suggested that Rb may have a role in regulating differentiation and migration (Takahashi et al., 2003; Ferguson et al., 2005; Chen et al., 2007; McClellan et al., 2007); however, the underlying mechanisms remain unknown. Clearly, indirect cross talk between the cell cycle machinery and differentiation pathways is essential to prevent premature differentiation of proliferating progenitors while promoting differentiation as cell division ceases. If the cell cycle proteins themselves could directly regulate genes required for differentiation, these two processes could become intimately coordinated.

Here we have uncovered a more direct role for cell cycle proteins in neuronal differentiation through the control of Dlx1 and Dlx2 homeodomain protein regulation, two key proteins that specify GABAergic neurons in the brain. Consistent with a deficit in *Dlx1/Dlx2* gene expression, mice lacking Rb exhibited a pro-

Received March 19, 2012; revised April 18, 2012; accepted April 24, 2012.

Author contributions: N.G., K.A.M., D.S.P., and R.S.S. designed research; N.G., M.G.A., D.S., S.M.A.L., L.J., K.A.M., and Y.D.R. performed research; M.E. and A.B. contributed unpublished reagents/analytic tools; N.G., M.G.A., D.S., L.J., K.A.M., R.K., M.E., A.B., D.S.P., and R.S.S. analyzed data; N.G., K.A.M., R.K., M.E., A.B., D.S.P., and R.S.S. wrote the paper.

This work was supported by a Canadian Institutes of Health Research (CIHR) grant to R.S.S., and grants from the Lebanese National Council for Scientific Research and the University Research Board at the American University of Beirut to N.G. N.G. was previously supported by a fellowship from the Heart and Stroke Foundation of Canada. M.G.A. is supported by a Heart and Stroke Foundation of Ontario studentship; L.M.J. and K.A.M. were supported by CIHR Canada Scholarships. We gratefully acknowledge equipment funding from the Centre for Stroke Recovery to R.S.S. and D.S.P. We thank Drs. Mireille Khacho, Renaud Vandenbosch, and Marc Germain for critical reading of the manuscript. We thank Jason MacLaurin, Rayan Naser, Carine Jaafar, and Maarouf Baghdadi for excellent technical assistance.

Correspondence should be addressed to Ruth S. Slack, Department of Cellular and Molecular Medicine, University of Ottawa, 451 Smyth Road, Ottawa, Ontario K1H 8M5, Canada. E-mail: rslack@uottawa.ca.

DOI:10.1523/JNEUROSCI.1344-12.2012

 0270-6474/12/328219-12$15.00/0

Cell Stem Cell
Article

Opposing Regulation of *Sox2* by Cell-Cycle Effectors E2f3a and E2f3b in Neural Stem Cells

Lisa M. Julian,[1] Renaud Vandenbosch,[1] Catherine A. Pakenham,[1] Matthew G. Andrusiak,[1] Angela P. Nguyen,[1] Kelly A. McClellan,[1] Devon S. Svoboda,[1] Diane C. Lagace,[1] David S. Park,[1] Gustavo Leone,[3] Alexandre Blais,[2,*] and Ruth S. Slack[1,*]

[1]Department of Cellular and Molecular Medicine
[2]Ottawa Institute of Systems Biology and Department of Biochemistry, Microbiology, and Immunology
University of Ottawa, 451 Smyth Road, Ottawa, ON K1H 8M5, Canada
[3]Solid Tumor Biology Program, Department of Molecular Virology, Immunology, and Medical Genetics and Department of Molecular Genetics, Comprehensive Cancer Center, The Ohio State University, Columbus, OH 43210, USA
*Correspondence: alexandre.blais@uottawa.ca (A.B.), rslack@uottawa.ca (R.S.S.)
http://dx.doi.org/10.1016/j.stem.2013.02.001

SUMMARY

The mechanisms through which cell-cycle control and cell-fate decisions are coordinated in proliferating stem cell populations are largely unknown. Here, we show that E2f3 isoforms, which control cell-cycle progression in cooperation with the retinoblastoma protein (pRb), have critical effects during developmental and adult neurogenesis. Loss of either E2f3 isoform disrupts *Sox2* gene regulation and the balance between precursor maintenance and differentiation in the developing cortex. Both isoforms target the *Sox2* locus to maintain baseline levels of *Sox2* expression but antagonistically regulate Sox2 levels to instruct fate choices. E2f3-mediated regulation of *Sox2* and precursor cell fate extends to the adult brain, where E2f3a loss results in defects in hippocampal neurogenesis and memory formation. Our results demonstrate a mechanism by which E2f3a and E2f3b differentially regulate *Sox2* dosage in neural precursors, a finding that may have broad implications for the regulation of diverse stem cell populations.

INTRODUCTION

Stem cell-fate decisions, such as self-renewal, precursor cell maintenance, and commitment to differentiation have critical outcomes for embryonic development, tissue maintenance, tumor suppression, and regeneration. Cortical development depends on a precisely regulated balance of self-renewal within stem cell-like apical precursors (APs), production of rapidly proliferating basal progenitors (BPs), and differentiation of postmitotic neurons (Englund et al., 2005; Farkas and Huttner, 2008; Hutton and Pevny, 2011) (Figure 1A). Identifying mechanisms that control this balance can inform our understanding of developmental neurogenesis and, more broadly, reveal stem cell biological principles extending to embryonic stem cell differentiation, tumor formation, and tissue regeneration.

The pluripotency factor Sox2 is an established regulator of neural precursor proliferation, self-renewal, and differentiation during development and is also required for maintenance of adult stem cell populations in many different tissues (reviewed in Sarkar and Hochedlinger, 2013). Overexpression of Sox2 in both mouse and chick embryonic neural precursor cells (NPCs) results in maintenance of the $Sox2^+$ population and defective neurogenesis (Bani-Yaghoub et al., 2006; Graham et al., 2003). Conversely, loss of function of Sox2 in neural precursors leads to precursor loss and reduced or aberrant differentiation, depending on the tissue type and degree of Sox2 loss (Cavallaro et al., 2008; Favaro et al., 2009; Ferri et al., 2004; Graham et al., 2003; Miyagi et al., 2008; Taranova et al., 2006). Taken together, these studies reveal that the function of Sox2 is strongly influenced by dosage; thus, fine-tuning of transcription from the *Sox2* locus is crucial for the generation of the correct proportion of precursors versus differentiated cell types. Interestingly, a recent study finds that the Cyclin-dependent kinase inhibitor 1A (p21) binds a *Sox2* enhancer region to regulate Sox2 expression and adult neurogenesis, linking cell-cycle regulation with Sox2-mediated control of neural stem cell (NSC) expansion (Marqués-Torrejón et al., 2013).

Previous evidence suggests that the cell cycle machinery plays a key role in regulating the proliferative expansion and self-renewal capacity of NPCs (Nishino et al., 2008; Ruzhynsky et al., 2007; Vanderluit et al., 2004). However, how specific cell-cycle regulatory proteins function in this context remains poorly defined. The retinoblastoma pocket protein (pRb) family controls cell-cycle progression by binding and inhibiting the E2f family of transcription factors. E2fs are classified into the "activator" subclass, which drives proliferation and transcription, and the "repressor" subclass, the members of which are thought to repress gene transcription by modifying chromatin structure through association with pocket proteins (Asp et al., 2009). Earlier work has reported that E2f3 is the most highly expressed E2f family member in wild-type and pRb-deficient neural precursors (Callaghan et al., 1999), suggesting that it may be an important regulator of NPC functions. Understanding how the *E2f3* gene functions to regulate the cell cycle is not entirely straightforward, because the two isoforms (*E2f3a* and *E2f3b*) expressed from its locus have identical domains important for DNA binding, transactivation, and pocket-protein binding, and only their N termini are unique. Mice lacking both

MCB Journals.ASM.org

Interaction and Antagonistic Roles of NF-κB and Hes6 in the Regulation of Cortical Neurogenesis

Laurent Methot,[a] Robert Hermann,[a]* Yeman Tang,[a] Rita Lo,[a] Hosam Al-Jehani,[a,c] Sumit Jhas,[a] Devon Svoboda,[b] Ruth S. Slack,[b] Philip A. Barker,[a] Stefano Stifani[a]

Montreal Neurological Institute, McGill University, Montreal, Quebec, Canada[a]; Department of Cellular and Molecular Medicine, University of Ottawa, Ottawa, Ontario, Canada[b]; Department of Neurosurgery, Faculty of Medicine, Dammam University, Dammam, Saudi Arabia[c]

The involvement of nuclear factor kappa B (NF-κB) in several processes in the postnatal and adult brain, ranging from neuronal survival to synaptogenesis and plasticity, has been documented. In contrast, little is known about the functions of NF-κB during embryonic brain development. It is shown here that NF-κB is selectively activated in neocortical neural progenitor cells in the developing mouse telencephalon. Blockade of NF-κB activity leads to premature cortical neuronal differentiation and depletion of the progenitor cell pool. Conversely, NF-κB activation causes decreased cortical neurogenesis and expansion of the progenitor cell compartment. These effects are antagonized by the proneuronal transcription factor Hes6, which physically and functionally interacts with RelA-containing NF-κB complexes in cortical progenitor cells. In turn, NF-κB exerts an inhibitory effect on the ability of Hes6 to promote cortical neuronal differentiation. These results reveal previously uncharacterized functions and modes of regulation for NF-κB and Hes6 during cortical neurogenesis.

Development of the mammalian cerebral cortex initiates with mitotic neural progenitor cells located in the ventricular zone (VZ) of the embryonic neocortex. These cells initially undergo symmetric divisions to generate two new undifferentiated progenitors. At the onset of neurogenesis, certain neural progenitors begin to undergo asymmetric divisions that generate a new progenitor and a neuron. Regulation of the balance between progenitor maintenance and neuronal differentiation is essential for correct cortical development, but the mechanisms regulating these processes remain incompletely characterized (1, 2).

Hairy/enhancer of split (Hes) transcription factors, including Hes1 and Hes5, are important regulators of the balance between proliferation and differentiation during cortical neurogenesis. Hes1 and Hes5 act downstream of the Notch receptors to inhibit neuronal differentiation and promote maintenance of the undifferentiated progenitor state (3–5). The antineurogenic role of Notch-induced Hes proteins is antagonized, at least in part, by a related Hes family member, Hes6, which is not activated by Notch signaling and instead functions downstream of proteins that promote neuronal differentiation (6–8).

Functions of the Notch pathway are often modulated by cross talk with the transcription factor, nuclear factor kappa B (NF-κB) (9, 10). NF-κB is a heterodimer that controls the expression of many genes involved in regulating cell proliferation, survival, and differentiation during numerous physiological processes (11, 12). NF-κB dimers are ubiquitously expressed but are usually maintained in an inactive state in the cytosol by mechanisms that prevent and/or revert their nuclear translocation, including the association with factors generally referred to as inhibitors of NF-κB (IκBs). A variety of different stimuli lead to the activation of NF-κB by causing the phosphorylation and degradation of IκBs (13, 14).

NF-κB is important for nervous system processes like neuronal survival, dendrite development, synaptic plasticity, and learning (15–18). Little is known, however, about the involvement of NF-κB in early stages of brain development. Here, we show that mouse NF-κB is selectively activated in neocortical neural progenitor cells, where it inhibits neuronal differentiation and maintains the undifferentiated progenitor state. This effect is antagonized by Hes6, which interacts physically and functionally with NF-κB. This antagonism is bidirectional, since NF-κB suppresses Hes6-mediated promotion of cortical neurogenesis. Together, these results reveal a previously uncharacterized function for NF-κB during cortical neurogenesis and provide evidence that mutually repressive interactions between NF-κB and Hes6 drive signaling events that are critical for normal cerebral cortex development.

MATERIALS AND METHODS

DNA plasmids. The following expression and reporter plasmids have been described previously: pCAGGS-GFP (where GFP is green fluorescent protein) (19); pcDNA3-IκBαM (20); pAd-Track-IKKβ-DN (where IKKβ-DN is dominant negative form of IκB kinase subunit beta) (21, 22); pCMV2-FLAG-Hes6WT, pCMV2-FLAG-Hes6Δ55-95, pCMV2-FLAG-Hes6ΔWRPW, pCMV2-FLAG-Hes1WT, and pEGFP (23, 24); pCMV-p65/RelA (pCMV-RelA) and pNF-κB-luciferase (25); and pRSV-β-gal (7, 24). The IκBαM coding sequence was subcloned as an EcoRI fragment into the EcoRI site of the pCIG2 vector, which contains a cDNA-internal ribosome entry site (IRES)-enhanced GFP (EGFP) expression cassette under the control of a cytomegalovirus (CMV) enhancer and chicken β-actin promoter (26). The IKKβ-DN coding sequence was subcloned as a blunt-ended NotI/HindIII fragment into the SmaI site of pCIG2.

Received 29 November 2012 Returned for modification 12 February 2013
Accepted 13 May 2013
Published ahead of print 20 May 2013

Address correspondence to Stefano Stifani, stefano.stifani@mcgill.ca.
* Present address: Robert Hermann, Neurobiology of Brain Tumors, German Cancer Research Center, Heidelberg, Germany.

Supplemental material for this article may be found at http://dx.doi.org/10.1128/MCB.01610-12.

doi:10.1128/MCB.01610-12